The metabolism of 11β-hydroxyandrostenedione by steroidogenic enzymes yields metabolites contributing to the androgen pool in prostate cancer

by
Therina du Toit

Dissertation presented for the degree of Doctor of Philosophy
(Biochemistry) in the Faculty of Science at Stellenbosch University

UNIVERSITEIT
iYUNIVESITHI
STELLENBOSCH
UNIVERSITY

100
1918·2018

Promoter: Prof Amanda C. Swart

March 2018

Declaration

By submitting this thesis electronically, I declare that the entirety of the work contained therein is my own, original work, that I am the sole author thereof (save to the extent explicitly otherwise stated), that reproduction and publication thereof by Stellenbosch University will not infringe any third party rights and that I have not previously in its entirety or in part submitted it for obtaining any qualification.

This thesis includes 4 original papers published in peer-reviewed journals. The development and writing of the papers were the principal responsibility of myself and, for each of the cases where this is not the case, a declaration is included in the thesis indicating the nature and extent of the contributions of co-authors.

T du Toit

March 2018

Ter herinnering aan Katherina Helena (Ina) Theron

Dankie vir my naam, ek mis Ouma

Summary

This study describes:

- The development and validation of three ultra-performance convergence chromatography tandem mass spectrometry (UPC^2-MS/MS) analytical methods which were applied in the detection and quantification of C_{19} and C_{21} steroids, including C11-oxy C_{19} and C11-oxy C_{21} steroids;

- The investigation into the contribution of adrenal 11β-hydroxyandrostenedione (11OHA4) and 11β-hydroxytestosterone (11OHT) to the pool of active androgens in the prostate, by following androgen metabolism in normal epithelial prostate PNT2, benign prostatic hyperplasia (BPH-1) and prostate cancer LNCaP, C4-2B and VCaP cell models;

  Steroid profiles revealed 11β-hydroxysteroid dehydrogenase type 2 (11βHSD2) activity in all the cell models, confirmed in the conversion of 11OHA4 to 11keto-androstenedione (11KA4), with reductive 17β-hydroxysteroid dehydrogenase (17βHSD) enzymes metabolising 11KA4, ultimately yielding 11keto-testosterone (11KT).

- The *in vitro* investigation into the inactivation, reactivation, glucuronidation and sulfation of 11OHA4, 11OHT and their downstream metabolites;

  In prostate cancer (PCa) cell models, the conjugation of 11KT and 11keto-dihydrotestosterone (11KDHT) were hampered compared to testosterone (T) and dihydrotestosterone (DHT), while the inactivation and reactivation of the C11-oxy C_{19} steroids were less efficient than the C_{19} steroids in BPH-1 cells.

- The *in vivo* steroid profiles in PCa, BPH and castration-resistant prostate cancer (CRPC) tissue and plasma of healthy and PCa patients;

  Analyses of the C_{19} and C11-oxy C_{19} steroids, together with glucuronide and sulfate conjugates, showed increased unconjugated levels of 11KT and 11KDHT in plasma of PCa patients compared to a healthy subject, and 11OHA4, 11KT and 11KDHT levels were prominent in PCa tissue, while downstream inactive C11-oxy 3α-reduced metabolites were identified in BPH and CRPC tissue.

Opsomming

Hierdie studie beskryf die volgende:

- Die ontwikkeling en validering van drie *UPC²-MS/MS* analitiese metodes wat vervolgens toegepas is in die skeiding en kwantifisering van steroïedmetaboliete.

- Die ondersoek na 11OHA4 and 11OHT se bydrae tot die aktiewe androgeen poel in die prostaat;

  Androgeen metabolisme is in normale epiteel prostaat PNT2, BPH-1 en prostaat kanker LNCaP, C4-2B en VCaP selmodelle ondersoek. Die steroïdprofiele bevestig die teenwoordigheid van 11βHSD2 aktiwiteit in al die modelle in die omsetting van 11OHA4 na 11KA4, sowel as die aktiwiteit van 17βHSD wat vervolgens die omsetting van 11KA4 na 11KT gekataliseer het.

- Die *in vitro* inaktivering, heraktivering en konjugering van 11OHA4 en 11OHT metaboliete;

  In prostaatkanker selmodelle was 11KT en 11KDHT konjugering oneffektief in vergelyking met T en DHT, en die inaktivering van die C11-oksie C_{19} steroïede was nie optimaal in vergelyking met die C_{19} steroïede in BPH-1 selmodelle nie.

- Die *in vivo* steroïedprofiele in prostaatkankerweefsel, BPH weefsel en kastrasie-weerstandige prostaatkankerweefsel en in plasma van gesonde normale individuë en prostaatkanker pasiënte, asook die teenwoordigheid van ongekonjugeerde en gekonjugeerde steroïedmetaboliete in sirkulasie;

  Analiese toon dat ongekonjugeerde 11KT en 11KDHT hoër was in die plasma van pasiënte met prostaatkanker; 11OHA4, 11KT en 11KDHT vlakke was abnormaal hoog in die prostaatkankerweefsel, terwyl onaktiewe C11-oksie 3α-gereduseerde metaboliete geïdentifiseer was in BPH weefsel en in kastrasie-weerstandige prostaatkankerweefsel.

Acknowledgements

I hereby wish to express my sincere gratitude and appreciation to:

Prof Amanda C Swart, a remarkable woman, who has helped me discover myself, my inquisitive nature for science and the world. Without you none of this would have been possible, thank you. You are an amazing supervisor and role-model, I hope that we will always find the time to talk about our day and have a G&T.

Prof Pieter Swart, thank you for teaching me to appreciate the 'everyday'. I will always cherish our conversations around the dinner table.

Ralie Louw, a wonderful laboratory manager, who was always willing to help me and order the products needed for my project – thank you!

The technical and administrative staff of the Biochemistry department, especially Reggie Brandt for all the nitrogen canisters you had to carry for me.

Dr. Maria 'Marietjie' Stander and her CAF team at Stellenbosch University for their technical expertise during UPC^2-MS/MS and UPLC-MS/MS analyses.

My fellow students – this journey was worth it because of all of you!

Colin – you are my best friend and my favourite person to talk to, you mean the world to me, never forget that.

My mother – your support and unconditional love is what motivates me, keep me safe, allows me to dream and has provided me with a home and an amazing life.

Contents

Abbreviations

<u>General</u>

21OHD	21-hydroxylase deficiency
ADT	Androgen deprivation therapy
AR	Androgen receptor
BO	Bilateral orchiectomy
BPH	Benign prostatic hyperplasia
CAH	Congenital adrenal hyperplasia
CRPC	Castration-resistant prostate cancer
CYP450	Cytochrome P450
Cyt b_5	Cytochrome b_5
DSD	Disorders of sex development
ER(β)	Estrogen receptor (beta)
GC-MS	Gas chromatography mass spectrometry
HPLC	High-performance liquid chromatography
HSD	Hydroxysteroid dehydrogenase
HSE	Hydroxysteroid epimerase
HSP	Heat shock protein
LC-MS/MS	Liquid chromatography tandem mass spectrometry
NADH	Nicotinamide adenine dinucleotide
NADPH	Nicotinamide adenine dinucleotide phosphate
OATP	Organic anion transporter protein

PAPS	3'-phosphoadenosine-5'-phosphosulfate
PAPSS	PAPS synthase
PCa	Prostate cancer
PCOS	Polycystic ovary syndrome
POR	P450 oxidoreductase
PSA	Prostate-specific antigen
SCF	Supercritical fluid
StAR	Steroidogenic acute regulatory protein
TURP	Transurethral resection of the prostate
UDP	Uridine diphosphate
UHPLC-MS/MS	Ultra-high performance liquid chromatography tandem mass spectrometry
UPC^2-MS/MS	Ultra-performance convergence chromatography tandem mass spectrometry
UPLC-MS/MS	Ultra-performance liquid chromatography tandem mass spectrometry
ZF	Zona fasciculata
ZG	Zona glomerulosa
ZR	Zona reticularis

<div align="center">Enzymes</div>

11βHSD	11β-hydroxysteroid dehydrogenase
11βHSD1	11β-hydroxysteroid dehydrogenase type 1
11βHSD2	11β-hydroxysteroid dehydrogenase type 2

17βHSD	17β-hydroxysteroid dehydrogenase
17βHSD2	17β-hydroxysteroid dehydrogenase type 2
17βHSD3	17β-hydroxysteroid dehydrogenase type 3
17βHSD6	17β-hydroxysteroid dehydrogenase type 6
3αHSD	3α-hydroxysteroid dehydrogenase
3βHSD	3β-hydroxysteroid dehydrogenase
3βHSD1	3β-hydroxysteroid dehydrogenase type 1
3βHSD2	3β-hydroxysteroid dehydrogenase type 2
AKR1C1	3α-hydroxysteroid dehydrogenase type 4
AKR1C2	3α-hydroxysteroid dehydrogenase type 3
AKR1C3	17β-hydroxysteroid dehydrogenase type 5
AKR1D1	Aldo-keto reductase family 1
CYP11A1	Cytochrome P450 cholesterol side chain cleavage
CYP11B1	Cytochrome P450 11β-hydroxylase
CYP11B2	Cytochrome P450 aldosterone synthase
CYP17A1	Cytochrome P450 17α-hydroxylase/17,20 lyase
CYP21A2	Cytochrome P450 steroid 21-hydroxylase
H6PDH	Hexose-6-phosphate dehydrogenase
RL-HSD	Retinol-like hydroxysteroid dehydrogenase
SRD5A	5α-reductase
SRD5A1	5α-reductase type 1
SRD5A2	5α-reductase type 2

SRD5A3	5α-reductase type 3
STS	Steroid sulfatase
SULT	Sulfotransferase
SULT2A1	Sulfotransferase
SULT2B1a	Sulfotransferase
SULT2B1b	Sulfotransferase
UGT	Uridine diphosphate glucuronosyltransferase
UGT2B15	Uridine diphosphate glucuronosyltransferase 2B type 15
UGT2B17	Uridine diphosphate glucuronosyltransferase 2B type 17
UGT2B28	Uridine diphosphate glucuronosyltransferase 2B type 28

Steroid hormones

11,16-diOHPROG	4-pregnen-11β,16α-diol-3,20-dione
11K-3αDIOL	11keto-5α-androstane-3α,17β-diol
11K-3βDIOL	11keto-5α-androstane-3β,17β-diol
11K-5αDIONE	11keto-5α-androstanedione
11KA4	11keto-androstenedione/4-androsten-3,11,17-trione
11KAST	11keto-androsterone/5α-androstan-3α-ol-11,17-dione
11KDHPROG	11keto-dihydroprogesterone/5α-pregnan-3,11,20-trione
11KDHT	11keto-dihydrotestosterone/5α-androstan-17β-ol-3,11-dione
11K-epiAST	5α-androstan-3β-ol-11,17-dione
11K-etiocholanolone	5β-androstan-3α-ol-11,17-dione
11KPdiol	5α-pregnan-3α,17α-diol-11,20-dione

11KPdione	5α-pregnan-17α-ol-3,11,20-trione
11KPROG	11keto-progesterone/4-pregnen-3,11,20-trione
11KT	11keto-testosterone/4-androsten-17β-ol-3,11-dione
11OH-5αDIONE	11β-hydroxy-5α-androstanedione
11OHA4	11β-hydroxyandrostenedione/4-androsten-11β-ol-3,17-dione
11OHAST	11β-hydroxyandrosterone/5α-androstan-3α,11β-diol-17-one
11OHDHPROG	11β-hydroxydihydroprogesterone/5α-pregnan-11β-ol-3,20-dione
11OHDHT	11β-hydroxydihydrotestosterone/5α-androstan-11β,17β-diol-3-one
11OH-epiAST	5α-androstan-3β,11β-diol-17-one
11OH-epietiocholanolone	5β-androstan-3β,11β-diol-17-one
11OH-etiocholanlone	5β-androstan-3α,11β-diol-17-one
11OHPdiol	5α-pregnan-3α,11β,17α-triol-20-one
11OHPdione	5α-pregnan-11β,17α-diol-3,20-dione
11OHT	11β-hydroxytestosterone/4-androsten-11β,17β-diol-3-one
11αOHPROG	11α-hydroxyprogesterone/4-pregnen-11α-ol-3,20-dione
11βOHPROG	11β-hydroxyprogesterone/4-pregnen-11β-ol-3,20-dione
16OHPROG	16α-hydroxyprogesterone/4-pregnen-16α-ol-3,20-dione
17OHPREG	17α-hydroxypregnenolone/5-pregnen-3β,17α-diol-20-one
17OHPROG	17α-hydroxyprogesterone/4-pregnen-17α-ol-3,20-dione
18OHCORT	18-hydroxycorticosterone/4-pregnen-11β,18,21-triol-3,20-dione
21-dE	21-deoxycortisone/17α-dihydroxypregn-4-ene-3,11,20-trione
21-dF	21-deoxycortisol/11β,17α-dihydroxypregn-4-ene-3,20-dione

3,11-diOHDHPROG	5α-pregnan-3α,11β-diol-20-one
3αDIOL	5α-androstane-3α,17β-diol
3βDIOL	5α-androstane-3β,17β-diol
5αDIONE	5α-androstanedione/5α-androstan-3,17-dione
5βDIONE	5β-androstanedione/5β-androstan-3,17-dione
A4	Androstenedione/4-androsten-3,17-dione
ACTH	Adrenocorticotropic hormone
Alfaxalone	5α-pregnan-3α-ol-11,20-dione
Allopregnanolone	5α-pregnan-3α-ol-20-one
Androstenediol	Androsta-5-ene-3β,17β-diol
AST	Androsterone/5α-androstan-3α-ol-17-one
CORT	Corticosterone/4-pregnen-11β,21-diol-3,20-dione
Cortisol	4-pregnen-11β,17α,21-triol-3,20-dione
Cortisone	4-pregnen-17α,21-diol-3,11,20-trione
CRH	Corticotropin-releasing hormone
DHEA	Dehydroepiandrosterone/5-androsten-3β-ol-17-one
DHPROG	Dihydroprogesterone/5α-pregnan-3,20-dione
DHT	Dihydrotestosterone/5α-androstan-17β-ol-3-one
DOC	11-deoxycorticosterone/4-pregnen-21-ol-3,20-dione
EpiAST	Epiandrosterone/5α-androstan-3β-ol-17-one
Epietiocholanolone	5β-androstan-3β-ol-17-one
EpiT	Epitestosterone/4-androsten-17α-ol-3-one

Etiocholanolone	5β-androstan-3α-ol-17-one
G	Glucuronide
GnRH	Gonadotropin-releasing hormone
LH	Luteinizing hormone
LHRH	Luteinizing hormone-releasing hormone
Pdiol	5α-pregnane-3α,17α-diol-20-one
Pdione	5α-pregnane-17α-ol-3,20-dione
PREG	Pregnenolone/5-pregnen-3β-ol-20-one
Pregnanetriol	5β-pregnan-3α,17α,20α-triol
PROG	Progesterone/4-pregnen-3,20-dione
S	Sulfate
T	Testosterone/4-androsten-17β-ol-3-one

<u>Mathematical symbols</u>

K_m	Michaelis constant
V_{max}	Maximum velocity/rate
$\dfrac{V_{max}}{K_m}$	Catalytic efficiency

Chapter 1

General introduction

Steroids produced in the adrenals serve as precursors for the biosynthesis of steroid hormones in the prostate (Sharifi and Auchus 2012), and while the biosynthesis of active steroids is essential in the progression of prostate cancer (PCa), the inactivation and conjugation of steroids in the prostate microenvironment are also important. The production, inactivation and elimination of active steroids must be finely regulated within the prostate to maintain homeostasis, however, dysregulation of these pathways contributes to the initiation and development of PCa. Overproduction of active steroids and impeded inactivation pathways, in addition to promiscuous receptor binding, together all contribute to PCa progression.

The adrenal steroids relevant to PCa which are the focus of this thesis are divided into two categories: the C_{19} and C_{21} steroids, which consists of either 19 or 21 carbon atoms in the steroid backbone structures, respectively. C_{19} steroids include the androgens, while C_{21} steroids include the mineralocorticoids and glucocorticoids. C_{19} and C_{21} steroids can be metabolised by adrenal steroidogenic enzymes that either hydroxylate the carbon 11 (C11) or convert the C11-hydroxy group to a keto group, resulting in the production of C11-oxy C_{19} and C11-oxy C_{21} steroids, respectively. These C11-oxy steroids are produced in the adrenals, released into circulation, where after they exert physiological effects once taken up by peripheral target tissue. An important adrenal C11-oxy C_{19} steroid, 11β-hydroxyandrostenedione (11OHA4) is abundantly produced in the adrenals (Rege et al. 2013), and although this steroid is not androgenic, it is metabolised to potent downstream

1

androgens in the prostate (Storbeck et al. 2013; Swart et al. 2013; Bloem et al. 2015). 11OHA4, together with its metabolites, have been identified as role-players in the progression of PCa and are metabolised in a metabolic pathway termed, the 11OHA4-pathway. The pathway is particularly important in the context of castration-resistant prostate cancer (CRPC), in which gonadal androgens are negligible and adrenal steroids remain in abundance. To date, the metabolism of 11OHA4 and its metabolites have been shown in non-steroidogenic cells transfected with appropriate steroidogenic enzymes and in LNCaP cells, which endogenously express steroidogenic enzymes (Storbeck et al. 2013; Swart et al. 2013). In addition, the androgenic capability of downstream 11OHA4 metabolites towards the androgen receptor (AR) has been reported (Yazawa et al. 2008; Rege et al. 2013; Storbeck et al. 2013; Campana et al. 2016). These studies have shown that the relevance of the 11OHA4-pathway lies within two C11-keto metabolites: 11keto-testosterone (11KT) and 11keto-dihydrotestosterone (11KDHT). Both steroids bind and activate the AR, induces the expression of AR-regulated genes, while also increasing cell proliferation in PCa cell models (Pretorius et al. 2016). 11KT and 11KDHT have been determined to be equipotent to testosterone (T) and dihydrotestosterone (DHT), respectively, with T and DHT historically established as potent androgens in the steroid arena. While *in vitro* studies have reported the contributory role of 11OHA4 and its metabolites to PCa, *in vivo* evidence of these steroids in PCa or benign prostatic hyperplasia (BPH) has not been established, in addition to the presence of these C11-oxy C_{19} steroids in normal physiology. Both BPH and PCa are androgen dependent prostate diseases, however, these are two different diseases in terms of their origin and aggressiveness, with BPH considered a precursor disease to the development of PCa (Penning 2010). Moreover, while the biosynthesis of the C11-oxy C_{19} steroids and their metabolism to active androgens are now well documented, the inactivation and conjugation of these steroids, to

date, have not been clarified. The presence of these C11-oxy C_{19} steroids *in vivo*, together with their inactivation being inefficient, will firmly establish these steroids as major role-players in PCa. Another important concept to consider is the role of adrenal C11-oxy C_{21} steroids in PCa. Recent *in vitro* studies have shown the contribution of adrenal C11-oxy C_{21} precursor steroids to the androgen pool – producing 11KDHT via the backdoor pathway in non-steroidogenic cells transfected with the appropriate steroidogenic enzymes, and in LNCaP cells (Barnard et al. 2017), adding another layer of complexity to the role of C11-oxy steroids in the progression of PCa.

The analyses and quantification of steroids in the research and clinical setting have been accomplished by gas chromatography mass spectrometry (GC-MS) and liquid chromatography tandem mass spectrometry (LC-MS/MS) for many years, however, progress in technologies regarding mass spectrometry, combining aspects of both GC-MS and LC-MS/MS, has led to the introduction of ultra-performance convergence chromatography tandem mass spectrometry (UPC^2-MS/MS) enabling the separation of chemically similar steroid structures, within minutes, as well as the accurate quantification of steroids present at very low concentrations (Quanson et al. 2016). Using the state-of-the-art UPC^2-MS/MS in the analyses of these C11-oxy steroids has allowed not only the evaluation of the influence of these steroids on PCa progression, but has also showed that comprehensive steroid profiles can be applied in the analyses of steroidogenic pathways.

The PhD study conducted will be presented as follows:

Chapter 2 provides an overview of adrenal steroidogenesis and highlights steroid metabolic pathways and the enzymes involved in the biosynthesis and inactivation of steroid hormones in the prostate. This chapter furthermore reviews the C11-oxy C_{19} steroids and their contribution to disease, highlighting

their receptor action. The chapter concludes with a discussion on the progression of PCa to CRPC and current clinical treatment regimens.

The aims of this thesis, which have been addressed in Chapters 3, 4, 5 and 6, can be summarised as follows:

- to develop and validate UPC^2-MS/MS analytical methods for the separation and quantification of C_{19}, C11-oxy C_{19}, C_{21} and C11-oxy C_{21} steroids;

- to investigate the metabolism of 11OHA4 and 11β-hydroxytestosterone (11OHT) and their downstream metabolites in normal epithelial PNT2 cells, epithelial BPH cells and in cancer cell models, LNCaP, VCaP and C4-2B cells;

- to evaluate the inactivation by 3α-hydroxysteroid dehydrogenases (3αHSDs) and reactivation by retinol-like hydroxysteroid dehydrogenase (RL-HSD) of the C11-oxy C_{19} and C_{19} steroids in BPH-1, LNCaP, VCaP and C4-2B cells, which are cells that endogenously express 3αHSDs and RL-HSD;

- to compare the glucuronidation of C11-oxy C_{19} and C_{19} steroids by endogenously expressed uridine-diphosphate glucuronosyltransferases (UGTs) in LNCaP, C4-2B and VCaP cells and to evaluate the sulfation of C11-oxy C_{19} and C_{19} steroids by endogenously expressed sulfotransferases (SULTs) in LNCaP cells;

- to determine circulating C11-oxy C_{19} and C_{19} steroid glucuronide and sulfate levels;

- to evaluate to presence of the C11-oxy C_{19} steroids in BPH, PCa and CRPC tissue, together with determining steroid profiles in plasma of healthy subjects and in PCa patients.

Chapter 3 is presented in the form of three published manuscripts. The first manuscript (Du Toit and Swart 2016) provides a review on prostate steroidogenesis with the focus on the conjugating enzymes, UGT2Bs, in regulating steroid action. A perspective is furthermore given on the role of the specific UGT2B type 28 (UGT2B28) isoform in PCa, while also discussing aspects still unknown in terms of the regulation of the UGT2B enzymes. In the second manuscript (Du Toit et al. 2017), C11-oxy C_{19} steroids are profiled in PNT2 and LNCaP cells and the glucuronidation of the C_{19} steroids, T, DHT, androsterone (AST) and 5α-androstane-3α, 17β-diol (3αDIOL) are analysed and compared to the glucuronidation of 11KT and 11KDHT in LNCaP cells. Furthermore, *in vivo* levels of the C11-oxy C_{19} are shown in steroid panels determined in PCa tissue and in plasma of PCa patients. The third manuscript (Du Toit and Swart 2018) describes the inefficient UGT-conjugation of the C11-oxy C_{19} steroids in LNCaP, C4-2B and VCaP cell models. In addition, the metabolism of the C11-oxy C_{19} and C_{19} steroids are described in the aforementioned cell models, while the inactivation and reactivation of DHT and 11KDHT by enzymes endogenously expressed in the cell models are also described. Comprehensive steroid panels of the C11-oxy C_{19} and C_{19} steroids in CRPC tissue are also presented, and C11-oxy C_{19} and C_{19} steroid glucuronides in plasma of a healthy subject and in PCa patients are shown.

Chapter 4 describes a preliminary investigation into the SULT-conjugation of the C11-oxy C_{19} steroids in LNCaP cells. Firstly, the development of an in-laboratory dual deconjugating protocol, which deconjugates steroid glucuronides and steroid sulfates, is discussed. This protocol was subsequently applied to deconjugate steroid glucuronides and sulfates present in aliquots collected after *in vitro* enzymatic conversion assays were conducted, and in plasma samples. The conjugation of T- and DHT-metabolites are discussed, comparing the C11-oxy C_{19} steroids to the C_{19} steroids. In addition, the

SULT-conjugation of ketosteroids (androstenedione [A4] and 11OHA4) are shown in LNCaP cells, together with *in vivo* steroid sulfate levels determined in plasma of healthy subjects and in a PCa patient.

In Chapter 5 the metabolism of 11OHA4 and its downstream metabolites in BPH-1 cells are presented, together with a comparison of the inactivation by 3αHSD and reactivation by RL-HSD of the C11-oxy C_{19} and C_{19} steroids. In addition, *in vivo* evidence establishing the presence of the C11-oxy C_{19} steroids in BPH tissue is presented and depicted as steroid panels.

Chapter 6 describes a novel UPC^2-MS/MS method that was developed and validated for the separation and quantification of C_{19} and C_{21} steroids, including their C11-hydroxy and C11-keto derivatives. This chapter discusses the application of the method in the evaluation of augmented steroid metabolic pathways and steroid levels in adrenal-linked endocrine diseases. In addition, preliminary unpublished results concerning the application of this method in the analysis of C11-oxy steroids *in vivo* is summarised.

Chapter 7 presents a general discussion of the results described in this thesis, highlights the main conclusions that were drawn from these findings and concludes with recommendations for future studies.

Chapter 2

The biosynthesis of the C11-oxy C$_{19}$ steroids and their contribution to prostate cancer

2.1 Introduction

Steroid hormones are involved in normal physiological development, including cellular growth and sexual maturation. However, these same hormones are implicated in steroid-dependent diseases with for example, steroid hormones having been linked to PCa since 1946 (Huggins 1946; Huggins and Bergenstal 1952). In addition, the clinical diseases and disorders known today that result from androgen excess or androgen deficiency include congenital adrenal hyperplasia (CAH), polycystic ovary syndrome (PCOS), 21-hydroxylase deficiency (21OHD), as well as the excess or deficit production of steroid hormones which presents as disorders of sex development (DSD) in newborns (Rauh 2009; Auchus and Miller 2012; Auchus 2015; Turcu and Auchus 2015). During childhood, adrenarche is linked to androgen imbalances (Auchus and Rainey 2004), while in maturing females, PCOS present with androgen excess (Azziz et al. 1998). The development of breast cancer, as with PCa, is androgen dependent, wherein androgens are converted to estrogens, which in turns drives hormone-dependent tumour growth (Risbridger et al. 2010). In addition, insufficient production of the stress hormone, cortisol, in Addison's disease or excess cortisol production in Cushing's syndrome are both consequences of hormonal imbalances (Ten et al. 2001; Rang et al. 2003; Løvås et al. 2009; Couchman et al. 2011). Other conditions, including male pattern baldness, pre- and post-menopause, premenstrual syndrome, metabolic syndrome and skin conditions, all of which have been linked to steroid hormones (Anagnostis et al. 2009; Couchman et al. 2011; Slominski et al. 2013).

7

The inactivation and conjugation of steroid hormones, which interrupts steroid signalling and terminates physiological effects, contribute to the development of steroid-dependent diseases when not proceeding efficiently. In addition, steroid receptor interactions causing downstream effects also contribute to disease, with active steroid hormones binding receptors and while non-androgenic steroids may not bind receptors, these steroids may be channelled to downstream potent steroids as in the case of the adrenal C11-oxy C_{19} steroid, 11OHA4.

This chapter will summarize the biosynthesis of androgens in the adrenals, focusing on the production of the C11-oxy C_{19} steroids. Peripheral steroid metabolic pathways and the respective enzymes involved in these pathways will be highlighted, together with the implication of the C11-oxy steroids in disease states. Lastly, androgen receptor action will be reviewed, as well as the progression of PCa to CRPC, together with treatment regimens currently employed in the clinical setting.

2.2 Adrenal steroidogenesis

The adrenal glands are found atop the kidneys in the human body, comprising of three layers: the outer capsule, the adrenal cortex, and the inner medulla. The adrenal cortex, in turn, also consists of three layers wherein adrenal steroidogenesis takes place: the zona glomerulosa (ZG), the zona fasciculata (ZF) and the zona reticularis (ZR) (Messiano and Jaffe 1997). The steroid hormone output of the adrenal cortex is controlled by corticotropin-releasing hormone (CRH) from the hypothalamus, which stimulates the release of adrenocorticotropic hormone (ACTH) from the pituitary corticotropes, with ACTH in turn stimulating the ZF and the ZR to produce their respective steroid hormones. This signalling pathway, termed the HPA-axis, representing the hypothalamus-pituitary-adrenal pathway that regulates steroid hormone production. The ZG is, however, under the regulation of angiotensin II, which forms part of the renin-angiotensin system, with the extracellular potassium concentration also

8

involved in this regulation (Hammer et al. 2005). The zones of the adrenal cortex are not only defined

by their physiological compartmentalization, but also by their differential enzyme expression. As the

layers are divided into three sections, so also is adrenal steroidogenesis divided into three pathways:

the mineralocorticoid pathway within the ZG, the glucocorticoid pathway within the ZF and the

androgen pathway within the ZR (Fig. 2.1). While the steroid hormones produced in the first two

pathways are termed C_{21} steroids, the androgen pathway represents the production of C_{19} steroids.

The C_{21} steroids produced in the mineralocorticoid pathway represents steroid hormones that are

involved in regulating the electrolyte and water balance of the human body, including the regulation of

blood pressure, denoted by the production of aldosterone. The C_{21} steroids produced in the

glucocorticoid pathway represent steroid hormones that are involved in the stress response of the

human body, denoted by the production of cortisol (and cortisone). Moreover, these steroids are also

involved in carbohydrate-, protein- and lipid metabolism, as well as in immune and inflammatory

responses. Although the mineralocorticoids and glucocorticoids are involved in steroid-dependent

diseases, these steroids will not be the primary focus of this thesis.

The C_{19} steroids produced in the androgen pathway of adrenal steroidogenesis are involved in sexual

development and growth, and will be the focus of this thesis. C_{19} androgens are produced from the

universal precursor of all steroid hormones, the 27-carbon cholesterol. Cholesterol is transported from

the outer to the inner mitochondrial membrane by steroidogenic acute regulatory protein (StAR)

(Clark et al. 1994; Ghayee and Auchus 2007), and subsequently oxidized by cytochrome P450

side-chain cleavage (CYP11A1) to produce the C_{21} steroid, pregnenolone (PREG) (Fig. 2.1). This reaction

occurs in all three zones of the adrenal cortex, however, the subsequent production of androgens

occurs only in the ZR. The hydroxylase catalytic activity of 17α-hydroxylase/17,20-lyase (CYP17A1), a

microsomal cytochrome P450 enzyme, subsequently converts PREG to 17-hydroxypregnenolone (17OHPREG), followed by the conversion of 17OHPREG, catalysed by the lyase activity of CYP17A1, to the C_{19} androgen precursor, dehydroepiandrosterone (DHEA) (Fig. 2.2). 3β-hydroxysteroid dehydrogenase type 2 (3βHSD2) catalyses the conversion of Δ^5 to Δ^4 steroids and biosynthesizes two androgens namely, A4 from DHEA, and T from androstenediol, the 17β-hydroxysteroid dehydrogenase (17βHSD) product of DHEA (Miller and Auchus 2011). DHEA, if not channelled to androstenediol or A4, can be inactivated by SULTs, specifically SULT2A1, to DHEA-sulfate (DHEA-S), while androstenediol is also sulfated (Rege et al. 2016). Although the sulfation pathway is dominant in the adrenals, steroid sulfation is reversible as steroid sulfatase (STS) removes the sulfate group, and is expressed in the adrenal cortex (Dalla Valle et al. 2007; Mueller et al. 2015).
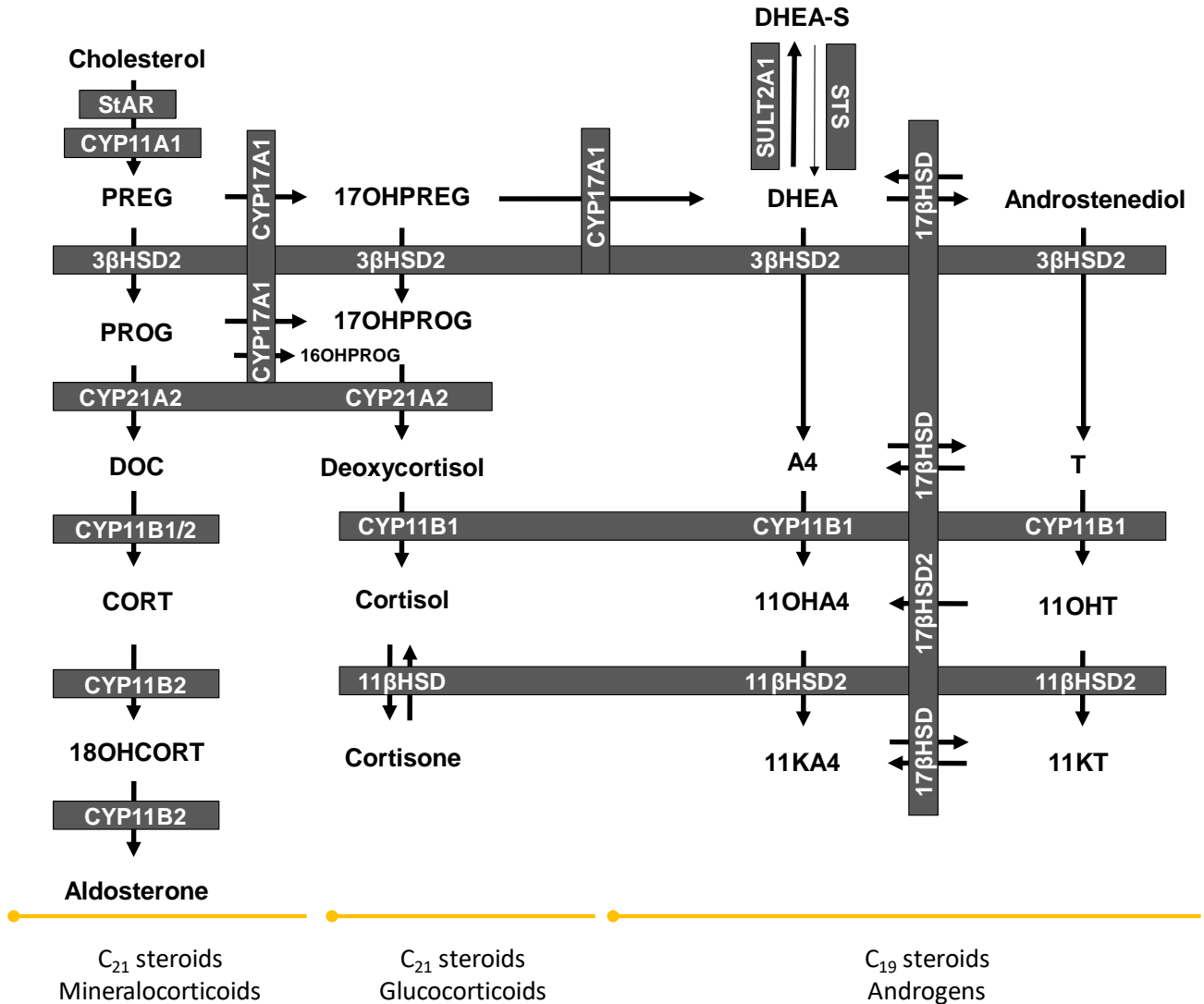
Figure 2.1 Adrenal steroidogenesis representing the three pathways of steroid hormone production; the mineralocorticoid-, the glucocorticoid- and the androgen pathways.

The lyase activity of CYP17A1 is therefore a key enzyme required for the production of androgens, as the absence of the lyase activity of CYP17A1 will channel steroids into the glucocorticoid pathway. Indeed, in the absence of the 17,20-lyase activity in the ZF, 3βHSD2 converts 17OHPREG to 17-hydroxyprogesterone (17OHPROG), followed by the sequential conversion of 17OHPROG by cytochrome P450 steroid 21-hydroxylase (CYP21A2) producing 11-deoxycortisol which is converted by

11

cytochrome P450 11β-hydroxylase (CYP11B1), to produce cortisol in the glucocorticoid pathway. In the ZG, CYP17A1 is absent, hence 3βHSD2 converts PREG to progesterone (PROG), followed by the conversion of PROG to deoxycorticosterone (DOC) by CYP21A2, where after cytochrome P450 aldosterone synthase (CYP11B2) sequentially converts DOC to corticosterone (CORT), 18-hydroxy-CORT (18OH-CORT) and finally aldosterone, in the mineralocorticoid pathway. Of note, while CYP17A1 hydroxylates PROG at C17, the enzyme also hydroxylates PROG at C16, producing 16-hydroxyprogesterone (16OHPROG) (Swart et al. 1993).

Adrenal steroid production is divided between the endoplasmic reticulum, for the 3βHSD2, CYP17A1 and CYP21A2 catalysed reactions, while the CYP11A1, CYP11B1 and CYP11B2 catalysed reactions occur in the mitochondria. The latter reactions require an electron shuttle system, adrenodoxin/adrenodoxin reductase for their hydroxylase or oxidase activity, while the endoplasmic reticulum localized enzymatic reactions require electrons from nicotinamide adenine dinucleotide phosphate (NADPH) using the enzymatic action of P450 oxidoreductase (POR) (Miller and Auchus 2011). Moreover, the lyase activity of CYP17A1 requires the co-factor cytochrome b_5 (cyt b_5), a flavoprotein which facilitates both CYP17A1 and POR (Storbeck et al. 2013).

While cholesterol can be biosynthesized *de novo* from acetate in the endoplasmic reticulum, recruited from intracellular sources, such as cytosolic vacuoles, or recruited from outer cellular circulatory lipoproteins, free cholesterol ($C_{27}H_{46}O$) is derived from cholesterol esters (low-density lipoprotein and high-density lipoprotein) and possess a chemical structure based on the common cyclopentanoperhydrophenanthrene ring structure (You 2004), which is the chemical backbone for all steroid hormones (Fig. 2.2).
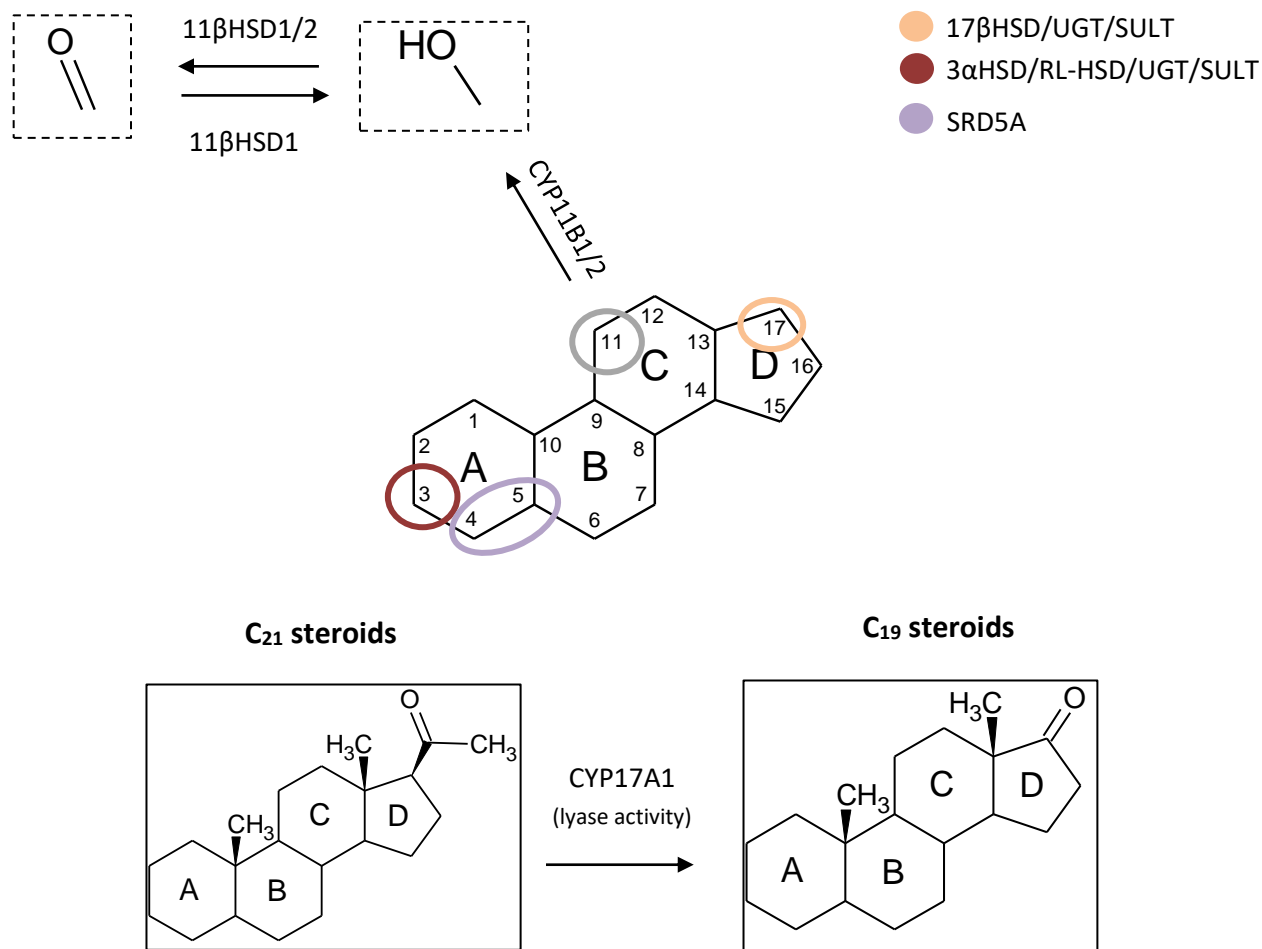
Figure 2.2 Common cyclopentanoperhydrophenanthrene ring structures, representing the carbons whereupon steroidogenic enzymes act. The addition of the hydroxyl group at C11 by CYP11B1/2, the interconversion of the C11-hydroxy and C11-keto group by 11βHSDs, and the conversion of C_{21} to C_{19} steroids catalysed by CYP17A1 are shown.

2.2.1 The production of C11-oxy steroids by cytochrome P450 11β-hydroxylase and aldosterone synthase

While CYP11B1 and CYP11B2 are crucial in the production of cortisol and aldosterone, respectively, these enzymes both biosynthesise C11-oxy C_{19} steroids *in vitro*. However, in the androgen pathway of adrenal steroidogenesis (Fig. 2.1) CYP11B1 would be the enzyme catalysing the hydroxylation at C11.

The production of C11-hydroxy C_{19} steroids catalysed by CYP11B has been reported using recombinant bovine CYP11B (Mathew et al. 1990), guinea pig CYP11B1 and B2 (Bülow et al. 1996; Bülow and Bernhardt 2002) and by human CYP11B1 and B2 (Schloms et al. 2012; Swart et al. 2013). CYP11B1 and B2 are mitochondrial enzymes, which utilize NADPH as an electron donor and transfer an electron via the flavoprotein, adrenodoxin reductase, and subsequently via adrenodoxin, a nonheme iron-sulfur protein, ultimately transferring the electron to the substrate via the P450 heme group, producing the hydroxylated steroid product. Both CYP11B1 and CYP11B2 are able to catalyse the biosynthesis of 11OHA4 and 11OHT from A4 and T, respectively (Fig. 2.1, 2.2). While CYP11B2 is expressed in the ZG only, CYP11B1 has been shown to be expressed in the ZF and the ZR (Gomez-Sanchez et al. 2014). This suggests that CYP11B1 catalyses the C11 hydroxylation of A4 and T in the ZR. Interestingly, CYP11B2 has been shown to convert T to 11OHT more efficiently compared to the hydroxylation of A4 *in vitro* (Swart et al. 2013).

The first report of 11OHA4 was in 1953, when Jeanloz et al. (1953), showed the production of 11OHA4 in bovine adrenal glands following perfusion with A4, while 11OHA4 was also identified as a downstream metabolite of DHEA and A4 by Dorfman (1954), and in human adrenals (Touchstone et al. 1955). Adrenal steroidogenesis in guinea pigs also showed the production of 11OHA4, with its production being increased following ACTH stimulation (Bélanger et al. 1993), suggesting the involvement of the ZF and ZR and the enzymes expressed in these zones. The ACTH dependent increase in 11OHA4 has been shown repeatedly (Bloch et al. 1957; Dyrenfurth et al. 1960; Cohn and Mulrow 1963; Rege et al. 2013), and ACTH has been linked to increased 11β-hydroxylation activity (Kowal 1969; Kowal et al. 1970; Ganguly et al. 1977). While the side-chain cleavage of cortisol by CYP17A1 producing 11OHA4 is plausible, this conversion has not been proven without a doubt and A4

14

remains the main precursor in the production of 11OHA4 in the adrenals. In addition, while the gonadal contribution to the production of 11OHA4 cannot be ruled out, as CYP11B has been shown in the testes, ovaries (Imamichi et al. 2016) and in testicular tumours (Savard et al. 1960; Lipsett et al. 1966), the adrenal remains the primary steroid producing organ in the production of 11OHA4.

Moreover, the hydroxylation of A4 by CYP11B has been shown in H295R adrenocarcinoma cells (Xing et al. 2011; Schloms et al. 2012; Swart et al. 2013) –in the presence of a 3βHSD2 inhibitor, trilostane, 11OHA4 was produced when A4 was assayed and in the presence of a CYP11B1 inhibitor, etomidate, 11OHA4 could not be recovered when A4 was assayed (Schloms et al. 2012). Clearly, 11OHA4 is produced from the CYP11B hydroxylation of A4. The hydroxylation of T has also been reported (Swart et al. 2013), and 11OHT has been detected *in vivo* in adrenal vein samples (Rege et al. 2013), but 11OHT levels were ~300-fold lower than 11OHA4, under stimulated and unstimulated conditions (Rege et al. 2013). Although the expression of 17βHSD type 5 (AKR1C3) has been reported in the adrenals (Rege et al. 2013), the AKR1C3 and 17βHSD type 3 (17βHSD3) catalysed conversion of 11OHA4 to 11OHT does not occur (Storbeck et al. 2013). Furthermore, following the addition of ^{14}[C]T, 11OHT was recovered in adrenal tissue homogenates (Chang et al. 1963), establishing that 11OHT is predominantly produced from T by CYP11B enzymes in the adrenals.

Once 11OHA4 and 11OHT are biosynthesised in the adrenal, 11β-hydroxysteroid dehydrogenase type 2 (11βHSD2) can catalyse the conversion of these C11-hydroxy metabolites to 11keto-androstenedione (11KA4) and 11KT, respectively (Fig. 2.1, 2.2). Indeed, these conversions have been shown *in vitro* in non-steroidogenic cells transfected with 11βHSD2 (Swart et al. 2013) and 11KA4 has been identified in

normal subjects and in patients with diseased adrenals (Goldzieher and Beering 1969). Furthermore, 11KA4 and 11KT were also identified *in vivo* in adrenal vein samples, and although comparable to 11OHT levels, the C11-oxy steroids were much lower than 11OHA4 (Rege et al. 2013). 11βHSD1, which catalyses the reverse reaction of 11βHSD2 (Fig. 2.2), has also been shown to convert 11KA4 and 11KT to 11OHA4 and 11OHT, respectively (Swart et al. 2013). Moreover, 11OHA4, 11OHT, 11KA4 and 11KT were shown to be better substrates for the 11βHSD enzymes than the glucocorticoids, cortisol and cortisone. Once 11KA4 and 11KT are produced in the adrenals, 17βHSDs expressed in the ZR (Rege and Rainey 2012; Rege et al. 2013), interconvert these metabolites, while oxidative 17βHSDs also convert 11OHT to 11OHA4 (Storbeck et al. 2013; Swart et al. 2013) (Fig. 2.1). However, as the adrenals express low levels of 11βHSD2 and 17βHSDs, the adrenal output of 11OHA4 surpasses that of 11OHT, 11KA4 and 11KT, and also that of A4 (Bloch et al. 1957; Rege et al. 2013).

Up until this point the CYP11B enzymes has been discussed in terms of C_{19} steroid substrates (A4 and T), producing C11-oxy C_{19} and C_{21} steroids (DOC, CORT, 18OHCORT and deoxycortisol). These enzymes are, however, also critical in the production of 11-hydroxyprogesterone (11OHPROG) from PROG and 21-deoxycortisol (21-dF) from 17OHPROG (Barnard et al. 2017; Van Rooyen et al. 2017), steroid hormones detected in 21OHD patients which are important in the initial reactions in the backdoor pathway (section 2.3), together with the production of 11,16-diOHPROG from 16OHPROG by CYP11B2 (Van Rooyen et al. 2017).

In circulation, steroids are bound to carrier plasma proteins (>95%), with free unbound steroids being taken up by target tissue, such as the prostate, signifying them biologically active upon binding to receptors (Barahona et al. 1980; Fernlund et al. 1990). In a recent review, Turcu and Auchus (2017),

highlighted that the binding of the C11-oxy C_{19} steroids to plasma proteins, such as sex-hormone binding globulin and albumin, in circulation has, to date, not been elucidated. While it has not been reported how these steroids are transported in circulation, their biosynthesis in and secretion from the adrenals as well as their contribution to the androgen pool through steroid metabolic pathways in the prostate, has been the subject of a number of recent reports.

2.3 Steroid metabolic pathways in the prostate

The testes predominantly contribute to circulatory T under normal condition, however, under castrate conditions, it is the adrenals that provide the C_{19} androgen precursors. Once these androgen precursors are taken up by the prostate, they are efficiently metabolised in the classic-, alternative- and 11OHA4-pathways. Moreover, adrenal C_{21} steroid precursors may also be metabolised in the prostate via the backdoor pathway, given the required enzymes are abundantly expressed. These metabolic pathways will be discussed below.

2.3.1 The classic and alternative pathway to DHT production

Adrenal C_{19} steroid precursors, T (negligible), DHEA and A4 contribute to the production of the potent steroid, DHT, in the classic and alternative pathways in the prostate (Mostaghel 2013). In the classic pathway, once A4 is converted to T by reductive 17βHSDs, 5α-reductase type 1 (SRD5A1) and 5α-reductase type 2 (SRD5A2) converts T to DHT (Russell and Wilson 1994) (Fig. 2.3). A4 either contributes directly to T, or is firstly metabolised from adrenal DHEA, by 3βHSD type 1 (3βHSD1) or 3βHSD2 (Chang et al. 2011). Again, it is worth mentioning that under normal physiological condition, the testes provide T in abundance, which is directly converted to DHT by SRD5As in the prostate. While the classic pathway to DHT production has been recognized as the dominant pathway for decades, the alternative '5α-androstanedione (5αDIONE)' pathway is taking center stage (Auchus 2004;

Luu-The et al. 2008; Miller and Auchus 2011; Chang and Sharifi 2012). In this pathway, DHT is predominantly produced from A4 via 5αDIONE as an intermediate metabolite, and SRD5A1 has been shown to preferentially convert A4 to 5αDIONE rather than T to DHT in CRPC models and in tissue (Thigpen et al. 1993; Chang et al. 2011). Moreover, SRD5A1 silencing hampered the conversion of A4 to 5αDIONE and the ultimate production of DHT in CRPC, suggesting the upregulation of SRD5A1 reported in CRPC would surely increase the flux via the alternative pathway (Chang et al. 2011; Sharifi 2012).
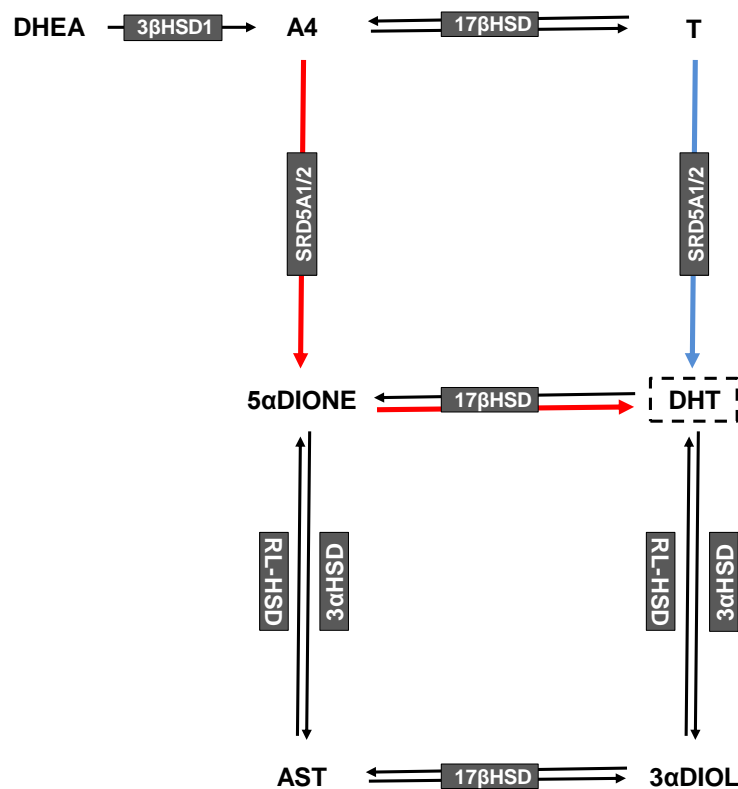
Figure 2.3 The classic- (blue arrow) and alternative (red arrows) pathways leading to the production of DHT from adrenal C_{19} steroid precursors in the prostate (Boxed steroid; potent steroid).

Following its production, DHT can be inactivated to 3αDIOL by 3αHSD enzymes present in the prostate, and while reactivation by RL-HSD enzymes are also possible, DHT may also be conjugated by UGTs and

SULTs. Furthermore, AST, produced from 5αDIONE by 3αHSDs may also be conjugated, together with T and 3αDIOL.

2.3.2 The 11OHA4-pathway to 11KT and 11KDHT production

Adrenal 11OHA4 is metabolised to the potent C11-oxy C_{19} steroids, 11KT and 11KDHT, in the 11OHA4-pathway in the prostate (Fig. 2.4). In addition, as trace amounts of 11OHT, 11KA4 and 11KT are produced in the adrenals, these steroid hormones are also capable of contributing to prostate steroids and 11KT and 11KDHT levels, however, it is generally accepted that 11KA4 and 11KT only contribute to the 11OHA4-pathway once 11OHA4 and 11OHT are metabolised in the prostate (Turcu and Auchus 2017). The following section will describe and summarize the production of the C11-oxy C_{19} steroids from 11OHA4 in the 11OHA4-pathway as has been reported by Bloem et al. (2013), Storbeck et al. (2013) and Swart et al. (2013).

In the prostate, 11βHSD2 is a key enzyme metabolising adrenal 11OHA4 to 11KA4, which initiates the 11OHA4-pathway. The subsequent conversions by reductive 17βHSDs and SRD5As ultimately yields 11KT and 11KDHT, respectively. In transfected non-steroidogenic cells, reductive 17βHSD3 and AKR1C3, have been shown to catalyse the conversion of C11-keto A4-metabolites to C11-keto T-metabolites, while SRD5A1 and SRD5A2 catalyse the production of 11β-hydroxy-5α-androstanedione (11OH-5αDIONE), 11keto-5α-androstanedione (11K-5αDIONE), 11β-hydroxydihydrotestosterone (11OHDHT) and 11KDHT. Furthermore, oxidative 17βHSD type 2 (17βHSD2) catalyses the conversion of 11OHT, 11KT, 11OHDHT, 11KDHT and 11keto-5α-androstane-3α, 17β-diol (11K-3αDIOL) to their respective C11-oxy A4-metabolites, while both 11β-hydroxysteroid dehydrogenase type 1 (11βHSD1) and 11βHSD2 have been revealed to be involved in the interconversions between C11-hydroxy and C11-keto metabolites (Swart and Storbeck 2015). In addition, 11βHSD2 has been shown to be

expressed in LNCaP prostate cells (Page at al. 1994; Dovio et al. 2009), and therefore reported to catalyse the metabolism of 11OHA4 in these cells, while 11βHSD2 has also been shown in prostate tissue (Albiston et al. 1994; Pelletier et al. 2004) Clearly, 11βHSDs, 17βHSDs and SRD5As are essential in the metabolism of adrenal 11OHA4 in the prostate. Furthermore, SRD5A conversions assays have shown that 11OHA4 and 11KA4 are preferentially converted to their 5α-reduced products compared to the T-metabolites, 11KT and 11OHT, comparable to the alternative pathway in DHT production described above. In addition, AKR1C3 has been shown to preferentially convert 11KA4 and 11K-5αDIONE to their T-derivatives, compared to the conversion of A4 to T (Swart and Storbeck, 2015) and, to date, 11OHDHT and 11K-3αDIOL have not been shown to be substrates for 3αHSDs and 11βHSD1, respectively.

Figure 2.4 11OHA4-pathway leading to the production of 11KT and 11KDHT from adrenal 11OHA4 in the prostate (Boxed steroids; potent steroids).

Following its production, 11KDHT can be inactivated to 11K-3αDIOL by 3αHSD enzymes present in the prostate, and while reactivation by RL-HSD enzymes are also possible, 11KDHT may also be conjugated by UGTs and SULTs. Furthermore, 11β-hydroxyandrosterone (11OHAST) and 11keto-androsterone (11KAST), produced by 3αHSDs from 11OH-5αDIONE and 11K-5αDIONE, respectively, may also be conjugated, together with 11OHT, 11KT, 11OHDHT and 11K-3αDIOL. While the adrenals have been described as the primary source of 11OHA4 in circulation, CYP11B1 and CYP11B2 have been shown to

be expressed in human primary prostate and metastatic primary prostate carcinomas (Biancolella et al. 2007; Mitsiades et al. 2012). Therefore, it is possible that within the prostate microenvironment, adrenal A4 and T, together with gonadal T, may be converted to 11OHA4 and 11OHT, respectively.

2.3.3 The backdoor pathway to DHT and 11KDHT production

The backdoor pathway, also termed 'the alternative backdoor pathway', was initially described as the conversion of 3αDIOL to DHT, thereby bypassing T and A4 as precursors and was reported in testes of tammar wallaby pouch young and immature mouse testis by Auchus (2004). In human physiology, the backdoor pathway has been described in 21OHD patients, in which the accumulation of adrenal PROG and 17OHPROG levels leads to androgen excess and specifically to the production of DHT (Kamrath et al. 2012). Since hampered CYP21A2 activity in these patients results in an accumulation in PROG and 17OHPROG levels *in vivo*, SRD5A enzymes are able to convert PROG and 17OHPROG to dihydroprogesterone (DHPROG) and 5α-pregnan-17α-ol-3,20-dione (Pdione), respectively. DHPROG and Pdione are subsequently substrates for 3αHSDs, producing allopregnanolone and 5α-pregnan-3α,17α-diol-20-one (Pdiol), respectively, followed by the lyase activity of CYP17A1 yielding AST (Fig. 2.5). Indeed, Pdiol has been reported to be an excellent substrate for CYP17A1 (Gupta et al. 2003). Ultimately, AST can be converted to DHT, following 3αHSD (RL-HSD) and reductive 17βHSD catalysed reactions (Fig. 2.3 and 2.5). In addition to 21OHD patients, the backdoor pathway may also be active in diseases and adrenal disorders clinically characterized by androgen excess, including PCOS, 3βHSD deficiency and Antley-Bixler syndrome (POR deficiency) (Ghayee and Auchus 2007; Marti et al. 2017).
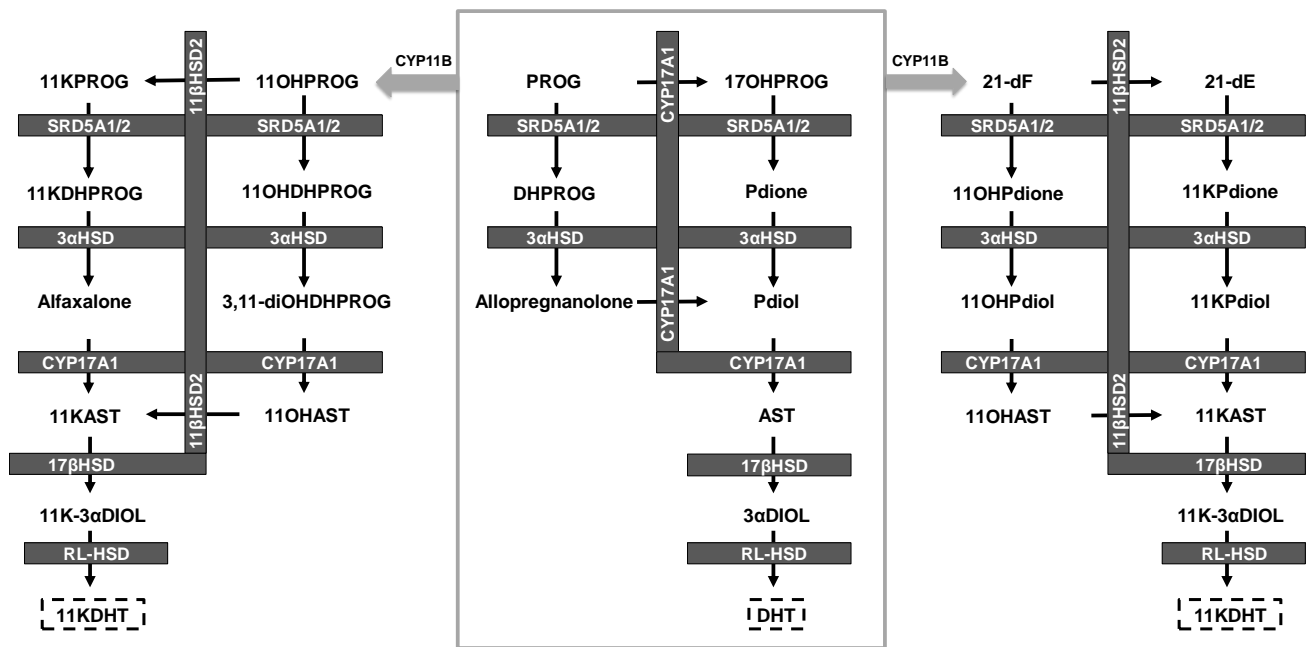
Figure 2.5 Backdoor pathway leading to the production of DHT from PROG and 17OHPROG, and 11KDHT from 11OHPROG, 11KPROG, 21-dF and 21-deoxycortisone (21-dE). (Boxed steroids, potent steroids; boxed pathway, represents the 'classical' backdoor pathway).

As previously mentioned, CYP11B enzymes convert PROG and 17OHPROG to 11OHPROG and 21-dF, respectively. These steroids, together with their 11βHSD2 products 11keto-progesterone (11KPROG) and 21-dE, are also substrates for the SRD5As and as such are able to contribute to the backdoor pathway, yielding 11KDHT (Barnard et al. 2017; Van Rooyen et al. 2017) (Fig. 2.5). Moreover, 16OHPROG has also recently been shown to be a substrate for CYP11B2, with this product (11,16-diOHRPOG) and 16OHPROG itself shown to be substrates for SRD5As *in vitro*. The SRD5A product of 16OHPROG was also in turn a substrate for the catalytic activity of 3αHSD (Van Rooyen et al. 2017). While the backdoor pathway would be active in peripheral tissue that readily express SRD5As (the initial step in these pathways), 3αHSDs and 17βHSDs, the expression of CYP17A1 and 11βHSD2 may not be optimal in peripheral tissue. The adrenals do not express SRD5As (Auchus 2009), although

SRD5A activity has been reported in the fetal adrenal by Hanley and Arlt (2006). The testes and skin also express most of the enzymatic machinery; the testes express SRD5A2 (Flück et al. 2011), together with CYP17A1 and 17βHSD, while skin cells express CYP11B1, CYP17A1, 3βHSD, SDR5A1 and SRD5A2 (Dumont et al. 1992; Thigpen et al. 1993; Slominski et al. 1996d; Thiboutot et al. 2003; Slominski et al. 2004c). Clearly, some target tissue would produce some of the steroids in the backdoor pathways up until point, after which the steroids would be released into circulation, to be taken up by other peripheral target tissue and further metabolised dependent on the expression of enzymes required.

Interestingly, the prostate expresses all the enzymes involved in the backdoor pathway, together with CYP17A1, with mRNA transcripts having been reported in PCa cell lines (Dillard et al. 2008; Locke et al. 2008). Moreover, while *de novo* steroid biosynthesis from cholesterol has been suggested to occur in CRPC (Cai et al. 2011), the topic is controversial as others have reported the negligible contribution of *de novo* biosynthesis compared to the contribution of adrenal precursors to the androgen pool in the prostate (Hofland et al. 2010; Kumagai et al. 2013). Clearly, all the above mentioned pathways are able to metabolise a wide-array of precursor steroids, incorporating these to produce potent androgens within the prostate microenvironment.

2.4 Steroidogenic enzymes involved in steroid metabolic pathways in the prostate

While steroid metabolic pathways can utilize multiple adrenal precursor steroids, including C_{19} and C_{21} adrenal steroids, this thesis will focus mainly on the contribution of 11OHA4 and its metabolites to PCa, which is dependent on the expression of 11βHSDs, 17βHSDs and SRD5As as pre-receptor regulatory enzymes, together with 3αHSDs, RL-HSDs, UGTs and SULTs as post-receptor regulatory enzymes.

The epithelium lining the tube alveoli of the prostate consists of two steroidogenic cell layers adjacently located, namely basal (adjacent to the bloodstream) and luminal cells (above the basal cells). Steroids in circulation are taken up into the basal cells, where after androgen receptor action occurs in the luminal cells. 3βHSDs, 3αHSDs, 17βHSDs, SRD5As and UGTs are expressed in the basal cells, while SRD5As and UGTs are also expressed in the luminal cells, together with the AR (Labrie et al. 2001; Bélanger et al. 2003; Pelletier 2008). Basal cells are, therefore, actively involved in steroid metabolic pathways, while also supplying luminal cells with steroid precursors, and both cells are secretory cells, contributing to steroid conjugates in circulation.

2.4.1 11β-hydroxysteroid dehydrogenases

Traditionally, the role of 11βHSDs have been linked solely to the interconversion of the glucocorticoids, namely cortisol and cortisone, however, their role in the interconversion between C11-hydroxy and C11-keto androgens has recently come under the spotlight (Fig. 2.2). While the keto-metabolite, cortisone, is considered an inactive metabolite in the glucocorticoid pathway, the C11-keto metabolites in the androgen pathway are active steroid hormones, specifically considering 11KT and 11KDHT (section 2.5). The microsomal oxo-reductase, 11βHSD1, is a NADPH-dependent enzyme which converts the C11-keto moiety to a C11-hydroxy moiety (Cooper and Stewart 2009). The required NADPH is supplied by the microsomal NADPH regenerating enzyme, hexose-6-phosphate dehydrogenase (H6PDH), which favours the reductive activity of this enzyme, however, this enzyme also possesses dehydrogenase activity, which catalyses the reverse reaction, converting C11-hydroxy moieties to their C11-keto moieties. *In vivo* conditions, however, favour the oxo-reductase activity of 11βHSD1 and therefore the production of C11-hydroxy metabolites. Conversely, 11βHSD2 possesses only dehydrogenase activity, efficiently converting C11-hydroxy to C11-keto metabolites. Moreover, while

11βHSD2 has been reported to be involved in the production of C11-keto metabolites in the adrenals (Rege et al. 2013) (Fig. 2.1) and has been shown *in vitro* to produce C11-keto derivatives in the 11OHA4-pathway (Swart et al. 2013) (Fig. 2.4), this enzyme is also involved in the biosynthesis of novel C_{21} steroids as precursors to be metabolised in the backdoor pathway (Barnard et al. 2017) (Fig. 2.5). While 11βHSD2 is expressed in prostate tissue, it is also expressed in the adrenals (ZG, ZF, ZR), in addition to the placenta, testis, ovary, skin and kidneys (Miller and Auchus 2011; Mostaghel 2014).

2.4.2 17β-hydroxysteroid dehydrogenases

17βHSDs catalyse the interconversion between C17-hydroxy and C17-keto metabolites, with specific isoforms catalysing the reductive activity, while other isoforms catalyse the dehydrogenase reactions (Fig. 2.2). The isoforms catalysing the reductive activity utilize $NADPH/NADP^+$ as a cofactor, converting C17-keto to C17-hydroxy metabolites, while the dehydrogenases utilize $NAD^+/NADH$ to convert the C17-hydroxy to C17-keto metabolites (Luu-The 2001). The most well characterised reductive 17βHSDs are 17βHSD3 and AKR1C3, whereas 17βHSD2 is a commonly reported oxidative 17βHSD. 17βHSDs are intricately involved in the interconversion between A4 and T (Fig. 2.1, 2.3), as well as 11KA4 and 11KT (Fig. 2.4), with the reductive 17βHSDs catalysing the activation of androgens –both 17βHSD3 and AKR1C3 biosynthesize T and 11KT, with these transcripts, together with 17βHSD2 present in prostate tissue (Dumont et al. 1992; Martel et al. 1992; Akinola et al. 1996). Furthermore, 17βHSD isoforms are also expressed in other peripheral tissue, including the adrenals (in the ZR) and the testis (Dufort et al. 1999; Luu-The 2001; Mostaghel 2014).

2.4.3 5α-reductases

SRD5As reduces the C4-C5 double bond on the steroid backbone structure (Fig. 2.2). This reaction is irreversible and produces potent steroids, such as DHT and 11KDHT, and as such these steroids are

involved in the classic-, alternative-, 11OHA4-, and backdoor pathway (Fig. 2.3, 2.4, 2.5). SRD5As are NADPH-dependent enzymes (Russell and Wilson 1994; Soronen et al. 2004), with three isoforms isolated to date. SRD5A2 is known as the predominant isoform active in normal prostatic physiology, while SRD5A1 has been reported to be increased in PCa (Stanbrough et al. 2006; Chang et al. 2011). Both SRD5A1 and SRD5A2 has been identified to catalyse the production of 5α-reduced metabolites in the 11OHA4-pathway (Storbeck et al. 2013; Swart et al. 2013), however, the ability of the third SRD5A isoform, 5α-reductase type 3 (SRD5A3) (Uemura et al. 2008), to catalyse the production of 5α-reduced C11-oxy C_{19} steroids has, to date, not been clarified. SRD5As are expressed in multiple steroidogenic tissue, including the prostate, ovary, skin, liver and testes (Russell and Wilson 1994; Uemura et al. 2008)

2.4.4 3α-hydroxysteroid dehydrogenases

3αHSDs catalyse the reversible reduction of the C3-keto moiety to a C3-hydroxy moiety, thereby converting active 5α-reduced steroids to inactive 3α-reduced metabolites (Fig. 2.2), utilizing NADP(H) as cofactors (Miller and Auchus 2011). This reduction is considered an inactivation step in prostate steroidogenesis, as these reduced products are less androgenic and serve as potential substrates for elimination from the prostate microenvironment by conjugation. The specific isoform, 3α-hydroxysteroid dehydrogenase type 3 (AKR1C2), has been shown to mediate the inactivation of C_{19} steroids (Penning and Byrns 2009) and is therefore involved in the classic-, alternative- and 11OHA4-pathway (Fig. 2.3, 2.4). In the backdoor pathway (Fig. 2.5), however, AKR1C2 is essential in the conversion of 5α-reduced metabolites to their 3α-reduced products, which demonstrates that in this pathway 3αHSD catalyses an important step that is required for the conversion of adrenal C_{21} steroid precursors to active steroids (DHT and 11KDHT).

Interestingly, 3α-hydroxysteroid dehydrogenase type 4 (AKR1C1), a 20α(3β)-hydroxysteroid dehydrogenase, results in the formation of a β-hydroxyl moiety at C3 of C_{19} steroids, including 5α-androstane-3β-17β-diol (3βDIOL) and epiandrosterone (epiAST). AKR1C1 also has marginal 3αHSD activity and may therefore function as a 3α/β- and 20α-HSD (Steckelbroeck et al. 2003; Penning and Byrns 2009). However, in the prostate microenvironment, AKR1C2 would predominantly produce 3α-conformational steroids and AKR1C1 would produce 3β-conformational steroids (Penning et al. 2000). Moreover, although AKR1C3 has been discussed as a 17βHSD enzyme, AKR1C3 may also function as a 3α/3β-HSD, producing 3αDIOL (2.7 nmoles product/min/mg protein) and 3βDIOL (2.0 nmoles product/min/mg protein) (Penning and Byrns 2009). Clearly, HSD enzymes possess dual activities, and the preferred activity will depend on co-factor and steroid substrate availability, in addition to the stage of PCa development. While the role of C3β-hydroxy steroids in PCa still needs to be clarified, these metabolites may contribute to downstream physiological effects, such as AR or estrogen receptor (ER) binding. For instance, 3βDIOL has been shown to bind the ERβ, and was identified as a proapoptotic ligand which regulates growth in the prostate (Muthusamy et al. 2011).

2.4.5 Retinol-like hydroxysteroid dehydrogenases

RL-HSD enzymes catalyse the oxidation of the 3α-reduced steroids (Fig. 2.2), utilizing NAD(H) as cofactors (Miller and Auchus 2011). These enzymes are sometimes referred to as 3αHSDs, however, literature does distinguish between the reductive and dehydrogenase activities, while certain enzyme isoforms also possess dual activities. For this thesis, RL-HSDs functions by converting a C3-hydroxy moiety to a C3-keto moiety, thereby once again providing potent steroids to the androgen pool, in the classic-, alternative-, 11OHA4-, and backdoor pathways (Fig. 2.3, 2.4, 2.5).

Importantly, 17βHSD type 6 (17βHSD6) functions as a 3α/β-HSD (moderate activity), but more predominantly as a RL-HSD, converting 3αDIOL to DHT (Miller and Auchus 2011). 17βHSD6, also known as retinol dehydrogenase-like 3α-hydroxysteroid dehydrogenase, has also been shown to convert DHT to 3βDIOL (3-ketoreductase/3β-hydroxysteroid dehydrogenase activity), which activates the ERβ. Interestingly, in BPH 17βHSD6 and ERβ were co-expressed, while expression of both proteins was lost in PCa (Muthusamy et al. 2011). Moreover, in the presence of both DHT and 3αDIOL and 17βHSD6, ERβ activation was increased, suggesting 17βHSD6 has dual activity whereby both DHT (3βHSD activity) and 3αDIOL (3α→β epimerization activity) are converted to 3βDIOL (Muthusamy et al. 2011). This has also been shown for 5αDIONE, whereby a 3(α→β) hydroxysteroid epimerase (HSE) converted 5αDIONE to epiAST, while also metabolising AST to epiAST, however, this enzyme also converts epiAST to AST (<20% activity) (Huang et al. 2000). In addition, the conversion of 3αDIOL to DHT by 17βHSD6 (RL-HSD activity) has been reported (Biswas 1997; Bauman et al. 2006), as well as the RL-HSD conversion of AST to 5αDIONE (Belyaeva et al. 2007), further contributing to the complexities of steroidogenesis in the prostate. This enzyme may be a regulatory enzyme, especially in the context of C11-oxy C_{19} and C11-oxy C_{21} steroids, that requires further investigation. The C11-oxy C_{19} steroids with 3β-conformations, such as 5α-androstan-3β,11β-diol-17-one (11OH-epiAST), 5α-androstan-3β-ol-11,17-dione (11K-epiAST) and 11keto-5α-androstane-3β, 17β-diol (11K-3βDIOL) have not been shown to be produced *in vitro* by enzymatic conversions, neither have their levels been reported *in vivo* or their AR and ERβ activation been described. Furthermore, literature reports 3βDIOL levels to be increased 5-fold compared to 3αDIOL in the prostate (Bélanger et al. 1990; Matthews et al. 2006), and epiT (17α-epimer of T) has been shown in plasma (Starka et al. 1997) and to be increased in PCa tissue compared to BPH tissue (Heracek et al. 2007), while epiAST is not a

preferred substrate for UGT-conjugation (Beaulieu et al. 1996) –clearly indicating a role for epi-steroids in PCa.

2.4.6 Uridine-diphosphate glucuronosyltransferases

Once C_{19} steroids are reduced by 17βHSDs and 3αHSDs, UGT enzymes conjugate the C17 β- and C3 α-hydroxy groups by glucuronidation and thereby terminates the steroid signal (Fig. 2.2) These conversions are irreversible and requires the regenerating system which converts uridine diphosphate (UDP) glucose to UDP glucuronic acid by UDP glucose-6-dehydrogenase (Fig. 2.6). This system provides UDP glucuronic acid to the UGT enzymes, which subsequently adds the glucuronide group to the oxygen moiety on the steroid chemical backbone, and releases a hydrogen atom and UDP as products, together with the steroid glucuronide. While two superfamilies of UGTs exist, UGT1 and UGT2, this thesis focusses on the UGT2 family, which in turn is subdivided into UGT2A and UGT2B families. UGT2A enzymes are linked to the olfactory epithelium (Lazard et al. 1991), while UGT2Bs are expressed in the prostate and conjugate C_{19} steroids, phenols and fatty acids (Beaulieu et al. 1996). The UGT2B enzymes are expressed in the basal and luminal cells of the prostate, thereby regulating the potency of active steroids in both cell layers and, following glucuronidation, increases the water-solubility of the steroids, thereby facilitating their secretion from the cells (Tukey and Strassburg 2000). UGT steroid substrates in the classic- and alternative pathways include T, DHT, AST and 3αDIOL (Fig. 2.3) (Bélanger et al. 2003; Chouinard et al. 2007; Byrns et al. 2012), while potential substrates in the 11OHA4-pathway include; 11OHT, 11KT, 11OHDHT, 11KDHT, 11OHAST, 11KAST and 11K-3αDIOL (Fig. 2.4). In the backdoor pathway DHT, 11K-3αDIOL, 11KDHT, in addition to their 3αHSD products AST, 3αDIOL, 11KAST and 11OHAST are potential substrates for UGT2B enzymes (Fig. 2.5). Three

isoforms of UGT2B enzymes are present in the prostate: UGT2B type 15 (UGT2B15), UGT2B type 17 (UGT2B17) and UGT2B type 28 (UGT2B28), and are discussed in detail in chapter 3.
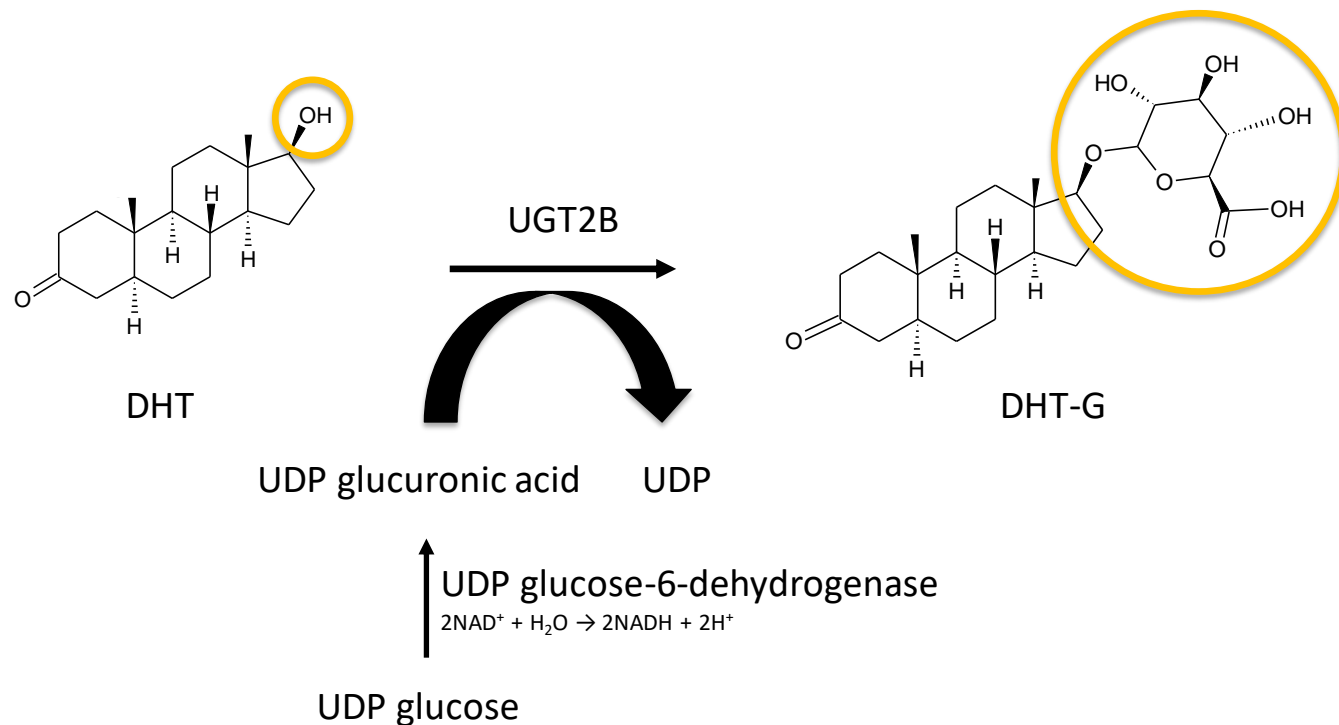
Figure 2.6 Regeneration system for the UGT2B catalysed reaction of DHT to DHT-glucuronide (DHT-G).

While literature has extensively explored the glucuronidation of C_{19} steroids, the glucuronidation of C11-oxy C_{19} has not been described. It has, however, been suggested that UGT2B17 is able to glucuronidate 11OHAST and AST, but that the presence of the C11α/β hydroxy group may interfere with the conjugation of these C_{19} steroids (Beaulieu et al. 1996), with impeded glucuronidation of the C11-oxy C_{19} steroids contributing to the potency of these steroids.

2.4.7 Sulfotransferases and sulfatases

It was previously discussed that SULT and STS enzymes are involved in adrenal steroidogenesis, regulating the conjugation of DHEA (Fig. 2.1). These enzymes are, however, also present in the prostate

31

and conjugate other C_{19} steroids. Cytosolic SULTs that conjugate steroids include, SULT2A1 and SULT2B1a and SULT2B1b, and while SULT2A1 is the predominant form in the adrenals, the expression of SULT2B1b is greater than SULT2B1a in the prostate (Geese and Raftogianis 2011). PREG, 17OHPREG, AST, DHEA and androstenediol are substrates for SULT2A1, PREG for SUL2B1a and cholesterol for SULT2B1b (Mueller et al. 2015). These SULT enzymes requires a sulfate supplied by 3'-phosphoadenosine-5'-phosphosulfate (PAPS), which is biosynthesized from ATP by PAPS synthase 1 and 2 (PAPSS1, PAPSS2) (Strott 2002), to conjugate hydrophobic steroids (Fig. 2.7). Notably, the sulfation of steroids is a reversible reaction, with the back reaction catalysed by membrane-bound microsomal STS, thereby providing androgens to the steroid pool in peripheral tissue. STS catalyses the hydrolysis of steroid sulfates, such as DHEA-S, PREG-sulfate (PREG-S) and cholesterol-sulfate (Mueller et al 2015) and is expressed in normal (Farnsworth 1973) and cancerous prostate tissue (Nakamura et al. 2006), while also being expressed in LNCaP cells (Day et al. 2009).
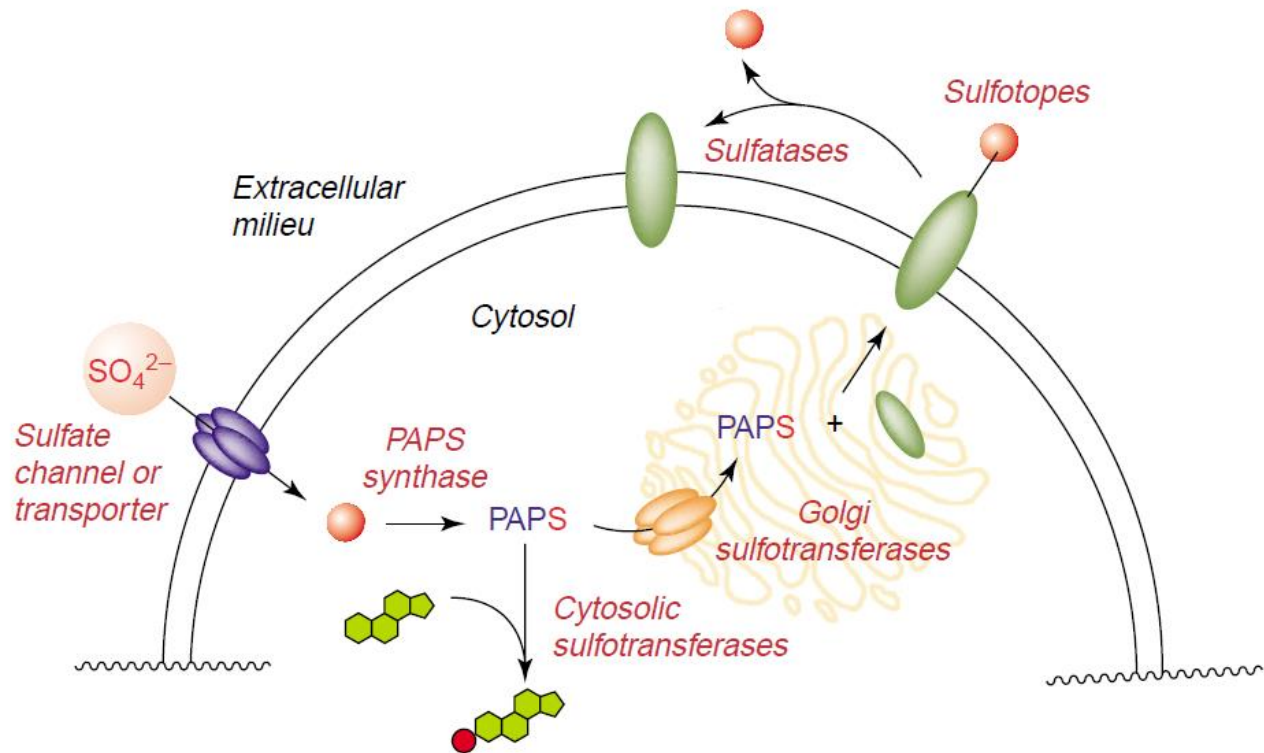
Figure 2.7 Sulfation cycle representing the transfer of sulfate through sulfate channels, enzyme activity of PAPSS and the ultimate sulfation of the steroid backbone structure. Reproduced from Hemmerich et al. 2004.

Interestingly, upregulation and downregulation of sulfation has been linked to diseases: in 21OHD, DHEA and DHEA-S levels have been shown to be reduced, while PREG-S levels were reported to be higher (Turcu et al. 2016); in PCOS, high DHEA and DHEA-S levels have been reported, while impaired DHEA sulfation due to PAPSS2 deficiency has been shown in a PCOS patient (Noordam et al. 2009); in adrenarche, DHEA-S levels have been shown to be elevated and is therefore considered a biomarker for this occurrence. In the latter scenario circulatory 11OHA4 has also been shown to be involved, increasing from 2.5 to 6.4 nM during childhood in boys and girls (Holownia et al. 1992). Clearly, C11-oxy C_{19} steroids and their sulfation and desulfation may be important in adrenarche, in addition to their potential influence in clinical conditions such as 21OHD, PCOS and PCa.

The steroid metabolic pathways and steroidogenic enzymes involved in these pathways, as discussed above, are active in prostate cell models, such as PNT2, BPH-1, LNCaP, C4-2B and VCaP, which were cell models used to conduct the studies presented in this thesis. These cell models are excellent for studying prostate enzymatic conversions involved in the metabolism of C_{19} and C11-oxy C_{19} steroids, as these cells express both pre-receptor and post-receptor regulatory enzymes. Chapters 3 and 4 will include data relating to LNCaP metabolic pathways, while Chapter 3 will also discuss metabolic pathways in PNT2, VCaP and C4-2B cells and Chapter 5 will discuss metabolic pathways in BPH-1 cells. PNT2 prostate epithelial cells are derived from normal human prostatic epithelium and have been immortalized (Cussenot 1991), however, while they have retained most of the characteristics of normal epithelial cells and are non-tumorigenic, PCa related genetic alterations are also present in these cells (Berthon 1995; Blanchere et al 1998). The BPH-1 prostate epithelial cells are androgen-independent and non-tumorigenic, originating from human prostate tissue obtained by transurethral resection and subsequently primary cell cultures from a male which displayed a BPH phenotype (Hayward 1995). LNCaP prostate cancer epithelial cells are hormone-dependent, show low tumorgenicity and originated from a supraclavicular lymph node metastasis (Horoszewicz et al. 1983), while VCaP prostate cancer cells are androgen dependent, non-tumorigenic and derived from a vertebral metastasis in a patient representing an advanced PCa and a castrate resistant phenotype (Korenchuk et al. 2001). C4-2B prostate cancer cells are androgen-independent, represented as 'androgen ablation resistance' and highly tumorigenic with CRPC characteristics. Interestingly, C4-2B cells are derived from bone metastatic tumours maintained in intact athymic male mice, which originated from LNCaP cells (Thalmann et al. 2000).

2.5 C11-oxy C$_{19}$ steroids and their implications in disease

Adrenal C11-oxy C$_{19}$ steroids, once secreted, would have implications in peripheral target tissue, while C11-oxy C$_{19}$ steroids produced within peripheral tissue will also have downstream effects. In this regard, the androgenicity of steroid hormones are important, as most physiological effects are mediated through receptors, and intraprostatic androgenicity are specifically mediated through the AR. As pre-receptor and post-receptor regulations are in place in the prostate microenvironment, there is a balance maintained between these two mechanisms, regulating the availability of AR agonists. When this balance is, however, perturbed, AR agonists are produced in abundance causing cellular effects implicated in the initiation and development of PCa, and the progression to CRPC.

2.5.1 Androgen receptor action

The AR protein is expressed in the nuclei of luminal cells of the prostate epithelium and is a member of the steroid hormone receptor family of ligand-activated nuclear transcription factors (Labrie et al. 2001; Pelletier 2008). In the cytoplasm of the luminal cells, the AR is inactive and unliganded, although attached to heat shock proteins (HSPs) which stabilize their tertiary structure (Smith and Toft 1993). Once the AR binds its ligand, it disassociates from the HSPs, dimerizes with other ARs, undergoes phosphorylation and translocates into the nucleus (McEwan 2000; Prins 2000). Thereafter, the AR-ligand complex binds DNA, followed by the recruitment of transcriptional- and co-factors, in order to activate genetic pathways (Habib 2004). The androgenicity of steroid hormones are, therefore, determined by the binding and activation of the AR, the induction of AR regulated gene expression, and cell proliferative effects, with DHT deemed the most potent AR ligand and, preferentially to T, binds the AR.

To date, the transactivation of the AR by the C11-oxy C_{19} steroids has been shown (Yazawa et al. 2008; Rege et al. 2013; Storbeck et al. 2013; Campana et al. 2016), in addition to the binding of the C11-oxy C_{19} steroids to the human AR (Pretorius et al. 2016) (Table 2.1). While the androgenicity of 11OHA4 was determined to be negligible since the 1960s already (Rosemberg et al. 1958; Dorfman et al. 1966), other authors have also confirmed that 11OHA4 is non-androgenic (Rege et al. 2013; Storbeck et al. 2013; Campana et al. 2016), however, the C11 keto metabolite, 11KA4, has been shown to have similar, albeit low, androgenicity compared to A4 (Rege et al. 2013; Campana et al. 2016). Considering the T-metabolites, 11KT and T exhibit comparable androgenicity, while the androgenicity of 11OHT was 2-fold lower than that of T and 11KT. Furthermore, 11KDHT showed androgenicity comparable to DHT, at 1 nM, while 11OHDHT was not as potent as DHT (Storbeck et al. 2013). It was, however, shown at 10 nM that 11OHT, 11OHDHT, 11KT and 11KDHT activate the AR comparable to DHT (Bloem et al. 2015). Furthermore, the induction of AR regulated gene expression in LNCaP cells, which express a mutated AR (Veldscholte et al. 1990), was shown, suggesting the C11-oxy C_{19} steroids also bind this mutant, while the induction of AR regulated genes by C11-oxy C_{19} steroids were also shown in VCaP cells, which express the wild-type AR. Importantly, the authors concluded that 11KT and 11KDHT are equipotent steroids compared to T and DHT, respectively (Pretorius et al. 2016).

Table 2.1 Androgenicity of C11-oxy C_{19} steroids indicated by AR binding, AR activation, induction of AR-regulated genes and cell proliferative effects. Comparing 11KDHT and 11OHDHT to DHT, and 11KT and 11OHT to T.

		11KDHT	11OHDHT	11KT	11OHT
Whole cell binding assays	*wild-type* hAR[a]	√ =	-	√ =	-
Transactivation assays (hAR)	at 1 nM[b]	√ =	√ <	√ =	√ <
	at 10 nM[c]	√ =	√ =	√ =	√ =
	at 100 nM[d]	-	-	√ =	√ <
Cell proliferation assays (at 1 nM)	In LNCaP cells[a]	√ >	-	√ >	-
	In VCaP cells[a]	√ =	-	√ =	-
Induction of AR-regulated gene expression (In LNCaP cells at 1 nM)	*KLK3*[a]	√	-	√	-
	TMPRSS2[a]	√	-	√ > (p=0.052)	-
	FKBP5[a]	√	-	√ > (p<0.05)	-

[a]Data from (Pretorius et al. 2016); [b]Data from (Storbeck et al. 2013); [c]Data from (Bloem et al. 2015); [d]Data from (Rege et al. 2013); -, steroid not included in the assay; =, equal comparison; > compared more efficient; < compared less efficient

The intraprostatic androgenicity of the C11-oxy C_{19} steroids is evident, clearly showing that the C11-oxy C_{19} steroids, 11KT and 11KDHT, are potent steroids and their androgenic activity comparable to that of C_{19} steroids. In PCa, the activation of the AR is integral to disease progression, positioning 11KT and 11KDHT as role players in PCa and CRPC.

2.5.2 Castration-resistant prostate cancer

While PCa is driven by gonadal T, with the contribution of adrenal steroid hormones to the uncastrated prostate microenvironment being minimal, CRPC is driven by adrenal androgens, including the C_{19}, C11-oxy C_{19}, C_{21} and C11-oxy C_{21} steroids. The difference between PCa and CRPC is not only the

different origins of precursor steroids and the aggressiveness of the disease, but also the expression of steroidogenic enzymes which is altered, in addition to the presence of mutated ARs. In terms of the AR, mutations in the ligand binding domain produces mutated AR variants that bind promiscuously or which are constitutively active (Mohler et al. 2004), in addition to reduced AR specificity and AR gene amplifications, with the latter reported in one third of the cases (Taplin et al. 1995; Holzbeierlein et al. 2004). Furthermore, ligand-independent activation of AR signalling pathways may also occur. In terms of steroidogenic enzymes, subcellular localization may change, in addition to post-translational changes, while the availability of cofactors may impede activity, leading to a preference for the binding of alternative steroid substrates (Mizrachi and Auchus 2009; Sharifi 2012; Sharifi and Auchus 2012).

While both 3βHSD1 and 3βHSD2 expression is increased in CRPC, 3βHSD1 is also 10-fold more efficient than 3βHSD2 in the production of Δ^4 androgens (Miller and Auchus 2011). In addition, SRD5A1 has been shown to be increased in PCa and CRPC (Titus et al. 2005; Stanbrough et al. 2006; Montgomery et al. 2008), together with SRD5A3 (Uemura et al. 2008; Titus and Mohler 2009; Godoy et al. 2011; Azzouni et al. 2012; Mitsiades et al 2012). Up-regulation of AKR1C3 has also been shown in PCa and CRPC (Lin et al. 2004; Fung et al. 2006; Penning et al. 2006; Stanbrough et al. 2006; Luu-The et al. 2008; Montgomery et al. 2008; Mitsiades et al. 2012), while increased 17βHSD3 and decreased 17βHSD2 expression has also been reported (Koh et al. 2002). While the above mentioned enzymes would biosynthesize active androgens, the expression of UGT2B17 is increased in PCa, compared to BPH (Paquet et al. 2012), while UGT2B15 is also increased in androgen-independent PCa (Stanbrough et al. 2006), and in CRPC (Mostaghel 2013), suggesting alterations also occur to counter the increase in steroid production. The aforementioned AR mutations and enzymatic changes,

38

however, represents the adaptations prostate cells undergo to survive, producing a cancerous growth, and in the case of CRPC, shows high fatality with an average survival of only 1-2 years in these patients (Ross et al. 2008).

2.5.3 Treatments regimens in PCa and CRPC

Prior to discussing treatment options with patients, PCa needs to be accurately diagnosed. Diagnosis is based upon clinical and histological parameters. While histological data will accurately diagnose PCa, this is an invasive biopsy which has a high morbidity and mortality rate, showing minor and major complications, in 69.7 % and 1-3% in patients, respectively. Clinical data instead includes a digital rectal examination supported by imaging evidence of cancerous growth, in addition to determining prostate-specific antigen (PSA) circulatory levels. Clinical evidence is less invasive with lower risk of infections, and while it has its own pitfalls, as PSA determination results in false positives, PSA is still correlated to PCa risk and diagnosis of PCa based on clinical data is still considered the better option, as well as being cost effective. Following diagnosis, surgery and radiation is suggested as treatment options. If, however, prognosis shows the continued increase in PCa risk, denoted by Gleason scoring, tumour stage and PSA levels, bilateral orchiectomy (BO) is suggested as the first line of androgen-deprivation therapy (ADT) treatment, reported in 56.2% cases as the treatment option employed (Heyns et al. 2014). While physical castration through BO is a once-off treatment and is the more cost-effective option, chemical castration requires medication to be taken regularly, together with monthly payments, with patient compliances adding to the complications of this form of ADT (Mariani et al. 2001; Heyns et al. 2014). It is worth mentioning that the hypothalamus-pituitary-gonadal axis is involved in testicular steroidogenesis, and works through pulses of gonadotropin-releasing hormone (GnRH) released by the hypothalamus, which in turn stimulates

the pituitary gland to release luteinizing hormones (LH), which ultimately stimulate the testis to produce T. T in turn has a negative feedback mechanism on the hypothalamus and the pituitary to suppress T production. Chemical castration, therefore, involves the intake of GnRH antagonists such as degarelix, which blocks the GnRH receptor and the release of LH or long-acting GnRH/LH-releasing hormones (LHRH) agonists, such as leuprolide acetate and goserelin, which continues the stimulation of GnRH, and over time desensitization occurs, and as such less LH is released and T produced (Tolis et al. 1982). Interestingly, physical and chemical castration have been shown to be equally effective, with relapse also being similar. The measurement of PSA levels is routinely employed to assess the relapse, which is expected within 48 months up until 16 years (Heyns et al. 2014).

Biochemically CRPC has adapted to survive, even after ADT treatment, and therefore necessitates the need for targeted enzymatic treatments. Indeed, steroidogenic enzymes involved in prostate metabolic pathways are currently being targeted. CYP17A1 inhibition, by abiraterone acetate, has been shown to be effective in PCa patients (Attard et al. 2009). As CYP17A1 is a branch point in adrenal steroidogenesis, in the production of mineralocorticoids, glucocorticoids and androgens (Fig. 2.1), this treatment is, however, not without its disadvantages. With CYP17 inhibition, less C_{21} steroids are shunted into the androgen pathway, which in turn leads to the accumulation of precursor steroids, metabolised to mineralocorticoids and glucocorticoids. Patients on abiraterone treatment therefore need to be monitored for mineralocorticoid excess and a potential increase in cardiovascular risk (Pia et al. 2013). Other enzymes for targeted inhibition are SRD5As, with dutasteride and finasteride shown to be successful pharmaceutical compounds, and while dutasteride inhibits both SRD5A1 and SRD5A2, finasteride only inhibits SRD5A2 (Luo et al. 2003; Shah et al. 2009). The inhibition of SRD5A is a more specific target than the inhibition of CYP17A1, as SRD5A is directly involved in the production of

40

DHT, however, dutasteride and finasteride do not block SRD5A3, suggesting this isoform is a potential target to be explored. The inhibition of CYP17A1 and SRD5As as monotherapies, or in combination, would decrease the influence of adrenal steroids in CRPC, as SRD5As are involved in the classic-, alternative-, 11OHA4- and backdoor pathways, while CYP17A1 is also required for the backdoor pathway. Furthermore, the inhibition of AKR1C3 may also be a potential target. Inhibiting this enzyme would reduce the adrenal and peripheral production of active androgens, such as T and 11KT, together with depriving the AR of a co-activator (Yepuru et al. 2013). AKR1C3 inhibition would, however, only limit the alternative-, 11OHA4- and backdoor pathways, but the classic pathway would still contribute to intraprostatic DHT levels from T as a precursor steroid. Under castrated conditions, however, minimal T is produced by the adrenal which highlights AKR1C3 as a viable enzymatic target specifically in CRPC. Two additional enzymatic targets are 3βHSD1 and STS. While the inhibition of 3βHSD1 would limit the contribution of DHEA to the intraprostatic androgen pool as the conversion of DHEA to A4 is inhibited, this treatment should be specific to this isoform as the inhibition of 3βHSD2 would also influence the mineralocorticoid and glucocorticoid pathways (Fig. 2.1). Inhibition of STS would limit the contribution of DHEA-S, together with other steroid sulfates, to the androgen pool, however, inhibiting STS would limit the production of cholesterol from cholesterol sulfate, ultimately obstructing steroidogenesis (Penning 2014).

While the addition of hormones seems an unlikely treatment option, the use of exogenous steroid hormones has been employed in PCa patients, notably, estrogens (diethyl stilbestrol) and progestins (synthetic progesterones). Both these compounds activate the negative feedback of the hypothalamus thereby reducing GnRH and LH pulses. These compounds have the advantage of not activating the AR, however, side effects have been reported, including gynecomastia and thromboembolism. Clinically,

the use of GnRH/LHRH analogues are, therefore, favoured above the use of these exogenous hormones (Sharifi and Auchus 2012).

Another treatment regime in PCa patients is the use of AR antagonists, which are compounds that bind the AR and renders the AR non-functional. These compounds include; flutamide, bicalutamide, nilutamide and enzalutamide (Tran et al. 2009). This form of treatment, however, has a high occurrence of resistance, as the AR mutates or binds ligands promiscuously, while the AR may also be constitutively active without ligand binding. In addition, bicalutamide has been reported to act as an antagonist of the AR, while over time, under androgen ablation, bicalutamide becomes a AR agonist (Culig et al. 1999).

While the above mentioned treatment regimens have advantages and disadvantages as individual treatments, the combination of these treatments may be the most advantageous in PCa and CRPC patients. For instance, abiraterone treatment in combination with prednisone, a synthetic glucocorticoid receptor agonist which suppresses CRH and ACTH release, has shown potential in CRPC treatment approaches (Ryan et al. 2013; Rathkopf et al. 2014). The combination of abiraterone and enzalutamide has also been employed, however, the combination treatment did not deter relapse of the cancer, and requires further investigation (Loriot et al. 2013; Noonan et al. 2013; Bianchini et al. 2014; Schrader et al. 2014).

2.6 Summary

From this chapter it is clear that adrenal steroidogenesis contributes an important adrenal androgen to the androgen pool, namely 11OHA4. Adrenal 11OHA4 is a key precursor steroid which is metabolised in the 11OHA4-pathway, producing potent steroids, 11KT and 11KDHT, that bind and activate the AR,

while also upregulating AR regulated genes –pinpointing these C11-oxy steroids as crucial role-players in CRPC. In the clinical setting, however, the C11-oxy C_{19} steroids have not, to date, been considered in the diagnosis of PCa or prognostic scoring of PCa patients, nor are these steroid levels determined *in vivo* to assess treatment efficacy. The aim of this thesis is to establish the metabolism of the C11-oxy C_{19} steroids in PCa in the research setting, with potential implications in the clinical setting.

While the pre-receptor metabolism and receptor action of C11-oxy C_{19} steroids have been investigated, the inactivation and glucuronidation of these steroids have not been described. Of particular interest for this PhD study is to ascertain whether the glucuronidation of the C11-oxy C_{19} steroids is hampered when compared to the C_{19} steroids. Furthermore, the presence of the C11-oxy C_{19} steroid *in vivo* have also not been described nor has the metabolism of these steroids been investigated in normal prostate cells. In the next chapter, presented in the form of three published manuscripts, the investigation into the inactivation and glucuronidation of the C11-oxy C_{19} steroids, and their presence in plasma and tissue, together with their metabolism in different prostate cell models, will be discussed.

Chapter 3

Published Manuscripts

3.1 Introduction

Adrenal C_{19} steroids serve as precursors to active androgens once metabolized in peripheral tissue, such as the prostate. One such is 11OHA4 which was discovered in the 1950's (Jeanloz et al. 1953; Dorfman 1954; Touchstone et al. 1955; Masuda 1957; Goldzieher and Beering 1969), but considered an inactive androgen with no specific physiological role (Dorfman et al. 1966). Our group has shown that adrenal 11OHA4 and 11OHT are metabolized to potent AR agonists, 11KT and 11KDHT, the latter as potent as DHT at 1 nM (Bloem et al. 2013; Storbeck et al. 2013; Swart et al. 2013). The rediscovery of 11OHA4 and the identification of androgenic downstream metabolites has brought about a new perspective on adrenal C11-oxy C_{19} steroids and their contribution to PCa. In this regard our laboratory has identified novel enzymatic pathways in the metabolism of 11OHA4 and 11OHT and their metabolites, with these C11 hydroxy- and C11 keto C_{19} steroids also being produced in prostate cells (Bloem et al. 2013; Storbeck et al. 2013; Swart et al. 2013). Although many advances have been made in elucidating the downstream metabolism of 11OHA4 and its metabolites in PCa, further research was undertaken regarding this adrenal steroid. The aim of this section of the thesis was therefore to present recent reports undertaken in the PhD study identifying and quantifying C_{19} steroids and their C11-oxy derivatives *in vitro*, in prostate cell models and *in vivo*, in prostate tissue and plasma using the state-of-the-art UPC^2-MS/MS technology. Firstly, a review is presented on UGT2B enzymes which regulate active androgen levels by conjugating androgens and terminating their physiological signal. A specific perspective is given on the UGT2B28 isoform which has been attributed a role in the

44

progression of PCa, as its expression in tissue has been correlated with conjugated steroid levels, PSA levels, Gleason scoring and PCa risk. The glucuronidation of C_{19} and C11-oxy C_{19} steroids was subsequently investigated in PCa cell models that endogenously express UGT isoforms –in LNCaP cells, together with C4-2B and VCaP cells. In addition, the metabolism of C11-oxy C_{19} steroids in normal PNT2 prostate cells are shown, as well as their metabolism in LNCaP, C4-2B and VCaP cells. Furthermore, the inactivation and reactivation of the C_{19} steroid, DHT, and the C11-oxy C_{19} steroid, 11KDHT, are highlighted. UPC^2-MS/MS analysis also allowed for the quantification, at nM level, of C11 hydroxy- and C11 keto C_{19} steroids in PCa tissue and human plasma obtained from PCa patients. *In vivo* circulating glucuronide levels were also determined in PCa patients and compared to normal levels. These studies are presented in the three manuscripts included in this chapter.[1]

---

[1]Author contributions to the manuscript entitled *Profiling adrenal 11β-hydroxyandrostenedione metabolites in prostate cancer cells, tissue and plasma: UPC^2-MS/MS quantification of 11β-hydroxytestosterone, 11keto-testosterone and 11keto-dihydrotestosterone*: LMB generated and supplied the data presented in Fig. 6A and B and added minor corrections to the final draft of the manuscript; JLQ advised with UPC^2-MS/MS method development and validation; RE contributed towards the data presented in Fig.8 in the analysis of 11KDHT only; AMS supplied tissue and plasma samples.

Perspective

Perspective on the regulatory role of UGT2B28 as a conjugating enzyme in the progression of prostate cancer

Therina du Toit, Amanda C. Swart

Department of Biochemistry, Stellenbosch University, Stellenbosch 7600, South Africa

Correspondence to: Amanda C. Swart. Department of Biochemistry, Stellenbosch University, Private Bag X1, Matieland, 7602, South Africa. Email: acswart@sun.ac.za.

Provenance: This is an invited Perspective commissioned by Section Editor Peng Zhang (Department of Urology, Union Hospital, Tongji Medical College, Huazhong University of Science and Technology, Wuhan, China).

Comment on: Belledant A, Hovington H, Garcia L, *et al.* The UGT2B28 Sex-steroid Inactivation Pathway Is a Regulator of Steroidogenesis and Modifies the Risk of Prostate Cancer Progression. Eur Urol 2016;69:601-9.

Abstract: The maintenance of steroid homeostasis in the prostate is critical, with perturbation of steroidogenesis contributing to the modulation of active ligands in the androgen pool. In this scenario, enzymes catalysing the biosynthesis, inactivation and conjugation of steroids are the key players, regulating active ligand levels and in so doing, the activation of the androgen receptor (AR). The glucuronidation of potent ligands renders them unable to bind the AR, allowing the secretion of conjugated steroids. Uridine diphosphate glucuronosyltransferase 2B type 28 (UGT2B28), one of the UGT enzymes catalyzing the glucuronidation of androgens, has recently been given a prominent role in the regulation of prostate steroidogenesis—one which stands in contrast to the accepted dogma that lower androgen levels resulting from increased conjugation are associated with decreased prostate cancer (PCa) risk and disease progression. Increased DHT and its precursors, T and androstenediol, were reported to be associated with increased UGT2B28 tumor expression levels, linked to lower PSA levels but higher Gleason scores and increased PCa risk. In addition, the complete deletion of UGT2B28, was associated with decreased T, DHT and glucuronide derivatives when compared to patients carrying both alleles. UGT2B28 is encoded by a single gene giving rise to UGT2B28 type I which catalyses androgen glucuronidation and, due to alternative splicing, also produces two distinct transcripts, UGT2B28 type II and III. Type II with its premature stop codon, is devoid of the cofactor binding domain while type III is devoid of the substrate binding domain, both catalytically inactive, truncated proteins. Increased UGT2B28 mRNA expression was reported in primary tumours, and while variable nuclear and strong cytoplasmic staining were distinctive of tumour cells, the expression levels and compartmentalization of the specific protein isoforms remain unknown. While increased expression of type I would contribute towards lowering androgen levels, increased expression of types II and III would not. The abundance of type III transcripts in multiple tissues may provide insight into a regulatory role with truncated isoforms possibly affecting androgen levels by regulating substrate and/or co-factor availability, dimerization or the formation of protein complexes with other UGTs, while protein-protein interaction may also impact cascade signaling pathways in PCa development and disease progression.

Keywords: 11keto-testosterone; copy-number variation; dihydrotestosterone; prostate cancer prognosis; UDP-glucuronosyltransferase

In their article "The UGT2B28 sex-steroid inactivation pathway is a regulator of steroidogenesis and modifies the risk of prostate cancer progression" published in *Eur Urol* in April 2016, Belledant *et al*. report a regulatory role to the enzyme uridine diphosphate glucuronosyltransferase 2B type 28 (UGT2B28), modulating prostate cancer (PCa) progression. This role is separate from that of UGT2B28's function as a conjugative inactivating enzyme, with UGT2B28 influencing circulating androgen levels in PCa patients as well as clinical and pathologic factors associated with the disease (1).

Placing the work in context, we will discuss the contribution of steroidogenic enzymes towards the production and maintenance of active androgens which interact with the androgen receptor (AR) and the crucial role that these enzymes play—not only in normal prostate homeostasis but also in PCa. We will also briefly discuss genetic variability within UGT2B enzymes, focusing on B28, after which we will review the concepts highlighted by Belledant *et al*. and provide a perspective on the role of this conjugating enzyme in PCa.

Active androgen levels are maintained by both metabolic and catabolic enzymes with 5α-reductase type 1 (SRD5A1) and type 2 (SRD5A2) catalyzing the biosynthesis of dihydrotestosterone (DHT) from testosterone (T) or alternatively from androstenedione (A4) and the 5α-androstane-3,17-dione (5αDIONE) intermediate. The interconversion of A4 and T and their 5α-reduced metabolites by the reductive or oxidative 17β-hydroxysteroid dehydrogenase (17βHSD) enzymes further adds to the complexity of steroidogenesis in the prostate. The equilibrium is however perturbed in PCa and tumour development is associated with the modulation of enzyme expression. Increased expression of the reductive enzyme 17βHSD3 (31-fold) has been reported in the prostate tumour microenvironment (2) as well as increases in 17βHSD5 (AKR1C3) expression ranging 2–5-fold, favouring T biosynthesis. In conjunction with the increased expression of the reductive enzymes, a 7-fold decrease in the expression of the oxidative enzyme 17βHSD2 which catalyzes the reverse conversion of T to A4, has been reported which again diverts the flux towards T production. In addition, while SRD5A2, which is expressed in normal prostate tissue, is decreased (2–4-fold), the expression of SRD5A1 has been shown to be increased (2-fold) in castration-resistant prostate tumours thus maintaining DHT levels in the prostate [(3) and the references therein].

Contributing to the active androgen levels in the prostate microenvironment are the inactivating and conjugating enzymes. Only androgens with a hydroxyl group at C17 or C3 are potential substrates for conjugation by UGTs and as such both T and DHT can be converted to their glucuronide derivatives, rendering them inactive to be secreted into circulation. DHT together with 5αDIONE are, however, also inactivated by 3α-hydroxysteroid dehydrogenase type 3 (AKR1C2), which catalyzes the reduction of the keto group at C3, forming 5α-androstane-3α,17β-diol (3αDIOL) and androsterone (AST), respectively, allowing the subsequent addition of the glucuronide moiety at C3. While AKR1C2 also exhibits oxidative activity, this reverse reaction is primarily catalyzed by 17βHSD6, 17βHSD10 and retinol dehydrogenase 5 expressed in the prostate (4-7). In primary PCa, AKR1C2 expression levels have been reported to be significantly decreased compared to benign tissues (7-9), which contributes to significantly higher DHT levels in primary PCa tumours (10). In malignant epithelial cells, increased expression (3-fold) of 17βHSD10, which mediates the conversion of 3αDIOL to DHT, increased DHT tumour production (11). Furthermore, androgen deprivation therapy led to a 2-fold increase in 17βHSD6 expression levels, also associated with the biochemical progression of PCa (11). It is therefore apparent that the intricate homeostasis in the prostate is modulated by the perturbed expression of the steroidogenic enzymes catalyzing DHT production and those catalyzing the inactivation of androgens.

The expression of the UGT2B enzymes are tissue and substrate specific. UGT2B7, B15 and B17 are the three major UGT2Bs primarily responsible for androgen conjugation in humans and of these only B15 and B17 are actively expressed in the prostate (12). The UGT2B enzymes conjugate androgens in a regiospecific manner, either catalyzing the addition of the glucuronide moiety at C17 and/or at C3. UGT2B7 conjugates 3αDIOL and AST at C3 and T, DHT and 3αDIOL at C17; UGT2B15 only at C17 of T and 5α-reduced androgens, DHT and 3αDIOL; UGT2B17 at C3 and C17 of T, DHT, 3αDIOL and AST and UGT2B28 conjugates 3αDIOL at both C3 and C17 (low efficiency), as well as AST and T. Although UGT2B28 conjugates 3αDIOL, its capacity to conjugate 3αDIOL is much lower than that of B15 and B17 (12,13). In addition, UGT2B28 also conjugates estradiol (E2), etiocholanolone and 5β-androstane-3α,17β-diol. The latter is the product of androstenediol (5-diol) catalyzed by AKR1C2 and SRD5A (13,14). Interestingly, 5-diol was shown by Belledant *et al*. to be increased and associated with increased UGT2B28 levels in prostate tumour tissue.

S1498

du Toit and Swart. The role of UGT2B28 in prostate cancer

In contrast to the steroidogenic enzymes catalyzing biosynthesis pathways, the genes encoding the UGT enzymes are characterized by substantial genetic variability brought about by polymorphisms, the production of alternative transcripts through alternative splicing/last exon/internal exon use and exon skipping, together with copy number variation (CNV) and alternative promoters. These factors all contribute to the complexity of the role of the UGT enzymes in steroid inactivation, impacting protein expression levels and enzymatic activities which in turn impact circulating androgen levels and PCa outcomes (15).

While comparative studies relating to circulating hormone levels are complicated by interindividual variations, biochemical studies inevitably yield tangible data regarding enzyme kinetics as, for example, in the case of the Asp85Tyr polymorphism of UGT2B15. This functional polymorphism encodes a protein with the Asp85Tyr mutation and has been shown to be expressed either homozygously for one or the other as well as heterozygously in patients with both alleles. Similar Km values for DHT and 3αDIOL are reported but the enzyme containing Tyr residue catalyzes the inactivation more efficiently with a 2-fold higher Vmax value (16,17). UGT2B15, B17 and B28 are encoded by a single gene (15), with polymorphisms in the former two genes having been shown to significantly impact circulating levels of free unconjugated T and AST (18-20), and the intra-prostatic levels of 3αDIOL-3G and 3αDIOL-17G (21). Whole gene deletions were reported for UGT2B28 in this paper and previously by Nadeau *et al.* (18), in which they also showed that in UGT2B17 (–/–) PCa patients circulating 3αDIOL-17G levels were significantly reduced. Although T and DHT levels were not significantly lower, AST levels were increased, indicative of increased flux in these metabolic pathways and if unconjugated, would allow the reactivation of AST and a concomitant increase in AR signaling. This study also showed that in UGT2B28 (+/–) patients, circulating androgen levels were not affected. However, patients with a single copy in conjunction with the UGT2B17 (–/–) deletion not only had significantly increased AST levels but also significantly decreased AST-G and 3αDIOL-17G levels (15,18).

Investigations into complete UGT2B28 deficiency by Belledant *et al.* (1) reported significantly decreased circulating T, DHT AST-G, and 3αDIOL (both C3 and C17 derivatives) in patients when compared to UGT2B28 (+/+) patients. In addition, their study also reported that high tumour expression levels of UGT2B28 were associated with lower protein specific antigen (PSA), smaller tumour volume, but with higher Gleason score and positive nodal status. Patients with increased nuclear and cytosolic UGT2B28 expression in tumours together with significantly increased circulating T and DHT levels suggested an association with progression to a more aggressive disease.

It should be noted that three UGT2B28 isoforms are expressed in humans—type I, II and III characterized in 2001 by Lévesque *et al.* (13). RT-PCR data identified the three transcripts in mammary gland tissue and in LNCaP prostate cancer cells with only type III expressed in prostate and benign prostatic hyperplasia tissue. The active UGT2B28 type I was shown to catalyze the conjugation of E2, T, AST and 3αDIOL efficiently. UGT2B28 type II contained a 308 bp deletion, amino acid residues 335 to 437 in the cofactor binding domain and contained a premature stop codon, and UGT2B28 type III lacked residues 105 to 221 in the putative substrate binding domain. Both truncated isoforms yielded a non-functional protein. Western blot analyses, using the polyclonal EL-93 anti-UGT2B17 antiserum, specific to the UGT2B enzymes, showed the three isoforms to have apparent molecular masses of 52, 35 and 42 kDa, respectively. While UGT2B protein was also shown to be present in liver preparations together with RT-PCR identifying UGT2B28 type II and III transcripts (13), the present study by Belledant *et al.* showed the polyclonal EL-93 antibody yielding a positive signal for all the UGT2B proteins. In contrast, the UGT2B28 antibody was shown to specifically bind UGT2B28 protein only and since it was raised against a peptide sequence spanning residues 113–124 the antibody only recognizes the type I and type II isoforms. Since only type III mRNA transcripts were shown in normal prostate (a single prostate tissue sample purchased from Clontech) (13), it is therefore interesting that immunohistochemistry (IHC) analyses showed the presence of UGT2B28 in normal prostate tissue, in the nucleus of basal and some secretory cells, pointing to the presence of both the type I and II isoforms. Cancer tumour cells from UGT2B28 (+/+), on the other hand, showed strong nuclear and cytoplasmic staining (1) and while it is very possible that type III is also present, the data cannot distinguish between type I and II. Interestingly comparative analyses of UGT2B28 expression and gene copy number showed, in both the nuclei and cytoplasm, that expression levels were similar between +/+ and +/– patients. Strong nuclear staining was associated with significantly lower PSA levels and patients presented with smaller tumours, while strong cytoplasmic staining was associated with higher Gleason scores and positive nodal status. Considering circulating androgens, significantly

increased T and DHT levels were also associated with increased nuclear UGT2B28 expression. Although these androgens also increased with increased cytosolic expression, their levels were not significant. 5-diol, the product of dehydroepiandrosterone catalyzed by AKR1C3/17βHSD3, also increased with increased nuclear (P=0.079) and cytoplasmic (P=0.026) expression of UGT2B28 (1), and would as such contribute towards T levels due to the presence of 3β-hydroxysteroid dehydrogenase type 2 catalyzing the conversion of 5-diol to T.

Analyses of circulating androgens in UGT2B28 (–/–) PCa patients showed significantly reduced T, DHT as well as downstream conjugated metabolites, AST-G and 3αDIOL-3G and 3αDIOL-17G levels in comparison to UGT2B28 (+/+) patients. Circulating A4 was significantly increased in the UGT2B28 (–/–) cohort (1) which would contribute to the production of DHT via the 5αDIONE pathway in prostate steroidogenesis (22). Although all downstream intermediate steroid metabolites were not reported in this study, analyses of the ratio of A4, T and DHT to their conjugated metabolites, 8.59 [UGT2B28 (+/+)] and 8.97 [UGT2B28 (–/–)] offers some perspective into the metabolic flux. However, these steroids cannot be regarded in isolation as we have also shown the hydroxylation of A4 by cytochrome P450 11β-hydroxylase leads to the production of 11β-hydroxyandrostenedione (11OHA4) in the adrenal, which would also be increased in UGT2B28 (–/–) patients with higher A4 levels, and would certainly contribute to the androgen pool via the 11OHA4-derived pathway (23,24).

The data presented is certainly open to interpretation and the manner in which the enzyme isoforms would impact PCa complex. Inactive androgens in circulation are also products of other UGT enzymes. When considering increased circulating T, DHT and 5-diol being associated with increased tumour expression of UGT2B28, it is prudent to note that androgens in the prostate and in circulation would be conjugated by UGT enzymes expressed either in the prostate itself or in other target tissue and therefore circulating levels cannot be regarded in isolation. In addition, the expression levels of UGT2B28 isoforms in the prostate and prostate tumours are unclear, since the expression can be that of type I or type II. It is furthermore possible that type III is also present. In the translation of UGT2B28 transcripts encoding type II, the deletion of exon 4 and 5 excises the UDPGA binding site and disrupts the open reading frame with the ensuing premature stop codon yielding a protein fold different

to that of type I. Despite not having a transmembrane domain, the truncated type II was reported to nevertheless be present in the endoplasmic reticulum and in the perinuclear membrane as in the case of type I. Type III on the other hand contains all the relevant structural domains but not the substrate binding domain. Although the data was not shown Lévesque et al. also reported that type III was capable of homodimerization (13). It is interesting to note that in their study in which the three isoforms were expressed in HEK293 cells, Western blotting showed type I and III to be represented by single bands while only type II showed additional bands of greater apparent masses indicting possible protein aggregation, either type II with itself or with the other two isoforms. Although one would normally not expect protein aggregation under denaturing electrophoretic conditions, it is fairly common that proteins form stable aggregates as for example in the case of cytochrome b_5, which electrophoreses as dimer and tetramer aggregates even under stringent denaturing conditions (25). Besides the IHC data not distinguishing between type I and II, it is unclear if isoform expression would be compartmentalized as in the case of UGT2B15 and 17 with the former being expressed in the luminal cells and the latter in the basal cells (26), further contributing towards the fine regulation brought about by compartmentalized conjugation and ligand availability to the AR. An interesting aspect brought to the fore by the Belledant et al. study is indeed a novel tier of regulation other than that of the inactivation of androgens. Increased T and DHT levels associated with increased UGT2B28 protein expression and more aggressive PCa could perhaps also be indicative of decreased UGT2B15 and B17 expression since androgens have been shown to negatively regulate their conjugation by these enzymes (27).

While an increase in the active isoform may contribute towards high levels of circulating conjugated androgens, the expression of the inactive forms would not contribute towards conjugated androgen levels. Linking UGT2B28 (+/+) to an increase in biochemical recurrence (BCR) and overexpression to increased PCa risk and potent androgens, would possibly implicate the expression of the inactive isoforms and an impaired ability to conjugate androgens. On the other hand, the isoforms may aggregate as has been shown for the UGT1 and UGT2 enzymes (28,29)—not only forming dimer-dimer complexes but also aggregates with other UGT2B enzymes thus rendering them unable to catalyze the conjugation of androgens.

Whether UGT2B28 is the active androgen-inactivating

S1500

du Toit and Swart. The role of UGT2B28 in prostate cancer

UGT isoform under high-androgen exposure as the authors suggested is unclear as the expression of UGT2B28 in the prostate remains to be fully characterized. While type I would certainly contribute towards androgen inactivation in the prostate, the expression of the isoform types in normal and PCa tissue and the expression level of the three isoforms as well as possible compartmentalization remain unknown. Since data thus far indicate tissue-specific processing of mRNA transcripts, investigations into the regulation of post-transcriptional activities in the expression of UGT enzymes will shed light on the role of the UGT2B28 isoforms. It is possible that type III may be involved in regulating co-factor availability while type II may sequester androgens, rendering them unavailable for AR activation, depending on the level of expression. In addition, the role of UGT2B28 type I in the inactivation of estrogens rendering these steroids incapable of activating the estrogen receptor, AR or mutated AR may be one of critical importance. Furthermore, UGT2B28 has been considered only in terms of T and DHT—C_{18}, C_{21} and C11-oxy steroids would certainly also impact PCa and possibly find associations with BCR. Previously published data suggests a regulatory role for UGT2B28 in terms of estrogen conjugation as AST and E2 were efficiently conjugated while more than 50% estrone (E1) remained in the free form in breast cyst fluid (13). Lévesque *et al.* (13) showed the presence of all three isoforms of UGT2B28 in mammary gland tissue, however, when transiently expressed, E1 was not conjugated by UGT2B28 type I—suggesting that other UGT2B enzymes are involved in the conjugation of E1. However, since the conjugation of E2 has been shown, a role for UGT2B28 in breast cancer is highlighted. Furthermore, with perturbed UGT2B28 expression and E2 conjugation decreased, promiscuous binding of E2 to the mutated AR in PCa may also occur (30). Interestingly while the three UGT2B28 transcripts were detected in breast tissue none were detected in the ovary or placenta and thus the presence of UGT2B28 type III in the testis, prostate and BPH tissue (13) suggests a prominent role for UGT2B28 in male steroid homeostasis. It was previously reported that the C11-oxy C_{19} steroids were poor substrates for conjugation and that UGT2B17 exhibits lower catalytic activity towards C_{19} steroids containing a C11-hydroxyl group, even though it has been shown that 5α-androstane-3α,11α/β-17β triol and T are conjugated at similar rates (15,31). We recently reported that 11OHA4 is metabolized to 11keto-dihydrotestosterone in PCa cells and have shown that it is as potent as DHT in activating the AR (32). We have since shown that 11keto-testosterone is not glucuronidated efficiently in LNCaP cells and as such would readily activate the AR as T and DHT are fully conjugated. Furthermore, we reported that the C11-oxy C_{19} steroids are present at significantly higher levels than the C_{19} steroids in circulation, in PCa tissue (33) and in BPH tissue (unpublished data), drawing attention to C11-oxy metabolites in PCa.

In summary, the contribution of UGT2B enzymes to active ligand availability can only be fully assessed in the context of all steroids which may contribute to PCa and its aggressive progression. This will certainly lead to a better understanding of the complex regulation by these inactivating enzymes, modulating receptor signaling, not only in terms of C_{19} steroids but also in terms of the C_{18} and C_{21} steroids as well as the C11-oxy steroids. As has been demonstrated by this study, genetic variations together with tissue-specific mRNA processing and the biosynthesis of different isoforms, as well as CNVs, contribute to the complexities of the UGT enzymes and their impact on PCa development and disease progression. Both UGT2B15 and B17 have also been reported to conjugate pharmacological compounds while the contribution of UGT2B28 to drug inactivation remains unknown. UGT2B17 and B28 are also among the UGT genes of the human genome which are the most commonly deleted genes and as such may impact drug metabolism and therapeutic strategies. While the usage of an alternative promoter may modulate the expression and/or activity of UGTs, it may also contribute to variability in the glucuronidation pathway and steroid hormone levels observed in patients. In the case of UGT2B17, gene deletions and CNVs have been shown to affect steroid inactivation, altering tissue and circulating androgen levels, supporting the general hypothesis of reduced inactivation by UGT enzymes resulting in increased active ligands, risk of PCa and its recurrence (34). The current report by Belledant *et al.* (1) showing increased UGT2B28 expression linked with increased T, DHT and 5-diol and a more aggressive disease, together with CNV associating gene deletion with decreased active AR ligands and conjugated downstream derivatives, points to other mechanisms at play involving pathways other than steroid inactivation.

Acknowledgements

of genetic aspects.

Footnote

Conflicts of Interest: The authors have no conflicts of interest to declare.

References

1. Belledant A, Hovington H, Garcia L, et al. The UGT2B28 Sex-steroid Inactivation Pathway Is a Regulator of Steroidogenesis and Modifies the Risk of Prostate Cancer Progression. Eur Urol 2016;69:601-9.

2. Koh E, Noda T, Kanaya J, et al. Differential expression of 17beta-hydroxysteroid dehydrogenase isozyme genes in prostate cancer and noncancer tissues. Prostate 2002;53:154-9.

3. Zhang A, Zhang J, Plymate S, et al. Classical and Non-Classical Roles for Pre-Receptor Control of DHT Metabolism in Prostate Cancer Progression. Horm Cancer 2016;7:104-13.

4. Penning TM, Bauman DR, Jin Y, et al. Identification of the molecular switch that regulates access of 5alpha-DHT to the androgen receptor. Mol Cell Endocrinol 2007;265-266:77-82.

5. Rizner TL, Lin HK, Peehl DM, et al. Human type 3 3alpha-hydroxysteroid dehydrogenase (aldo-keto reductase 1C2) and androgen metabolism in prostate cells. Endocrinology 2003;144:2922-32.

6. Rizner TL, Lin HK, Penning TM. Role of human type 3 3alpha-hydroxysteroid dehydrogenase (AKR1C2) in androgen metabolism of prostate cancer cells. Chem Biol Interact 2003;143-144:401-9.

7. Ji Q, Chang L, VanDenBerg D, et al. Selective reduction of AKR1C2 in prostate cancer and its role in DHT metabolism. Prostate 2003;54:275-89.

8. Yun H, Xie J, Olumi AF, et al. Activation of AKR1C1/ERβ induces apoptosis by downregulation of c-FLIP in prostate cancer cells: A prospective therapeutic opportunity. Oncotarget 2015;6:11600-13.

9. Khvostova EP, Otpuschennikov AA, Pustylnyak VO, et al. Gene expression of androgen metabolising enzymes in benign and malignant prostatic tissues. Horm Metab Res 2015;47:119-24.

10. Ji Q, Chang L, Stanczyk FZ, et al. Impaired dihydrotestosterone catabolism in human prostate cancer: critical role of AKR1C2 as a pre-receptor regulator of androgen receptor signaling. Cancer Res 2007;67:1361-9.

11. Ishizaki F, Nishiyama T, Kawasaki T, et al. Androgen deprivation promotes intratumoral synthesis of dihydrotestosterone from androgen metabolites in prostate cancer. Sci Rep 2013;3:1528.

12. Bélanger A, Pelletier G, Labrie F, et al. Inactivation of androgens by UDP-glucuronosyltransferase enzymes in humans. Trends Endocrinol Metab 2003;14:473-9.

13. Lévesque E, Turgeon D, Carrier JS, et al. Isolation and characterization of the UGT2B28 cDNA encoding a novel human steroid conjugating UDP-glucuronosyltransferase. Biochemistry 2001;40:3869-81.

14. Turgeon D, Chouinard S, Belanger P, et al. Glucuronidation of arachidonic and linoleic acid metabolites by human UDP-glucuronosyltransferases. J Lipid Res. 2003;44:1182-91.

15. Guillemette C, Lévesque E, Harvey M, et al. UGT genomic diversity: beyond gene duplication. Drug Metab Rev 2010;42:24-44.

16. Lévesque E, Beaulieu M, Green MD, et al. Isolation and characterization of UGT2B15(Y85): a UDP-glucuronosyltransferase encoded by a polymorphic gene. Pharmacogenetics 1997;7:317-25.

17. Bélanger A, Hum DW, Beaulieu M, et al. Characterization and regulation of UDP-glucuronosyltransferases in steroid target tissues. J Steroid Biochem Mol Biol 1998;65:301-10.

18. Nadeau G, Bellemare J, Audet-Walsh É, et al. Deletions of the androgen-metabolizing UGT2B genes have an effect on circulating steroid levels and biochemical recurrence after radical prostatectomy in localized prostate cancer. J Clin Endocrinol Metab 2011;96:E1550-7.

19. Coviello AD, Haring R, Wellons M, et al. A genome-wide association meta-analysis of circulating sex hormone-binding globulin reveals multiple Loci implicated in sex steroid hormone regulation. PLoS Genet 2012;8:e1002805.

20. Sun T, Oh WK, Jacobus S, et al. The impact of common genetic variations in genes of the sex hormone metabolic pathways on steroid hormone levels and prostate cancer aggressiveness. Cancer Prev Res (Phila) 2011;4:2044-50.

21. Olsson M, Ekström L, Guillemette C, et al. Correlation between circulatory, local prostatic, and intra-prostatic androgen levels. Prostate 2011;71:909-14.

22. Chang KH, Li R, Papari-Zareei M, et al. Dihydrotestosterone synthesis bypasses testosterone to drive castration-resistant prostate cancer. Proc Natl Acad Sci U S A 2011;108:13728-33.

23. Schloms L, Storbeck KH, Swart P, et al. The influence of Aspalathus linearis (Rooibos) and dihydrochalcones

Stellenbosch University https://scholar.sun.ac.za

S1502   du Toit and Swart. The role of UGT2B28 in prostate cancer

on adrenal steroidogenesis: quantification of steroid intermediates and end products in H295R cells. J Steroid Biochem Mol Biol 2012;128:128-38.

24. Swart AC, Schloms L, Storbeck KH, et al. 11β-hydroxyandrostenedione, the product of androstenedione metabolism in the adrenal, is metabolized in LNCaP cells by 5α-reductase yielding 11β-hydroxy-5α-androstanedione. J Steroid Biochem Mol Biol 2013;138:132-42.

25. Storbeck KH, Swart AC, Lombard N, et al. Cytochrome b(5) forms homomeric complexes in living cells. J Steroid Biochem Mol Biol 2012;132:311-21.

26. Chouinard S, Pelletier G, Bélanger A, et al. Cellular specific expression of the androgen-conjugating enzymes UGT2B15 and UGT2B17 in the human prostate epithelium. Endocr Res 2004;30:717-25.

27. Gauthier-Landry L, Bélanger A, Barbier O. Multiple roles for UDP-glucuronosyltransferase (UGT)2B15 and UGT2B17 enzymes in androgen metabolism and prostate cancer evolution. J Steroid Biochem Mol Biol 2015;145:187-92.

28. Ikushiro S, Emi Y, Iyanagi T. Protein-protein interactions between UDP-glucuronosyltransferase isozymes in rat hepatic microsomes. Biochemistry 1997;36:7154-61.

29. Meech R, Mackenzie PI. UDP-glucuronosyltransferase,

the role of the amino terminus in dimerization. J Biol Chem 1997;272:26913-7.

30. Taplin ME, Bubley GJ, Shuster TD, et al. Mutation of the androgen-receptor gene in metastatic androgen-independent prostate cancer. N Engl J Med 1995;332:1393-8.

31. Beaulieu M, Lévesque E, Hum DW, et al. Isolation and characterization of a novel cDNA encoding a human UDP-glucuronosyltransferase active on C19 steroids. J Biol Chem 1996;271:22855-62.

32. Bloem LM, Storbeck KH, Swart P, et al. Advances in the analytical methodologies: Profiling steroids in familiar pathways-challenging dogmas. J Steroid Biochem Mol Biol 2015;153:80-92.

33. du Toit T, Bloem LM, Quanson JL, et al. Profiling adrenal 11β-hydroxyandrostenedione metabolites in prostate cancer cells, tissue and plasma: UPC2-MS/MS quantification of 11β-hydroxytestosterone, 11keto-testosterone and 11keto-dihydrotestosterone. J Steroid Biochem Mol Biol 2017;166:54-67.

34. Guillemette C, Lévesque É, Rouleau M. Pharmacogenomics of human uridine diphospho-glucuronosyltransferases and clinical implications. Clin Pharmacol Ther 2014;96:324-39.
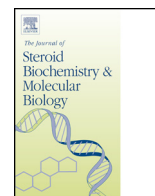
Original research

Profiling adrenal 11β-hydroxyandrostenedione metabolites in prostate cancer cells, tissue and plasma: UPC²-MS/MS quantification of 11β-hydroxytestosterone, 11keto-testosterone and 11keto-dihydrotestosterone

Therina du Toit[a], Liezl M. Bloem[a], Jonathan L. Quanson[a], Riaan Ehlers[a], Antonio M. Serafin[b], Amanda C. Swart[a],*

[a] Department of Biochemistry, Stellenbosch University, Stellenbosch 7600, South Africa
[b] Division of Radiobiology, Department of Medical Imaging and Clinical Oncology, Faculty of Medicine and Health Sciences, Stellenbosch University, Tygerberg 7505, South Africa

ABSTRACT

Adrenal C_{19} steroids serve as precursors to active androgens in the prostate. Androstenedione (A4), 11β-hydroxyandrostenedione (11OHA4) and 11β-hydroxytestosterone (11OHT) are metabolised to potent androgen receptor (AR) agonists, dihydrotestosterone (DHT), 11-ketotestosterone (11KT) and 11-ketodihydrotestosterone (11KDHT). The identification of 11OHA4 metabolites, 11KT and 11KDHT, as active androgens has placed a new perspective on adrenal C11-oxy C_{19} steroids and their contribution to prostate cancer (PCa).

We investigated adrenal androgen metabolism in normal epithelial prostate (PNT2) cells and in androgen-dependent prostate cancer (LNCaP) cells. We also analysed steroid profiles in PCa tissue and plasma, determining the presence of the C_{19} steroids and their derivatives using ultra-performance liquid chromatography (UHPLC)- and ultra-performance convergence chromatography tandem mass spectrometry (UPC²-MS/MS).

In PNT2 cells, sixty percent A4 (60%) was primarily metabolised to 5α-androstanedione (5αDIONE)(40%), testosterone (T)(10%), and androsterone (AST)(10%). T(30%) was primarily metabolised to DHT(10%) while low levels of A4, 5αDIONE and 3αADIOL (≈20%) were detected. Conjugated steroids were not detected and downstream products were present at <0.05 μM. Only 20% of 11OHA4 and 11OHT were metabolised with the former yielding 11keto-androstenedione (11KA4), 11KDHT and 11β-hydroxy-5α-androstanedione (11OH-5αDIONE) and the latter yielding 11OHA4, 11KT and 11KDHT with downstream products <0.03 μM. In LNCaP cells, A4 (90%) was metabolised to AST-glucuronide via the alternative pathway while T was detected as T-glucuronide with negligible conversion to downstream products. 11OHA4 (80%) and 11OHT (60%) were predominantly metabolised to 11KA4 and 11KT and in both assays more than 50% of 11KT was detected in the unconjugated form. In tissue, we detected C11-oxy C_{19} metabolites at significantly higher levels than the C_{19} steroids, with unconjugated 11KDHT, 11KT and 11OHA4 levels ranging between 13 and 37.5 ng/g. Analyses of total steroid levels in plasma showed significant levels of 11OHA4 (≈230–440 nM), 11KT (≈250–390 nM) and 11KDHT (≈19 nM). DHT levels (<0.14 nM) were significantly lower.

In summary, 11β-hydroxysteroid dehydrogenase type 2 activity in PNT2 cells was substantially lower than in LNCaP cells, reflected in the conversion of 11OHA4 and 11OHT. Enzyme substrate preferences suggest that the alternate pathway is dominant in normal prostate cells. Glucuronidation activity was not detected in PNT2 cells and while all T derivatives were efficiently conjugated in LNCaP cells, 11KT was not. Substantial 11KT levels were also detected in both PCa tissue and plasma. 11OHA4 therefore presents a significant androgen precursor and its downstream metabolism to 11KT and 11KDHT as well as its presence in PCa tissue and plasma substantiate the importance of this adrenal androgen.

© 2016 Elsevier Ltd. All rights reserved.

* Corresponding author at: Department of Biochemistry, Stellenbosch University, Private Bag X1, Matieland, 7602, South Africa.
E-mail address: acswart@sun.ac.za (A.C. Swart).

Contents

1. Introduction

Most prostate cancers (PCa) are androgen driven and as such androgen deprivation therapy (ADT) is currently the primary clinical approach in the treatment of the disease. Reducing circulating testosterone (T) levels is initially effective in lowering the production of the potent androgen, dihydrotestosterone (DHT), however, most cases progress to castration-resistant prostate cancer (CRPC). CRPC is androgen-dependent and in the absence of testicular T, adrenal C_{19} steroids serve as substrates for the intratumoral biosynthesis of androgen receptor (AR) agonists in the prostate [1–4]. Following castration and the elimination of testicular androgens, DHT is nevertheless still detected in the prostate, denoting the importance of the adrenal's contribution to the prostate androgen tumor micro-environment and cell proliferation [5,6].

The production of active androgens, their subsequent activation of the AR and transcription of AR-regulated genes, are prerequisites in the development and differentiation of the normal prostate, as well as in the development and progression of PCa [7]. The androgen signalling pathway is closely linked to tumor initiation and invasion, and the subsequent development of metastatic disease. Following ADT, the biosynthesis of active androgens in prostate cells are initiated by the uptake of circulating dehydroepiandrosterone (DHEA), androstenedione (A4), 11β-hydroxyandrostenedione (11OHA4) and T produced in the adrenal gland. In the adrenal, basal and adrenocorticotropic hormone (ACTH)-stimulated A4 levels, 79 and 585 nM respectively, are 100-fold greater than T levels, while 11OHA4 levels are even higher, 157 and 811 nM, respectively. 11-ketoandrostenedione (11KA4), 11β-hydroxytestosterone (11OHT) and 11-ketotestosterone (11KT) are also produced in the adrenal albeit at negligible levels, similar to that of T [8]. These aforementioned adrenal C_{19} steroids contribute to androgen production in the prostate with A4 and T being converted to DHT via the conventional and 'alternative' 5α-androstanedione (5αDIONE) pathways (Fig. 1) while the C11 hydroxy- and keto- A4 and T metabolites contribute to the production of 11keto-dihydrotestosterone (11KDHT) and 11β-hydroxy-dihydrotestosterone (11OHDHT) through much the same pathways, also known as the 11OHA4-derived pathway (Fig. 2) [9,10]. 11KDHT exhibits agonist activity towards the AR comparable to that of DHT, thereby implicating it as a role player in CRPC. In contrast, 11OHA4 exhibited negligible androgenic activity at 1 nM while the androgenic activity of 11OHT increased upon its

reduction to 11OHDHT. Even at 10 nM the androgenic activity of 11OHA4 remained weak, however, the androgenicity of the other metabolites in the pathway increased with both 11β-hydroxy-5α-androstanedione (11OH-5αDIONE) and 11KA4 exhibiting partial agonist activity and the remaining metabolites in the pathway showing full agonist activity [9,11,12].

The peripheral metabolism of adrenal androgens rely on the activity of 17β-hydroxysteroid dehydrogenase (17βHSD) and 5α-reductase (SRD5A) [7,13–17], while the activation of 11OHA4 relies on the presence of 11β-hydroxysteroid dehydrogenase type 2 (11βHSD2) [9–12,18]. The subsequent inactivation and conjugation relies on the expression of 3α-hydroxysteroid dehydrogenase (3αHSD) type 1 (AKR1C1) and type 3 (AKR1C2) and uridine diphosphate glucuronosytransferases (UGT2B15, UGT2B17 and UGT2B28) [19–23]. In the conventional C_{19} pathway, which primarily refers to the production of T by the testes and the subsequent biosynthesis of DHT from T in the prostate, it is the adrenal androgens, DHEA, A4 and to a lesser degree T, metabolised by the same enzymes that contribute towards the androgen pool in the recurrence of PCa. The uptake of A4 and T by prostate cells results in their interconversion by 17βHSD, followed by the conversion to 5α-reduced steroids (Fig. 1). Both 17βHSD3 and 17βHSD type 5 (also known as AKR1C3) are present in prostate
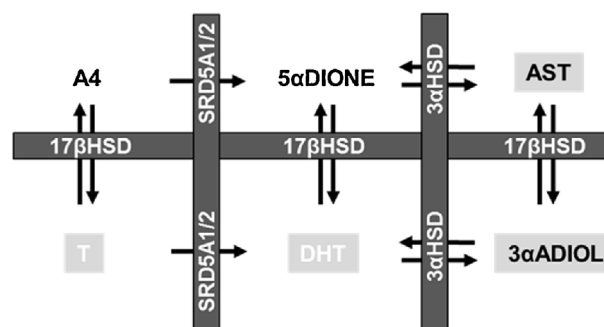
Fig. 1. C_{19} steroid metabolism in the conventional and alternate pathways. A4, androstenedione; T, testosterone; 5αDIONE, 5α-androstenedione; DHT, dihydrotestosterone; AST, androsterone; 3αADIOL, 5α-androstane-3α, 17β-diol; 17βHSD, 17β-hydroxysteroid dehydrogenase (downward reaction by 17βHSD3 and/or AKR1C3; upward reaction by 17βHSD2); SRD5A1/2, 5α-reductase type 1 and/or 2; 3αHSD, 3α-hydroxysteroid dehydrogenase (forward reaction by AKR1C1 or AKR1C2; reverse reaction by 17βHSD6). Steroids shaded in grey depict UGT2B substrates. Steroid metabolites in white text; human AR agonists at 1 nM.

Fig. 2. C11 hydroxy- and keto- C_{19} steroids metabolism in the 11OHA4-derived pathway. 11OHA4, 11β-hydroxyandrostenedione; 11OHT, 11β-hydroxytestosterone; 11KA4, 11-ketoandrostenedione; 11KT, 11-ketotestosterone; 11OH-5αDIONE, 11β-hydroxy-5α-androstenedione; 11K-5αDIONE, 11-keto-5α-androstenedione; 11KDHT, 11-ketodihydrotestosterone; 11OHDHT, 11β-hydroxy-dihydrotestosterone; 11OHAST, 11β-hydroxyandrosterone; 11KAST, 11-ketoandrosterone; 11K-3αADIOL, 11-keto-5α-androstane-3α,17β-diol; 17βHSD, 17β-hydroxysteroid dehydrogenase; 17βHSD2, 17β-hydroxysteroid dehydrogenase type 2; SRD5A1/2, 5α-reductase type 1 and 2; 3αHSD, 3α-hydroxysteroid dehydrogenase; 11βHSD2, 11β-hydroxysteroid dehydrogenase type 2. Steroids shaded in grey depict potential UGT2B substrates. Dashed arrows; conversions catalysed by 11βHSD2. Steroid metabolites in white text; human AR agonists at 1 nM.

tissue and play a dominant role in converting A4, 5αDIONE and androsterone (AST) to T, DHT and 5α-androstane-3α, 17β-diol (3αADIOL), respectively. However, 17βHSD2 is also expressed and catalyses the reverse reaction to produce A4, 5αDIONE and AST [24]. In the conventional pathway the production of DHT is reported to be via A4 being converted to T which is subsequently reduced by SRD5A1 and SRD5A2. In CRPC, however, the preferred route of DHT biosynthesis is the conversion of adrenal derived A4 to 5αDIONE by SRD5A1, followed by the reduction of this intermediate by 17βHSD in the 'alternative' 5αDIONE pathway [17,25].

The metabolism of 11OHA4 follows a similar route in that it is readily metabolised by the SRD5As while not being reduced to 11OHT by 17βHSD3 and/or AKR1C3. However, in the presence of 11βHSD2, both 11OHA4 and 11OHT are reduced to their C11 keto form (Fig. 2). In the 11OHA4-derived pathway, the conversion of 11OHA4 to produce 11KA4 is catalysed by 11βHSD2, which in turn is utilized by AKR1C3 and/or 17βHSD3 to produce 11KT with the latter subsequently being reduced to its dihydro-form, 11KDHT, by SRD5A1/2. However, 11OHA4 is also metabolised by SRD5A yielding 11OH-5αDIONE which is also not reduced by 17βHSDs. In the presence of 11βHSD2, 11OH-5αDIONE is converted to its keto derivative, 11-keto-5α-androstanedione (11K-5αDIONE) and upon reduction by 17βHSD, also yields 11KDHT. In addition, 11KA4 and 11OHT produced in the adrenal may also be metabolised in the prostate by SRD5A1 and SRD5A2 to their 5α-reduced forms, viz. 11K-5αDIONE and 11OHDHT, respectively [9–12,18].

As previously mentioned the subsequent inactivation and glucuronidation of androgens in the prostate are catalysed by 3αHSD and UGT2Bs (Figs. 1 and 2), with the reversible reduction of DHT and 5αDIONE to 3αADIOL and AST, respectively, which exhibit only weak androgenic activity, being catalysed by AKR1C2. AKR1C2 is also capable of converting 11OH-5αDIONE, 11K-5αDIONE and 11KDHT to 11OHAST, 11KAST and 11K-3αADIOL, respectively, while 11OHDHT is not a substrate for AKR1C2 (unpublished data). The

presence of 3(α/β)-hydroxysteroid epimerase in the prostate results in the β-conformations of these steroids also being produced, 3βADIOL [26] and epiAST [27,28] from DHT and 5αDIONE, respectively. It is also possible for this enzyme to catalyse the production of 11OH-epiAST, 11K-epiAST and 11K-3βADIOL. The enzyme mediating the reverse oxidoreduction of 3αADIOL and AST has been shown to be attributed to the retinol dehydrogenase (RoDH) like 3αHSDs (RL-HSD/17βHSD6 and 17βHSD10) [29], with 17βHSD6 having both oxidoreductase and epimerase activities. The reverse reaction for epiAST to 5αDIONE has also been shown [27]. The potential for 11OHAST, 11KAST, 11K-3αADIOL and their respective β-conformations to be oxidoreduced by 3αHSD is therefore also possible. Although the aforementioned reactions have been investigated regarding T, the inactivation and conjugation of the C11- hydroxy and keto C_{19} adrenal steroids and their derivatives remain unknown. Earlier studies in which 11OHAST and 11KAST were detected in urine, concluded that these were the products of the metabolism of 11OHA4 and 11KA4–the first evidence of the inactivation of the C11-oxy C_{19} steroids [30]. More recently, we reported these steroids, 11OHAST and 11KAST, in the LNCaP androgen-dependent PCa cell model [9,10]. It has also been reported that β-conformations of steroids, such as epiAST, are not readily glucuronidated, but rather sulfonated, compared to their α-counterparts which are more readily conjugated [31–33].

Our characterization of the metabolism of 11OHA4, using ultra high performance liquid chromatography tandem mass spectrometry (UHPLC–MS/MS), has identified novel steroid metabolites capable of activating the AR [9,10]. Although the inactivation and conjugation of these metabolites have not been elucidated, our studies clearly implicated 11OHA4's role in PCa with its metabolites contributing to the intratumoral androgen pool in CRPC. Further advancements in LC–MS led to the introduction of ultra performance convergence chromatography tandem mass spectrometry (UPC²-MS/MS) bringing about improved

chromatographic resolution, reduced run times and increased sensitivity resulting in more accurate analyses of androgen metabolites and steroid profiles in the prostate.

The aim of this study was to firstly analyse the metabolism of C_{19} and C11-oxy C_{19} steroids in vitro, in a normal prostate epithelial cell model (PNT2) and in an androgen-dependent cancer cell model (LNCaP), in order to establish steroid profiles which would also allow downstream analyses of inactivation. Our previous studies focused primarily on characterising the activation of adrenal derived C11-oxy C_{19} steroids in the 11OHA4-derived pathway in LNCaP cells while the metabolism of C_{19} steroids have also not been fully described in a normal prostate cell model. We therefore analysed the metabolism of these steroids in PNT2 and LNCaP cells using UPC^2-MS/MS and in order to demonstrate the relevance of these steroid hormones in the physiological milieu, we investigated these C_{19} metabolites in PCa tissue as well as in PCa plasma. Our findings show for the first time 11OHA4 and 11OHT and their hydroxyl- and keto-metabolites to be present in human PCa tissue and plasma, with levels far exceeding those of A4, T and their metabolites.

2. Materials and methods

2.1. Tissue and plasma

Human PCa tissue and blood samples were collected in a study investigating clinical markers of PCa (reference no. N09/11/330; Faculty of Medicine and Health Sciences, Stellenbosch University and Tygerberg Hospital, South Africa). PCa tissue samples were obtained from patients (A) aged 71, untreated, prostate-specific antigen (PSA) 351 and (B) aged 67, 4 years after anti-androgen treatment commenced, PSA 60.8, and blood was obtained from patients (A) aged 74, who underwent bilateral orchiectomy, PSA 37.3 and (B) aged 66, luteinising hormone-releasing hormone analogue (LHRHa) treatment, PSA 7.1, 4.4 months and 1 year, respectively, after treatment commenced. Tissue samples, immediately snap-frozen in liquid nitrogen upon resection, and plasma samples were stored at $-80\,°C$ until further use.

2.2. Materials

Steroids (A4, T, 5αDIONE, DHT, AST, and 3αADIOL), β-glucuronidase (Type VII-A from *E. coli*, 5,292,000 units/g), RPMI-1640 medium, D-(+)-Glucose, dichloromethane (DCM) and methyl *tert*-butyl ether (MTBE) were purchased from Sigma-Aldrich (St. Louis, MO, USA). 11OHA4, 11OHT, 11KA4, 11KT, 11KDHT, 11OHAST, 11OH-epiAST, 11KAST, 11K-epiAST and DHT-glucuronide (DHT-G) were purchased from Steraloids (Wilton, USA). Corning® CellBIND® Surface 10-cm dishes, 6-well and 24-well plates were purchased from Corning® Life Sciences (NY, USA). PNT2 and LNCaP cells were obtained from the Sigma's European Collection of Cell Cultures (St. Louis, USA). Penicillin-streptomycin (penstrep), fetal bovine serum (FBS), trypsin-EDTA and phosphate buffered saline were obtained from Oxoid limited (Hampshire, England). Deuterated cortisol (9, 11, 12, 12-D4-cortisol), deuterated testosterone (Testosterone 1, 2-D2, 98%), deuterated progesterone (Progesterone 2,2,4,6,6,17A,21,21,21-D9, 98%) and deuterated 11β-hydroxyandrostenedione (4-androsten-11β-OL-3,17-DIONE 2,2,4,6,6,16,16-D7, 98%) were purchased from Cambridge isotopes (Andover, MA, USA). HEPES buffer (1 M) and sodium pyruvate (100 mM) were purchased from Biochrom (Berlin, Germany). The UPC^2 BEH and BEH 2-Ethylpyridine columns were purchased from Waters and the Kinetex PFP column was purchased from Phenomenex. All other chemicals were of analytical grade and supplied by reliable scientific houses.

2.3. Steroid metabolism in PNT2 and LNCaP cells

PNT2 cells were cultured in RPMI-1640 medium supplemented with 10% FBS, 1.5 g $NaHCO_3$/L (pH 7), 1% penstrep at 37 °C, in an atmosphere of 90% humidity and 5% CO_2. After 3–4 passages confluent cells were plated into 24-well plates (1×10^5 cells/mL, 0.5 mL/well) and incubated for 48 h. The medium was removed and replaced with 0.5 mL RPMI-1640 medium containing individual steroid substrates: A4, T, 11OHA4, 11OHT, 11KA4 and 11KT (1 μM). The cells were incubated for 48 h after which 0.5 mL aliquots were removed for analysis of free steroids.

LNCaP cells were cultured in RPMI-1640 growth medium, supplemented with 2.5 g D-(+)-Glucose, 1% HEPES and 1% sodium pyruvate and once confluent replated into 24 well Corning® CellBIND® surface plates (2×10^5 cells/mL, 0.5 mL/well). The same experimental protocols were followed as above and the metabolism of A4, T, 5αDIONE, DHT, AST, 3αADIOL, 11KT and 11KDHT (1 μM) assayed. Aliquots, 0.5 mL were removed after 48 h for analyses of free steroids. A second experiment was conducted to determine downstream metabolism of 11OHA4 and 11OHT (1 μM) in LNCaP cells, plated at 4×10^4 cells/mL. Cells were incubated with steroid substrates for a longer period (96 h) in phenol-free media, without serum supplementation, after which 0.5 mL aliquots were removed for analysis of free steroids.

Analysis of total steroids (free + conjugated) was carried out after treating duplicate 0.5 mL aliquots with 400 units (76 μL) of β-glucuronidase (*E. coli* Type VII-A; Sigma-Aldrich) at 37 °C, pH 6.5, for 24 h to deconjugate steroids. DHT-G (1 μM; in 0.5 mL media) was deconjugated and extracted, and used as a control for deconjugation efficiency, determined by the amount of DHT recovered using UHPLC-MS/MS (Supplemental Fig. 1).

2.4. Steroid extraction

In vitro assays were analysed after liquid/liquid steroid extractions were carried out with either DCM or MTBE. Cortisol-D4 (15 ng) and testosterone-D2 (15 ng), were added to each sample as internal standards prior to steroid extraction. A 10:1 vol of DCM was added to medium aliquots from A4, T, 5αDIONE, DHT, AST, 3αADIOL and 11KT assays in LNCaP cells and 11OHA4, 11KA4, 11OHT, 11KT, A4 and T assays in PNT2 cells, the samples vortexed at 1000 RPM for 15 min, and centrifuged for 5 min. Extracted media was aspirated, the DCM phase dried under nitrogen and the dried residues dissolved in 0.15 mL 50% methanol in water. A 3:1 vol of MTBE was added to medium aliquots from 11OHA4, 11OHT and 11KDHT assays in LNCaP cells, the samples vortexed at 1000 RPM for 15 min, and frozen at $-80\,°C$. Thereafter the organic phase was removed, dried under nitrogen, and the dried residues dissolved in 0.15 mL 50% methanol in water.

Frozen PCa tissue samples, 100 mg, were lyophilised overnight and homogenised in 5 mL MTBE after addition of internal standard containing testosterone-D2 (1.5 ng) and cortisol-D4 (15 ng), after which samples were sonicated for 10 min. Samples were transferred to screw cap tubes, shaken at 1000 RPM for 60 min, and centrifuged for 10 min. The supernatant was transferred and dried under nitrogen. Dried steroid residues were resuspended in 0.15 mL 50% methanol in water.

Plasma samples (1 mL) were thawed on ice and vortexed after which one 0.5 mL aliquot was deconjugated prior to extraction as described above. Internal standards testosterone-D2 and cortisol-D4, were prepared in MTBE and added to samples to a final concentration of 1.5 ng and 15 ng, respectively. The samples were vortexed in 5 mL MTBE for 15 min at 1000 RPM, and subsequently centrifuged for 5 min. The organic layer was removed and dried under nitrogen after which the dried steroid residue was dissolved in 0.15 mL 50% methanol in water.

T. du Toit et al. / Journal of Steroid Biochemistry & Molecular Biology 166 (2017) 54–67

All samples were stored at −20 °C prior to UHPLC- and UPC²-MS/MS analysis.

2.5. Separation and quantification of steroid metabolites

Stock solutions of A4, T, 5αDIONE, DHT, AST, 3αADIOL, 11OHA4, 11KA4, 11OHT, 11KT, 11KDHT, 11OHAST, 11OH-epiAST, 11KAST, 11K-epiAST and DHT-G were dissolved in absolute ethanol (2 mg/mL) and stored at −20 °C. Two sets of standards ranging from 0.001 to 1 ng/µL were prepared – one in 50% methanol and another series extracted from the appropriate cell culture media using the protocol described in 2.4.

Steroids analysed by UHPLC–MS/MS (ACQUITY UHPLC, Waters, Milford, USA) were separated using a Phenomenex UHPLC Kinetex PFP column (2.1 mm × 100 mm, 2.6 µm) (Torrance, CA, USA) as previously described [34], with modifications to the applied gradient (supplemental Tables 1 and 2). Briefly, the mobile phases consisted of 1% formic acid in water (A) and 49%: 49%: 2% methanol: acetonitrile: isopropanol (B). Steroids, in an injection volume of 5 µL, were eluted at a flow rate of 0.4 mL/min in a total run time of 5 min per sample. A Xevo triple quadrupole mass spectrometer (Waters, Milford, USA) was used for quantitative mass spectrometric detection and steroids were analysed in multiple reaction monitoring (MRM) mode. Electrospray in the positive ionization mode (ESI⁺) was utilized in the MRM mode. The capillary voltage of 3.5 kV, cone voltage of 15–35 V and collision energy of 4–36 eV was set during this quantification. The following settings were used: source temperature 120 °C, desolvation temperature 400 °C, desolvation gas 900 L/h and cone gas 50 L/h. Retention times (RT), parent and daughter ions, cone (V) and collision (eV) voltages, limit of detection (LOD) and limit of quantification (LOQ) are shown in supplemental Table 3.

The C₁₉ steroids analysed by ACQUITY UPC²–MS/MS (Waters Corporation, Milford, USA) were separated as previously described using an ACQUITY UPC² BEH column (3 mm × 100 mm, 1.7 µm particle size) for the A4 and T metabolites and an ACQUITY UPC² BEH 2-Ethylpyridine (EP) column (3 mm × 100 mm, 1.7 µm particle size) for the C11-oxy C₁₉ metabolites [9,35], shown in Fig. 3a and b, with modifications to the applied gradient (supplemental Tables 4 and 5).

The mobile phase consisted of CO_2 modified with methanol in which steroids, in an injection volume of 2 µL, were eluted at a flow rate of 2 mL/min in a total run time of 5 min per sample. The column temperature was set to 60 °C and the automated back pressure regulator (ABPR) was set to 2000 psi. A Xevo TQ-S triple quadrupole mass spectrometer (Waters, Milford, USA) was used for quantitative mass spectrometric detection and all steroids were analysed in MRM mode, using the ESI⁺ mode. A make-up pump was utilized in the system, which fed 1% formic acid in methanol into the mixer preceding the MS line at a constant flow rate of 0.2 mL/min. The capillary voltage of 3.8 kV, cone voltage of 15–35 V and collision energy of 8–30 eV was set during this quantification. The following settings were used: source temperature 120 °C, desolvation temperature 500 °C, desolvation gas 1000 L/h and cone gas 150 L/h. The mass transitions, RT, LOD and LOQ and additional relevant data is shown in Table 1. Data was collected and analysed with the MassLynx 4.1 (Waters Corporation) software program.

2.6. Method validation

Method validation regarding the extraction of steroid metabolites from RPMI-1640 cell culture media (0.5 mL) and subsequent separation and analyses of steroid metabolites using the UHPLC–MS/MS system has been reported previously by Swart et al. [18]. Biological repeats and instrumental repeats were completed and absolute recoveries of steroid metabolites (T, 11OHT, 11KT, A4, 11OHA4 and 11KA4) were reported to be 97.57 ± 14.64% [18]. The chromatographic separation of the steroid metabolites using UHPLC–MS/MS is shown in supplemental Fig. 2 (for separating C₁₉ steroids) and Supplemental Fig. 3 shows the chromatogram for 11KT. Method validation regarding the separation and analysis of steroid metabolites using UPC²-MS/MS was carried out by replicate analysis (n = 3) of cell culture media RPMI-1640 and FBS, spiked with each steroid at low (0.0002 ng/µL), middle (0.02 ng/µL) and high concentrations (0.1 ng/µL), as well as cortisol-D4 (15 ng), progesterone-D9 (15 ng) and testosterone-D2 (1.5 ng) as internal standards. Steroids were extracted and samples prepared as described in 2.4; spiked cell culture media was extracted using DCM and MTBE and spiked FBS was extracted using MTBE. Absolute recoveries and matrix effects, calculated as reported in Taylor et al. [36], are summarized in Supplemental Tables 6a and b. Method validation regarding the UPC²-MS/MS separation and analysis of steroid metabolites in human prostate tissue were carried out by replicate analysis (n = 3) of baboon prostatic tissue (100 mg), spiked with testosterone-D2 (1.5 ng), progesterone-D9 (15 ng), cortisol-D4 (15 ng) and 11β-hydroxyandrostenedione-D7 (15 ng), and steroids extracted as described in 2.4. Process efficiencies are summarized in supplemental Table 7.
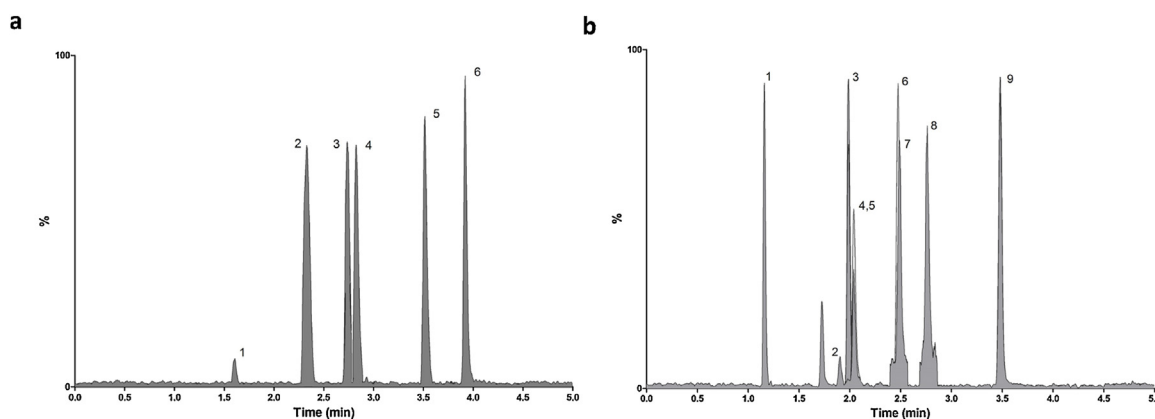
Fig. 3. UPC²-MS/MS separation of C₁₉ reference standards. (a) C₁₉ steroids, 2 µL each of a 0.1 ng/µL standard solution, are depicted in the elution order of (1) 5αDIONE, 1.66 min, (2) A4, 2.35 min, (3) DHT, 2.79 min, (4) AST, 2.86 min, (5) T, 3.53 min and (6) 3αADIOL, 3.93 min; (b) C11-oxy C₁₉ steroids, 2 µL each of a 0.1 ng/µL standard solution, are depicted in the elution order of (1) 11KA4, 1.16 min, (2) 11KAST, 1.91 min, (3) 11OHA4, 1.99 min, (4, 5) 11K-epiAST/11KDHT (clear peak), 2.04 min, (6) 11KT (clear peak), 2.47 min, (7) 11OHAST, 2.49 min, (8) 11OH-epiAST, 2.76 min and (9) 11OHT, 3.48 min.

Table 1

UPC^2-MS/MS detection and quantification of C$_{19}$ steroid standards. Parent molecular ion species and mass transitions of daughter ions; retention time (RT, min); limit of detection (LOD) and limit of quantification (LOQ) of steroids; mass spectrometer settings, cone voltages (CV), collision energy (CE); and internal deuterated standards, testosterone-D2, cortisol-D4 and progesterone-D9.

Steroid metabolite	RT (min)	Mass transitions		CV (V)		CE (eV)		LOD[a] (ng/μL)	LOQ[b] (ng/μL)	Calibration range (ng/μL)	Linearity (r²)
		Quantifier	Qualifier								
A4	2.35	287.2 > 96.9	287.2 > 108.8	30	30	15	15	<0.00001[c]	0.001	0.001−1	0.9968
T	3.53	289.2 > 97.2	289.2 > 109.0	30	30	22	22	<0.00001[c]	0.001	0.001−1	0.9940
5αDIONE	1.66	289.2 > 253.1	289.2 > 97.2	22	30	16	22	0.00025[c]	0.001	0.001−1	0.9993
DHT	2.79	291.2 > 255.0	291.2 > 273.0	25	25	15	20	0.00025[c]	0.001	0.001−1	0.9990
AST	2.86	273.2 > 105.3	291.3 > 273.3	30	18	30	8	0.00025[c]	0.001	0.001−1	0.9962
3αADIOL	3.93	275.2 > 257.0	275.2 > 175.0	15	15	15	15	0.0001[c]	0.001	0.001−1	0.9999
Testosterone-D2	3.53	291.0 > 99.1	291.0 > 111.2	30	30	20	30	–	–	–	–
Cortisol-D4	4.69	367.0 > 121.0		35		25		–	–	–	–
Progesterone-D9	2.18	324.2 > 100.0	324.2 > 113.0	30	30	20	25	–	–	–	–
11OHA4	1.99	303.2 > 267.2	303.2 > 121.0	30	30	30	15	0.00001[c]	0.001	0.001−1	0.9855
11OHT	3.48	305.3 > 121.0	305.3 > 269.0	35	35	20	15	0.00001[c]	0.001	0.001−1	0.9970
11KA4	1.16	301.2 > 257.0	301.2 > 265.2	35	35	25	25	0.00001[c]	0.001	0.001−1	0.9806
11KT	2.47	303.2 > 121.0	303.2 > 267.0	30	30	20	20	0.00001[c]	0.001	0.001−1	0.9955
11OH-5αDIONE	1.52	305.0 > 269.2	305.0 > 287.2	35	35	15	15	–	–	–	–
11K-5αDIONE	0.87	303.2 > 241.0	303.2 > 267.0	35	35	30	25	–	–	–	–
11OHDHT	3.59	307.0 > 253.0	307.0 > 271.0	35	35	20	20	–	–	–	–
11KDHT	2.04	305.2 > 243.0	305.2 > 269.0	30	30	20	20	0.00025[c]	0.001	0.001−1	0.9882
11OHAST	2.49	289.0 > 271.0	289.0 > 213.0	15	15	15	15	0.005[c]	0.01	0.01−1	0.9740
11OH-epiAST	2.76	289.0 > 271.0	289.0 > 213.0	15	15	15	15	0.005[c]	0.01	0.01−1	0.9935
11KAST	1.91	305.0 > 147.2	305.0 > 173.1	30	30	30	30	0.005[c]	0.01	0.01−1	0.9976
11K-epiAST	2.04	305.0 > 147.2	305.0 > 173.1	30	30	30	30	0.01[c]	0.01	0.01−1	0.9993
11K-3αADIOL	3.32	307.0 > 271.0	307.0 > 253.0	15	15	10	10	–	–	–	–
Testosterone-D2	1.71	291.0 > 99.1	291.0 > 111.2	30	30	20	30	–	–	–	–
Cortisol-D4	4.15	367.0 > 121.0		35		25					
Progesterone-D9	0.80	324.2 > 100.0	324.2 > 113.0	30	30	20	25				

[a] Limit of detection was defined as S/N ratio >3.
[b] Limit of quantification was defined as a S/N ratio >10.
[c] [35].

2.7. Statistical analysis

Experiments were performed in triplicate, representative of at least duplicate experiments and the results are given as means ± SEM. Data were processed using GraphPad Prism (version 5) software (GraphPad Software, San Diego, California). Steroids that were not commercially available were quantified by UPC^2-MS/MS, following peak integrations, using response factors, previously determined by Quanson (2015, p. 39) [37], as follows: for 11OH-5αDIONE relative to 11OHA4, 4.147 ± 0.640; for 11K-5αDIONE relative to 11KA4, 4.501 ± 0.549; for 11OHDHT relative to 11OHT, 3.812 ± 0.243 and for 11KDHT relative to 11KT, 2.973 ± 0.179. Standard curves were generated by integrating respective substrates to quantify aforementioned C11-oxy 5α-reduced steroids.

3. Results and discussion

The role of adrenal androgens in CRPC has been widely reported and with the emphasis on A4, the contribution of 11OHA4 to the intratumoral environment has been sorely neglected. The study into the metabolism of the C11 hydroxy- and keto- C$_{19}$ steroid metabolites in PNT2 and LNCaP cells, in conjunction with UPC^2-MS/MS, provides analysis of both free unconjugated and conjugated androgen levels, with steroid profiles highlighting the roles of the steroidogenic enzymes. Steroid profiles also allow for comparative analyses of C$_{19}$ and C11-oxy C$_{19}$ steroids in PCa tissue and in plasma, demonstrating the relevance of adrenal C$_{19}$ precursor steroids in PCa.
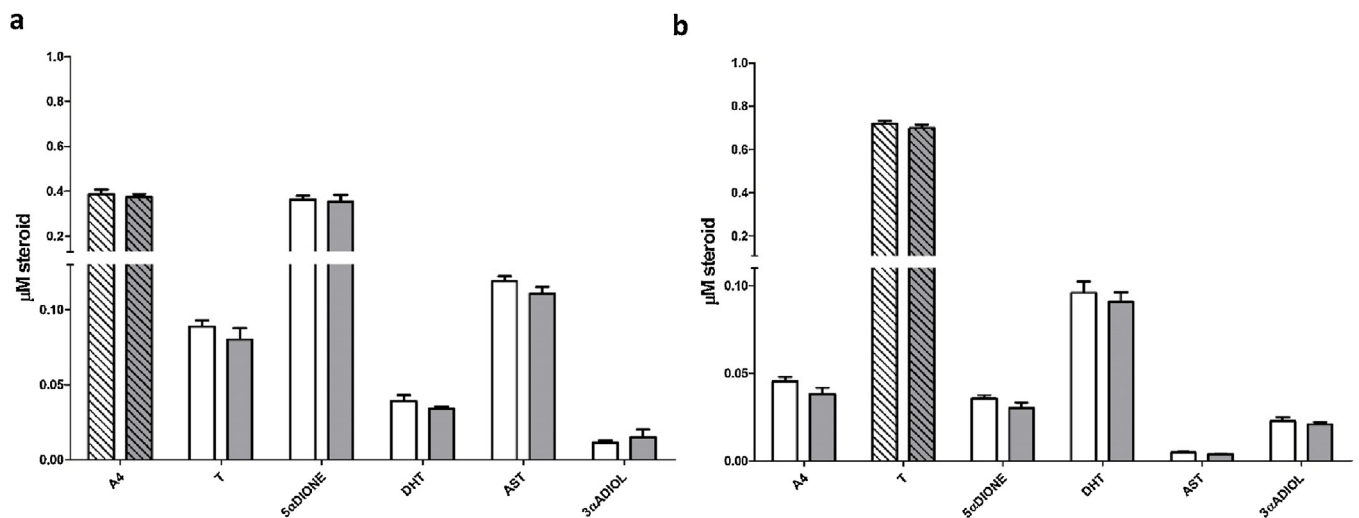
3.1. Androgen metabolism in PNT2 cells

The metabolism of the C11 hydroxy- and keto-metabolites of both A4 and T was firstly investigated in a normal prostate cell model. We assayed these steroids at 1 μM even though their production in the adrenal was reported to be lower, with the exception of 11OHA4 [8], as this allowed detection of their downstream metabolites. Analyses of 11OHA4 (Fig. 4a) and 11OHT (Fig. 4b) showed the conversion of these substrates to their C11-keto products, 11KA4 and 11KT, suggesting the presence of 11βHSD2 in these cells, albeit at very low levels. Only twenty percent 11OHA4 (20%) was converted to 11KDHT via 11KT, and to 11OH-5αDIONE by SRD5A with 80% 11OHA4 remaining after 48 h. The metabolism of 11OHT was similar − 20% was metabolised, yielding the same amount of 11KT. The metabolism of 11KA4 (Fig. 4c) and 11KT (Fig. 4d) was somewhat more efficient than the C11-hydroxy androgens− 40% was metabolised to downstream products. The conversion of 11KA4 yielded mainly 11KT due to catalysis by endogenous reductive 17βHSD activity, and also 11KDHT catalysed by SRD5A. Similarly, 11KT was oxidised to 11KA4 by 17βHSD2 and subsequently inactivated, evident from the levels of C11 keto-AST derivatives, while 10% of the 11KT was reduced by SRD5A yielding 0.1 μM 11KDHT.

While the inactivation of 11KDHT via the formation of 11K-3αADIOL was not evident, the C11-oxy AST derivatives were detected. In addition, glucuronidated steroids were negligibly low with most of the steroids detected at 48 h present in the free form.

In contrast, the metabolism of A4 was far more efficient than that of 11OHA4. More than 50% (0.6 μM) of the A4 substrate was converted to downstream products (Fig. 5a) compared to the significantly lower conversion of 11OHA4 (≈20%). Analysis of the
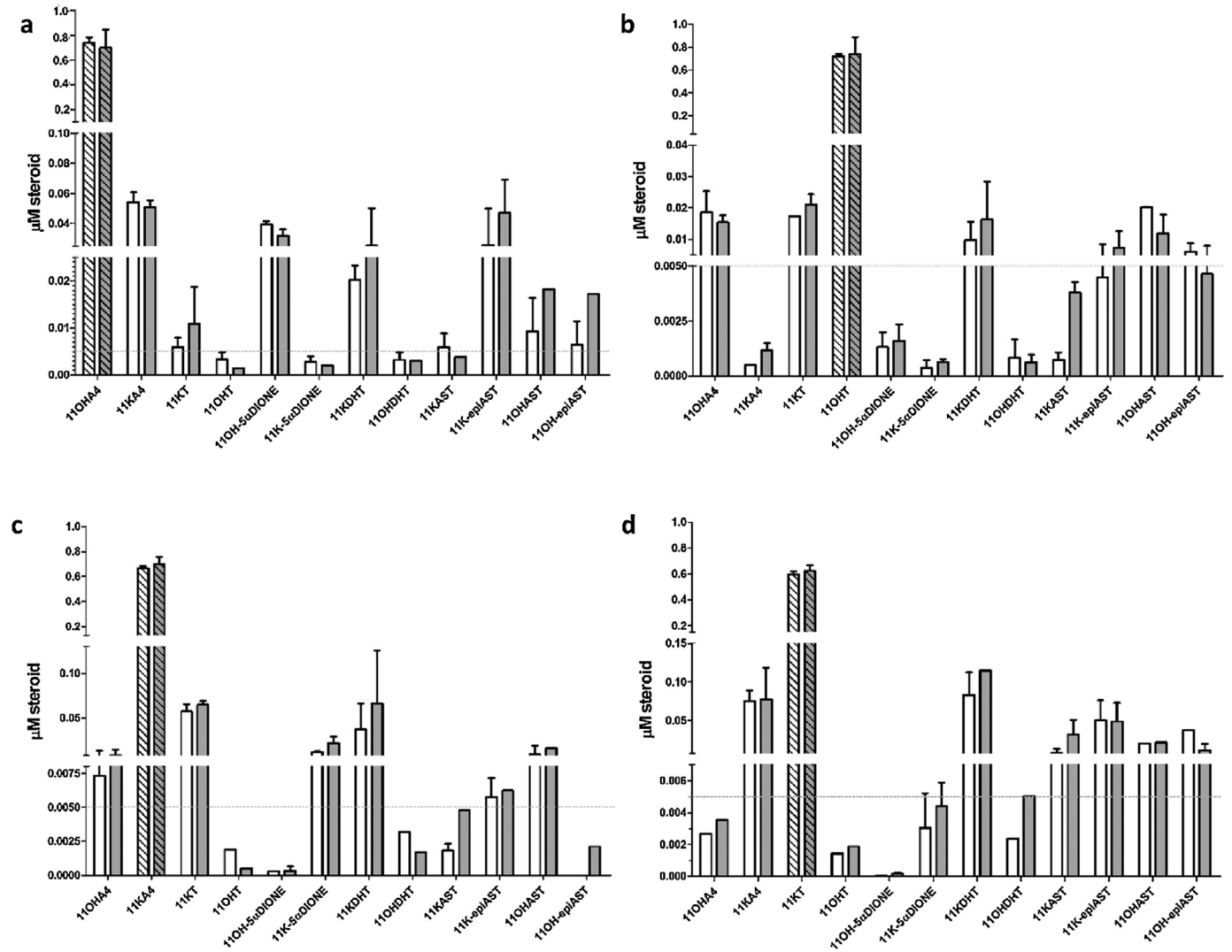
Fig. 4. C11-oxy androgen metabolism in PNT2 cells: (a) 11OHA4; (b) 11OHT; (c) 11KA4 and (d) 11KT. Steroid (1 μM; patterned bars) was assayed after 48 h and free unconjugated steroids depicted as clear bars and total steroids as shaded bars. The experiment was performed in triplicate, analysed by UPC^2-MS/MS and the results expressed as the mean ±SEM (n = 3). Steroid levels below the dashed grey line represent steroids detected below the level of accurate quantification.

Fig. 5. Steroid (1 μM; patterned bars) metabolism in PNT2 cells: (a) A4 and (b) T was assayed after 48 h and free unconjugated steroids depicted as clear bars and total steroids as shaded bars. The experiment was performed in triplicate, analysed by UPC^2-MS/MS, representative of two independent experiments. Results are expressed as the mean ± SEM (n = 6).

steroid profiles showed that the catalytic activity of SRD5A towards A4 was more efficient than that of the reductive 17βHSD activity was in catalysing T's biosynthesis, reflected in the significantly lower levels of T produced relative to 5αDIONE after 48 h. Although 17βHSD3 and AKR1C3 mRNA expression levels are similar to SRD5A1 and SRD5A2 in normal prostate tissue [2], A4 is nevertheless preferentially converted to 5αDIONE suggesting that the 'alternative' 5αDIONE pathway also takes precedence in normal cells. 5αDIONE, in turn, is further metabolised to DHT and AST. While DHT is formed from both 5αDIONE and T, DHT levels detected in the conversion of A4 are much lower than in the conversion of T, 0.05 μM and 0.1 μM, respectively. In addition, the conversion of T (Fig. 5b) to downstream metabolites appears to be less efficient with 70% of the substrate remaining after 48 h.

Data also suggests that the reductive 17βHSD activity is predominant compared to the oxidative activity since A4 was more readily converted to T (≈ 0.1 μM T; Fig. 5a) while the conversion of T to A4 (≈ 0.05 μM A4; Fig. 5b) was markedly lower. These findings are supported by data reported by Berthaut et al. [38] showing predominant 5α-reductase activity converting T to DHT with negligible conversion of T to A4 in isolated epithelial cells. Our data showed that the conversion of T and 11KT yielded similar levels of DHT and 11KDHT (≈ 0.1 μM), respectively– suggesting an equal contribution to the AR agonist pool provided by adrenal C_{19} precursors T and 11KT.

Interestingly, glucuronide derivatives of T, DHT and their inactive metabolites were not detected. UGT2B15 and 17 have however been shown in normal prostate tissue with UGT2B17 expressed only in basal epithelial cells of the alveoli where it catalyses the conjugation of T, DHT, ADT and 3αADIOL. UGT2B15 is expressed in luminal epithelial cells and since the inactivating enzymes are not expressed in these cells the enzyme modulates AR interaction by conjugating T and DHT [20,39]. Reports regarding steroid metabolism in PNT2 cells are limited and with our analyses showing no detectable glucuronides in the metabolism of A4 and T, together with negligible levels of conjugated downstream 11OHA4 and 11OHT metabolites (detected below the limit of accurate quantification), suggest that these UGT isoforms are not active. It has furthermore been reported that PNT2 cells, although derived from normal human prostatic epithelium tissue, exhibit some characteristics of prostatic tumours, and present with genetic alterations found in prostatic tumours [40].

Androgen metabolism has, to date, not been characterized in the PNT2 cell model. Our data shows no catalytic activity of UGTs towards T and its downstream metabolites, indicating that this cell line presents itself as an ideal cell model to study androgen metabolism in the absence of glucuronidation.

3.2. Androgen metabolism in LNCaP cells

Since LNCaP cells metabolise the C11-oxy C_{19} steroids to yield active androgens [12] and exhibit high glucuronidation activity [19,41–43], this cell model was used to investigate the downstream inactivation and conjugation of the C11-oxy steroids. In LNCaP cells, 11OHA4 is metabolised by 11βHSD2 and SRD5A to yield 11KA4 and 11OH-5αDIONE, respectively [44,45]. Analysis of steroid profiles showed that 11OHA4's metabolism (Fig. 6a) yielded predominantly 11KA4, together with the inactive C11-oxy AST derivatives. 11KT was the only C11-oxy T derivative detected with negligible 11OHT forming due to 11OHA4 not being reduced by 17βHSD. In addition, 50% of 11KT (0.06 μM) was in the free form after 96 h, while unconjugated 11KAST and 11OHAST were also detected, albeit at low levels, these steroids could recycle to active androgens. In contrast, 11OHT can be metabolised (Fig. 6b) by 17βHSD2, 11βHSD2 and SRD5A to yield 11OHA4, 11KT and 11OHDHT, respectively. Analysis showed that while 0.672 μM 11OHT had been conjugated with no free steroid present after 96 h, the steroid was also converted to 11OHA4 (0.164 μM), 11KA4 (0.121 μM) and 11KT (0.266 μM). 11KT was, however, also present in the free form at 0.078 μM ($\approx 30\%$). We did not detect 11KDHT or 11OHDHT in either of the assays. We also did not detect these metabolites in the metabolism of 11OHA4 and 11OHT in our previous study even though independent duplicate samples aliquots were pooled– 11KDHT was detected only when 1 μM 11OH-5αDIONE and 11OHDHT were assayed as substrates [9]. These data suggest that in the metabolism of 11OHA4 and 11OHT in LNCaP cells, the major C11-oxy T derivative to be produced is 11KT.

Considering the output of the adrenal in terms of 11OHA4 it would seem that 11KT, given the inefficiency of its conjugation, would contribute markedly to AR activation and downstream physiological effects. The expression of 11βHSD2 is central to the production of active androgens as is evident in the analysis of the conversion of 11OHA4 and 11OHT in LNCaP cells. However, in both cell lines, the presence of 11βHSD2 led to the production of 11KT.
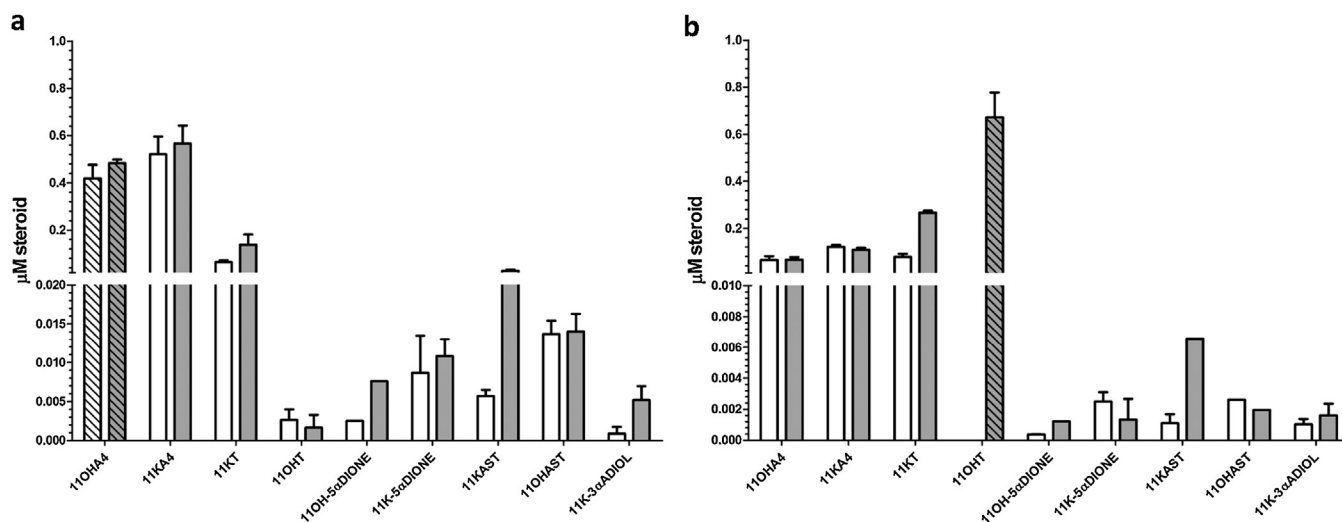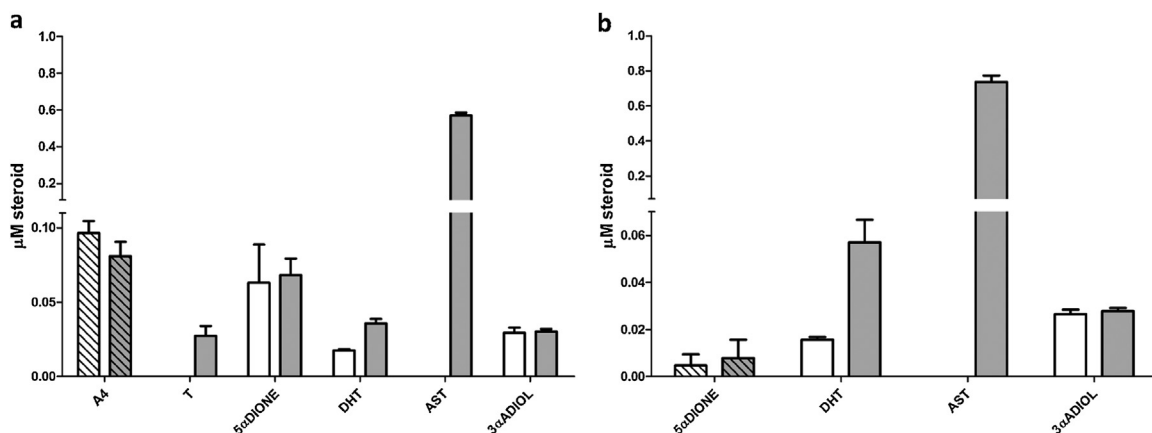

Fig. 6. Steroid (1 μM; patterned bars) metabolism in LNCaP cells: (a) 11OHA4 and (b) 11OHT was assayed after 96 h and free steroids depicted as clear bars and total steroids as shaded bars. The experiment was performed in triplicate, analysed by UPC²-MS/MS, the results are expressed as the mean ± SEM (*n* = 3).
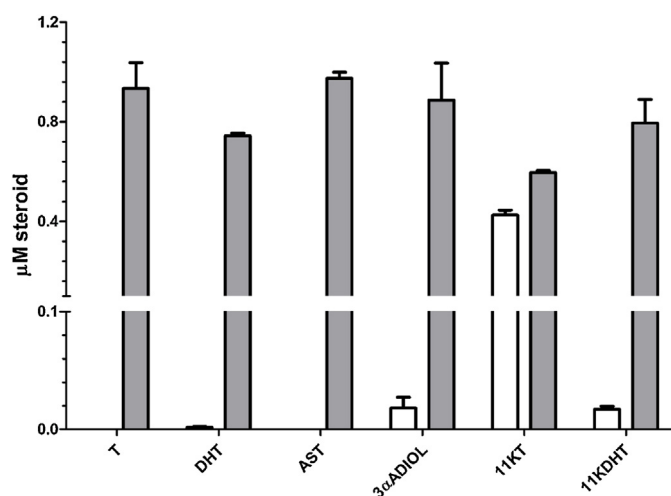
The conversion of 11OHT to 11KT by 11βHSD2, converts a partial agonist to a full agonist [11], placing 11βHSD2 central to the potency of these metabolites.

Analysis of A4 metabolism in LNCaP cells clearly demonstrated the preferred conversion of A4 to 5αDIONE, followed by the conversion of 5αDIONE to DHT by reductive 17βHSD− data supporting the predominant 'alternative' 5αDIONE pathway in the biosynthesis of DHT in these cells (Fig. 7a). Data showed that the catalytic activity of endogenously expressed SRD5A towards A4 in producing 5αDIONE was more efficient, compared to T in the biosynthesis of DHT (Supplemental Fig. 4a). In the conversion of A4, the major flux was towards AST ($\approx$0.6 µM) via 5αDIONE ($\approx$0.07 µM), with no free AST detected after 48 h. Analyses detected T, indicating conversion of A4 to T by reductive 17βHSD, however, at low levels and in the glucuronidated form only, with ±50% ($\approx$0.02 µM) of the detected DHT being unconjugated. Negligible conversion of T to DHT by SRD5A was further evident from the low DHT levels detected when T was assayed as substrate, again showing more efficient glucuronidation of T with $\approx$0.9 µM of the steroid present in the conjugated form. These steroid profiles also suggests that reductive 17βHSD activity, catalysing the conversion of the A4 derivatives to T derivatives, takes precedence over the oxidative 17βHSD activity catalysing the reverse reactions in these cells. It is, however, possible that the UGT2B isoforms, catalysing the conjugation were simply more efficient than 17βHSD. UGT2B15 and UGT2B17 are both expressed in LNCaP cells with the latter conjugating glucuronide formation at both C15 and C17 hydroxyl groups [42,46]. It was shown that UGT2B17, when transiently expressed in HEK293 cells, conjugated DHT most efficiently followed by AST, and 3αADIOL, while conjugation of T was 5-fold less efficient than that of DHT [46]. Our analyses, however, indicate downstream conversion of DHT with 0.74 µM being conjugated, while very little downstream conversion of T was detected with most of the steroid being conjugated (Supplemental Fig. 4a and b).

Effective inactivation and glucuronidation is further demonstrated in Fig. 7b in which 5αDIONE and DHT were converted to AST and 3αADIOL in reactions catalysed by AKR1C2. The conjugation of AST was highly efficient with no free AST being detected (also confirmed in Supplemental Fig. 4c). Most of the 3αADIOL was detected in the conjugated form when assayed as substrate (Supplemental Fig. 7d) with low levels of the free form present possibly accounting for the DHT detected. It is interesting to note that when DHT was assayed only conjugated DHT was detected after 48 h (Supplemental Fig. 4b). In contrast, when

Fig. 8. Analyses of conjugated steroid products in LNCaP cells. Individual steroid substrates (1 µM) were incubated for 48 h and metabolites analysed. Free unconjugated steroids depicted as clear bars and total steroids as shaded bars. The experiment was performed in triplicate, analysed by UHPLC–MS/MS (T, DHT, AST, 3αADIOL and 11KT) and UPC²-MS/MS (11KDHT), representative of two independent experiments. Results are expressed as the mean ± SEM (*n* = 6).

produced as an intermediate, the free form of DHT was always detected together with conjugated DHT, albeit at low levels.

We also assayed 11KT and 11KDHT in LNCaP cells after 48 h to determine free and conjugated steroid levels in order to compare the conjugation of the C_{19} and C11-oxy C_{19} steroids (Fig. 8). As discussed in the aforementioned text, AST and 3αADIOL, the inactive derivatives of 5αDIONE and DHT, may either be conjugated or may undergo reactivation by RL-HSDs (17βHSD6) or 17βHSD10 [15,20,47]. Although AST is conjugated at C3 only and 3αADIOL at both C3 and C17, the former was detected in the conjugated form (0.97 µM) only, indicating that the steroid had not been converted to 5αDIONE (Supplemental Fig. 4c). Negligibly lower levels of conjugated 3αADIOL (0.87 µM) was detected, together with free 3αADIOL (0.018 µM) which was also channelled to DHT (Supplemental Fig. 4d). When assayed, DHT was converted to downstream products evident from the 0.74 µM present in the conjugated form after 48 h, of which free DHT was negligible and 3αADIOL contributed 0.097 µM (Supplemental Fig. 4b). T was conjugated efficiently with minimal conversion to downstream

Fig. 7. Steroid (1 µM; patterned bars) metabolism in LNCaP cells: (a) A4 and (b) 5αDIONE was assayed after 48 h and free unconjugated steroids depicted as clear bars and total steroids as shaded bars. The experiment was performed in triplicate, representative of two independent experiments analysed by UHPLC–MS/MS. Results are expressed as the mean ± SEM (*n* = 6).

products (Supplemental Fig. 4a), 0.93 μM being present in the conjugated form with no free T present. In assaying 11KDHT as substrate our data showed that only ≈20% of the steroid was metabolised after 48 h, comparable to DHT, with 11KDHT-glucuronide levels detected at 0.78 μM. The level of free 11KDHT (0.017 μM) were significantly higher (10-fold) than the levels of free DHT.

It is interesting to note that the levels of the other C_{19} glucuronide metabolites were all greater than 0.75 μM. Glucuronidation is, however, not the only form of conjugation that occurs in vitro and in vivo, as androgens may also undergo sulphonation. Our assays and UHPLC- and UPC^2-MS/MS analyses did not include sulphonated conjugates or other steroid products that may have formed by endogenous CYP enzymes catalysing hydroxylation or methylations [48–56]. It is therefore possible that additional products may have formed during the long incubation periods.

11KT was predominantly present in the free form (70%) when 11KT was assayed as substrate, reflecting the inefficient glucuronidation of 11KT also observed for the metabolism of 11OHA4 and 11OHT in LNCaP cells – inefficient glucuronidation of 11KT possibly affecting elimination, together with subsequent reactivation would have implications in PCa. We previously showed that 11KT is able to bind the AR as a partial agonist at 1 nM and as a full agonist at 10 nM [9,11]. Since 11KT may thus remain available, the steroid may influence transcription levels of AR regulated genes, more so than T, DHT and 11KDHT in PCa. DHT has been shown to induce the upregulation of a number of androgen responsive genes in LNCaP cells in which the expression of UGT2B15 and UGT2B17 were silenced [20]. In addition, AR activation by 11KT could be exaggerated due to AR mutations in the ligand binding domain, reducing AR-ligand specificity with an ensuing increase in AR gene amplification and expression of mutated AR variants that are constitutively active in PCa [57,58]. Since 11KT may also bind mutant receptors more readily than other androgens the presence of this active androgen may lead to increased transcription and cell proliferation despite ADT, which targets only T in the biosynthesis of DHT.

3.3. In vivo C_{19} steroid profiles

We have shown that 11OHA4, in the presence of 11βHSD2, is metabolised in normal and PCa cell models in much the same manner as A4, with our data suggesting differential inactivation and conjugation of the 5α-reduced C11-oxy C_{19} steroids. It is possible that the hampering of the inactivation and conjugation, by the presence of either the functional hydroxyl or keto group at C11, may affect cellular processes via the AR. The relevance of these steroids in PCa and their contribution to the diseased state can only be assessed by establishing their presence in PCa tissue as well as in circulation. We thus analysed C_{19} steroid levels in prostate tissue as well as in plasma obtained from PCa patients using UPC^2-MS/MS, which allows a more sensitive and robust means of analysing and quantifying metabolites in the nM range.

3.3.1. PCa tissue

In this investigation we aimed at identifying the intratumoral C11-oxy C_{19} steroids, which have, to date, not been shown, and to quantitate these steroids relative to the known C_{19} androgens and their metabolites. Profiles of free, unconjugated steroid metabolites in PCa tissue from both patient tissue specimens (A and B) showed that 11OHA4 and its downstream metabolites were present at far higher levels that A4, T and their metabolites (Fig. 9). Comparative analyses of individual metabolites are hampered due to the variability of steroid levels reported to date, possibly due to sample collection strategies, steroid extraction and analytical techniques. For example, in both patient samples T levels, 2.56 and 6.3 ng/g, were detected to be far higher than those in normal tissue (0.2–1.8 ng/g) which is expected, but normal ranges for DHT (0.7–9.3 ng/g) [59], placed both patients at the lower end with their DHT levels, 1.06 and 1.77 ng/g. On the other hand, in PCa tissue DHT levels were reported between 0.66 and 6.98 ng/g with T levels 0.4–1.34 ng/g [59]. The data obtained in the case of patient A can however be compared to levels reported in a study by Heracek et al. [60], which included 121 untreated patients, with A4, T and DHT levels of 1.4, 1.3 and 2.5 ng/g,
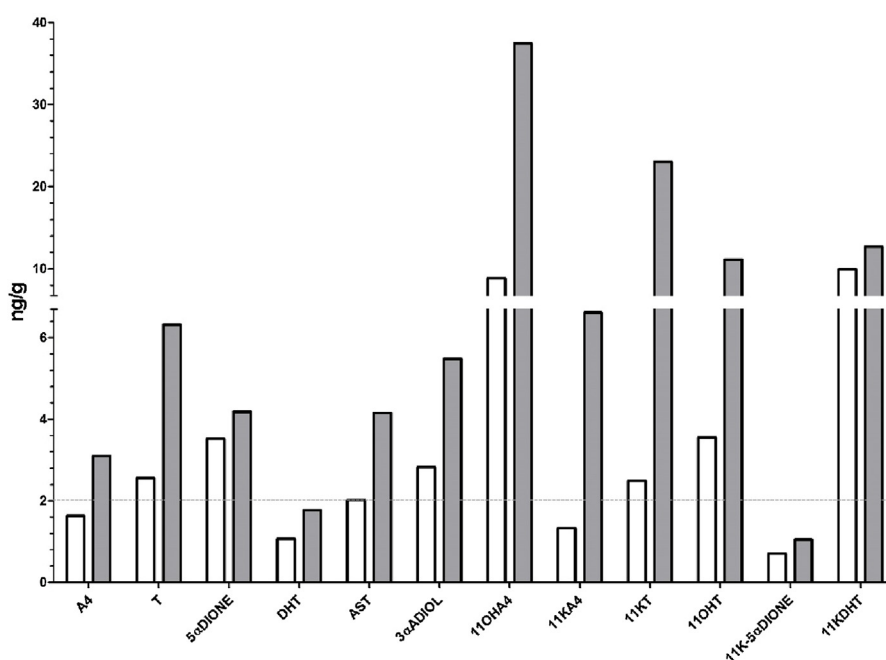
Fig. 9. UPC^2-MS/MS analysis of C_{19} steroid levels in PCa tissue. Steroids represented as free unconjugated steroids; clear bars, patient A, no prior treatment; shaded bars, patient B, treatment with an androgen antagonist. Steroids below the dashed line represent steroids detected below the level of accurate quantification.

respectively. However, the ±SEM values were high indicating possible inter-patient variability also contributing to the wide ranges that have been reported for normal and disease values. In both patients the downstream metabolites of A4 and T followed a similar profile, with the exception of 5αDIONE. Regardless of the higher A4 levels in patient B, 5αDIONE levels were comparable which indicate that patient B formed less of the intermediate than patient A, suggesting differences in SRD5A activity. Also suggestive of a greater SRD5A activity in patient A, are the comparable levels of 11KDHT (9.9 and 12.6 ng/g) despite the 11KT precursor being 9-fold lower in patient A's tissue.

In the steroid profiles only two SRD5A products, namely 11KDHT and 11K-5αDIONE (a 11KDHT precursor steroid) were detected whilst 11OHDHT and 11OH-5αDIONE were not. It is possible that 11OHDHT may be present in the conjugated form and that 11OH-5αDIONE together with 11K-5αDIONE may have been inactivated by AKR1C2 and subsequently conjugated. No other 5α- or 3α-reduced metabolites were detected in the free form, other than 11KDHT and 11K-5αDIONE – which suggests either the predominant production of these keto-dihydro derivatives or alternatively, the inactivation and conjugation of the other 5α-reduced metabolites.

Although the presence of 11OHA4, 11KA4, 11OHT and 11KT in the tissue samples was not an unexpected finding since these are produced by the adrenal, the levels at which the latter three metabolites were detected was surprising. The expression of 11βHSD2 in peripheral tissue, as well as in PCa tissue [44,45] will yield 11KA4 and 11KT from their respective C11-hydroxy precursors [18] and while the adrenal produces high levels of 11OHA4, which can account for the high levels thereof in PCa, the high 11OHT levels cannot be attributed solely to adrenal production. Although CYP11B1 and CYP11B2 have been reported to be expressed in human primary prostate carcinomas and metastatic primary prostate carcinomas [48,49], we have not detected hydroxylation of A4 or T at C11 in LNCaP cells. T has been shown to be hydroxylated at C11 in liver microsomal preparations [61–63] and by CYP3A4 [48,50] and CYP3A5 [51] which are expressed in PCa tissue and may thus produce 11OHT, and may as such contribute towards the pool of C11 hydroxy- and keto C_{19}

metabolites observed in prostate tissue [52–56]. 11OHT can furthermore be converted by the oxidative activity of 17βHSD2 to 11OHA4 and subsequently to 11KA4. Both 11KA4 as well as 11OHT can be converted to 11KT, further accounting for the high 11KT levels (23 ng/g).

Although DHT levels were significantly lower than 11KDHT in both patient samples cases (7- and 9-fold), the DHT levels were comparable with other studies [3,59,64,65] and still fell within the physiological relevant range able to activate the AR. It is apparent that the presence of 11OHA4 in both patients suggests a major influx from adrenal origin, and together with the downstream metabolites, present a pool of intratumoral C_{19} steroids of which 11KDHT and 11KT are the most prominent in the tissue.

3.3.2. Plasma

Since androgens play an important role in the progression of PCa, ADT, the mainstay in metastatic PCa treatment, strives to eliminate the source of DHT by decreasing circulating T levels. Circulating C_{19} steroids are indicators of ADT efficacy and are generally accepted to be <0.69 nM (20 ng/dL) [66]. This is, however, not always achieved in all PCa patients and the variations reported are likely due to the contribution of adrenal C_{19} steroids [67,68]. We therefore profiled the adrenal C_{19} steroids in plasma samples obtained from PCa patients and showed that the levels of 11OHA4 and its downstream metabolites far exceed those of A4, T and their downstream metabolites. In Fig. 10 we show C_{19} steroid levels in two patients after treatment, one who had undergone physical and the other chemical castration. Although the C_{19} steroid levels A4, 0.77 and 0.306 nM; T, 3.5 and 2.38 nM and DHT, 0.138 and 0.114 nM were low and T specifically well below the normal circulating T levels (15.4 ≈ 5.6 nmol/L) [69], collectively the C_{19} steroids were above the cut-off for ADT efficacy. However, while T levels were higher than the generally accepted castrate levels, DHT levels were similar to the reported DHT castrate levels (0.5–0.18 nM) [66–68]. It is interesting to note that the down-stream inactive products of DHT and 5αDIONE ranged from 22 to 170 nM. The levels of AST and 3αADIOL may also be of significance as, when in circulation, these steroids can be taken up by the prostate and oxidised by RL-HSDs to DHT. Analysing the complete
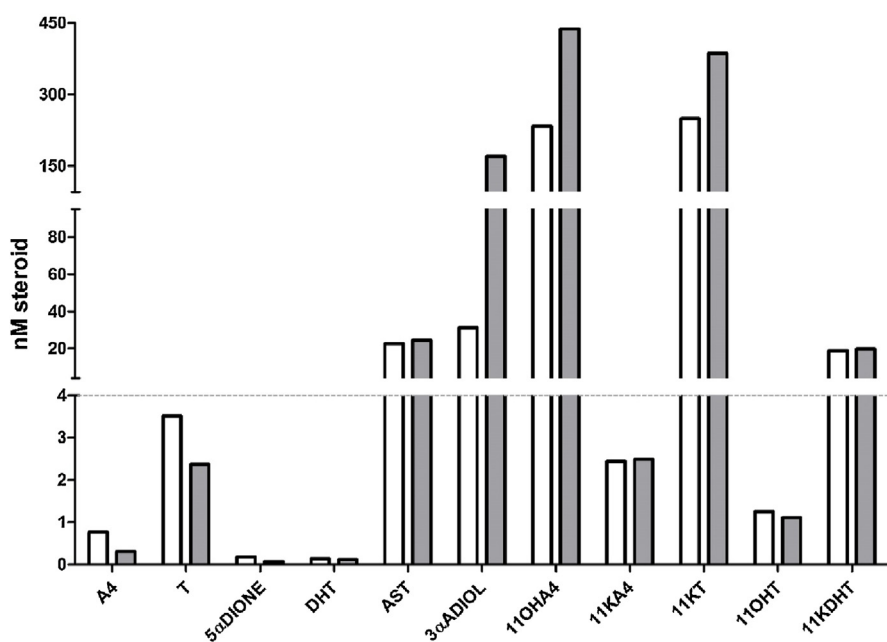
Fig. 10. UPC²-MS/MS analysis of plasma C_{19} steroid levels of PCa patients. Steroids represented as total steroids; clear bars, patient treatment BO, shaded bars, patient treatment LHRH analogue. Steroids below the dashed line represent steroids detected below the level of accurate quantification.

C_{19} panel and not only T and DHT, indicates a shunt of C_{19} steroids in the alternate or conventional pathways and also highlights the fact that these are downstream products of A4 and T in peripheral tissue.

In targeting T only in order to circumvent DHT in treatment regimes, the C11-oxy androgens are overlooked. These steroids could certainly be considered in combination therapies which would include, in addition to chemical/surgical castration, CYP17A1 or CYP11B1 inhibitors to either inhibit the biosynthesis of A4 and T by CYP17A1, for instance by abiraterone acetate, which has been proven to be effective in survival of CRPC patients [70,71] or the biosynthesis of 11OHA4 and 11OHT by CYP11B1 in the adrenal. Our analysis show 11OHA4 and 11KT, C11-oxy derivatives of A4 and T, to be present at levels significantly higher than the C_{19} steroids, $\approx$850-fold and $\approx$115-fold, respectively (Fig. 10). 11KDHT was detected at levels $\approx$136- and $\approx$170-fold more than DHT and while no other C11-oxy 5α- or 3α-reduced metabolites were detected, 11KT was present at significantly higher levels than 11KDHT, 13- and 19-fold. Our data obtained in LNCaP cells which suggest that 11KT is poorly conjugated by the UGT enzymes together with the high levels of 11KT detected in plasma samples, certainly implicate 11KT as a role player in PCa. This is the first analyses of the C11-oxy C_{19} steroids in plasma obtained from PCa patients and serve only to demonstrate the presence of these steroids in circulation. Although 11OHA4, 11KA4, 11OHT and 11KT have been shown in iliac vein samples in women diagnosed with adrenal aldosterone-producing adenoma, these were reported to be very low (<3.5 nM) both pre- and post ACTH stimulation [8]. It is interesting to note that, although the analysis of tissue and plasma represents four different PCa patients, 11KDHT levels were high in all cases and at these levels in prostatic tissue 11KDHT would certainly activate the AR, suggesting that circulating adrenal androgens contribute to post-castration tissue androgen levels.

In our analyses we also investigated the glucuronidation of these C11-oxy steroids in plasma and found the glucuronide conjugates to be negligible. Our data therefore presents unconjugated steroid levels only. It is possible that these steroids may have been sulphonated, which may also be the case in the PCa tissue analysed. Although sulphonation of steroids by SULT2B has been reported in prostate tissue, glucuronidation is a major route of C_{19} steroid catabolism, with reports showing urinary T predominantly present as T-glucuronide compared to its sulfonated conjugated form [33]. In addition, the reduced expression of SULT2B has been reported in PCa specimens [72]. It should be noted that β-conformations of steroids, such as T (C17 hydroxyl group) and AST (C3 hydroxyl group) have been shown to be predominantly sulphonated and not glucuronidated [31,33,46], however, the production of these epi(3β)-steroids were minimal in steroid conversion assays in prostate cell models, and none of these steroids were detected in PCa tissue or plasma (data not shown). Conjugation of the C11-oxy C_{19} steroids in tissue still remains to be investigated.

4. Conclusion

Taken together, these studies show that while C11-oxy C_{19} steroids are metabolised in the androgen-dependent cancer cell model and in the normal cell model, albeit to a lesser degree, 11βHSD2 has an integral role in driving the 11OHA4-derived pathway, most prominent in the LNCaP cells. On the other hand, SRD5A was more efficient than the reductive 17βHSDs expressed endogenously in PNT2 and LNCaP cells regarding the metabolism of A4 suggesting that the alternative pathway is the preferred pathway in PNT2 cells as is the case in LNCaP cells. Although glucuronidation activity in PNT2 cells was negligible, steroid

conjugation was efficient in LNCaP cells (T-glucuronide > DHT-glucuronide > 11KDHT-glucuronide) – with the exception of 11KT. Inefficient conjugation of 11KT and activation of the AR would further impact PCa progression in ADT regimes targeting T only. 11KT is inevitably shunted to downstream metabolites since it is only marginally glucuronidated, with free 11KT and its downstream metabolites able to exert physiological effects via the AR.

The relevance of these C11-oxy C_{19} steroids came to the fore in our steroid profile analysis of PCa tissue and plasma. This is the first report of C11-oxy C_{19} steroids in vivo, and our data show that these steroid levels are significantly higher compared to the C_{19} steroids, both in circulation and in tissue of PCa patients. In addition, 11KT and 11KDHT were significantly higher than DHT in plasma which was also the case in tissue, together with high 11OHT levels. Since the data represent four case studies only, no deductions other than comparing C11-oxy C_{19} steroid levels to the C_{19} steroid levels and analysing the respective pathways, can be made. However, steroid profiles generated using UPC^2-MS/MS, highlight subtle differences that would otherwise have been overlooked in the analyses of only single steroids – for example; low A4, T and DHT plasma levels present no indication of inactive products formed from these precursor steroids in the tumor microenvironment.

The steroid profiles presented in this study substantiate the importance of adrenal 11OHA4 as a significant androgen precursor underscoring its role in PCa. Although 11OHA4 exhibits no androgenic activity, our findings clearly show that this much neglected adrenal androgen can no longer be excluded when assessing the progression of PCa and the efficacy of treatment regimes.

Conflict of interest

The authors declare that there is no conflict of interest.

Acknowledgements

Appendix A. Supplementary data

Supplementary data associated with this article can be found, in the online version, at http://dx.doi.org/10.1016/j.jsbmb.2016.06.009.

References

[1] M. Stanbrough, G.J. Bubley, K. Ross, T.R. Golub, M.A. Rubin, T.M. Penning, et al., Increased expression of genes converting adrenal androgens to testosterone in androgen-independent prostate cancer, Cancer Res. 66 (2006) 2815–2825, doi:http://dx.doi.org/10.1158/0008-5472.CAN-05-4000.

[2] V. Luu-The, A. Bélanger, F. Labrie, Androgen biosynthetic pathways in the human prostate, Best Pract. Res. Clin. Endocrinol. Metab. 22 (2008) 207–221, doi:http://dx.doi.org/10.1016/j.beem.2008.01.008.

[3] R.B. Montgomery, E.A. Mostaghel, R. Vessella, D.L. Hess, T.F. Kalhorn, C.S. Higano, et al., Maintenance of intratumoral androgens in metastatic prostate cancer: a mechanism for castration-resistant tumor growth, Cancer Res. 68 (2008) 4447–4454, doi:http://dx.doi.org/10.1158/0008-5472.CAN-08-0249.

[4] M.N. Stein, S. Goodin, R.S. Dipaola, Abiraterone in prostate cancer: a new angle to an old problem, Clin. Cancer Res. 18 (2012) 1848–1854, doi:http://dx.doi.org/10.1158/1078-0432.CCR-11-1805.

[5] F. Labrie, Intracrinology: its impact on prostate cancer, Curr. Opin. Urol. 3 (1993) 381–387.

[6] J.F. Larsen, S. Walter, T. Krarup, Complete androgen blockade as primary treatment for advanced metastatic cancer of the prostate, Int. Urol. Nephrol. 22 (1990) 249–255, doi:http://dx.doi.org/10.1007/BF02550402.

[7] N. Sharifi, R.J. Auchus, Steroid biosynthesis and prostate cancer, Steroids 77 (2012) 719–726, doi:http://dx.doi.org/10.1016/j.steroids.2012.03.015.

[8] J. Rege, Y. Nakamura, F. Satoh, R. Morimoto, M.R. Kennedy, L.C. Layman, et al., Liquid chromatography – tandem mass spectrometry analysis of human adrenal vein 19-carbon steroids before and after ACTH stimulation, J. Clin. Endocrinol. Metab. 98 (2013) 1182–1188, doi:http://dx.doi.org/10.1210/jc.2012-2912.

[9] L.M. Bloem, K.H. Storbeck, P. Swart, T. Du Toit, L. Schloms, A.C. Swart, Advances in the analytical methodologies: profiling steroids in familiar pathways-challenging dogmas, J. Steroid Biochem. Mol. Biol. 153 (2015) 80–92, doi:http://dx.doi.org/10.1016/j.jsbmb.2015.04.009.

[10] A.C. Swart, K. Storbeck, 11β-Hydroxyandrostenedione: downstream metabolism by 11βHSD 17βHSD and SRD5A produces novel substrates in familiar pathways, Mol. Cell. Endocrinol. 408 (2015) 114–123, doi:http://dx.doi.org/10.1016/j.mce.2014.12.009.

[11] K. Storbeck, L.M. Bloem, D. Africander, L. Schloms, P. Swart, A.C. Swart, 11β-Hydroxydihydrotestosterone and 11-ketodihydrotestosterone, novel C_{19} steroids with androgenic activity: a putative role in castration resistant prostate cancer? Mol. Cell. Endocrinol. 377 (2013) 135–146, doi:http://dx.doi.org/10.1016/j.mce.2013.07.006.

[12] L.M. Bloem, K.H. Storbeck, L. Schloms, A.C. Swart, 11β-Hydroxyandrostenedione returns to the steroid arena: biosynthesis, metabolism and function, Molecules 18 (2013) 13228–13244, doi:http://dx.doi.org/10.3390/molecules181113228.

[13] W.L. Miller, R.J. Auchus, The molecular biology, biochemistry, and phsiology of human steroidogenesis and its disorders, Endocr. Rev. 32 (2011) 81–151, doi:http://dx.doi.org/10.1210/er.2010-0013.

[14] J. Rege, W.E. Rainey, The steroid metabolome of adrenarche, J. Endocrinol. 214 (2012) 133–143, doi:http://dx.doi.org/10.1530/JOE-12-0183.

[15] E.A. Mostaghel, Steroid hormone synthetic pathways in prostate cancer, Transl. Androl. Urol. 2 (2013) 212–227, doi:http://dx.doi.org/10.3978/j.issn.2223-4683.2013.09.16.

[16] R. Mindnich, G. Möller, J. Adamski, The role of 17 beta-hydroxysteroid dehydrogenases, Mol. Cell. Endocrinol. 218 (2004) 7–20, doi:http://dx.doi.org/10.1016/j.mce.2003.12.006.

[17] K. Chang, R. Li, M. Papari-zareei, L. Watumull, Y. Daniel, R.J. Auchus, Dihydrotestosterone synthesis bypasses testosterone to drive castration-resistant prostate cancer, Proc. Natl. Acad. Sci. 108 (2011) 13728–13733, doi:http://dx.doi.org/10.1073/pnas.1107898108/-/DCSupplemental. www.pnas.org/cgi/doi/10.1073/pnas.1107898108.

[18] A.C. Swart, L. Schloms, K. Storbeck, L.M. Bloem, T. Du Toit, J.L. Quanson, et al., 11β-Hydroxyandrostenedione, the product of androstenedione metabolism in the adrenal, is metabolized in LNCaP cells by 5α-reductase yielding 11β-hydroxy-5α-androstanedione, J. Steroid Biochem. Mol. Biol. 138 (2013) 132–142, doi:http://dx.doi.org/10.1016/j.jsbmb.2013.04.010.

[19] S. Chouinard, O. Barbier, A. Bélanger, UDP-glucuronosyltransferase 2B15 (UGT2B15) and UGT2B17 enzymes are major determinants of the androgen response in prostate cancer LNCaP cells, J. Biol. Chem. 282 (2007) 33466–33474, doi:http://dx.doi.org/10.1074/jbc.M703370200.

[20] O. Barbier, A. Bélanger, Inactivation of androgens by UDP-glucuronosyltransferases in the human prostate., Best Pract, Res. Clin. Endocrinol. Metab. 22 (2008) 259–270, doi:http://dx.doi.org/10.1016/j.beem.2008.01.001.

[21] M. Beaulieu, E. Levesque, D.W. Hum, A. Belanger, Isolation and characterization of a novel cDNA encoding a human UDP-glucuronosyltransferase active on C19 steroids, J. Biol. Chem. 271 (1996) 22855–22862, doi:http://dx.doi.org/10.1074/jbc.271.37.22855.

[22] R.H. Tukey, C.P. Strassburg, Human UDP-glucuronosyltransferases: metabolism, expression, and disease, Annu. Rev. Pharmacol. Toxicol. 40 (2000) 581–616, doi:http://dx.doi.org/10.1146/annurev.pharmtox.40.1.581.

[23] E.A. Mostaghel, A. Zhang, S. Plymate, UDP-glucuronosyltransferase enzymes in prostate cancer progression: is only androgen catabolism involved? Eur. Urol. (2015) 9–11, doi:http://dx.doi.org/10.1016/j.eururo.2015.08.025.

[24] L. Wu, M. Einstein, W.M. Geissler, H.K. Chan, K.O. Elliston, S. Andersson, Expression cloning and characterization of human 17β-hydroxysteroid dehydrogenase type 2, a microsomal enzyme possessing 20α-hydroxysteroid dehydrogenase activity, J. Biol. Chem. 268 (1993) 12964–12969.

[25] M.A. Titus, C.W. Gregory, O.H. Ford, M.J. Schell, S.J. Maygarden, J.L. Mohler, Steroid 5α-reductase isozymes I and II in recurrent prostate cancer, Clin. Cancer Res. 11 (2005) 4365–4371, doi:http://dx.doi.org/10.1158/1078-0432.CCR-04-0738.

[26] S. Muthusamy, S. Andersson, H. Kim, R. Butler, L. Waage, U. Bergerheim, et al., Estrogen receptor β and 17β-hydroxysteroid dehydrogenase type 6, a growth regulatory pathway that is lost in prostate cancer, Proc. Natl. Acad. Sci. 108 (2011) 20090–20094, doi:http://dx.doi.org/10.1073/pnas.1117772108.

[27] X.F. Huang, V. Luu-The, Molecular characterization of a first human 3 (α → β)-hydroxysteroid epimerase, J. Biol. Chem. 275 (2000) 29452–29457, doi:http://dx.doi.org/10.1074/jbc.M000562200.

[28] O.V. Belyaeva, S.V. Chetyrkin, A.L. Clark, N.V. Kostereva, K.S. SantaCruz, B.M. Chronwall, et al., Role of microsomal retinol/sterol dehydrogenase-like short-chain dehydrogenases/reductases in the oxidation and epimerization of 3α-hydroxysteroids in human tissues, Endocrinology 148 (2007) 2148–2156, doi:http://dx.doi.org/10.1210/en.2006-1491.

[29] D.R. Bauman, S. Steckelbroeck, M.V. Williams, D.M. Peehl, T.M. Penning, Identification of the major oxidative 3α-hydroxysteroid dehydrogenase in human prostate that converts 5α-androstane-3α, 17β-diol to 5α-dihydrotestosterone: a potential therapeutic target for androgen-dependent disease, Mol. Endocrinol. 20 (2006) 444–458, doi:http://dx.doi.org/10.1210/me.2005-0287.

[30] R.I. Dorfman, In vivo metabolism of neutral steroid hormones, J. Clin. Endocrinol. Metab. 14 (1954) 318–325, doi:http://dx.doi.org/10.1210/jcem-14-3-318.

[31] D. Turgeon, J.-S. Carrier, E. Levesques, D.W. Hum, A. Belanger, Relative enzymatic activity, protein stability, and tissue distribution of human steroid-metabolizing UGT2 B subfamily members, Endocrinology 142 (2001) 778–787, doi:http://dx.doi.org/10.1210/endo.142.2.7958.

[32] A.F. Gazdar, H.K. Oie, C.H. Shackleton, T.R. Chen, T.J. Triche, C.E. Myers, et al., Establishment and characterization of a human adrenocortical carcinoma cell line that expresses multiple pathways of steroid biosynthesis, Cancer Res. 50 (1990) 5488–5496.

[33] T. Sten, I. Bichlmaier, T. Kuuranne, A. Leinonen, J. Yli-kauhaluoma, M. Finel, UDP-Glucuronosyltransferases (UGTs) 2B7 and UGT2B17 display converse specificity in testosterone and epitestosterone glucuronidation, whereas UGT2A1 conjugates both androgens similarly, Drug Metab. Dispos. 37 (2009) 417–423, doi:http://dx.doi.org/10.1124/dmd.108.024844.concentration.

[34] L. Schloms, K.-H. Storbeck, P. Swart, W.C.A. Gelderblom, A.C. Swart, The influence of *Aspalathus linearis* (Rooibos) and dihydrochalcones on adrenal steroidogenesis: quantification of steroid intermediates and end products in H295R cells, J. Steroid Biochem. Mol. Biol. 128 (2012) 128–138, doi:http://dx.doi.org/10.1016/j.jsbmb.2011.11.003.

[35] J.L. Quanson, M. Stander, E. Pretorius, A. Taylor, C. Jenkinson, K.-H. Storbeck, High-throughput analysis of 19 endogenous androgenic steroids by ultra-performance convergence chromatography tandem mass spectrometry (Personal communication).

[36] P.J. Taylor, Matrix effects: the Achilles heel of quantitative high-performance liquid chromatography-electrospray-tandem mass spectrometry, Clin. Biochem. 38 (2005) 328–334, doi:http://dx.doi.org/10.1016/j.clinbiochem.2004.11.007.

[37] J.L. Quanson, The characterisation of the catalytic activity of human steroid 5α-reductase towards novel C_{19} substrates, MSc thesis (2015) Stellenbosch University, http://scholar.sun.ac.za/handle/10019.1/97057.

[38] I. Berthaut, M. Portois, O. Cussenot, I. Mowszowicz, Human prostatic cells in culture: different testosterone metabolic profile in epithelial cells and fibroblasts from normal or hyperplastic prostates, J. Steroid Biochem. Molec. Biol. 58 (1996) 235–242.

[39] S. Chouinard, G. Pelletier, A. Bélanger, O. Barbier, Isoform-specific regulation of uridine diphosphate-glucuronosyltransferase 2B enzymes in the human prostate: differential consequences for androgen and bioactive lipid inactivation, Endocrinology 147 (2006) 5431–5442, doi:http://dx.doi.org/10.1210/en.2006-0229.

[40] P. Berthon, O. Cussenot, L. Hopwood, A. Leduc, N. Maitland, Functional expression of SV40 in normal human prostatic epithelial and fibroblastic cells – differentiation pattern of nontumorigenic cell-lines, Int. J. Oncol. 6 (1995) 333–343.

[41] C. Guillemette, A. Belanger, Glucuronosyltransferase activity in human cancer cell line LNCaP, Mol. Cell. Endocrinol. 107 (1995) 131–139, doi:http://dx.doi.org/10.1016/0303-7207(94)03434-U.

[42] G. Bélanger, M. Beaulieu, B. Marcotte, E. Levesque, C. Guillemette, D.W. Hum, et al., Expression of transcripts encoding steroid UDP-glucuronosyltransferases in human prostate hyperplastic tissue and the LNCaP cell line, Mol. Cell. Endocrinol. 113 (1995) 165–173, doi:http://dx.doi.org/10.1016/0303-7207(95)03627-J.

[43] A. Bélanger, D.W. Hum, M. Beaulieu, E. Levesque, C. Guillemette, A. Tchernof, et al., Characterization and regulation of UDP-glucuronosyltransferases in steroid target tissues, J. Steroid Biochem. Mol. Biol. 65 (1998) 301–310, doi:http://dx.doi.org/10.1016/S0960-0760(97)00183-0.

[44] A. Dovio, M.L. Sartori, S. De Francia, S. Mussino, P. Perotti, L. Saba, et al., Differential expression of determinants of glucocorticoid sensitivity in androgen-dependent and androgen-independent human prostate cancer cell lines, J. Steroid Biochem. Mol. Biol. 116 (2009) 29–36, doi:http://dx.doi.org/10.1016/j.jsbmb.2009.04.007.

[45] N. Page, N. Warriar, M.V. Govindan, 11β-Hydroxysteroid dehydrogenase and tissue specificity of androgen action in human prostate cancer cell LNCaP, J. Steroid Biochem. Mol. Biol. 49 (1994) 173–181, doi:http://dx.doi.org/10.1016/0960-0760(94)90008-6.

[46] M. Beaulieu, E. Levesque, D.W. Hum, A. Belanger, Isolation and characterization of a novel cDNA encoding a human UDP-glucuronosyltransferase active on C19 steroids, J Biol. Chem. 271 (1996) 22855–22862.

[47] T.M. Penning, D.R. Bauman, Y. Jin, T.L. Rizner, Identification of the molecular switch that regulates access of 5α-DHT to the androgen receptor, Mol. Cell. Endocrinol. 265–266 (2007) 77–82, doi:http://dx.doi.org/10.1016/j.mce.2006.12.007.

[48] N. Mitsiades, C.C. Sung, N. Schultz, D.C. Danila, B. He, V.K. Eedunuri, et al., Distinct patterns of dysregulated expression of enzymes involved in androgen synthesis and metabolism in metastatic prostate cancer tumors, Cancer Res. 72 (2012) 6142–6152, doi:http://dx.doi.org/10.1158/0008-5472.CAN-12-1335.

[49] M. Biancolella, A. Valentini, D. Minella, L. Vecchione, F.D. Amico, G. Chillemi, et al., Effects of dutasteride on the expression of genes related to androgen metabolism and related pathway in human prostate cancer cell lines, Invest.

New Drugs. 25 (2007) 491–497, doi:http://dx.doi.org/10.1007/s10637-007-9070-7.

[50] T. Fujimura, S. Takahashi, T. Urano, J. Kumagai, T. Murata, K. Takayama, et al., Expression of cytochrome P450 3A4 and its clinical significance in human prostate cancer, Urology 74 (2009) 391–397, doi:http://dx.doi.org/10.1016/j.urology.2009.02.033.

[51] K.A. Usmani, R.L. Rose, E. Hodgson, Inhibition and activation of the human liver microsomal and human cytochrome P450 3A4 metabolism of testosterone by deployment-related chemicals, Drug Metab. Dispos. 31 (2003) 384–391, doi:http://dx.doi.org/10.1124/dmd.31.4.384.

[52] A.-M. Moilanen, J. Hakkola, M.H. Vaarala, S. Kauppila, P. Hirvikoski, J.T. Vuoristo, et al., Characterization of androgen-regulated expression of CYP3A5 in human prostate, Carcinogenesis 28 (2007) 916–921, doi:http://dx.doi.org/10.1093/carcin/bgl222.

[53] N. Finnstrom, C. Bjelfman, T.G. Soderstrom, G. Smith, L. Egevad, B.J. Norlen, et al., Detection of cytochrome P450 mRNA transcripts in prostate samples by RT-PCR, Eur. J. Clin. Invest. 31 (2001) 880–886, doi:http://dx.doi.org/10.1046/j.1365-2362.2001.00893.x.

[54] J.A.G. Agúndez, C. Martínez, M. Olivera, L. Gallardo, J.M. Ladero, C. Rosado, et al., Expression in human prostate of drug- and carcinogen-metabolizing enzymes: association with prostate cancer risk, Br. J. Cancer. 78 (1998) 1361–1367, doi:http://dx.doi.org/10.1038/bjc.1998.685.

[55] Y. Yamakoshi, T. Kishimoto, K. Sugimura, H. Kawashima, Human prostate CYP3A5: identification of a unique 5′-untranslated sequence and characterization of purified recombinant protein, Biochem. Biophys. Res. Commun. 260 (1999) 676–681, doi:http://dx.doi.org/10.1006/bbrc.1999.0960.

[56] I. Koch, R. Weil, R. Wolbold, J. Brockmöller, E. Hustert, O. Burk, et al., Interindividual variability and tissue-specificity in the expression of cytochrome P450 3A mRNA., Drug Metab, Dispos 30 (2002) 1108–1114, doi:http://dx.doi.org/10.1124/dmd.30.10.1108.

[57] R.M. Attar, C.H. Takimoto, M.M. Gottardis, Castration-resistant prostate cancer: locking up the molecular escape routes, Clin. Cancer Res. 15 (2009) 3251–3255, doi:http://dx.doi.org/10.1158/1078-0432.CCR-08-1171.

[58] N. Sharifi, The 5α-androstanedione pathway to dihydrotestosterone in castration-resistant prostate cancer, J. Investig. Med. 60 (2012) 1–8 doi:10.231/JIM.0b013e31823874a4.

[59] T.M. van der Sluis, A.N. Vis, R.J.A. van Moorselaar, H.N. Bui, M.A. Blankenstein, E.J.H. Meuleman, et al., Intraprostatic testosterone and dihydrotestosterone. Part I: concentrations and methods of determination in men with benign prostatic hyperplasia and prostate cancer, BJU Int. 109 (2012) 176–182, doi:http://dx.doi.org/10.1111/j.1464-410X.2011.10651.x.

[60] J. Heracek, R. Hampl, H. Richard, M. Hill, H. Martin, L. Starka, et al., Tissue and serum levels of principal androgens in benign prostatic hyperplasia and prostate cancer, Steroids 72 (2007) 375–380, doi:http://dx.doi.org/10.1016/j.steroids.2007.01.004.

[61] K. Monostory, Z. Dvorak, Steroid regulation of drug-metabolizing cytochromes P450, Curr. Drug Metab. 12 (2011) 154–172, doi:http://dx.doi.org/10.2174/138920011795016854.

[62] M.H. Choi, P.L. Skipper, J.S. Wishnok, S.R. Tannenbaum, Characterization of testosterone 11β-hydroxylation catalyzed by human liver microsomal cytochromes P450, Pharmacology 33 (2005) 714–718, doi:http://dx.doi.org/10.1124/dmd.104.003327.

[63] J. Zielinski, M. Mevissen, Inhibition of *in vitro* metabolism of testosterone in human, dog and horse liver microsomes to investigate species differences, Toxicol. Vitro 29 (2015) 468–478, doi:http://dx.doi.org/10.1016/j.tiv.2014.12.018.

[64] B. Bélanger, A. Bélanger, F. Labrie, A. Dupont, L. Cusan, G. Monfette, Comparison of residual C-19 steroids in plasma and prostatic tissue of human, rat and guinea pig after castration: unique importance of extratesticular androgens in men, J. Steroid Biochem. 32 (1989) 695–698.

[65] T. Nishiyama, T. Ikarashi, Y. Hashimoto, K. Wako, K. Takahashi, The change in the dihydrotestosterone level in the prostate before and after androgen deprivation therapy in connection with prostate cancer aggressiveness using the Gleason score, J. Urol. 178 (2007) 1282–1289, doi:http://dx.doi.org/10.1016/j.juro.2007.05.138.

[66] M.G. Oefelein, A. Feng, M.J. Scolieri, D. Ricchiutti, M.I. Resnick, Reassessment of the definition of castrate levels of testosterone: implications for clinicaldecision making, Urology 56 (1995) 1021–1024, doi:http://dx.doi.org/10.1016/S0090-4295(00)00793-7.

[67] T. Nishiyama, Serum testosterone levels after medical or surgical androgen deprivation: a comprehensive review of the literature, Urol. Oncol. 32 (2014) 38.e17–38.e28, doi:http://dx.doi.org/10.1016/j.urolonc.2013.03.007.

[68] E.A. Mostaghel, Beyond T and DHT – novel steroid derivatives capable of wild type androgen receptor activation, Int. J. Biol. Sci. 10 (2014) 602–613, doi:http://dx.doi.org/10.7150/ijbs.8844.

[69] B.B. Yeap, O.P. Almeida, Z. Hyde, P.E. Norman, S.A.P. Chubb, K. Jamrozik, In men older than 70 years, total testosterone remains stable while free testosterone declines with age the health in men study, Eur. J. Endocrinol. 156 (2007) 585–594, doi:http://dx.doi.org/10.1530/EJE-06-0714.

[70] C.J. Ryan, M.R. Smith, J.S. de Bono, A. Molina, C.J. Logothetis, P. de Souza, et al., Abiraterone in metastatic prostate cancer without previous chemotherapy, N. Engl. J. Med. 368 (2013) 138–148, doi:http://dx.doi.org/10.1056/NEJMoa1209096.

[71] J.S. de Bono, C.J. Logothetis, A. Molina, K. Fizazi, S. North, L. Chu, et al., Abiraterone and increased survival in metastatic prostate cancer, N. Engl. J. Med. 364 (2011) 1995–2005.

[72] Y.-K. Seo, N. Mirkheshti, C.S. Song, S. Kim, S. Dodds, S.C. Ahn, et al., SULT2B1b sulfotransferase: induction by vitamin D receptor and reduced expression in prostate cancer, Mol. Endocrinol. 27 (2013) 925–939, doi:http://dx.doi.org/10.1210/me.2012-1369.
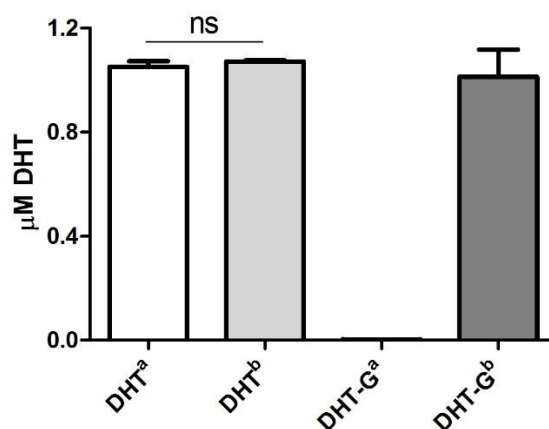
Supplementary Fig. 1: UHPLC-MS/MS analyses of deconjugation efficiency of DHT-G. Free steroid[a] in experimental samples before β-glucuronidase treatment, clear bars; and total steroid[b] (free + conjugated) after β-glucuronidase treatment, grey bars. The experiment was performed in triplicate and results are depicted as the mean ±SEM (*ns*=not significant).

Supplementary table 1: Gradient specifications of the UHPLC separation of C_{19} steroid metabolites.

Step	Time (min)	Solvent A (%)	Solvent B (%)	Curve
1	0	85	15	Initial
2	1.00	60	40	6
3	3.50	45	55	6
4	3.60	0	100	6
5	4.00	0	100	6
6	4.01	85	15	6
7	5.00	85	15	6

Supplementary table 2: Gradient specifications of the UHPLC separation of C11-oxy C_{19} steroid metabolites.

Step	Time (min)	Solvent A (%)	Solvent B (%)	Curve
1	0	85	15	Initial
2	3.50	61.5	38.5	4
3	3.60	0	100	6
4	4.00	0	100	6
5	4.01	85	15	6
6	5.00	85	15	6

Supplementary table 3: UHPLC-MS/MS detection and quantification of C_{19} steroid standards. Parent molecular ion species and mass transitions of daughter ions; retention time (RT, min); limit of detection (LOD) and limit of quantification (LOQ) of steroids; mass spectrometer settings, cone voltages (CV), collision energy (CE); and internal deuterated standards, testosterone-D2 (T-D2) and cortisol-D4.

|	Steroid metabolite	RT (min)	Precursor ion	CV	Product ion A	CE	Product ion B	CE	Product ion C	CE	Internal standard	LOD[a] (ng/µL)	LOQ[b] (ng/µL)	Calibration range (ng/µL)	Linearity (r^2)
C_{19} steroids	A4	3.13	287.2	30	96.9	15	108.8	15			T-D2	0.002[c]	0.02	0.02-2	0.9996
	T	2.98	289.2	30	97.2	22	109.0	22			T-D2	0.002[c]	0.02	0.02-2	0.9989
	5αDIONE	3.57	289.2	30	119.2	35	171.2	35			T-D2	<0.02	0.02	0.02-2	0.9995
	DHT	3.35	291.2	25	255.0	15	273.0	20			T-D2	<0.02	0.02	0.02-2	0.9998
	AST	3.60	273.2	30	105.3	30	147.0	25			T-D2	<0.02	0.02	0.02-2	0.9997
	3αADIOL	3.26	275.2	15	161.0	15	175.0	15	257	15	T-D2	<0.02	0.02	0.02-2	0.9993
	Testosterone-D2	2.98	291.0	30	99.1	20	111.25	20			-				
	Cortisol-D4	1.95	367.0	35	121.0	25					-				
C11 oxy C_{19} steroids	11KT	3.16	303.2	30	121.0	20	267.0	20			T-D2	0.0007[d]	0.02	0.02-2	0.9999
	Testosterone-D2	4.21	291.0	30	99.1	20	111.25	20			-				
	Cortisol-D4	2.51	367.0	35	121.0	25					-				

[a]Limit of detection was defined as S/N ratio >3

[b]Limit of quantification was defined as a S/N ratio >10

[c][34]

[d][18]

Supplementary table 4: Gradient specifications of the UPC^2 separation of C$_{19}$ steroid metabolites.

Step	Time (min)	Solvent A (%)	Solvent B (%)	Curve
1	0	99	1	Initial
2	4.0	91	9	7
3	4.1	75	25	6
4	5.0	99	1	6

Supplementary table 5: Gradient specifications of the UPC^2 separation of C11-oxy C$_{19}$ steroid metabolites.

Step	Time (min)	Solvent A (%)	Solvent B (%)	Curve
1	0	98	2	Initial
2	4.0	90.5	9.5	6
3	4.1	75	25	6
4	5.0	98	2	6
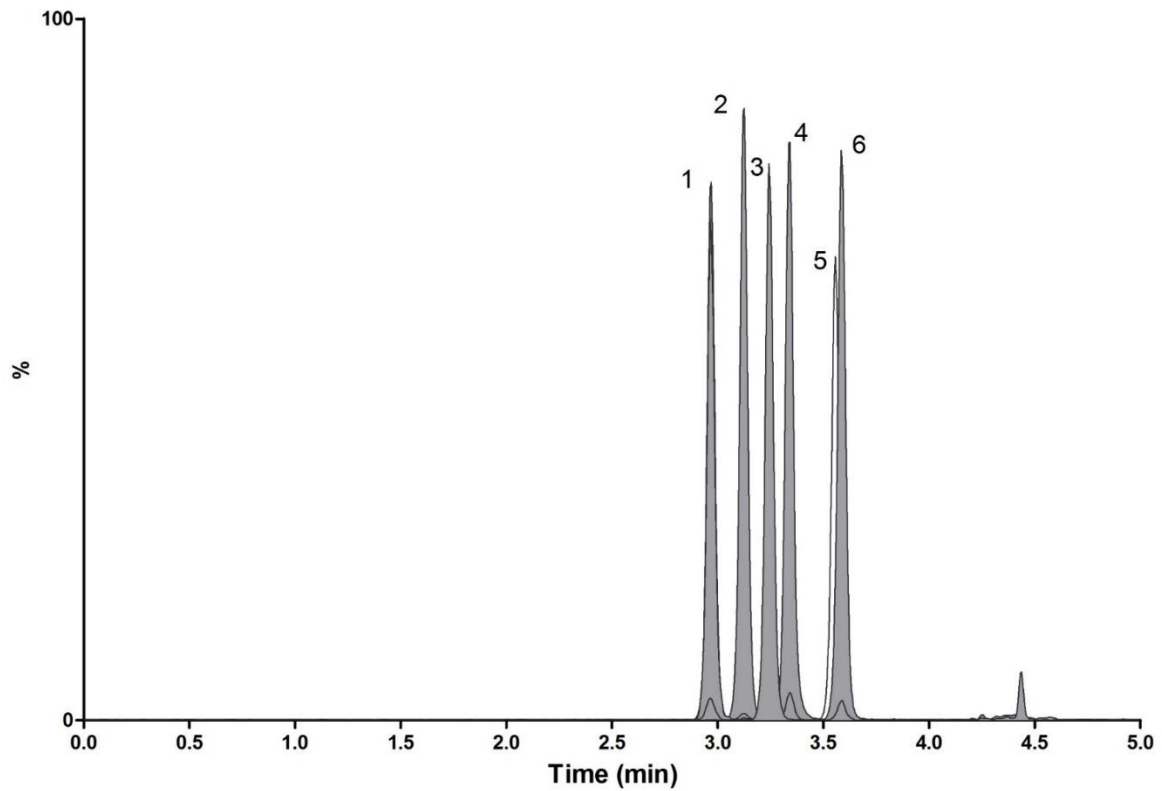
Supplementary Fig. 2: UHPLC-MS/MS separation of 6 C_{19} steroids. Standards, 5 µL each of a 2 ng/µL standard solution, are depicted in the elution order of (1) T, 2.97 min; (2) A4, 3.12 min; (3) 3αADIOL, 3.24 min; (4) DHT, 3.33 min; (5) 5αDIONE (clear peak), 3.55 min and (6) AST, 3.57 min.
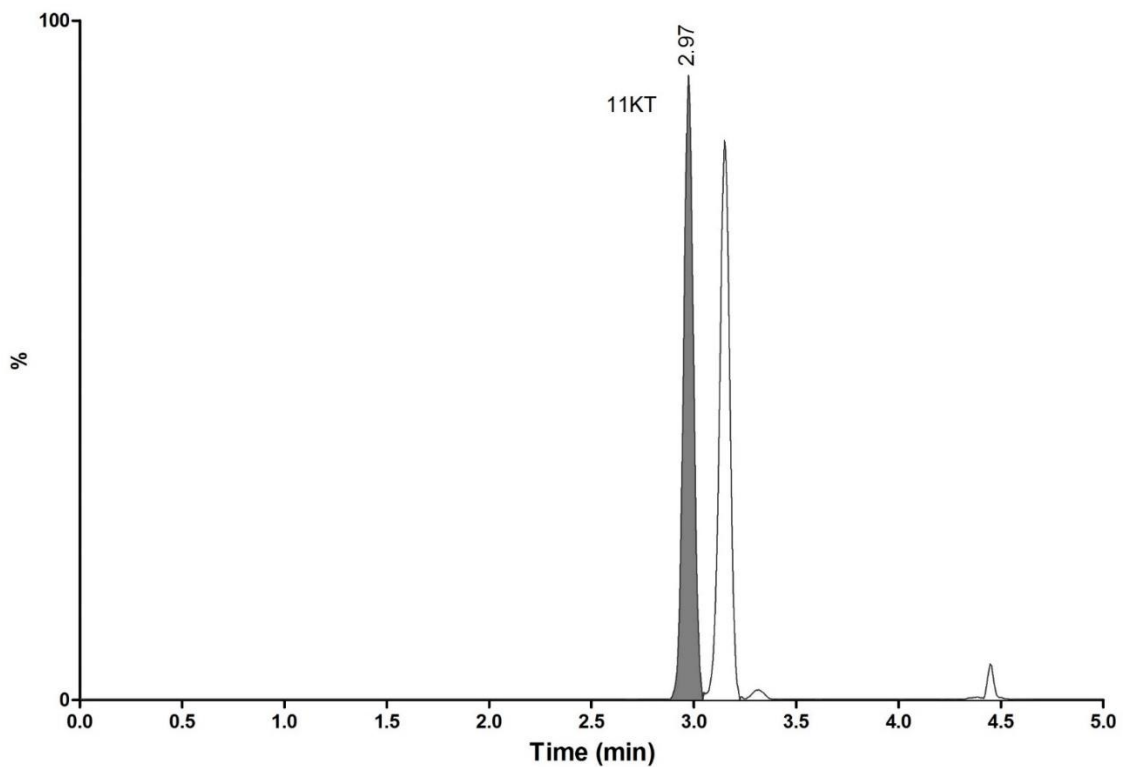
Supplementary Fig. 3: UHPLC-MS/MS analysis of 11KT. A Standard (shaded peak), 5 µL of 2 ng/µL standard solution, is depicted at 2.97 min (peak at 3.15 min represent 11OHA4 cross-talk).

Supplementary table 6a: UPC^2-MS/MS method validation for the extraction of steroids from cell culture media using DCM and MTBE, organic solvents for steroid extractions. Three steroid concentrations were analysed to determine recovery (%, n=3) and matrix effect (%, n=3)*.

Organic solvent extraction	Steroid metabolite	Recovery (%) ng/µL			Matrix effect (%) ng/µL		
		0.002	0.02	0.1	0.002	0.02	0.1
MTBE	11OHA4	279	111	99	21	3	-4
	11OHT	284	106	100	7	1	-2
	11KA4	249	108	100	38	10	-2
	11KT	297	107	100	4	8	-6
	11KDHT	259	89	100	-33	17	-4
	11OHAST	<LOQ	132	99	<LOQ	16	0
	11OH-epiAST	<LOQ	95	100	<LOQ	-2	-2
	11KAST	<LOQ	133	93	<LOQ	4	-3
	11K-epiAST	<LOQ	87	100	<LOQ	8	-10
DCM — C_{19} steroids	A4	196	94	100	31	-3	5
	T	217	98	100	37	1	1
	5αDIONE	202	93	100	21	-3	9
	DHT	193	100	100	20	-8	3
	AST	195	94	100	-14	-1	-2
	3αADIOL	197	84	101	16	4	-3
DCM — C11 oxy C_{19} steroids	11OHA4	332	143	98	43	-2	-7
	11OHT	329	143	98	27	3	-2
	11KA4	326	157	98	63	11	-6
	11KT	333	143	104	42	3	-6
	11KDHT	285	143	101	-48	-9	-10
	11OHAST	<LOQ	148	98	<LOQ	3	-2
	11OH-epiAST	<LOQ	149	98	<LOQ	4	0
	11KAST	<LOQ	130	99	<LOQ	35	10
	11K-epiAST	<LOQ	133	99	<LOQ	9	-13

Supplementary table 6b: UPC^2-MS/MS method validation for the extraction of steroids from FBS. Three steroid concentrations were analysed to determine recovery (%, *n*=3) and matrix effect (%, *n*=3)*.

	Steroid metabolite	Recovery (%) ng/µL			Matrix effect (%) ng/µL		
		0.002	0.02	0.1	0.002	0.02	0.1
C$_{19}$ steroids	A4	183.1	111.1	99.5	206	-18	-0.5
	T	177	122	99	216	-59	-46
	5αDIONE	145	78	101	123	-31	-7
	DHT	128	83	101	160	-23	-4
	AST	94	74	101	256	-25	-18
	3αADIOL	330	114	99	128	-12	-5
C11 oxy C$_{19}$ steroids	11OHA4	275	120	99	184	1	-7
	11OHT	268	139	98	162	8	7
	11KA4	237	127	99	169	5	-2
	11KT	251	137	98	148	4	-5
	11KDHT	209	130	99	-30	-17	-14
	11OHAST	<LOQ	174	97	<LOQ	7	8
	11OH-epiAST	<LOQ	92	100	<LOQ	-12	-16
	11KAST	<LOQ	136	98	<LOQ	-3	6
	11K-epiAST	<LOQ	120	99	<LOQ	5	-12

*Absolute recoveries were calculated by generating standard curves and comparing the concentration of the standards extracted from cell culture media and FBS to that of the expected concentrations. Matrix effects were determined by comparing the area of the steroid standards after post-extraction addition to that of steroid standards in 50% methanol. The difference in the responses of the steroids added post-extraction and those of the standards in 50% methanol was divided by the response of the latter.

Supplementary table 7: UPC^2-MS/MS method validation for the extraction of deuterated steroids from baboon prostatic tissue, recovery (%, n=3); matrix effect (%, n=3) and process efficiency (%, n=3)*.

	Deuterated steroid	Recovery (%)	Matrix effect (%)	Process efficiency (%)
C$_{19}$ steroids	Testosterone-D2[a]	109	-48	56
	Progesterone-D9[b]	78	-68	25
	Cortisol-D4[b]	99	-23	77
C11 oxy C$_{19}$ steroids	Testosterone-D2[a]	75	-60	30
	Progesterone-D9[b]	52	-63	19
	Cortisol-D4[b]	55	-14	47
	11β-hydroxy-androstenedione-D7[b]	46	-56	20

[a]Determined at the concentration of 0.01 ng/μL
[b]Determined at the concentration of 0.1 ng/μL

*Deuterated steroid recovery was calculated by comparing the area of the spiked deuterated steroid, added before the extraction of baboon prostatic tissue (representative of human prostatic tissue) described in 2.4, to that of post-extraction addition of deuterated steroids. Matrix effects were determined by comparing the area of the deuterated steroids recovered after post-extraction addition to that of steroid standards in 50% methanol (not extracted). The difference in area between samples added post-extraction and the standards in methanol was divided by the response of the latter. According to Taylor et al. [36] the overall process efficiency may subsequently be calculated by comparing the area of spiked steroids extracted from tissue to that of standards in 50% methanol.
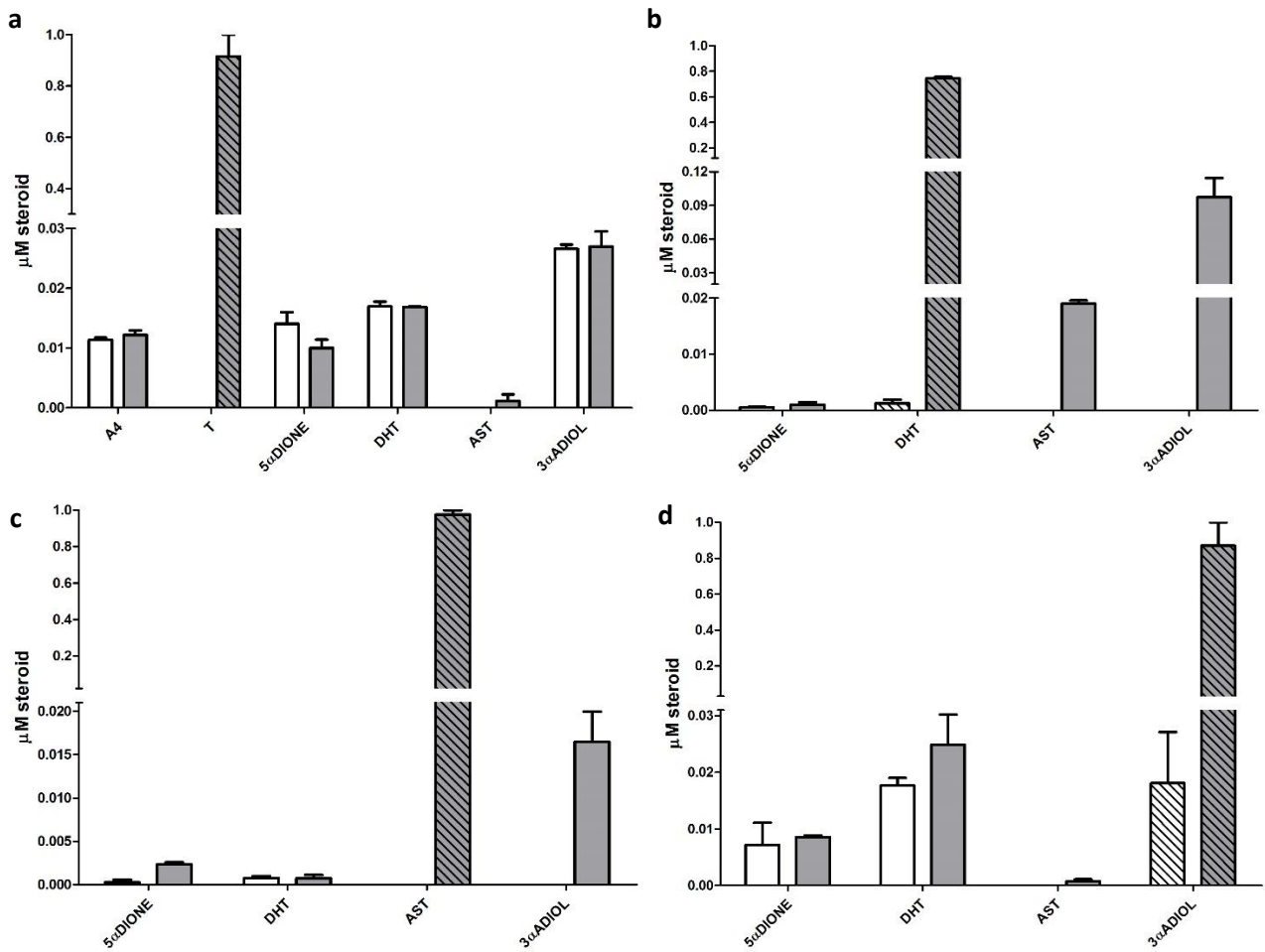
Supplementary Fig. 4: C_{19} Steroid metabolism in LNCaP cells. Steroid substrates (1 µM; patterned bars) were incubated and after 48 h free and total steroid metabolites analysed. Metabolism of (a) T, (b) DHT, (c) AST and (d) 3αADIOL with free steroids depicted as clear bars and total steroids as shaded bars. The experiment was performed in triplicate, representative of two independent experiments analysed by UHPLC-MS/MS. Results are expressed as the mean ±SEM (*n*=6).

CrossMark

Inefficient UGT-conjugation of adrenal 11β-hydroxyandrostenedione metabolites highlights C11-oxy C$_{19}$ steroids as the predominant androgens in prostate cancer

Therina du Toit, Amanda C. Swart*

Department of Biochemistry, Stellenbosch University, Stellenbosch 7600, South Africa

ABSTRACT

Although the adrenal C$_{19}$ steroids, androstenedione and testosterone, contribute to prostate cancer (PCa) progression the full complement of adrenal androgens, including the C11-oxy C$_{19}$ steroids, 11β-hydroxyandrostenedione (11OHA4) and 11β-hydroxytestosterone (11OHT) and their androgenic metabolites, 11keto-testosterone (11KT) and 11keto-dihydrotestosterone (11KDHT) have, to date, not been considered. This study investigated the contribution of 11OHA4 and 11OHT to the pool of active androgens in the prostate. Steroid profiles were determined in LNCaP, C4-2B and VCaP cell models, in PCa tissue, and in plasma focussing on the inactivation, reactivation and glucuronidation of 11OHA4, 11OHT and their downstream products using ultra-performance convergence chromatography tandem mass spectrometry (UPC^2-MS/MS). The C11-oxy C$_{19}$ steroids were the predominant steroids with the production of 11KT and 11KDHT in prostate cell models identifying 11β-hydroxysteroid dehydrogenase type 2 activity. Active:inactive steroid ratios indicated efficient inactivation of dihydrotestosterone (DHT) and 11KDHT by 3α-hydroxysteroid dehydrogenases, while the reactivation of DHT by retinol-like dehydrogenases was greater than the reactivation of 11KDHT. In PCa tissue, inactive C11-oxy C$_{19}$ steroids ranged from 27 to 30 ng/g, whereas inactive C$_{19}$ steroids were below 1 ng/g. Steroid glucuronidation was impeded: in VCaP cells, the C11-oxy C$_{19}$ steroids were unconjugated and the C$_{19}$ steroids fully conjugated; in C4-2B cells, all steroids were unconjugated, except for DHT of which 50% was conjugated; in LNCaP cells only androsterone, 11KT and 11β-hydroxyandrosterone were unconjugated. In PCa patients' plasma 11KDHT was present only in the unconjugated form, with 11KT also predominantly unconjugated (90–95%). Even though plasma and tissue sample numbers were limited, this study serves to demonstrate the abundance of C11-oxy C$_{19}$ steroids, with notable differences in their metabolism, dictated by steroidogenic enzymes and hampered conjugation, affecting active androgen levels. Larger cohorts are required to analyse profiles in modulated metabolic pathways, in order to shed light on treatment outcomes. The C11-oxy C$_{19}$ steroids are involved in PCa, with impeded glucuronidation in PCa ascribing a dominant role to these steroids in disease progression.

© 2017 Elsevier B.V. All rights reserved.

1. Introduction

It is widely accepted that although the adrenal C_{19} steroids, commonly referred to as androgens, do not exhibit androgenic activity, they serve as precursors to more potent androgens biosynthesized in peripheral tissue. This holds true when considering dehydroepiandrosterone (DHEA), androstenedione (A4) and 11β-hydroxyandrostenedione (11OHA4) (Bloem et al., 2015; Chang et al., 2011; Du Toit et al., 2017; Mizokami et al., 2009; Mohler et al., 2011; Mostaghel, 2014; Storbeck et al., 2013; Swart et al., 2013). In addition, the adrenal also produces 11β-hydroxytestosterone (11OHT) and 11keto-testosterone (11KT) (Rege et al., 2013) which, at 10 nM, have been shown to be capable of activating the androgen receptor (AR), comparable to dihydrotestosterone (DHT) (Bloem et al., 2015). Testosterone (T) is targeted in androgen deprivation therapy (ADT) aimed at reducing DHT, and has been the primary approach in the treatment of metastatic prostate cancer (PCa) for decades. The disease, which is dependent on active androgens, nevertheless progresses to castration-resistant prostate cancer (CRPC) with intratumoral DHT levels still capable of activating the AR (Chang et al., 2011; Mohler et al., 2011; Mostaghel, 2014). Adrenal A4 has been implicated in driving PCa in the absence of testicular T as it is converted to DHT in the prostate via 5α-androstanedione (5αDIONE) in the alternative pathway. The conversion of A4 to 5αDIONE, catalysed by 5α-reductase (SRD5A) is more efficient than that of T, with the upregulation of SRD5A type 1 (SRD5A1) and the concomitant down-regulation of SRD5A type 2 (SRD5A2) confirmed in the progression to CRPC (Chang et al., 2011; Montgomery et al., 2008; Stanbrough et al., 2006; Thomas et al., 2008; Titus et al., 2005).

A4 is however not the only adrenal androgen precursor contributing to CRPC with 11OHA4 also in circulation with levels having been reported to be ~2 fold higher than A4 (Rege et al., 2013). We have shown that 11OHA4 is converted to potent androgens, 11KT and 11-ketodihydrotestosterone (11KDHT) by the same steroidogenic enzymes catalysing the production of DHT with 11β-hydroxysteroid dehydrogenase type 2 (11βHSD2) and SRD5A playing pivotal roles (Bloem et al., 2015; Storbeck et al., 2013; Swart et al., 2013). The adrenal also produces 11-ketoandrostenedione (11KA4), 11OHT and 11KT, albeit at levels considerably lower than 11OHA4 (~0.99, 0.48, 0.39 and 157 nM, respectively) measured in female adrenal vein samples (Rege et al., 2013). These C11-oxy steroids are readily reduced by SRD5A, with 11KT and 11KDHT capable of activating the AR to the same degree as DHT, and of inducing androgen dependent gene expression (Bloem et al., 2015; Pretorius et al., 2016; Storbeck et al., 2013). Due to the improved capabilities of analytical technologies in the field of liquid chromatography tandem mass spectrometry (LC-MS/MS), we have also shown that these steroids are present in serum and tissue of PCa patients (Du Toit et al., 2017), which therefore begs the question as to the exclusivity of DHT being the sole potent androgen in terms of contributing to the progression of PCa. Furthermore, it is evident that the steroid profile in PCa remains incomplete and skewed since neither the C11-oxy androgens nor their conjugation are taken into account.

The biosynthesis of active androgens from their adrenal precursor C_{19} steroids and their subsequent inactivation are dependent on the expression levels of the relevant steroidogenic enzymes in peripheral tissue. Furthermore, the conjugation by the uridine diphosphate (UDP)-glucuronosyltransferase (UGT) isoforms adds another level of complexity with the expression of these enzymes characterized by copy number variation, the use of alternative promoters, polymorphisms, alternative splicing and exon skipping (Guillemette et al., 2010; Du Toit and Swart, 2016). We have shown 11KT is not conjugated as readily as T, DHT or 11KDHT by the UGT enzymes (Du Toit et al., 2017). The irreversible conjugation by the UGT enzymes contributing to the inactivation and reactivation equilibrium directly impact active androgen levels, not only in the prostate affecting PCa treatment strategies, but also in other clinical conditions which are characterized by adrenal-derived androgen excess. Increased C11-oxy C_{19} steroid levels have been detected in classic 21-hydroxylase deficiency patients and it has been suggested that these steroids could act as specific biomarkers of adrenal androgen excess (Turcu et al., 2016).

In the C_{19} steroid metabolic pathway, T, DHT, androsterone (AST) and 5α-androstane-3α,17β-diol (3αDIOL) are substrates for the conjugation by the UDP-glycosyltransferase 2 family, polypeptide B (UGT2B) enzymes (Fig. 1). DHT is inactivated by the 3α-hydroxysteroid dehydrogenase (3αHSD) enzymes to 3αDIOL, and, if not conjugated and secreted, 3αDIOL may be reactivated to DHT by the retinol-like hydroxysteroid dehydrogenase (RL-HSD) enzymes. AST can undergo the same conversion by the RL-HSD enzymes to 5αDIONE, followed by the 17β-hydroxysteroid dehydrogenase (17βHSD) reduction producing DHT (Supplemental Fig. 1).

In the C11-oxy C_{19} steroid metabolic pathway, 11OHT, 11KT, 11β-hydroxydihydrotestosterone (11OHDHT), 11KDHT, 11β-hydroxyandrosterone (11OHAST), 11-ketoandrosterone (11KAST) and 11-keto-5α-androstane-3α,17β-diol (11K-3αDIOL) are potential substrates for glucuronidation enzymes (Fig. 1). 11KDHT may be inactivated by the 3αHSD enzymes to 11K-3αDIOL, which may be reactivated to 11KDHT by the RL-HSD enzymes if unconjugated. 11OHAST and 11KAST may undergo the same conversion by RL-HSD enzymes to 11β-hydroxy-5α-androstenedione (11OH-5αDIONE) and 11-keto-5α-androstenedione (11K-5αDIONE), respectively. The subsequent conversion of 11OH-5αDIONE by 11βHSD2 to 11K-5αDIONE, followed by the 17βHSD reduction of the latter leads to the production of 11KDHT. 11OHDHT is not converted by the 3αHSD enzymes (Supplemental Fig. 1).

The aim of this study was to investigate the inactivation, reactivation and UGT-conjugation in the metabolism of the C_{19} and the C11-oxy C_{19} steroids in PCa cell models, plasma and tissue. The metabolism of 11OHA4 and 11OHT was firstly assayed in C4-2B and VCaP cell models together with that of T and 11OHDHT. Steroid profiles were established which allowed the analyses of active and inactive androgen levels. The reversible inactivation and reactivation of DHT and 11KDHT by 3αHSD and RL-HSD enzymes were subsequently assayed in LNCaP, VCaP and C4-2B prostate models expressing these enzymes endogenously. Analyses of the unconjugated steroids in prostate tissue of a CRPC patient produced profiles for comparative analyses of the full spectrum of active and inactive androgens. In addition, PCa cell models were used to assess glucuronidation in terms of unconjugated and conjugated metabolites. The C_{19} and the C11-oxy C_{19} glucuronide metabolites were subsequently identified in normal and in PCa plasma.

2. Material and methods

2.1. Tissue and plasma

Human PCa tissue and plasma samples were collected in a study investigating clinical markers of PCa (reference no. N09/11/330; Faculty of Medicine and Health Sciences, Stellenbosch University and Tygerberg Hospital, South Africa). The PCa tissue sample was obtained from a patient aged 83, classified as having CRPC, who underwent a bilateral orchiectomy (BO). Plasma was obtained from a normal subject, aged 59 and PCa patients, aged 74 who underwent BO and aged 66 who received luteinising hormone-releasing hormone analogue treatment (LHRHa). The tissue sample was snap-frozen in liquid nitrogen upon resection and stored with plasma samples at −80 °C.
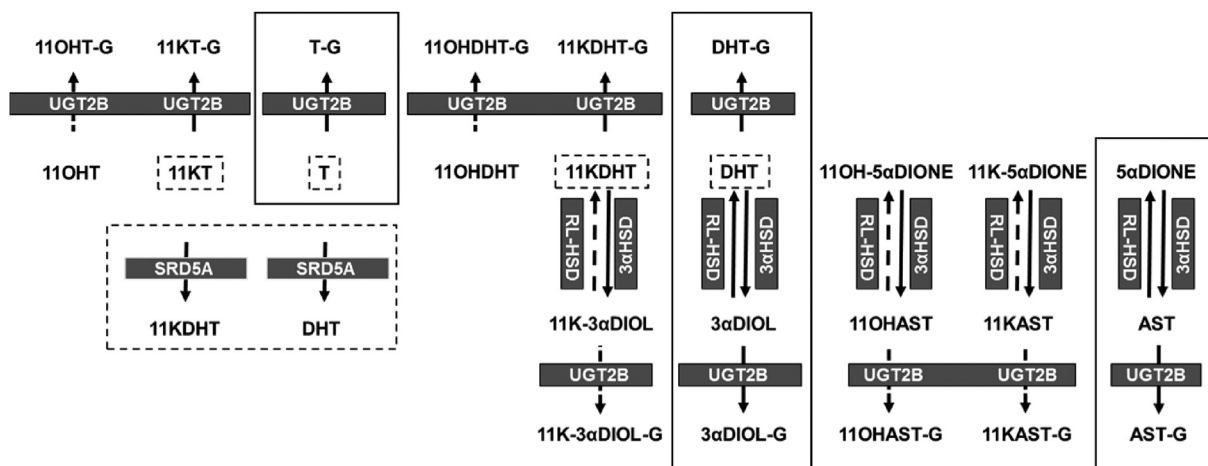
Fig. 1. C_{19} and C11 hydroxy and keto C_{19} steroids metabolism. Boxed steroid pathways depict C_{19} steroid metabolism; boxed steroid pathways (dashed line) depict activation of steroid androgens and boxed steroids (dashed line) depict human AR agonists at 1 nM.

2.2. Materials

Dulbecco's Modified Eagle medium (DMEM), Roswell Park Memorial Institute (RPMI)-1640 medium, D-(+)-Glucose, β-glucuronidase (Type VII-A from *E. coli*, 5,292,000 units/g; G7646), D-(+)-Glucose, dichloromethane (DCM), methyl tert-butyl ether (MTBE) and steroids (A4, T and DHT) were purchased from Sigma-Aldrich (St. Louis, MO, USA). All other steroids were from Steraloids (Wilton, USA). All cell culture plates were purchased from Corning® Life Sciences (NY, USA). LNCaP: C4-2B cell line (C4-2B cells) was donated by Prof DE Neal (Nuffield Department of Surgery, Oxford, United Kingdom). HEK293 (CRL-1573) and VCaP (CRL-2876) cells were bought from American Type Culture Collection (Johannesburg, South Africa) and LNCaP cells (Cat no. 89110211) were obtained from the Sigma's European Collection of Authenticated Cell Cultures (St. Louis, USA). Penicillin-streptomycin (penstrep), fetal bovine serum (FBS), trypsin-ethylenediaminetetraacetic acid (EDTA) and phosphate buffered saline (PBS) were obtained from Oxoid limited (Hampshire, England). Pierce™ BCA Protein determination kit was purchased from Thermo Fischer Scientific (South Africa). All deuterated steroids were purchased from Cambridge isotopes (Andover, MA, USA), and all other chemicals were of analytical grade and supplied by reliable scientific houses.

2.3. Steroid metabolism in LNCaP, C4-2B and VCaP cells

LNCaP cells were cultured in RPMI-1640 growth medium supplemented with 10% FBS, 1.5 g NaHCO$_3$/L (pH 7), 1% penstrep, 2.5 g D-(+)-Glucose, 1% HEPES and 1% sodium pyruvate at 37 °C, in an atmosphere of 90% humidity and 5% CO$_2$, and once confluent replated into 12-well Corning® CellBIND® surface plates at 2×10^5 cells/mL. C4-2B cells were cultured in RPMI-1640 medium, supplemented with 2.5 g D-(+)-Glucose as described above and confluent cells replated at 1×10^5 cells/mL. VCaP cells were cultured in DMEM medium as described above and confluent cells replated at 2×10^5 cells/mL. After 48 h, the medium was replaced with 1 mL cell-culture medium containing steroid substrates (1 μM): A4, T, 5αDIONE, DHT, AST, 3αDIOL, 11OHA4, 11OHT, 11KA4, 11KT, 11KDHT, 11KAST, 11OHAST, 11OHDHT and 11K-3αDIOL. 11OHDHT and 11K-3αDIOL were prepared (supplemental file) as these are not available commercially. Duplicate aliquots were removed for analysis of unconjugated steroids (0.5 mL) and of total

(unconjugated + conjugated) steroids (0.5 mL), following deconjugation with β-glucuronidase (supplemental file), as previously described (Du Toit et al., 2017). Protein concentrations were determined to normalise data. Briefly, cells were lysed and collected with 0.5 mL trypsin-EDTA, washed with 0.5 mL 1× PBS, after which 50 μL passive cell lysis buffer was added to the cells. The cells were vortexed, sonicated for 20 min, subjected to 2 freeze-thaw-cycles and incubated overnight at −20 °C, after which a Pierce® BCA protein determination was carried out.

In vitro assays were analysed after liquid/liquid steroid extractions using DCM (supplemental file). Cortisol-D4 (15 ng), testosterone-D2 (D2T, 1.5 ng), progesterone-D9 (D9PROG, 15 ng), androstenedione-D7 (D7A4, 15 ng) and 11β-hydroxyandrostenedione-D7 (D711OHA4, 15 ng) were added as internal standards. Frozen prostate tissue samples (100 mg) were analysed after steroids were extracted using MTBE after addition of internal standard, D2T (1.5 ng), cortisol-D4 (15 ng), D7A4 (15 ng) and D711OHA4 (15 ng). Steroids were extracted from plasma samples using MTBE with 0.5 mL extracted for the analyses of unconjugated steroids and 0.5 mL subjected to deconjugation prior to extraction for the analyses of total steroids. Internal standards D2T (1.5 ng) and cortisol-D4 (15 ng) were added to samples prior to extraction. Extracted steroids were dissolved in 0.15 mL 50% methanol in water. All samples were stored at −20 °C prior to ultra-performance convergence chromatography tandem mass spectrometry (UPC^2-MS/MS) analysis.

2.4. Separation and quantification of steroid metabolites

The C_{19} and C11-oxy C_{19} steroids were analysed by ACQUITY UPC^2–MS/MS (Waters Corporation, Milford, USA) as previously described, with method validation, including recovery and matrix effect as published (Du Toit et al., 2017), with modifications to the gradient (Supplemental Tables 1 and 2). Further method validation, including accuracy and precision, is shown in Supplemental Tables 3 and 4. UPC^2-MS/MS separation of the C_{19} and C11-oxy C_{19} steroids are shown in Supplemental Fig. 1a and b, respectively. The mass transitions, limit of detection (LOD) and limit of quantification (LOQ) are shown in Supplemental Table 5. Data were collected and analysed with the MassLynx 4.1 (Waters Corporation) software program.

2.5. Statistical analysis

Experiments were performed in triplicate and representative of at least duplicate experiments. Statistics were calculated by an unpaired *t*-test using GraphPad Prism (version 5) software (GraphPad Software, San Diego, California). Differences were considered statistically significant at $P < 0.05$.

3. Results

3.1. 11OHA4, 11OHT, T and 11OHDHT metabolism in C4-2B and VCaP cells

The metabolism of 11OHA4 and 11OHT was firstly investigated in PCa cells. It should be noted that both 11βHSD2 and SRD5A catalysed reactions are irreversible with 11βHSD2 converting the C11 hydroxyl group to a keto group, while SRD5A reduces the C4/C5 double bond. The 17βHSD enzymes exhibit either a reductive or oxidative activity. The reductive activity converts the C17 keto group of A4 and its derivatives to the hydroxyl group characteristic of T and its derivatives, and the oxidative activity catalyses the conversion of the hydroxyl group back to a keto group. 11OHA4 is converted either by 11βHSD2 or SRD5A as it is not a substrate for the 17βHSDs (Supplemental Fig. 1). 11βHSD2's conversion of 11OHA4 to 11KA4, 0.73 μM, was confirmed in C4-2B cells (Fig. 2a) with the 5α-reduction by SRD5A yielding 11OH-5αDIONE (~0.007 μM) and the subsequent 3α-reduction by 3αHSD yielding 11OHAST (~0.013 μM) — both at low levels. Although 11KDHT levels were negligible, the precursor steroid 11KT (0.05 μM), produced in the conversion of 11KA4 by the 17βHSDs, was detected. 11OHA4's metabolism in VCaP cells, although minimal, shows the production of 11KA4 (0.03 μM) by 11βHSD2 and 11OH-5αDIONE (~0.003 μM; below the LOQ) by SRD5As (Fig. 2b). Only low conjugated levels of 11KDHT (~0.006 μM), via 11KT (0.012 μM), was produced from 11OHA4 in this cell line, showing the pathway of 11OHA4 to 11KA4 (11βHSD2 activity), and subsequently to 11KT (17βHSD activity) followed by the 5α-reduction to 11KDHT (SRD5A activity). In contrast, 11OHT is a substrate for 11βHSD2 and SRD5A as well as 17βHSD2 (Supplemental Fig. 1). The metabolism of 11OHT in C4-2B cells showed the conversion by 17βHSD2 to 11OHA4 (0.016 μM) and by 11βHSD2 to 11KT, 0.49 μM (Fig. 2c). However, 11KT can also be biosynthesized from 11OHT via 11OHA4 and 11KA4 and subsequently to 11KT. Although no 5α-reduction of 11OHT could be detected, minimal 5α-reduction of 11KT to 11KDHT was detected (~0.0013 μM, below the LOQ). No other downstream 3α-reduced metabolites were detected. 11OHT's metabolism in VCaP cells showed the production of 11OHA4 (0.16 μM) and 11KT (0.1 μM) catalysed by 17βHSDs and 11βHSD2, respectively (Fig. 2d). The 5α-reduction of 11OHT to 11OHDHT (~0.0016 μM; below the LOQ) was also detected, however, no other 5α- or 3α-reduced metabolites were detected. Although 11OHT appears to be conjugated after 48 h in VCaP cells, following normalisation to protein, steroid levels were not significantly different (see Fig. 5c).

T's metabolism in C4-2B cells showed the predominant 5α-reduction to DHT (0.1 μM) by SRD5As, while lower A4 levels were detected, 0.044 μM (Fig. 2e). Downstream metabolism showed the 3αHSD reduction of DHT and 5αDIONE, to 3αDIOL (0.078 μM) and AST (0.057 μM), respectively. No conjugation of T derivatives was detected in this cell line following the addition of T after 48 h. In VCaP cells, unconjugated T levels were low, 0.05 μM, after 48 h (92.4% present in the conjugated form) (Fig. 2f). The endogenous SRD5As catalysed the conversion of T, producing DHT (0.019 μM unconjugated, 72.9% present in the conjugated form), while T was also converted to A4 (0.11 μM) by endogenous 17βHSDs. 3αHSD subsequently converted both 5αDIONE and DHT to AST (0.03 μM

unconjugated; 50.2% present in the conjugated form) and 3αDIOL (0.025 μM unconjugated), respectively. A substantial level of 5αDIONE (0.14 μM) was also produced from T via A4.

In both cell models 11OHDHT was metabolised efficiently (92.9% in C4-2B cells and 52.6% in VCaP cells) with only the unconjugated form being detected in C4-2B (0.07 μM) (Fig. 2g) and in VCaP cells (0.45 μM) (Fig. 2h). The steroid is predominantly converted to 11KDHT by 11βHSD2 in the cell models with the subsequent inactivation resulting in the production of 11K-3αDIOL, 15-fold higher in C4-2B cells, with 11KDHT and 11K-3αDIOL present at comparable levels in C4-2B cells. 11OHDHT was also converted to 11OH-5αDIONE (0.23 μM) in VCaP cells at levels comparable to 11KDHT (0.16 μM). 11OH-5αDIONE's subsequent metabolism is two directional − either inactivated to 11OHAST or converted to 11K-5αDIONE with its subsequent inactivation yielding 11KAST. Only 11KAST (0.012 μM) was detected in C4-2B cells and only 11OHAST (0.054 μM) was detected in VCaP cells.

### 3.2. Androgen inactivation and reactivation in prostate cell models

T and its derivatives are either conjugated at C17 or, upon reduction, at C3 by the 3αHSD enzymes. In the case of the A4 derivatives, conjugation occurs once the steroid is reduced at C3, with subsequent conjugation preventing conversion back to active androgens. As androgen inactivation and reactivation by the 3αHSD and RL-HSD enzymes would impact the levels of active androgens, we assayed the inactivation and reactivation by these enzymes with the relevant steroids in LNCaP, VCaP and C4-2B cells. In LNCaP cells, DHT and 11KDHT were more readily inactivated to 3αDIOL and 11K-3αDIOL, 2- and 15-fold greater, than the respective active forms (Fig. 3). In addition, 0.12 μM 11K-3αDIOL was produced in the metabolism of 11KDHT in these cells, 2-fold higher than 3αDIOL produced in DHT's metabolism, highlighting a more efficient inactivation of 11KDHT in LNCaP cells. In contrast, in VCaP and C4-2B cells, the inactivation and reactivation of DHT was similar, reflected in the 1:1 ratio. Interestingly, the inactivation and reactivation of 11KDHT is markedly different in both these models − the inactivation of 11KDHT was more efficient than the activation of 11K-3αDIOL back to 11KDHT, 11-fold in VCaP and 17-fold in C4-2B cells, with the metabolism of 11KDHT yielding 0.21 μM 11K-3αDIOL in VCaP cells and 0.40 μM in C4-2B cells.

3.3. C_{19} and C11-oxy C_{19} steroid profiles in prostate tissue

Analyses of unconjugated intratumoral androgens and downstream inactive metabolites in CRPC prostate tissue showed that the C11-oxy C_{19} steroids were present at considerably higher levels than the C_{19} steroids, comprising of the inactive 11OHAST (27.34 ng/g) and 11KAST (29.60 ng/g) steroids (Fig. 4). These inactive C11-oxy C_{19} steroids were present at levels higher than AST. The level of A4 (7.99 ng/g) was the highest C_{19} steroid present while the T level was detected at levels generally reported for normal tissue (0.2–1.8 ng/g). All other C_{19} steroids were below the LOQ, and no 3αDIOL was detected. Interestingly, 11KDHT was detected at ~0.97 ng/g, significantly higher than DHT, detected at ~0.23 ng/g.

3.4. Androgen conjugation in prostate cell models

Since the conjugation of C_{19} steroids would remove T derivatives and inactive androgens from the active androgen pool, we investigated the activity of the UGT enzymes towards the relevant androgens in prostate cell models. We previously reported that the conjugation of 11KT was inefficient in LNCaP cells (Du Toit et al., 2017), with present data again showing inefficient conjugation (Fig. 5a) with 0.027 μM 11KT (~15%) present in the unconjugated
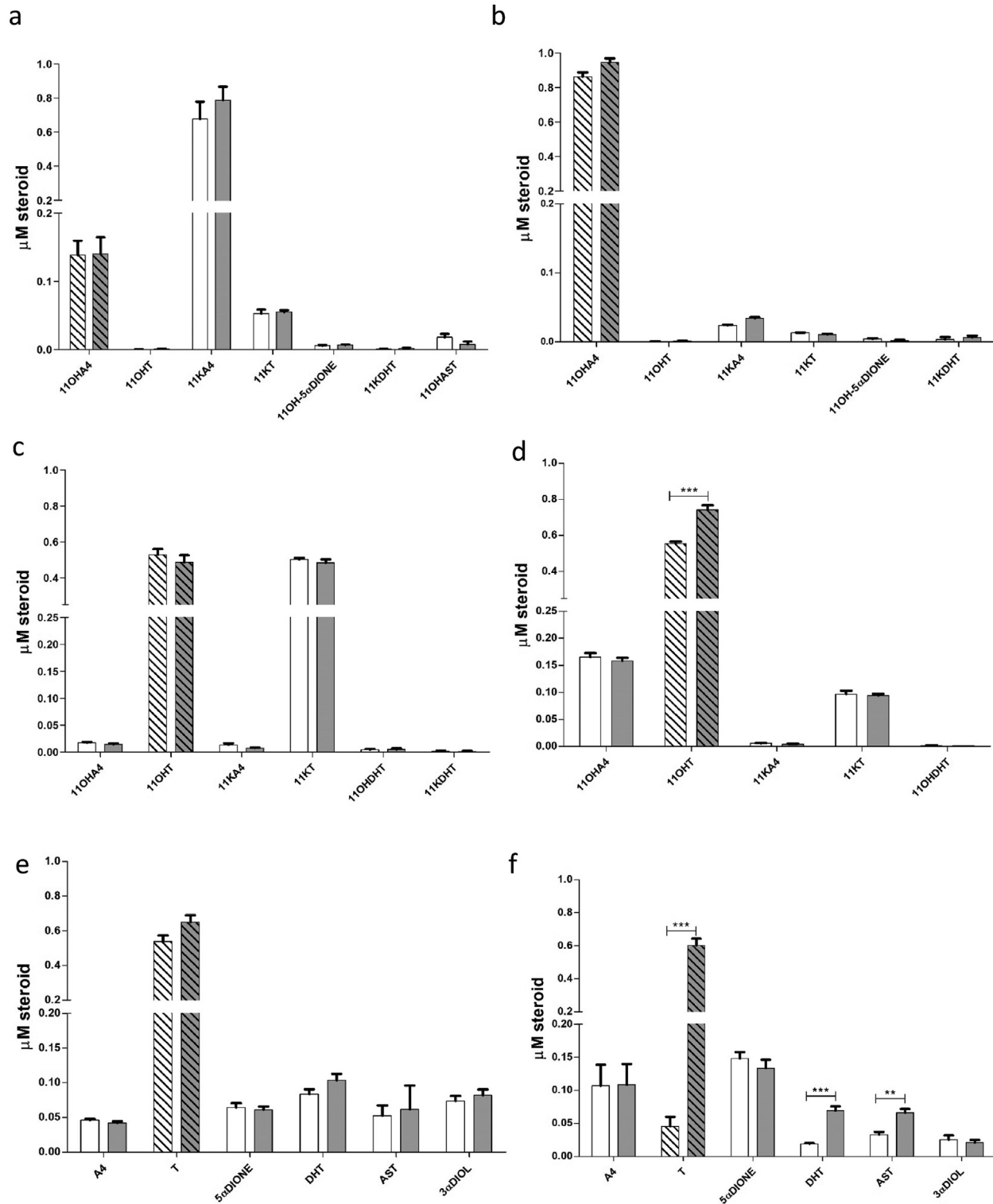
Fig. 2. C_{19} and C11-oxy C_{19} steroid metabolism in C4-2B and VCaP cells. 11OHA4 metabolism in (a) C4-2B and (b) VCaP cells; 11OHT metabolism in (c) C4-2B and (d) VCaP cells; T metabolism in (e) C4-2B and (f) VCaP cells and 11OHDHT metabolism in (g) C4-2B and (h) VCaP cells. 11OHA4, 11OHT, T and 11OHDHT (1 μM; patterned bars) metabolism was assayed after 48 h. Clear bars, unconjugated steroids; shaded bars; total steroids. Experiments were performed in triplicate, analysed by UPC^2-MS/MS and the results expressed as the mean ± STD DEV (11OHA4 $n = 3$, for all other substrates $n = 6$, **$P < 0.01$, ***$P < 0.001$).

form. No other steroids were present in the unconjugated form at 48 h, except for AST (0.016 μM) and 11OHAST (0.014 μM).

UGT-conjugation in androgen-independent C4-2B and VCaP cell models was markedly different. In C4-2B cells all C_{19} and C11-oxy C_{19} steroids remained unconjugated after 48 h. However, low levels of unconjugated DHT, 0.012 μM, were detected with ~50%
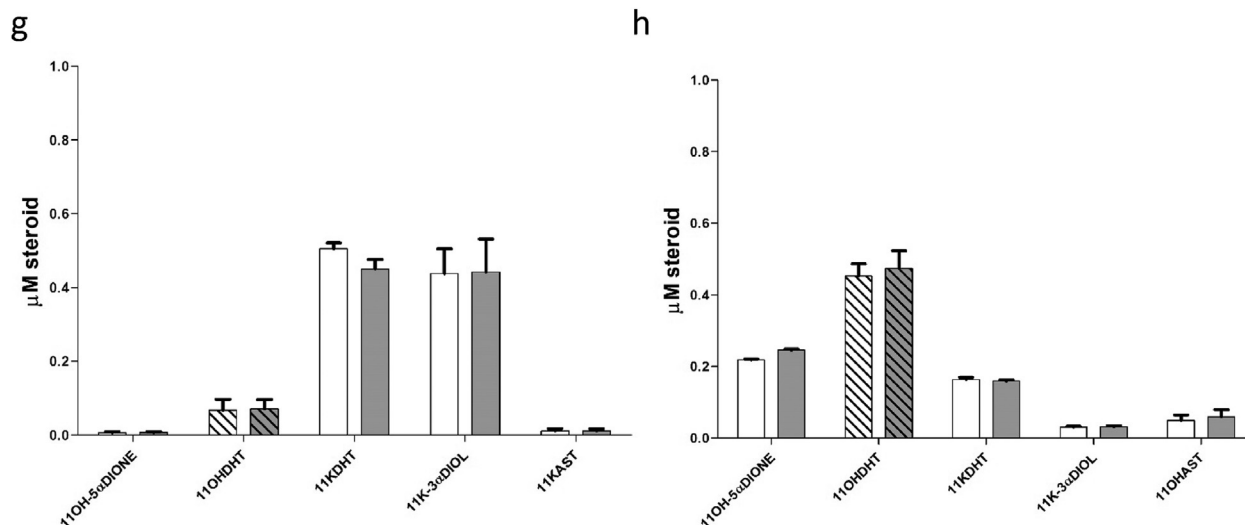
g

h

Fig. 2. (*continued*).

being present in the glucuronidated form (Fig. 5b). In contrast, in VCaP cells (Fig. 5c) the C_{19} steroids were predominantly present in the glucuronidated form with negligible unconjugated T and DHT (<1 nM) and low levels of unconjugated inactive AST, 0.026 μM, and 3αDIOL, ~0.011 μM. All the C11-oxy C_{19} steroids were predominantly present in the unconjugated form.

3.5. Conjugated androgen plasma levels

Glucuronidated C11-oxy C_{19} steroids levels in circulation have, to date, not been reported. Since glucuronide C11-oxy C_{19} steroid standards are unavailable, we chose to deconjugate plasma steroid metabolites to assess the C_{19} and C11-oxy C_{19} steroid glucuronide profiles showing total steroids as unconjugated and glucuronidated (Table 1). Comparative analyses (Fig. 6a, b and c) showed that the C11-oxy C_{19} steroid levels were higher than the C_{19} levels in all samples. Although data depicts a single sample, we have found that unconjugated C11-oxy C_{19} steroids are present at significantly higher levels than the unconjugated C_{19} steroids (~1.4-fold) in plasma of nineteen healthy subjects (unpublished results). While DHT was below the LOQ in all samples, in the healthy subject, T was detected in its unconjugated form only, while only 11KDHT-glucuronide was present (Fig. 6a). 11KT was the most abundant steroid with a greater portion present as unconjugated steroid, as only 26% was glucuronidated. Glucuronidated AST and 11OHAST comprised ~14% of the total steroids detected with 11KAST present in its glucuronidated form only. The two conjugated glucuronide derivatives of 3αDIOL *viz.* 3αDIOL-17G and 3αDIOL-3G, could not be resolved chromatographically, and are shown as unconjugated and total 3αDIOL (17G and 3G). Although the data obtained in the analyses of the PCa plasma samples does not represent a cohort of patients, the analyses clearly demonstrate different UGT activities towards the steroids. The androgens detected in the PCa patient (Fig. 6b), although markedly lower than in the healthy subject, showed only 11KT in the glucuronidated form, albeit at only 3%, significantly lower than in the healthy subject. In the PCa sample, in which the patient had progressed to CRPC (Fig. 6c), T levels were negligible, 3αDIOL of which ~50% was glucuronidated was, however, higher than in the healthy and the other PCa sample (Fig. 6b). In both PCa samples, AST was detected only as unconjugated while 11OHAST levels were considerably higher in the CRPC sample. Of the active C11-oxy C_{19} steroids, 11KT was present predominantly in

the unconjugated form in all the samples, with markedly lower levels of the glucuronidated form being detected in the PCa samples (10- to 20-fold). In both PCa patient plasma samples 11KDHT was present at comparable levels, however, only in the unconjugated form (Fig. 6b and c).

4. Discussion

Our present study shows that the C11-oxy C_{19} steroids are the predominant androgens in PCa cell models, PCa tissue and in circulation. The metabolism of adrenal 11OHA4 and 11OHT yielded active androgens in VCaP and C4-2B cells − predominantly 11KT and very low levels of 11KDHT and 11OHDHT. The conversion of 11OHA4 and 11OHT (Fig. 2a, b, c and d) to 11KA4 and 11KT respectively, in both models indicates the presence of 11βHSD2. In addition, in 11OHA4's metabolism, 11KA4 and 11KT levels are markedly higher in the C4-2B cells compared to VCaP cells, 25- and 4.5-fold respectively, suggesting higher expression levels of 11βHSD2 in C4-2B cells. The more efficient reduction of the C11-hydroxy moiety in C4-2B cells is substantiated in the conversion of 11OHDHT to 11KDHT (Fig. 2g) in which negligible 11OH-5αDIONE was detected, while this intermediate was detected in VCaP cells (Fig. 2h) at levels slightly higher than 11KDHT, which, in turn was 2.8-fold lower than in C4-2B cells.

Considering the metabolism of T, in which the presence of 11βHSD2 would not influence the conversion by steroidogenic enzymes, the data (Fig. 2e and f) depicts similar levels of A4 and DHT in both cell models, however, efficient conjugation of T and DHT occurred in VCaP cells only. Even though 5αDIONE levels were ~2.3-fold higher in VCaP cells together with 3αDIOL present only in the unconjugated form, with both these metabolites able to contribute to DHT, the level of unconjugated DHT remained markedly lower in VCaP cells, even though all the steroids were unconjugated in C4-2B cells. While only the inactive downstream 3αHSD metabolites, 3αDIOL and AST, were detected in C4-2B and VCaP cells, 11OHAST was formed in the metabolism of 11OHA4 in the former with the downstream 5α-reduced 11OHA4 and 11OHT metabolites, mid-tier of the pathway, remaining low (<20 nM).

These data show that 11OHA4 and 11OHT metabolites remain predominantly in the top tier of the metabolic pathway (Supplemental Fig. 1b) in C4-2B and VCaP cells, at levels higher than previously reported in LNCaP cells (Bloem et al., 2015). However,
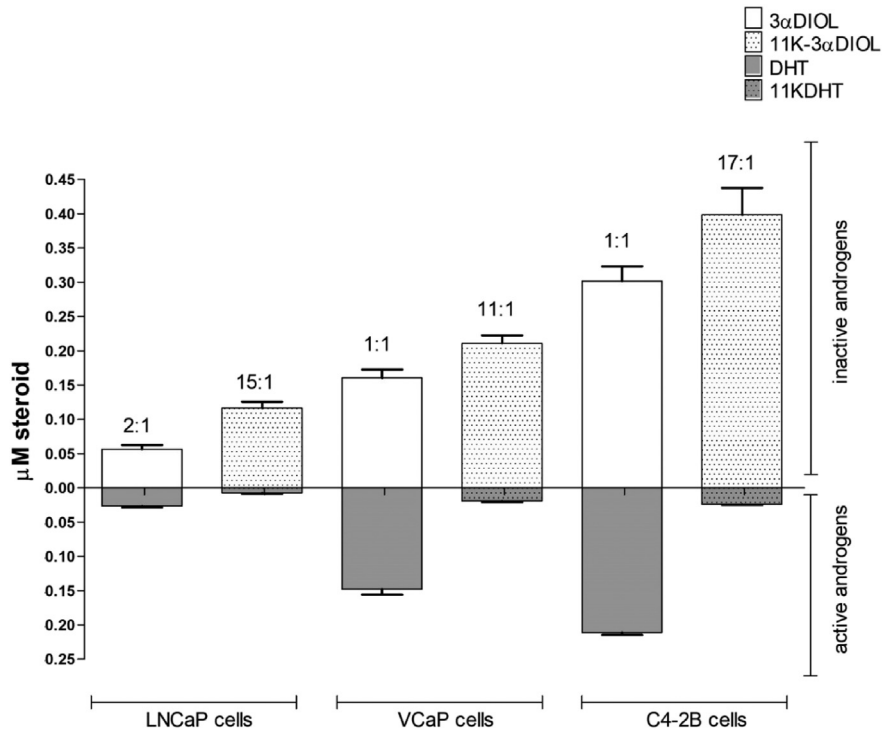
Fig. 3. Ratios of inactive androgens catalysed by 3αHSD enzymes and active androgens catalysed by RL-HSD enzymes in LNCaP, VCaP and C4-2B cells. Cells were incubated with DHT, 11KDHT, 3αDIOL and 11K-3αDIOL (1 μM) for 48 h. Bars show product formation with inactive androgens (white bars) representing the 3αHSD conversion of DHT to 3αDIOL and 11KDHT to 11K-3αDIOL and active androgens (grey bars) representing the RL-HSD conversion of 3αDIOL to DHT and 11K-3αDIOL to 11KDHT. Experiments were performed in triplicate, total steroids were analysed by UPC^2-MS/MS and the results expressed as the mean ± STD DEV ($n = 3$).
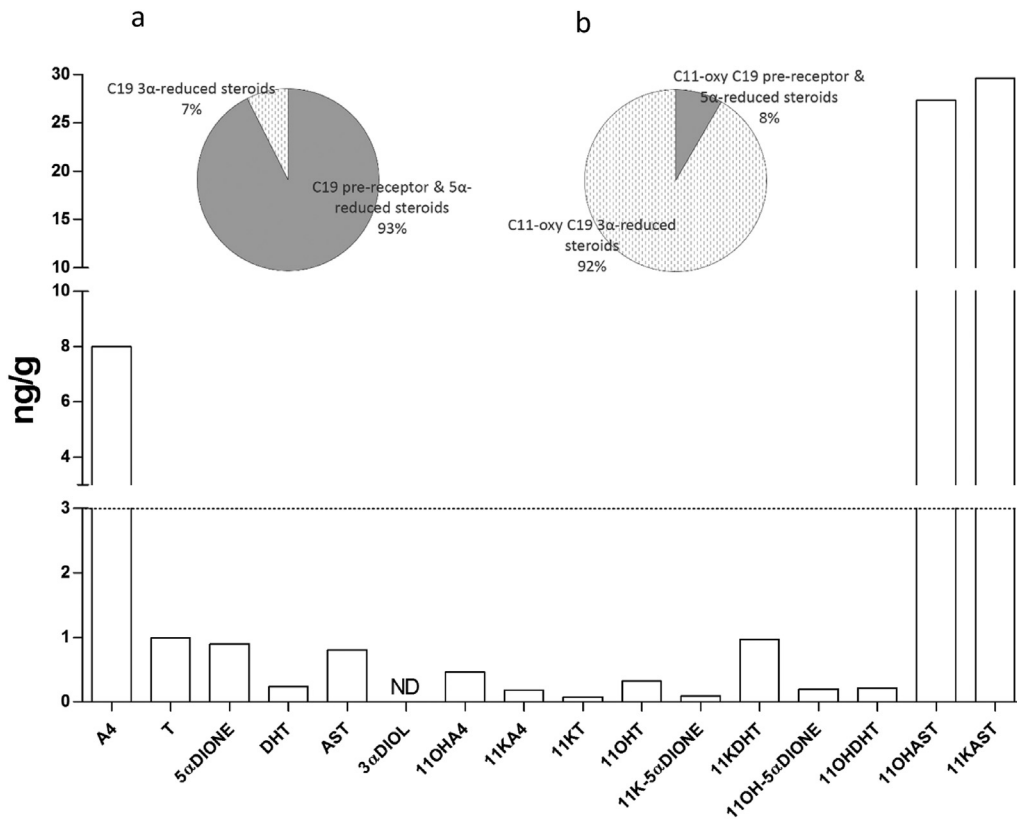
Fig. 4. UPC^2-MS/MS analysis of free, unconjugated C_{19} steroid profiles in prostate tissue. Steroids below the dashed line represent steroids detected below the LOQ. *ND*: not detected. Insert; relative contribution of the active and inactive (a) C_{19} and (b) C11-oxy C_{19} steroids to the patient's steroid profile.
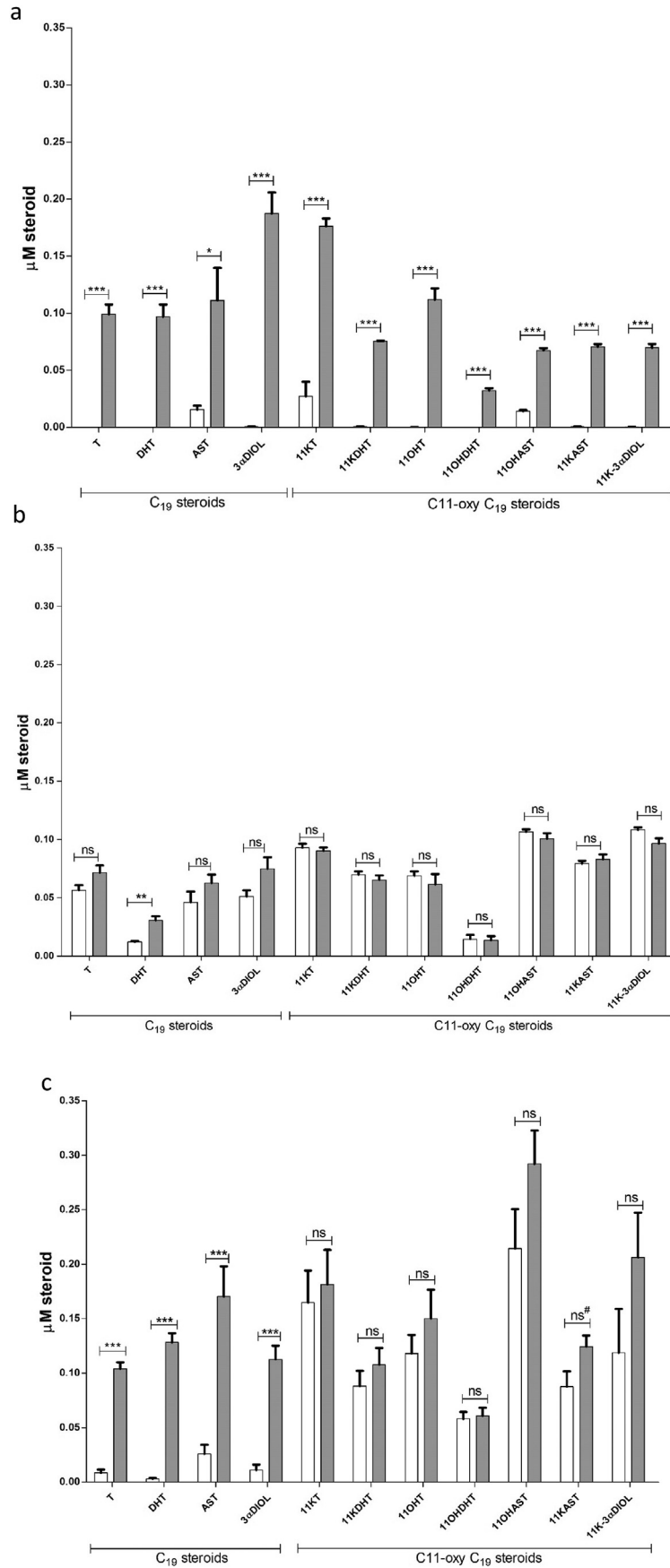
Fig. 5. Analyses of steroid glucuronidation. Substrate (μM normalised to mg protein), unconjugated (clear bars) and total (shaded bars), remaining after conversion of 1 μM in (a) LNCaP; (b) C4-2B and (c) VCaP cells after 48 h. Experiments were performed in triplicate, analysed by UPC^2−MS/MS and the results are expressed as the mean ± STD DEV ($n = 6$, ns = not significant, $^*P < 0.05$, $^{**}P < 0.01$, $^{***}P < 0.001$, $^#P = 0.0593$).

Table 1
Unconjugated, glucuronidated and total plasma steroid levels detected by UPC^2-MS/MS (Shaded steroids detected below the LOQ).

Steroid metabolite	Concentration (nM)								
	Healthy patient (Fig. 6a)			PCa patient (Fig. 6b)			PCa patient (Fig. 6c)		
	Unconjugated	Conjugated	Total	Unconjugated	Conjugated	Total	Unconjugated	Conjugated	Total
T	18.93	0.00	18.93	0.79	0.21	1	0.86	0	0.86
DHT	0.59	0.00	0.59	0.27	0.00	0.27	0.07	0.05	0.11
AST	6.93	12.41	19.34	8.84	0.00	8.84	10.75	0	10.75
3αDIOL	1.52	25.38	26.90	13.39	1.87	15.26	44.44	38.62	83.05
11OHT	0.28	1.92	2.20	0.35	0.91	1.26	1.67	0	1.67
11KT	203.63	71.60	275.23	237.74	11.75	249.49	351.05	35.40	386.44
11KDHT	0.00	49.11	49.11	24.70	0.00	24.70	26.42	0	26.42
11OHAST	26.00	54.76	80.76	75.19	1.51	76.70	17.90	318.74	336.64
11KAST	0.59	10.12	10.71	7.72	0.00	7.72	6.52	0	6.52
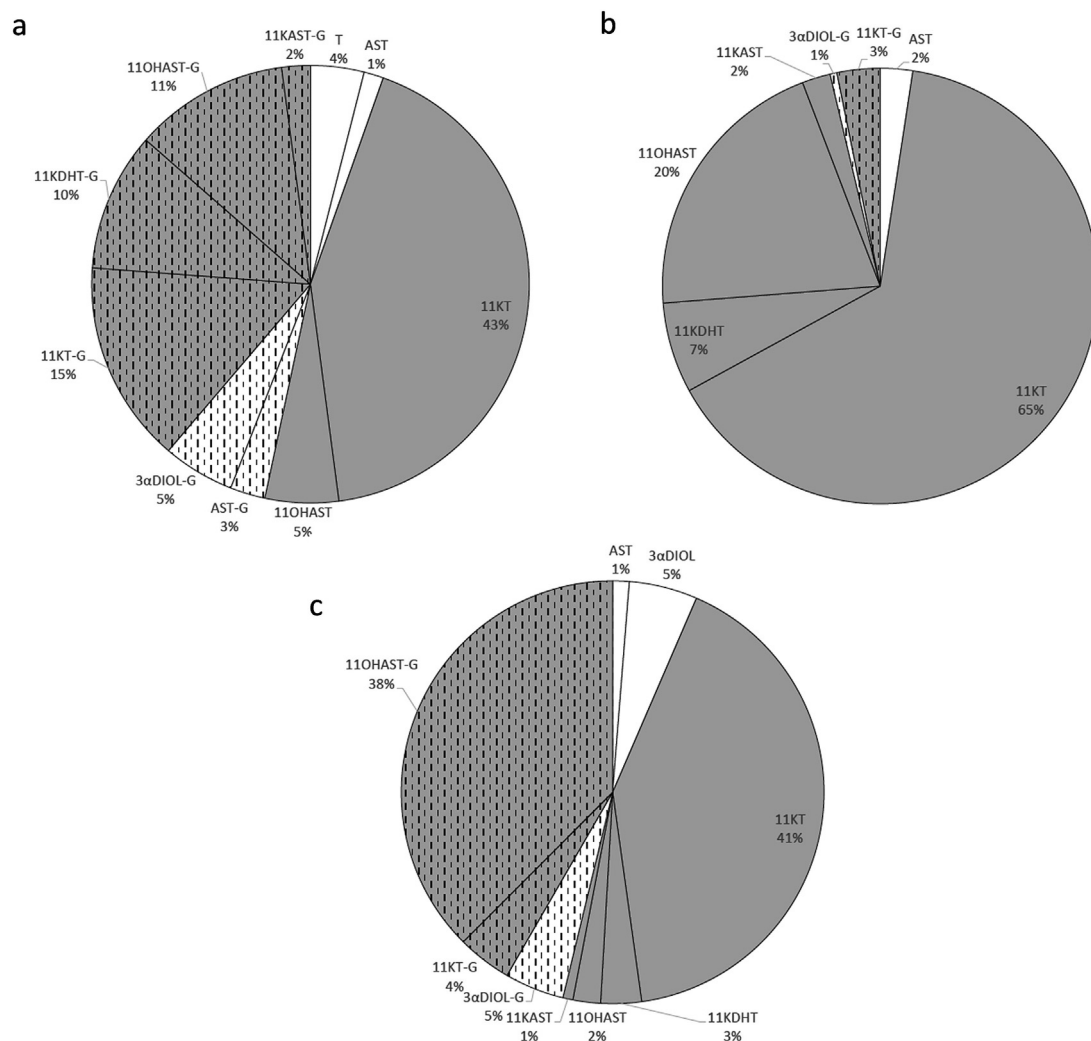
Fig. 6. Relative contribution of unconjugated and conjugated androgens to C$_{19}$ and C11-oxy C$_{19}$ plasma steroid profiles. (a) Healthy subject; (b) PCa patient (BO treatment) and (c) PCa patient (LHRHa treatment, progressed to CRPC). Clear wedges, C$_{19}$ steroids; shaded wedges, C11-oxy C$_{19}$ steroids and patterned wedges, conjugated steroids.

when assaying 11OHDHT, significantly higher levels of 11KDHT and 11K-3αDIOL were detected in C4-2B and VCaP cells than in LNCaP cells, suggesting a greater shunt of androgens in the metabolic pathways in the former two PCa models, which may be ascribed to the endogenous enzyme expression levels −17βHSD types 3, 5 and 6 and SRD5A1 in VCaP cells (Cai et al., 2011; Mitsiades et al., 2012; Sakai et al., 2016; Yepuru et al., 2013) and SRD5A1 and 3 in C4-2B

cells (Uemura et al., 2008). We previously reported that it was only in the conversion of 11OHDHT in LNCaP cells (and not when 11OHA4 was assayed as substrate), that we were able to detect 11KDHT in the unconjugated form, showing 11KDHT to be the predominant active androgen formed with low levels of 11KAST (Bloem et al., 2015). In the present study both 11OHA4 and 11OHT yielded active SRD5A reduced androgens 11KDHT and 11OHDHT,

albeit at low levels. The profile obtained in VCaP cells furthermore clearly indicate competition for 11OHDHT between the oxidative 17βHSDs and 11βHSD2, with the formation of 11OH-5αDIONE and 11KDHT respectively − higher 11OH-5αDIONE levels in VCaP cells than in C4-2B cells reflect higher levels of the oxidative 17βHSDs in VCaP cells than in C4-2B cells. This may be due to the expression of 17βHSD2 in VCaP cells, reported by Sakai et al. (2016). However, the formation of 11OH-5αDIONE would also lead to 11K-5αDIONE production and subsequently 11KDHT (Supplemental Fig. 1). Interestingly the expression of SRD5A2 has, to date, not been reported in these two PCa cell models, possibly due to low expression levels, accrediting the conversion of the C_{19} and C11-oxy C_{19} pre-receptor steroids to their 5α-reduced forms to SRD5A1 (VCaP and C4-2B cells) and SRD5A3 (C4-2B cells). It is therefore clear that steroid profiles would be dictated by the expression levels of endogenous steroidogenic enzymes in the tumour microenvironment. However, the complete steroid profile can only be generated once all steroids in the pathway can be accurately identified and quantitated, currently dependent on the availability of the full cohort of steroid standards.

The levels of pre-receptor androgens produced from adrenal 11OHA4 and 11OHT would be influenced by inactivation and conjugation as well as the conversion of the inactive steroids back to their active forms. Both T and DHT were conjugated efficiently in VCaP cells in which negligible levels of unconjugated steroids were detected, while conjugation was negligible in C4-2B cells. No studies have, to date, reported on C_{19} steroid conjugation in this cell model. In both cell models, the active C11-oxy steroids were present in the unconjugated form, however, low levels of conjugated 11KDHT were detected in VCaP cells. We therefore determined the glucuronidation of the C_{19} and the C11-oxy C_{19} steroids in these models as well as in LNCaP cells (Fig. 5a, b, c). The prostate expresses UGT2B type 15, 17 and 28 with these enzymes conjugating androgens by adding a glucuronide group either at C17 and/or C3: UGT2B15 conjugates androgens (T, DHT, 3αDIOL) at C17 only; UGT2B17 conjugates androgens (T, DHT, 3αDIOL, AST) at C3 and C17; and UGT2B28 conjugates androgens (T, 3αDIOL, AST) at both C3 and C17. It should be noted that UGT2B28 does not conjugate DHT, while also conjugating 3αDIOL with a lower efficiency compared to the other two enzymes (Bélanger et al., 2003; Du Toit et al., 2017; Lévesque et al., 2001).

In LNCaP cells which express all the aforementioned UGTs (Beaulieu et al., 1996; Bélanger et al., 1995; Guillemette et al., 1995; Lévesque et al., 2001), 11KT was detected in the unconjugated form, while none of the C11-oxy C_{19} steroids were conjugated in the C4-2B cells. It is possible that the specific UGT isozymes in C4-2B cells, are expressed at very low levels thus accounting for the detected of DHT conjugation only, or it may perhaps be that the non-functional UGT isoforms are being expressed. Conjugation of C_{19} steroids in VCaP cells has not been characterized. An investigation by Bao et al. (2008), into AR mediated expression of the UGT isoforms, showed that UGT2B15 gene transcripts were expressed in VCaP cells while UGT2B17 was not detected. In a more recent study, UGT2B28 was detected by RT-qPCR in VCaP cells, however, primers, common to three UGT2B28 isoforms, spanned exon one and it cannot therefore be concluded that these transcripts would reflect the expression of a functional protein (Malinen et al., 2015). UGT2B28 type I isoform actively conjugates androgens, with type II possessing a 308 bp deletion, amino acid residues 335−437 in the co-factor binding domain, producing an inactive isoform and type III lacking residues in the substrate binding domain also producing an inactive isoform (Du Toit and Swart, 2016; Lévesque et al., 2001). Having shown that UGT2B15 is present in VCaP cells, our data allows perhaps a tentative speculation that UGT2B15 does not catalyse the conjugation of the C11-oxy C_{19} steroids and since the enzyme acts

specifically at C17 of the C_{19} steroids, it is possible that the inability to conjugate the C11-oxy derivatives suggests that the C11-oxy moiety hampers substrate binding to and/or positioning in the active pocket which readily accommodates the C_{19} steroids (Du Toit et al., 2017; Guillemette et al., 1995). In contrast, it appears that the C11 moiety does not affect inactivation by 3αHSD and in the PCa cell models, 11KDHT was predominantly present in the inactive form while DHT and 3αDIOL were present at equimolar concentrations, however, at markedly higher concentrations than 11KDHT and 11K-3αDIOL.

Our study thus far has investigated the metabolism of the C11-oxy C_{19} steroids depicting their inactivation, reactivation and conjugation in prostate cell models, which is dependent on the expression of steroidogenic enzymes. The resulting steroid profiles permits the postulation and identification of physiologically relevant enzymatic conversions. However, it was reported by Sakai et al. (2016), that *in vitro* findings may perhaps not be reflected *in vivo* and using prostate cell models to study steroid metabolism may be an inaccurate way of investigating steroid biosynthesis. Human prostate samples may contain different transcripts encoding for enzymes and proteins not necessarily detected in prostate cell models (Sakai et al., 2016). Interpreting steroid panels in prostate tissue is therefore fundamental in understanding C11-oxy C_{19} steroid metabolism *in vivo*.

Analyses of tissue clearly demonstrate the different manner in which the C_{19} and the C11-oxy C_{19} steroids are metabolised *in vivo* and the levels at which they are present in their active, inactivated and unconjugated forms. Although our data only includes a single patient's profile, these steroid panels serve to show, not only the abundance of the C11-oxy C_{19} steroids *in vivo*, but also that these steroids are present at significantly higher levels than the C_{19} steroids. These findings corroborate our previous findings (Du Toit et al., 2017), showing too that profiles vary markedly between patients. In addition, the C_{19} steroids are present primarily as DHT and pre-receptor derivatives with inactivated steroids, AST (3αDIOL not detected) comprising only 7%. In contrast, the inactivated C11-oxy C_{19} steroids 11OHAST and 11KAST (11K-3αDIOL not detected) comprised 92%. The high levels of inactivated steroids suggest that while inactivation of the C11-oxy C_{19} steroids appear efficient, conjugation may be less efficient, hampering elimination. 11OHAST and 11KAST in their unconjugated form may be reactivated to 11KDHT, however, neither 3αDIOL nor 11K-3αDIOL were detected suggesting that these were either reactivated or eliminated following conjugation. The reactivation pathway of 11KAST and 11OHAST has been observed in preliminary studies conducted in prostate cells (unpublished results), however, this is dependent on the endogenous expression of the RL-HSD enzymes. We previously reported unconjugated androgen profiles in PCa tissue of patients prior to castration and on LHRH treatment in which the steroids were present at far higher levels than those of the CRPC patient profiled in this study, with the exception of A4. In the previous study 11KAST and 11OHAST were below the LOD with AST and 3αDIOL at 2−5 ng/g, while DHT and 11KDHT were also markedly higher than in the CRPC patient. The significantly higher levels of unconjugated 11KAST and 11OHAST detected in this study indicate an increased shunt in the C11-oxy C_{19} steroid pathway.

Plasma analyses showed, in the healthy subject, that the inactivated C11-oxy C_{19} steroids were ~2-fold higher than the inactivated C_{19} steroids, however, in both PCa patients the inactive C11-oxy C_{19} steroids were ~3.4-fold higher, also indicating a higher throughput of steroids in the 11OHA4 pathway. The contribution of adrenal DHEA to the pool of inactive C_{19} steroids in plasma was, however, not measured. Furthermore, even though T and DHT levels were negligible in treated patients, 11KT and 11KDHT present in their unconjugated form together ranged between 261 and

377 nM (8–11.5 µg/dL). While 11KDHT levels were 2-fold higher in normal plasma compared to treated patients, the steroid was fully glucuronidated. Analyses of circulating steroids also showed that the level of total androgens analysed were similar when comparing the normal subject and the patient who had undergone BO. In the patient who had progressed to CRPC total steroid levels were ~850 nM, 2-fold greater than the BO patient. It should be noted that the contribution of glucuronides detected in circulation are due to UGT2B15, UGT2B17, and UGT2B28 which are expressed in the liver (UGT2B28 I and II), kidney (UGT2B28 type III) and prostate (UGT2B28 type III), with UGT2B15 also expressed in adipose tissue (Beaulieu et al., 1996; Bélanger et al., 2003; Lévesque et al., 1997, 2001). In addition, UGT2B7, which is also capable of conjugating androgens (T, 3αDIOL and AST), is not expressed in the prostate, but is expressed in the liver and kidney, and as such would also contribute to conjugated steroid levels in circulation (Turgeon et al., 2001).

It is clear from our data that larger cohorts are required for conclusions to be drawn regarding active, inactive and glucuronidated androgen levels in PCa. For more accurate quantification, it is important to note that deuterated internal steroids are required for all the steroids which are being measured, however, most of the relevant deuterated steroids are currently commercially unavailable. Although it is possible that C11-oxy C_{19} steroids are conjugated by sulfation, their presence in the unconjugated form already suggests that the downstream metabolism of C_{19} and C11-oxy C_{19} steroids are very different. If unconjugated, these metabolites will remain available, shunted in the metabolic pathway towards 11KT and 11KDHT, activating the AR, possibly exacerbated by enzyme inhibitors. Androgen profiles, both in tissue and in circulation, indicating the necessity of the inclusion of C11-oxy C_{19} steroids in the assessment of not only PCa but also clinical conditions associated with androgen excess.

5. Conclusions

Our data show the C11-oxy C_{19} steroids are the predominant androgens in PCa tissue and in circulation, thereby corroborating our previous reports. Also in contrast to C_{19} steroids, a higher flux is observed in the metabolic pathway of the C11-oxy C_{19} steroids, reflected in higher levels of inactive 11OHAST and 11KAST compared to AST. Data also shows the efficient inactivation of the C11-oxy C_{19} steroids in PCa cell models, with the C_{19} ratio of DHT:3αDIOL being 1:1, compared to the C11-oxy C_{19} ratio of 11KDHT:11K-3αDIOL being >10:1, in all models. Furthermore, *in vitro* and *in vivo* data indicates the C11-oxy C_{19} steroids are not glucuronidated efficiently, with both 11KT and 11KDHT predominantly present in their unconjugated form, while T and DHT were predominantly in the glucuronidated form. In summary, the investigation identifies the presence of the C11-oxy C_{19} steroids and for the first time not only their abundance but, also their inactivation in tissue and glucuronide levels in plasma. These data warrant further *in vivo* studies to provide details regarding the contribution of inactivation and conjugation to the regulation of active androgen levels.

Conflict of interest

The authors declare that there is no conflict of interest.

Acknowledgments

Appendix A. Supplementary data

References

Bao, B.-Y., Chuang, B.-F., Wang, Q., Sartor, O., Balk, S.P., Brown, M., Kantoff, P.W., Lee, G.-S.M., 2008. Androgen receptor mediates the expression of UDP-glucuronosyltransferase 2 B15 and B17 genes. Prostate 68, 839–848. http://dx.doi.org/10.1002/pros.20749.

Beaulieu, M., Lévesque, É., Hum, D.W., Bélanger, A., 1996. Isolation and characterization of a novel cDNA encoding a human UDP-glucuronosyltransferase active on C_{19} steroids. J. Biol. Chem. 271, 22855–22862. http://dx.doi.org/10.1074/jbc.271.37.22855.

Bélanger, A., Pelletier, G., Labrie, F., Barbier, O., Chouinard, S., 2003. Inactivation of androgens by UDP-glucuronosyltransferase enzymes in humans. Trends Endocrinol. Metab. 14, 473–479. http://dx.doi.org/10.1016/j.tem.2003.10.005.

Bélanger, G., Beaulieu, M., Marcotte, B., Lévesque, É., Guillemette, C., Hum, D.W., Bélanger, A., 1995. Expression of transcripts encoding steroid UDP-glucuronosyltransferases in human prostate hyperplastic tissue and the LNCaP cell line. Mol. Cell. Endocrinol. 113, 165–173. http://dx.doi.org/10.1016/0303-7207(95)03627-J.

Bloem, L.M., Storbeck, K.-H., Swart, P., Du Toit, T., Schloms, L., Swart, A.C., 2015. Advances in the analytical methodologies: profiling steroids in familiar pathways – challenging dogmas. J. Steroid Biochem. Mol. Biol. 153, 80–92. http://dx.doi.org/10.1016/j.jsbmb.2015.04.009.

Cai, C., Chen, S., Ng, P., Bubley, G.J., Nelson, P.S., Mostaghel, E.A., Marck, B., Matsumoto, A.M., Simon, N.I., Wang, H., Chen, S., Balk, S.P., 2011. Intratumoral *de novo* steroid synthesis activates androgen receptor in castration-resistant prostate cancer and is upregulated by treatment with CYP17A1 inhibitors. Cancer Res. 71, 6503–6513. http://dx.doi.org/10.1158/0008-5472.CAN-11-0532.

Chang, K.-H., Li, R., Papari-Zareei, M., Watumull, L., Zhao, Y.D., Auchus, R.J., Sharifi, N., 2011. Dihydrotestosterone synthesis bypasses testosterone to drive castration-resistant prostate cancer. Proc. Natl. Acad. Sci. 108, 13728–13733. http://dx.doi.org/10.1073/pnas.1107898108.

Du Toit, T., Bloem, L.M., Quanson, J.L., Ehlers, R., Serafin, A.M., Swart, A.C., 2017. Profiling adrenal 11β-hydroxyandrostenedione metabolites in prostate cancer cells, tissue and plasma: UPC²-MS/MS quantification of 11β-hydroxytestosterone, 11keto-testosterone and 11keto-dihydrotestosterone. J. Steroid Biochem. Mol. Biol. 166, 54–67. http://dx.doi.org/10.1016/j.jsbmb.2016.06.009.

Du Toit, T., Swart, A.C., 2016. Perspective on the regulatory role of UGT2B28 as a conjugating enzyme in the progression of prostate cancer. Transl. Cancer Res. 5 (Suppl. 7), S1496–S1502. http://dx.doi.org/10.21037/tcr.2016.12.22.

Guillemette, C., Hum, D.W., Bélanger, A., 1995. Specificity of glucuronosyltransferase activity in the human cancer cell line LNCaP, evidence for the presence of at least two glucuronosyltransferase enzymes. J. Steroid Biochem. Mol. Biol. 55 (3/4), 355–362. http://dx.doi.org/10.1016/0960-0760(95)00183-2.

Guillemette, C., Lévesque, É., Harvey, M., Bellemare, J., Menard, V., 2010. UGT genomic diversity: beyond gene duplication. Drug Metab. Rev. 42 (1), 22–42. http://dx.doi.org/10.3109/03602530903210682.

Lévesque, É., Beaulieu, M., Green, M.D., et al., 1997. Isolation and characterization of UGT2B15(Y85): a UDP-glucuronosyltransferase encoded by a polymorphic gene. Pharmacogenetics 7, 317–325.

Lévesque, É., Turgeon, D., Carrier, J.-S., Montminy, V., Beaulieu, M., Bélanger, A., 2001. Isolation and characterization of the UGT2B28 cDNA encoding a novel human steroid conjugating UDP-glucuronosyltransferase. Biochem. 40, 3869–3881. http://dx.doi.org/10.1021/bi002607y.

Malinen, M., Toropainen, S., Jääskeläinen, T., Sahu, B., Jänne, O.A., Palvimo, J.J., 2015. Androgen receptor- and PIAS1-regulated gene programs in molecular apocrine breast cancer cells. Mol. Cell. Endocrinol. 414, 91–98. http://dx.doi.org/10.1016/j.mce.2015.07.024.

Mitsiades, N., Sung, C.C., Schultz, N., Danila, D.C., He, D., Eedunuri, V.K., Fleisher, M., Sander, C., Sawyers, C.L., Scher, H.I., 2012. Distinct patterns of dysregulated expression of enzymes involved in androgen synthesis and metabolism in metastatic prostate cancer tumors. Cancer Res. 72, 6142–6152. http://dx.doi.org/10.1158/0008-5472.CAN-12-1335.

Mizokami, A., Koh, E., Izumi, K., Narimoto, K., Takeda, M., Honma, S., Dai, J., Keller, E.T., Namiki, M., 2009. Prostate cancer stromal cells and LNCaP cells coordinately activate the androgen receptor through synthesis of testosterone and dihydrotestosterone from dehydroepiandrosterone. Endocr. Relat. Cancer 16, 1139–1155. http://dx.doi.org/10.1677/ERC-09-0070.

Mohler, J.L., Titus, M.A., Bai, S., Kennerley, B.J., Lih, F.B., Tomer, K.B., Wilson, E.M., 2011. Activation of the androgen receptor by intratumoral bioconversion of androstenediol by dihydrotestosterone in prostate cancer. Cancer Res. 71, 1486–1496. http://dx.doi.org/10.1158/0008-5472.CAN-10-1343.

Montgomery, R.B., Mostaghel, E.A., Vessella, R., Hess, D.L., Kalhorn, T.F., Higano, C.S., True, L.D., Nelson, P.S., 2008. Maintenance of intratumoral androgens in metastatic prostate cancer: a mechanism for castration-resistant tumor growth.

Cancer Res. 68, 4447—4454. http://dx.doi.org/10.1158/0008-5472.CAN-08-0249.

Mostaghel, E.A., 2014. Beyond T and DHT — novel steroid derivative capable of wild type androgen receptor activation. Int. J. Biol. Sci. 10, 602—613. http://dx.doi.org/10.7150/ijbs.8844.

Pretorius, E., Africander, D.J., Vlok, M., Perkins, M.S., Quanson, J.L., Storbeck, K.-H., 2016. 11-Ketotestosterone and 11-ketodihydrotestosterone in castration resistant prostate cancer: potent androgens which can no longer be ignored. PLoS One 11, e0159867. http://dx.doi.org/10.1371/journal.pone.0159867.

Rege, J., Nakamura, Y., Satoh, F., Morimoto, R., Kennedy, M.R., Layman, L.C., Honma, S., Sasano, H., Rainey, W.E., 2013. Liquid chromatography-tandem mass spectrometry analysis of human adrenal vein 19-carbon steroids before and after ACTH stimulation. J. Clin. Endocrinol. Metab. 98, 1182—1188. http://dx.doi.org/10.1210/jc.2012-2912.

Sakai, M., Martinez-Arguelles, D.B., Aprikian, A.G., Magliocco, A.M., Papadopoulos, V., 2016. De novo steroid biosynthesis in human prostate cell lines and biopsies. Prostate 76, 575—587. http://dx.doi.org/10.1002/pros.23146.

Stanbrough, M., Bubley, G.J., Ross, K., Golub, T.R., Rubin, M.A., Penning, T.M., Febbo, P.G., Balk, S.P., 2006. Increased expression of genes converting adrenal androgens to testosterone in androgen-independent prostate cancer. Cancer Res. 66, 2815—2825. http://dx.doi.org/10.1158/0008-5472.CAN-05-4000.

Storbeck, K.-H., Bloem, L.M., Africander, D.J., Schloms, L., Swart, P., Swart, A.C., 2013. 11β-hydroxydihydrotestosterone and 11-ketodihydrotestosterone, novel C19 steroids with androgenic activity: a putative role in castration resistant prostate cancer? Mol. Cell. Endocrinol. 377, 135—146. http://dx.doi.org/10.1016/j.mce.2013.07.006.

Swart, A.C., Schloms, L., Storbeck, K.-H., Bloem, L.M., Du Toit, T., Quanson, J.L., Rainey, W.E., Swart, P., 2013. 11β-Hydroxyandrostenedione, the product of androstenedione metabolism in the adrenal, is metabolized in LNCaP cells by 5α-reductase yielding 11β-hydroxy-5α-androstanedione. J. Steroid Biochem. Mol. Biol. 138, 132—142. http://dx.doi.org/10.1016/j.jsbmb.2013.04.010.

Thomas, L.N., Douglas, R.C., Lazier, C.B., Too, C.K.L., Rittmaster, R.S., Tindall, D.J., 2008. Type 1 and type 2 5α-reductase expression in the development and progression of prostate cancer. Eur. Urol. 53, 244—252. http://dx.doi.org/10.1016/j.eururo.2007.10.052.

Titus, M.A., Gregory, C.W., Ford III, O.H., Schell, M.J., Maygarden, S.J., Mohler, J.L., 2005. Steroid 5α-reductase isozymes I and II in recurrent prostate cancer. Clin. Cancer Res. 11, 4365—4371. http://dx.doi.org/10.1158/1078-0432.CCR-04-0738.

Turcu, A.F., Nanba, A.T., Chomic, R., Upadhyay, S.K., Giordano, T.J., Shields, J.J., Merke, D.P., Rainey, W.E., Auchus, R.J., 2016. Adrenal-derived 11-oxygenated 19-carbon steroids are the dominant androgens in classic 21-hydroxylase deficiency. Eur. J. Endocrinol. 174 (5), 601—609. http://dx.doi.org/10.1530/EJE-15-1181.

Turgeon, D., Carrier, J.-S., Lévesque, É., Hum, D.W., Bélanger, A., 2001. Relative enzymatic activity, protein stability, and tissue distribution of human steroid-metabolizing UGT2B subfamily members. Endocrinol 142 (2), 778—787. http://dx.doi.org/10.1210/endo.142.2.7958.

Uemura, M., Tamura, K., Chung, S., Honma, S., Okuyama, A., Nakamura, Y., Nakagawa, H., 2008. Novel 5α-steroid reductase (SRD5A3, type-3) is overexpressed in hormone-refractory prostate cancer. Cancer Sci. 99, 81—86. http://dx.doi.org/10.1111/j.1349-7006.2007.00656.x.

Yepuru, M., Wu, Z., Kulkarni, A., Yin, F., Barrett, C.M., Kim, J., Steiner, M.S., Miller, D.D., Dalton, J.T., Narayanan, R., 2013. Steroidogenic enzyme AKR1C3 is a novel androgen receptor-selective coactivator that promotes prostate cancer growth. Cancer Res. 19, 5613—5625. http://dx.doi.org/10.1158/1078-0432.CCR-13-1151.

Supplemental Fig. 1 – (a) C_{19} and (b) C11-oxy C_{19} metabolic pathways. Boxed steroids (dashed line) depict human AR agonists at 1 nM; [a]11OHDHT has not been shown to be a substrate for AKR1C2 nor 11OHAST for 17βHSD3 and AKR1C3, and neither 11K-3αDIOL for 11βHSD1 co-transfected with hexose 6-phosphate dehydrogenase.

Supplemental table 1: Gradient specifications of the UPC^2 separation of C_{19} steroid metabolites.

Step	Time (min)	Solvent A (%)	Solvent B (%)	Curve
1	0	99	1	Initial
2	4.0	85	15	7
3	4.1	75	25	6
4	4.2	99	1	6
5	5.0	99	1	6

Supplemental table 2: Gradient specifications of the UPC^2 separation of C_{11}-oxy C_{19} steroid metabolites.

Step	Time (min)	Solvent A (%)	Solvent B (%)	Curve
1	0	98	2	Initial
2	4	85	15	6
3	4.1	75	25	6
4	4.2	98	2	6
5	5	98	2	6
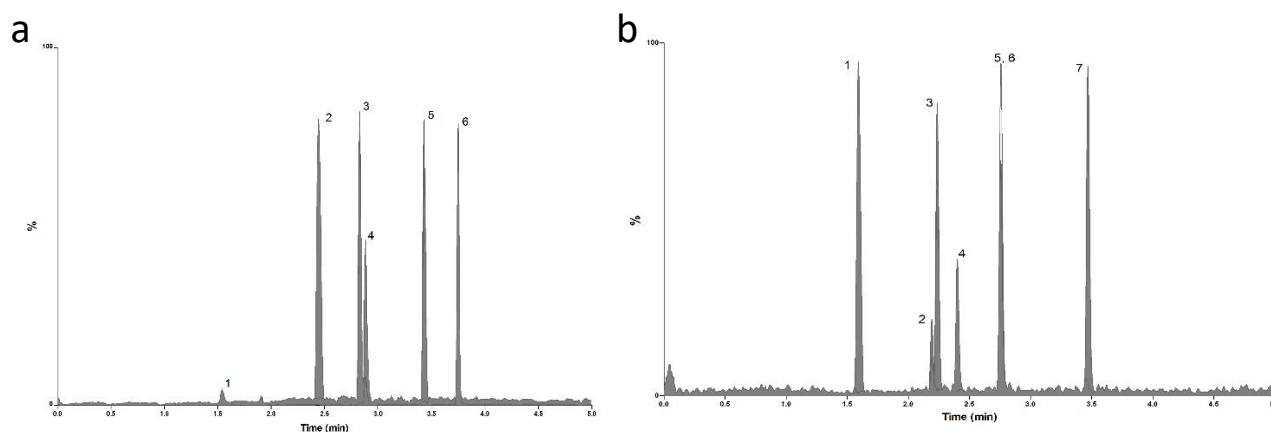
Supplemental Fig. 2 - UPC^2-MS/MS separation of C_{19} reference standards. (a) C_{19} steroids, 2 µL each of a 1 ng/µL standard solution, are depicted in the elution order of (1) 5αDIONE, 1.91 min, (2) A4, 2.44 min, (3) DHT, 2.83 min, (4) AST, 2.88 min, (5) T, 3.43 min and (6) 3αDIOL, 3.75 min; and (b) C_{11}-oxy C_{19} steroids, 2 µL each of a 1 ng/µL standard solution, are depicted in the elution order of (1) 11KA4, 1.59 min, (2) 11KAST, 2.19 min, (3) 11OHA4, 2.24 min, (4) 11KDHT, 2.40 min, (5) 11KT (clear peak), 2.76 min, (6) 11OHAST, 2.76 min and (7) 11OHT, 3.47 min.

Supplemental table 3: UPC[2]-MS/MS method validation for the extraction of steroids from cell culture media using DCM. Three steroid concentrations were analysed to determine accuracy[a] (%RSD, n=8) and precision[b] with inter day variability (%RSD, n=8).

	Steroid metabolite	Accuracy (%RSD) ng/µL			Precision (%RSD) ng/µL					
					Day 1			Day 2		
		0.002	0.02	0.1	0.002	0.02	0.1	0.002	0.02	0.1
C$_{19}$ steroids	A4	2.99	2.12	4.49	5.35	7.78	3.57	7.16	10.10	3.78
	T	4.24	1.98	2.26	4.97	10.60	5.05	9.28	9.03	10.93
	5αDIONE	12.92	3.27	4.20	9.49	9.17	4.44	8.76	7.25	2.50
	DHT	7.96	3.44	6.67	14.67	14.46	4.94	8.19	8.78	7.21
	AST	17.76	3.32	6.11	9.21	11.61	5.93	12.50	17.39	10.00
	3αDIOL	14.51	13.25	4.59	19.70	18.26	9.87	18.50	8.64	3.07
C11-oxy C$_{19}$ steroids	11OHA4	15.36	7.51	5.78	14.89	9.19	9.64	9.85	12.74	6.21
	11OHT	11.47	8.70	2.98	18.07	8.51	8.13	19.60	14.79	13.42
	11KA4	17.35	6.70	8.50	18.59	14.87	10.81	6.48	13.23	19.30
	11KT	18.67	5.46	12.70	19.95	18.94	9.34	9.55	9.56	4.37
	11KDHT	<LOQ	17.38	15.80	<LOQ	18.22	10.44	<LOQ	15.74	13.81
	11OHAST	<LOQ	18.50	12.83	<LOQ	19.69	12.37	<LOQ	18.63	13.35
	11KAST	<LOQ	18.83	15.63	<LOQ	16.09	10.69	<LOQ	10.50	7.76

[a]Accuracy: %RSD from the average calculated response following repeated injection; [b]Precision: %RSD from the average calculated response following independent replicates and was repeated over two days to assess inter day variability.

Supplemental table 4: UPC[2]-MS/MS method validation for the extraction of steroids from FBS using MTBE. Three steroid concentrations were analysed to determine accuracy[a] (%RSD, n=8) and precision[b] with inter day variability (%RSD, n=8).

	Steroid metabolite	Accuracy (%RSD) ng/µl			Precision (%RSD) ng/µL					
					Day 1			Day 2		
		0.002	0.02	0.1	0.002	0.02	0.1	0.002	0.02	0.1
C$_{19}$ steroids	A4	1.78	3.58	1.94	4.20	6.62	2.62	3.84	5.40	3.81
	T	1.27	2.10	1.86	2.16	8.25	1.50	10.11	7.28	4.21
	5αDIONE	3.52	5.09	2.49	5.55	9.10	5.08	6.69	9.56	3.70
	DHT	3.21	6.78	4.19	5.41	9.26	7.05	10.32	7.08	4.59
	AST	9.44	4.94	2.57	8.37	6.90	5.84	11.53	9.71	5.96
	3αDIOL	11.76	2.89	4.41	12.33	4.84	7.87	15.09	5.88	6.77
C11-oxy C$_{19}$ steroids	11OHA4	5.50	4.87	3.64	5.32	5.35	5.30	8.00	4.29	8.82
	11OHT	9.61	7.96	8.34	10.72	3.62	6.68	9.81	4.70	18.92
	11KA4	9.15	5.45	13.63	7.86	7.35	6.86	8.36	9.46	9.14
	11KT	8.92	5.02	3.37	8.74	4.19	6.89	10.60	5.15	7.72
	11KDHT	<LOQ	8.88	6.46	<LOQ	13.76	6.69	<LOQ	8.32	7.27
	11OHAST	<LOQ	13.38	8.70	<LOQ	13.42	8.90	<LOQ	3.05	3.67
	11KAST	<LOQ	10.03	5.40	<LOQ	11.45	6.85	<LOQ	9.23	8.81

[a]Accuracy: %RSD from the average calculated response following repeated injection; [b]Precision: %RSD from the average calculated response following independent replicates and was repeated over two days to assess inter day variability.

Supplemental table 5: UPC^2-MS/MS detection and quantification of C$_{19}$ steroid standards. Molecular ion species and mass transitions; retention time (RT, min); limit of detection (LOD) and limit of quantification (LOQ) of steroids; mass spectrometer settings, cone voltages (CV), collision energy (CE); and internal deuterated standards, testosterone-D2, cortisol-D4, progesterone-D9, androstenedione-D7 and 11β-hydroxyandrostenedione-D7.

Steroid metabolite	RT (min)	Mass transitions		CV (V)		CE (eV)		LOD[a] (ng/µL)[1]	LOQ[b] (ng/µL)
		Quantifier	Qualifier						
A4	2.44	287.2>96.9	287.2>108.8	30	30	15	15	<0.00001	0.0001
T	3.43	289.2>97.2	289.2>109.0	30	30	22	22	<0.00001	0.0001
5αDIONE	1.91	289.2>253.1	289.2>97.2	22	30	16	22	0.00025	0.001
DHT	2.83	291.2>255.0	291.2>273.0	25	25	15	20	0.00025	0.001
AST	2.88	273.2>105.3	291.3>273.3	30	18	30	8	0.00025	0.001
3αDIOL	3.75	275.2>257.0	275.2>175.0	15	15	15	15	0.0001	0.001
Testosterone-D2	3.43	291.0>99.1	291.0>111.2	30	30	20	30	-	-
Cortisol-D4	4.51	367.0>121.0		35		25		-	-
Progesterone-D9	2.28	324.2>100.0	324.2>113.0	30	30	20	25	-	-
Androstenedione-D7	2.43	294.3>100.0	294.3>113.0	25	25	25	25	-	-
11β-hydroxyandrostenedione-D7	3.56	310.2>99.8	310.2>147.2	25	25	30	25	-	-
11OHA4	2.24	303.2>267.2	303.2>121.0	30	30	30	15	0.00001	0.0001
11OHT	3.47	305.3>121.0	305.3>269.0	35	35	20	15	0.00001	0.0001
11KA4	1.59	301.2>257.0	301.2>265.2	35	35	25	25	0.00001	0.0001
11KT	2.76	303.2>121.0	303.2>267.0	30	30	20	20	0.00001	0.0001
11OH-5αDIONE	1.81	305.0>269.2	305.0>287.2	35	35	15	15	-	-
11K-5αDIONE	1.28	303.2>241.0	303.2>267.0	35	35	30	25	-	-
11OHDHT	3.06	307.0>253.0	307.0>271.0	35	35	20	20	-	-
11KDHT	2.40	305.2>243.0	305.2>269.0	30	30	20	20	0.00025	0.01
11OHAST	2.76	289.0>271.0	289.0>213.0	15	15	15	15	0.005	0.01
11KAST	2.19	305.0>147.2	305.0>173.1	30	30	30	30	0.005	0.01
11K-3αDIOL	3.37	307.2>271.0	307.2>253.0	15	15	10	10	-	-
Testosterone-D2	2.14	291.0>99.1	291.0>111.2	30	30	20	30	-	-
Cortisol-D4	3.74	367.0>121.0		35		25		-	-
Progesterone-D9	1.14	324.2>100.0	324.2>113.0	30	30	20	25	-	-
Androstenedione-D7	1.17	294.3>100.0	294.3>113.0	25	25	25	25	-	-
11β-hydroxyandrostenedione-D7	2.22	310.2>99.8	310.2>147.2	25	25	30	25	-	-

[a]Limit of detection was defined as S/N ratio >3 for the quantifier ion; [b]Limit of quantification was defined as a S/N ratio >10 for the quantifier ion and >3 for the qualifier ion; [1]Quanson et al., 2016.

Preparation of commercially unavailable steroids

11OHDHT and 11K-3αDIOL were prepared as follows: HEK293 cells were transfected with SRD5A1 (0.5 μg) and SRD5A2 (0.5 μg) and with AKR1C3 (1 μg). After 72 hrs, 11OHT (2 μM) was added to HEK293 cells expressing SRD5A1/2 and incubated for 24 hrs to produce 11OHDHT. 11KAST (2 μM) was converted to 11K-3αDIOL in HEK293 cells expressing AKR1C3 following the same protocol. Media were collected from HEK293 cells, diluted (1:1) with prostate cell-specific culture media and added at 1 μM to LNCaP, C4-2B and VCaP cells.

Steroid extraction

A 10:1 volume of dichloromethane (DCM) was added to sampled aliquots for assays in prostate cells, vortexed at 1000 RPM for 15 min, and centrifuged for 5 min. Extracted media was aspirated, the DCM phase dried under nitrogen and the dried residues dissolved in 0.15 mL 50% methanol in water.

Frozen prostate tissue samples were homogenised with 3 mL deionized water and the samples lyophilised overnight. Dried samples were homogenised in 5 mL methyl tert-butyl ether (MTBE), after which samples were sonicated for 10 min. Samples were transferred to screw cap tubes, shaken at 1000 RPM for 60 min, and centrifuged for 10 min. The supernatant was transferred and dried under nitrogen. Dried steroid residues were resuspended in 0.15 mL 50% methanol in water.

Plasma samples (1 mL) were thawed on ice and vortexed after which one 0.5 mL was extracted, and the other 0.5 mL subjected to deconjugation (see below), prior to extraction. Internal standards testosterone-D2 and cortisol-D4 were prepared in MTBE and added to samples prior to extraction. The samples were vortexed in 5 mL MTBE for 15 min at 1000 RPM, the organic layer was removed and dried under nitrogen. The dried steroid residue was dissolved in 0.15 mL 50% methanol in water.

Deconjugation of steroids

Aliquots (0.5 mL) were treated with 400 units (76 μL) of β-glucuronidase (Type VII-A from *E.coli*, 5,292,000 units/g; G7646 from Sigma-Aldrich; St.Louis, MO, USA) at 37 °C, pH 6.5, for 24 hrs to deconjugate steroids. DHT-G (1 μM; in 0.5 mL media) was deconjugated and extracted, and used as a control for deconjugation efficiency, confirmed by the amount of DHT recovered using UPC[2]-MS/MS.

Separation and quantification of steroid metabolites

Stock solutions of steroids were dissolved in absolute ethanol (2 mg/mL) and stored at -20°C. Standards were prepared as follows: a standard range, 0.00025 – 0.5 ng/μL prepared in deionized water applied in tissue sample analysis, a standard range, 0.0001 to 1 ng/μL, prepared (i) in RPMI-

1640 cell culture media applied in analysis of cell model assays and (ii) in FBS for plasma sample analysis. The prepared steroid standards were extracted using the protocol described above.

Steroids that were not commercially available were quantified by UPC^2-MS/MS, following peak integrations, using response factors, previously determined by Quanson (2015), as follows: for 11OH-5αDIONE relative to 11OHA4, 4.147±0.640; for 11K-5αDIONE relative to 11KA4, 4.501±0.549; and for 11OHDHT relative to 11OHT, 3.812±0.243 (tissue samples only). Standard curves were generated by integrating respective substrates to quantify C11-oxy 5α-reduced steroids. For enzymatic assays completed in prostate cells, 11OHDHT and 11K-3αDIOL concentrations were calculated relative to the ionisation when only the product is present, representing 100% conversion of substrate to product (1 µM of 11OHT converted to 1 µM 11OHDHT after 24 hrs in transiently SRD5A1/2 transfected HEK293 cells and 1 µM of 11KAST converted to 1 µM 11K-3αDIOL after 24 hrs in transiently AKR1C3 transfected HEK293 cells). Standard curves were generated by integrating respective substrates to quantify C11-oxy 5α-reduced steroids.

The C_{19} steroids were analysed by ACQUITY UPC^2–MS/MS (Waters Corporation, Milford, USA), separated using ACQUITY UPC^2 BEH column (3 mm x 100 mm, 1.7 µm particle size) for the A4 and T metabolites and an ACQUITY UPC^2 BEH 2-EP column (3 mm x 100 mm, 1.7 µm particle size) for the C11-oxy C_{19} metabolites. Briefly, the mobile phase consisted of CO_2 modified with methanol in which steroids, injection volume, 2 µL, were eluted at a flow rate of 2 mL/min in a total run time of 5 min per sample. The column temperature was set to 60°C and the automated back pressure regulator (ABPR) was set to 2000 psi. A Xevo TQ-S triple quadrupole mass spectrometer (Waters, Milford, USA) was used for quantitative mass spectrometric detection and all steroids were analysed in MRM mode, using the ESI$^+$ mode. A make-up pump was utilized in the system, which fed 1% formic acid in methanol into the mixer preceding the MS line at a constant flow rate of 0.2 mL/min. The capillary voltage of 3.8 kV, cone voltage of 15-35 V and collision energy of 8-30 eV was set during this quantification. The following settings were used: source temperature 120 °C, desolvation temperature 500 °C, desolvation gas 1000 L/h and cone gas 150 L/h.

References:

Quanson, J.L. 2015. The characterisation of the catalytic activity of human steroid 5α-reductase towards novel C19 substrates, MSc thesis, Stellenbosch University, http://scholar.sun.ac.za/handle/10019.1/97057.

Quanson, J.L., Stander M., Pretorius E., Taylor, A., Storbeck, K.-H., 2016. High-throughput analysis of 19 endogenous androgenic steroids by ultraperformance convergence chromatography tandem mass spectrometry. J. Chromatogr. B 1031, 131–138. https://doi.org/10.1016/j.jchromb.2016.07.024.

3.2 Summary

The *in vitro* and *in vivo* data clearly show that the C11-oxy C_{19} steroids are not glucuronidated as efficiently as the C_{19} steroids. In LNCaP and C4-2B cells, 11KT-G and 11KDHT-G formation was inefficient compared to T-G and DHT-G formation, and while C_{19} steroids were glucuronidated in VCaP cells, the C11-oxy C_{19} steroids remained unconjugated. Furthermore, in PCa patients, circulatory 11KT and 11KDHT were present in their unconjugated forms, while 11KDHT-G was the predominant form present in the healthy subject. In addition, T and DHT levels were negligible in the PCa patients, with high levels of unconjugated T detected only in the healthy subject. Clearly, glucuronidation of 11KT and 11KDHT was impeded and the levels of these steroids detected as unconjugated metabolites in plasma and tissue, highlight the relevance of these steroids in PCa and their potential role in PCa progression.

Unique steroid profiles, which revealed enzyme activities and substrate preferences, were also established in prostate cell models. In both PNT2 and LNCaP cells DHT was predominantly produced from the precursor steroid, A4, highlighting SRD5A catalysing the alternative pathway as the preferred route to DHT in these cells. Interestingly, PNT2, C4-2B and VCaP cells produced equal amounts of DHT, although in VCaP cells, DHT was primarily present in the glucuronidated form. Considering the 17βHSD isoform, reductive 17βHSD activity was also more active compared to the oxidative 17βHSD isoform, thus promoting the biosynthesis of active androgens in both PNT2 and LNCaP cells. All cell models showed 11βHSD2 activity, able to convert C11-hydroxy to C11-keto metabolites, however, different preferences were evident. PNT2 cells exhibited the least 11βHSD2 activity when compared to VCaP cells, which in turn was lower than that in C4-2B cells when considering the conversions of 11OHA4 and 11OHT to 11KA4 and 11KT, respectively, suggesting C4-2B cells has the highest 11βHSD2 expression levels. C4-2B cells also metabolized 11OHDHT more readily compared to VCaP and LNCaP cells, while exhibiting

no conjugating activity towards the C11-oxy metabolites compared to the glucuronidation of DHT. Furthermore, both C4-2B and VCaP cells showed equal inactivation and reactivation activity towards DHT, while the inactivation of 11KDHT was very different. 11KDHT's inactivation by 3αHSDs endogenously expressed in LNCaP, VCaP and C4-2B cells was efficient, being greater than that of the inactivation of DHT, suggesting that the C11 keto-moiety did not affect the binding of the steroid to the enzyme. Conversely, the reactivation of 11KDHT when compared to DHT was hampered in all the cell models, suggesting the C11-keto moiety may affect steroid-enzyme binding.

Taking together, our *in vitro* metabolic assays, suggest that the C11-oxy C_{19} steroids (11OHA4, 11OHT, 11KA4 and 11KT) remained mainly in the top tier of the 11OHA4-pathway regarding the C4-2B and VCaP cells, more so than in LNCaP cells, which in turn was also higher than in the normal PNT2 cell model. This highlights a greater metabolic shunt of these C11-oxy steroids in the PCa cells, suggesting a more prominent role for these metabolites in PCa. 11KT, produced at high levels in these PCa cell models in the metabolism of 11OHA4 and 11OHT, and together with its hampered glucuronidation, places this steroid in the spotlight as the most prominent androgen in the 11OHA4-pathway.

In terms of UGT2B enzymes, while UGT2B15 and B17 are intricately involved in the inactivation of steroids and decreased UGT2B17 expression has been associated with reduced steroid glucuronide production, UGT2B28 has been shown to have a more prominent regulatory role in PCa rather than steroid inactivation. Moreover, whether the C11-oxy C_{19} are glucuronidated by specific isoforms still remains to be clarified. While LNCaP cells, which endogenously express all three isoforms, conjugated the C_{19} and the C11-oxy C_{19} steroids suggesting the involvement of all three UGT isoforms, VCaP cells which express UGT2B15 did not conjugate the C11-oxy C_{19} steroids –suggesting UGT2B17 is the isoform

involved in the glucuronidation of the C11-oxy C_{19} steroids. Although, in terms of these C11-oxy steroids, UGT2B28 cannot be disregarded as a conjugating enzyme, UGT2B28 has been shown to be a weaker UGT enzyme compared to UGT2B15 and B17 in the glucuronidation of the C_{19} steroids. UGT2B17 enzymatic conversion assays conducted with single steroid substrates, may provide insight into the conjugation at C17 and C3 of the C11-oxy C_{19} steroids, in addition to the possible glucuronidation of the C11-hydroxy group. It would also be interesting to determine whether increased conjugated C11-oxy C_{19} steroids are detected *in vivo*, together with the increased expression of UGT transcripts, as has been reported regarding the UGT2B28 isoform. If it is assumed that increased UGT2B28 expression allows isoform aggregation, leading to inactive UGT enzymes, decreased steroid glucuronidation and therefore increased C_{19} androgens in circulation –which may further contribute to increased active C11-oxy C_{19} steroids in circulation.

Collectively, our *in vivo* data show for the first time, that the C11-oxy C_{19} steroids are present at levels higher than the C_{19} steroids. Although our *in vivo* data did not include the analysis of DHEA as a contributing C_{19} steroid, this steroid is considered a precursor steroid to C_{19} steroids, which include the C11-oxy C_{19} steroids. This study, furthermore, quantified high levels of 11OHA4, 11KT and 11KDHT in PCa tissue and plasma of PCa patients; and in tissue samples 11KDHT, and 11OHAST and 11KAST were present at levels higher than DHT and AST, respectively –underscoring these C11-oxy metabolites as role-players in PCa.

Taken together, it is clear that targeting T alone cannot be justified in treatment regimes, nor can T and DHT be the only steroid metabolites measured for prognostic scoring and in ascertaining treatment efficacy in PCa patients. Adrenal 11OHA4 presents a significant androgen precursor and its downstream metabolism to 11KT and 11KDHT substantiates the important role of this adrenal androgen in PCa.

Chapter 4

A preliminary investigation into the conjugation of C11-oxy C_{19} steroids by sulfation in LNCaP prostate

cells and in plasma

4.1 Introduction

The sulfation of steroids is another form of conjugation, besides glucuronidation, that occurs in target

tissue such as, the adrenals, kidneys, liver and prostate (Javitt et al. 2001; Rainey and Nakamura 2008;

Riches et al. 2009; Rege et al. 2014). Sulfation proceeds with the addition of a sulfate group to the steroid

backbone structure, either at C3 or C17 with a hydroxy moiety and is catalysed by SULTs. In contrast to

glucuronidation, however, steroid sulfation is reversible whereby the sulfate group is hydrolysed,

catalysed by arylsulfatase C also known as STS, which restores the hydroxy group and provides once

again an androgen precursor to the pool of active androgens (Mueller et al. 2015). STS mRNA expression

and enzyme activity has been shown in the testis, ovary, adrenals, kidney and prostate (Reed et al. 2005;

Dalla Valle et al. 2007; Nardi et al. 2009). Although, steroid sulfation contributes to the inactivation of

the steroids, it is not a termination of the physiological signal since reactivation by desulfation is possible.

Steroid sulfation is possible only once sulfate is taken up into the target cell by sulfate transporters, the

subsequent conversion of the sulfate to PAPS by PAPSS1 and PAPSS2, and finally the transfer of the

sulfate group to the oxygen moiety by cytoplasmic SULTs (Hemmerich et al. 2004). SULTs that are

involved in steroid sulfation include SULT1A1 (also known as phenol sulfotransferase), SULT1E1 (also

known as estrogen sulfotransferase), SULT2A1 (also known as DHEA sulfotransferase) and SULT2B1a and

SULT2B1b (Strott 2002; Mueller et al. 2015). SULT2A1 has been shown to catalyse the sulfation of DHEA,

PREG and AST (Falany et al. 1989; Chang et al. 2001; Meloche and Falany 2001;

96

Fuda et al. 2002; Chang et al. 2004; Ekuase et al. 2011; Gulcan and Duffel 2011), with SULT2B1a catalysing

the sulfation of PREG and SULT2B1b the sulfation of cholesterol (Fuda et al. 2002). In addition to

SULT2A1, SULT1E1 and SULT2Bs would also catalyse the sulfation of DHEA (Hempel et al. 2000; Mueller

et al. 2015) (Fig. 4.1).
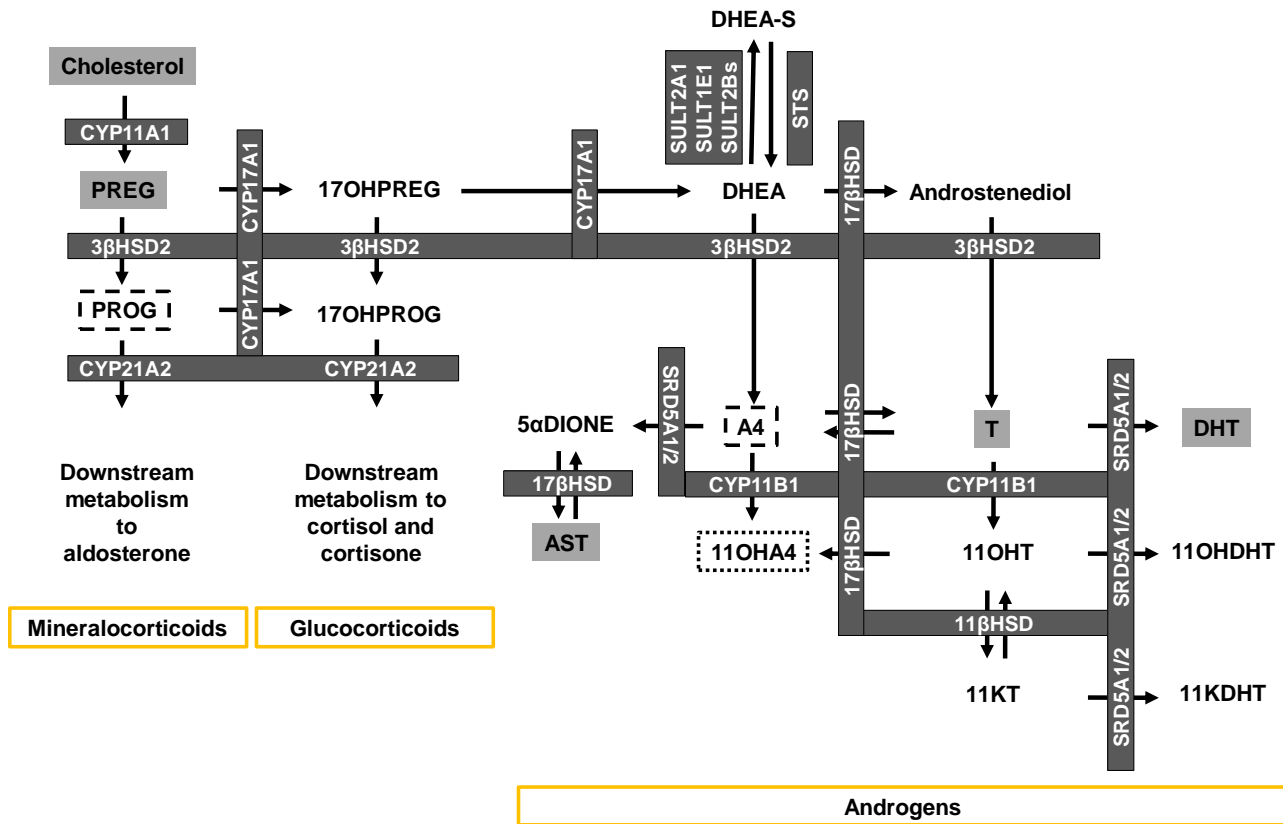
Figure 4.1 Adrenal and peripheral steroid metabolism. Shaded steroids, sulfated derivatives detected in circulation; Dashed boxed steroid, A4 and PROG, novel SULT2A1 ketosteroid substrates; 11OHA4, not a SULT2A1 substrate.

The most commonly reported adrenal steroids involved in sulfation and in desulfation are DHEA and

DHEA-S, respectively. DHEA, once produced from 17OHPREG by the CYP17A1 catalysed reaction, is the

first precursor in the androgen arm of adrenal steroidogenesis, and can either be converted to A4 by

3βHSD2 or inactivated to DHEA-S, specifically DHEA-3-sulfate, as the C3-hydroxy group of DHEA is sulfated by SULTs. Circulating DHEA-S levels range from 2000-1000 nmol/L in males, in premenopausal females from 1000-8000 nmol/L and in postmenopausal females from 1000-6000 nmol/L, with the DHEA:DHEA-S ratio shown to be 1:400, 1:200 and 1:300, respectively (Mueller et al. 2015). Although the sulfated C_{19} androgens are not as abundant, both AST-sulfate (AST-S, sulfate moiety at C3) and DHT-sulfate (DHT-S, sulfate moiety at C17) have been detected in circulation. Compared to DHEA-S, however, DHT-S levels are low, ranging between 50-100 nmol/L, with AST-S present at higher levels ranging from 0-5000 nmol/L in males (Mueller et al. 2015). Of note, both AST-S and DHT-S act as reservoirs to be reactivated to DHT by STS (Fig. 4.2) and steroidogenic enzymes (as is the case of AST-S). The sulfation of other C_{19} steroids, including T and 3αDIOL has not been widely reported, with both steroids possessing a C17-hydroxy group and 3αDIOL also possessing a C3-hydroxy group. It has been reported that SULTs prefer the C3-hydroxy group, therefore the sulfation of 3αDIOL would be expected, however, with the sulfation of DHT occurring at C17, the sulfation of T should also be possible.
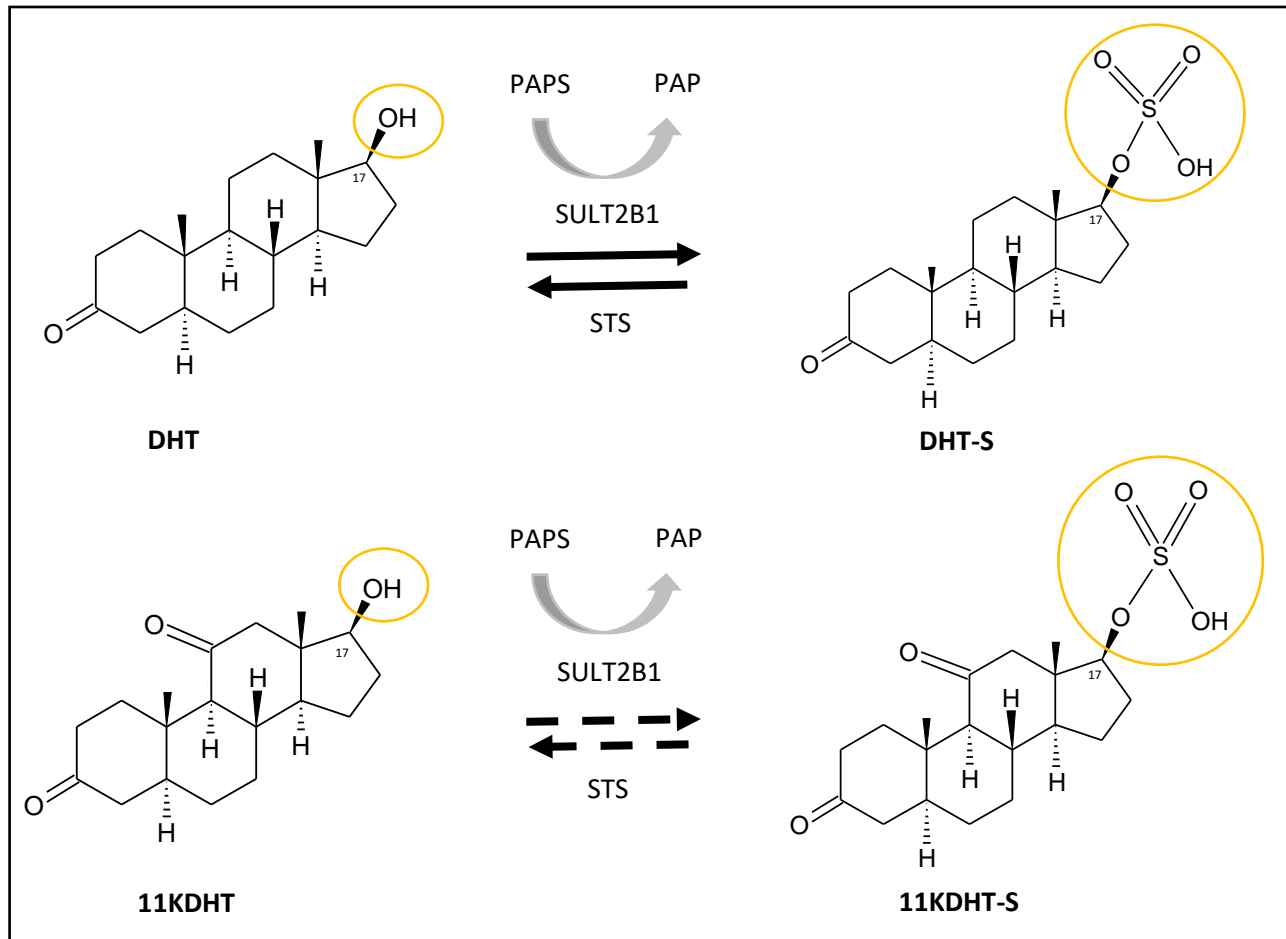
Figure 4.2 Sulfation and desulfation of DHT and 11KDHT at C17. 11KDHT-S, 11keto-dihydrotestosterone-sulfate.

Dysregulation of steroid sulfation and desulfation has been linked to androgen dependent diseases, such as PCa and PCOS, with the latter being an endocrine disease characterized by androgen excess, which would be expected as increased STS activity will increase active androgen levels due to the desulfation of steroid sulfates, while defective SULT activity will reduce the conjugation of active androgens and therefore favour their downstream metabolism. Indeed, SULT2B has been shown to be down-regulated (P<0.001) in malignant prostate tissue compared to adjacent non-malignant tissue, and the knockdown of SULT2B1b in LNCaP prostate cancer cells caused a significant increase in cell proliferation in the

99

presence of DHEA (He and Falany 2007; Seo et al. 2013). STS activity has also been confirmed in PCa tissue, while STS activity has also been shown in LNCaP prostate cancer cells (Nakamura et al. 2006; Day et al. 2009). Therefore, a fine equilibrium between sulfation and desulfation is important in the regulation of steroid action.

SULT2B1b is present in the cytosol of normal prostate, BPH and prostate adenocarcinoma tissue (He et al. 2004; He and Falany 2007). In LNCaP cells, SULT2B1b is also expressed in the cytosol (Vickman et al. 2016) and its expression has been shown to be regulated by the presence of DHT, while expression levels of SULT2B1a, SULT2A1 and SULT1E1 were not detected (He and Falany 2007). SULT2B1a and SULT2B1b isoforms are produced due to an alternative splicing on exon-1, and differ at the N-terminus (a 23-residue sequence in SULT2B1b and an 8-residue sequence in SULT2B1a) (Her et al. 1998; Fuda et al. 2002; Lee et al. 2003), and while the SULT2B1 antibody cannot discern between the two isoforms, their difference in weight, denoted as 39,6 kDa for SULT2B1a and 41,3 kDa for SULT2B1b (Meloche and Falany 2001), allows sodium dodecyl sulfate polyacrylamide gel electrophoresis to resolve these proteins, to distinguish between which isoform is present.

Of note, SULT2B1b shows selectivity for steroid sulfation at C3 with a β-hydroxy group (Fuda et al. 2002; Falany et al. 2006; He and Falany 2006; He and Falany 2007), while AST, T and DHT have been shown not to be ideal substrates (Meloche and Falany 2001). However, promiscuity and broad substrate specificity of the SULTs have been reported (Lewbart and Schneider 1956; Mueller et al. 2015), suggesting many different steroid substrates may be sulfated at C3 or C17, including those with a α-hydroxy group at C3 and perhaps even those such as 11KDHT with a hydroxy group at C17 (Fig. 4.2). Although, DHT is indeed a substrate for SULT2B1a and SULT2B1b, the latter exhibits a high K_m (~15.14 µM) and low V_{max} (~0.32 pmol/min/µg) towards DHT (V_{max}/K_m value of 0.02) compared to DHEA (V_{max}/K_m value of

0.37), with the SULT2B1b catalysed sulfation of DHT being 18.5-fold less efficient than DHEA (Geese and Raftogianis 2001). The sulfation of C11-oxy C_{19} steroids has, to date, not been reported. These steroids possess a α-hydroxy group at C3, as is the case for 11OHAST, 11KAST and 11K-3αDIOL, or a β-hydroxy group at C17, as is the case for 11OHT, 11KT, 11OHDHT, 11KDHT and 11K-3αDIOL. In addition, 11OHT, 11OHDHT and 11OHAST also possess a β-hydroxy group at C11, therefore, all the above mentioned steroids may serve as potential substrates for SULTs. It is interesting to note that SULT2A1 catalyses the sulfation of metabolites with a C3-hydroxy group in either the α or β conformation as well as at C17 of T (Falany et al. 1989; Falany et al. 1994). This isoform has, however, not been detected in LNCaP cells and is not readily expressed in prostate tissue, although it is prominent in the adrenals and liver (Falany et al. 1989; Falany 1997a; Javitt et al. 2001).

Recent reports have identified ketosteroids as a new class of substrates for cytosolic SULTs. Hashiguchi et al. (2017), showed that the C_{19} steroid, A4, and the C_{21} steroid, PROG, are substrates for the human SULT2A1 enzyme, reporting V_{max} values of ~170.5 and 5.5 pmol/min/mg enzyme, respectively. A4 possesses a keto-group at C3 and C17, and PROG at C3 and C20. Comparing A4 sulfation to DHEA sulfation, however, DHEA-S formation was more efficient with the catalytic efficiency (V_{max}/K_m) being ~360-fold higher than A4-sulfate formation. In addition, SULT2B1b exhibited weak activity towards A4 (V_{max} of 7.1 pmol/min/mg enzyme), while PROG was not sulphated by this isoform. The authors concluded that further *in vivo* data are needed to show the sulfation of ketosteroids. Interestingly, the authors showed that human SULT2A1 exhibited no activity towards 11OHA4 (Hashiguchi et al. 2017).

Since sulfation is a key step in regulating the cellular effects of steroids, conjugation by SULTs is important when we consider the C11-oxy C_{19} steroids, as the inactivation and conjugation of these steroids have not been fully investigated. Although immunoassays are generally used in the detection of sulfated and

non-sulfated steroids in the routine clinical setting, LC-MS/MS is currently gaining popularity (Rege et al. 2017). Most sulfated steroid reference standards, however, are not commercially available, thereby hampering quantification of *in vitro* and *in vivo* sulfated steroids. The aim of this study was therefore to investigate and compare the sulfation of the C11-oxy C_{19} and C_{19} steroids in LNCaP cells and to determine the levels of the sulfated steroid derivatives in plasma, by deconjugating steroids prior to extraction, enabling the quantification of all steroid metabolites using UPC^2-MS/MS.

4.2 Materials and methods

4.2.1 Materials

RPMI-1640 medium, D-(+)-Glucose, β-Glucuronidase (Type VII-A from *E.coli*, 5,292,000 units/g), Sulfatase (Type H-1 from *Helix Pomatia*, 53570 units/g), dichloromethane (DCM) and steroids (A4, DHEA, T and DHT) were purchased from Sigma-Aldrich (St. Louis, MO, USA). All other steroids were from Steraloids (Wilton, USA) and cell culture plates from Corning® Life Sciences (NY, USA). HEK293 cells were bought from American Type Culture Collection (Johannesburg, South Africa) and LNCaP cells from the Sigma's European Collection of Authenticated Cell Cultures (St. Louis, USA). The AKR1C3 pcDNA3 plasmid construct were obtained from Prof J. Adamski (Helmholtz Zentrum München, Institute of Experimental Genetics, Neuherberg, Germany) and the SRD5A1 and SRD5A2 pCMV7 plasmid constructs were a gift from Prof DW. Russell (Southwestern Medical Center, University of Texas, Dallas, USA). Penicillin-streptomycin (penstrep) were obtained from Oxoid limited (Hampshire, England) and fetal bovine serum (FBS) from Biochrom GmbH (Berlin, Germany). All deuterated steroids were purchased from Cambridge isotopes (Andover, MA, USA) and all other chemicals were of analytical grade and supplied by reliable scientific houses.

Male human blood samples were collected in a study investigating clinical markers of PCa (reference no. N09/11/330; Faculty of Medicine and Health Sciences, Stellenbosch University and Tygerberg Hospital, South Africa) from a normal subject, aged 59 and a PCa patient, aged 74 who underwent physical castration through BO. The female human blood left-over sample was collected under the clinical protocol 11-CH-0119 (Clinical Trials Number: NCT01313455) that was approved by the Eunice Kennedy Shriver National Institute of Child Health and Human Development Institutional Review Board (IRB), and kindly donated by Prof C.A. Stratakis (NICHD, Bethesda, MD, USA). All samples were stored at -80°C until further use.

4.2.2 Steroid conversion assays in LNCaP cells

LNCaP cells were cultured in RPMI-1640 growth medium supplemented with 10% FBS, 1.5 g $NaHCO_3$/L (pH 7), 1% penstrep, 2.5 g D-(+)-Glucose, 1% HEPES and 1% sodium pyruvate at 37°C, in 90% humidity and 5% CO_2, and once confluent replated into 12-well Corning® CellBIND® surface plates at 2×10^5 cells/mL. After 48 hrs, the medium was replaced with 1 mL culture medium containing steroid substrates (1 µM): T, DHT, AST, 3αDIOL, 11OHA4, 11OHT, 11KT, 11KDHT, 11KAST, 11OHAST, 11OHDHT, 11K-3αDIOL and DHEA for 12, 24 and 48 hrs. Commercially unavailable steroids, 11OHDHT and 11K-3αDIOL, were prepared as previously described (Du Toit and Swart 2018). Briefly, 11OHDHT and 11K-3αDIOL were prepared by transiently transfecting HEK293 cells, using XtremeGene HP® DNA transfection reagents, according to the manufacturer's instructions (Sigma-Aldrich, St. Louis, MO, USA), and adding the appropriate substrates —11OHT (2 µM) was added to cells transfected with SRD5A1 (0.5 µg) and SRD5A2 (0.5 µg) and converted to 11OHDHT. 11KAST (2 µM) was added to cells transfected with AKR1C3 (1 µg) and converted to 11K-3αDIOL. Media were collected, diluted (1:1) with culture media

and added to LNCaP cells. Steroid conversion was assayed by collecting aliquots (0.5 mL) at specific time intervals and stored at 4°C until extraction and UPC^2-MS/MS analyses.

Plasmid preparations for enzymatic assays in transiently transfected HEK293 cells

Luria-Bertani medium, 100 mL, containing ampicillin (100μg/mL), was inoculated with freezer stocks of plasmid-containing *E.coli* cells, 100 μL, overnight at 37°C at 230 rpm (Innova shaking incubator, New Brunswick) to prepare plasmids. The plasmid DNA was isolated using the Nucleobond® Midiprep DNA isolation kit, according to the manufacturer's instructions (Machery-Nagal). After precipitation, the DNA pellet was redissolved in nuclease free water, 200 μL, and the plasmid yield was calculated by UV spectrophotometry (Cary 60 UV-VIS; Agilent technologies), 260/280 nm. The average yield ranged from 100 μg - 200 μg per 100 mL.

4.2.3 β-glucuronidase and sulfatase deconjugation reactions

Three aliquots were collected at each time interval for the analysis of unconjugated steroids (A), total (unconjugated + glucuronidated) steroids (B) and total (unconjugated + glucuronidated + sulfated) steroids (C), after deconjugation with either β-glucuronidase for B or with sulfatase for C. Aliquots B were treated with 400 units (76 μL) β-glucuronidase at 37 °C, pH 6.5, for 24 hrs to deconjugate glucuronidated steroids (Du Toit et al. 2017; Du Toit and Swart 2018). Aliquots C were treated with 66 units (617 μL) sulfatase at 55°C, pH 5 (+ 110 μL sodium acetate buffer), for 3 hrs to deconjugate glucuronidated and sulfated steroids. DHT-G (1 μM) in 0.5 mL media was deconjugated and extracted, serving as a control for deglucuronidation efficiency, confirmed by DHT recovery from those samples, compared to DHT (1 μM) in 0.5 mL media extracted without prior treatment. DHEA-S (1 μM) in 0.5 mL media was desulfated and extracted, serving as a control for desulfation efficiency, confirmed by DHEA recovery

from those samples, compared to DHEA (1 µM) in 0.5 mL media extracted without prior treatment. Plasma aliquots (0.5 mL) underwent the same protocol as described above to deconjugate steroids.

4.2.4 Steroid extraction

Prior to steroid extractions, testosterone-D2 (D2T), 1.5 ng, progesterone-D9 (D9PROG), 15 ng, androstenedione-D7 (D7A4), 15 ng, and 11β-hydroxyandrostenedione (D711OHA4), 15 ng, were added as internal standards (100 µL) to cell model and plasma aliquots. *In vitro* and *in vivo* samples were analysed after a liquid/liquid steroid extraction using 5 mL DCM (10:1) was conducted (Du Toit et al. 2017). The samples in DCM were vortexed at 1000 rpm for 7 min, and centrifuged for 2 min, after which the extracted media was aspirated and the DCM phase dried under nitrogen. Dried residue was dissolved in 0.15 mL 50% methanol in water and all samples stored at −20°C until UPC^2-MS/MS analysis.

4.2.5 Separation and quantification of steroid metabolites

Stock solutions of steroids were dissolved in absolute ethanol (2 mg/mL) and stored at -20°C. A standard range, 0.0001 to 1 ng/µL, prepared in RPMI-1640 cell culture media and extracted as described above. 11OHDHT and 11K-3αDIOL concentrations were calculated relative to the ionisation signal when only the product is present, which represents 100% substrate conversion (1 µM 11OHT converted to 1 µM 11OHDHT and 1 µM of 11KAST converted to 1 µM 11K-3αDIOL after 48 hrs).

The C_{19} steroids were analysed by ACQUITY UPC$^{2®}$–MS/MS (Waters Corporation, Milford, USA), separated using an ACQUITY UPC^2 BEH column (3 mm x 100 mm, 1.7 µm particle size) for the A4 and T metabolites and DHEA, and an ACQUITY UPC^2 BEH 2-EP column (3 mm x 100 mm, 1.7 µm particle size) for the C11-oxy C_{19} metabolites. The mobile phase consisted of CO_2 modified with methanol in which

105

steroids, injection volume, 2 µL, were eluted at a flow rate of 2 mL/min in a total run time of 5 min per sample. The column temperature was set to 60°C and the automated back pressure regulator (ABPR) was set to 2000 psi. A Xevo TQ-S triple quadrupole mass spectrometer (Waters, Milford, USA) was used for quantitative mass spectrometric detection and all steroids were analysed in multiple reaction monitoring mode (ESI+). Preceding the MS line, a make-up pump mixed 1% formic acid in methanol at a constant flow rate of 0.2 mL/min. The following settings were used: capillary voltage of 3.8 kV, source temperature 120 °C, desolvation temperature 500 °C, desolvation gas 1000 L/h and cone gas 150 L/h. Data was collected and analysed with the MassLynx 4.1 (Waters Corporation) software program. The mass transitions of the steroids, limit of detection (LOD) and limit of quantification (LOQ) and method validation, including recovery, accuracy and precision has been previously published (Du Toit et al. 2017; Du Toit and Swart 2018; DHEA data reported in chapter 6). The cell model assay was performed in triplicate and representative of a single experiment, while plasma aliquots represent patient specific steroid profiling. Statistics were calculated by an unpaired t-test using GraphPad Prism (version 5) software (GraphPad Software, San Diego, California). Differences were considered statistically significant at P<0.05.
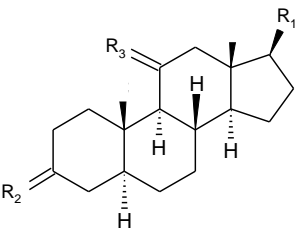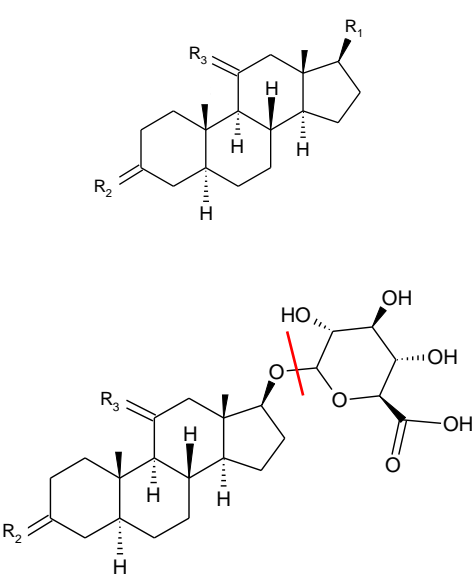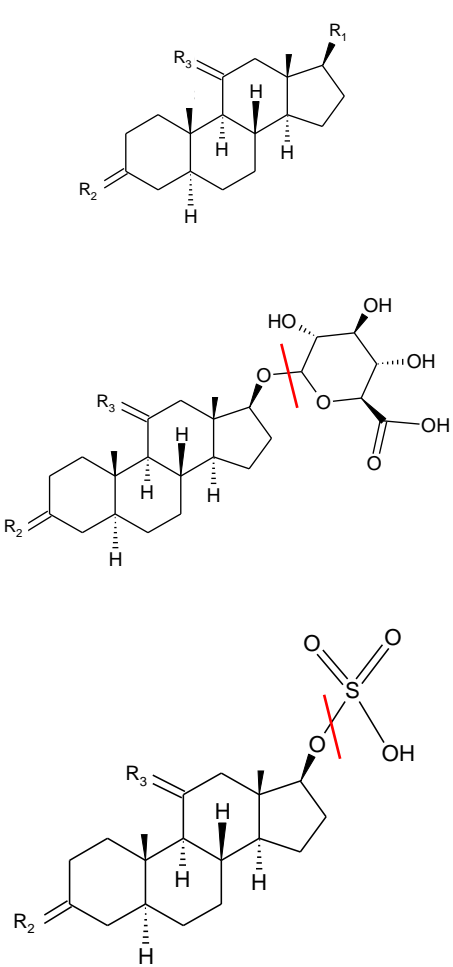
4.3 Results

In vitro sulfation of C_{19} and C11-oxy C_{19} steroids was investigated in LNCaP cells which express SULT2B1b endogenously. This is a well-established PCa cell model, in which conjugation of C_{19} steroids by glucuronidation was also investigated and described (Chapter 3). LNCaP cells, therefore, represent a cell model system capable of adding a sulfate or glucuronide to the steroid backbone structure with appropriate hydroxy moieties. Our laboratory does not currently hold a cell model in which steroids are only sulfated without glucuronidation, while in-laboratory steroid extraction protocols do not retain

water soluble conjugates. Dual deconjugating protocols, carried out prior to extraction and UPC^2-MS/MS quantification, were therefore developed with the aim of distinguishing conjugation by sulfation from conjugation by glucuronidation.

In order to analyse conjugation by glucuronidation, β-glucuronidase was used to deconjugate samples (B; section 4.2.3). In order to analyse conjugation by sulfation, sulfatase was used to deconjugate sulfated steroids (C; section 4.2.3). The latter enzyme, also has dual enzyme activity as this enzyme deconjugates glucuronidated and sulfated steroids, in a 3:1 ratio. Utilizing both deconjugating systems, the amount of steroid sulfates were calculated as follows: steroid sulfates = C - B (Table 4.1).

Table 4.1 Deconjugating enzymes employed in the analysis of conjugated metabolites in LNCaP cells and in plasma samples. R_1 = OH; R_2 = O or OH; R_3 = H, O or OH[1].

A	B	C
0.5 mL aliquot	0.5 mL aliquot	0.5 mL aliquot
Untreated	β-glucuronidase treated	Sulfatase treated
Unconjugated steroids extracted	Unconjugated + glucuronidated steroids extracted	Unconjugated + glucuronidated + sulfated steroids extracted

---

[1]Sulfation and glucuronidation is also possible at C3, if R2=OH.

4.3.1 Analyses of β-glucuronidase and sulfatase control reactions

Control reactions were conducted in parallel when *in vitro* and *in vivo* aliquots were deconjugated to determine the hydrolysis activity of β-glucuronidase and sulfatase. The complete hydrolysis of glucuronidated steroids by β-glucuronidase was monitored by deconjugating DHT-G (Fig. 4.3a). DHT-G was fully hydrolysed to DHT by β-glucuronidase, while DHEA-S was not desulfated following the same protocol (Fig. 4.3b). DHEA-S and DHT-G were used as controls, to analyse the dual hydrolysis activity of sulfatase. Sulfatase fully hydrolysed DHEA-S and DHT-G to DHEA and DHT, respectively (Fig.4.3c and d).
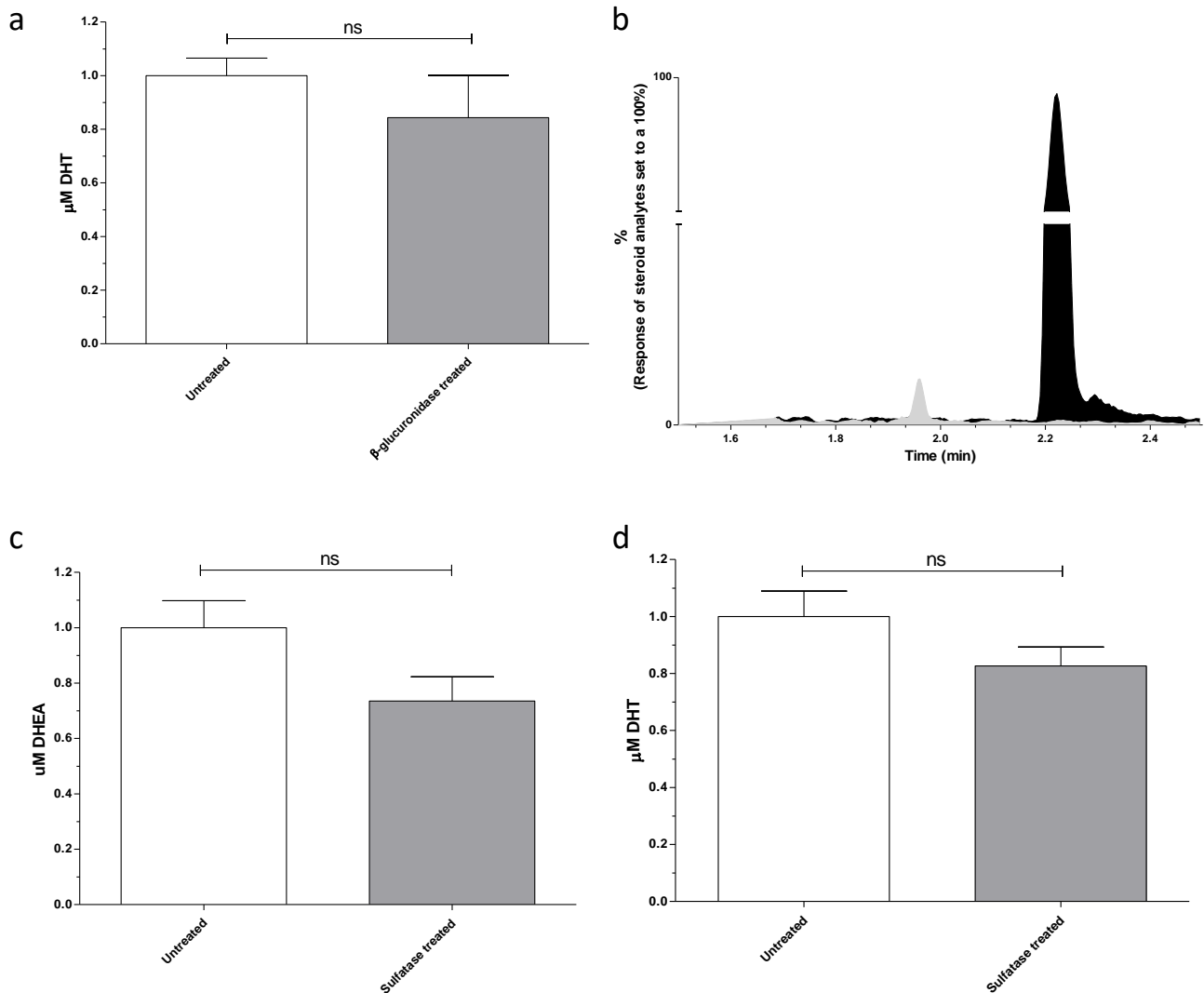
**Figure 4.3** Control reactions determining the hydrolysis activity of β-glucuronidase and sulfatase. (a) Untreated DHT (1 µM) extracted from media and DHT recovery from DHT-G (1 µM) after 24 hrs incubation with β-glucuronidase; (b) UPC^2-MS/MS chromatogram of DHEA (1 µM) (black chromatogram), with no DHEA peak detected after 24 hrs incubation of DHEA-S (1 µM) with β-glucuronidase (grey chromatogram); (c) untreated DHEA (1 µM) extracted from media and DHEA recovery from DHEA-S (1 µM) after 3 hrs incubation with sulfatase; and (d) untreated DHT (1 µM) extracted from media and DHT recovery from DHT-G (1 µM) after 3 hrs incubation with sulfatase. Experiments were performed in triplicate, analysed by UPC^2-MS/MS and the results expressed as the mean ± STD DEV (*n*=3 for a and b; *n*=4 for c and d; *ns*, not significant).

4.3.2 Analyses of steroid conjugation in LNCaP cells

Conjugation of T- and DHT-metabolites in LNCaP cells

The conjugation of T- and DHT-metabolites in LNCaP cells, would involve only the C17 β-hydroxy group of these steroids. Analysis of T levels (Fig. 4.4a) shows a rapid decrease in the free unconjugated steroid levels at 12 hrs, with negligible unconjugated T remaining at 24 and 48 hrs. T was predominantly in the glucuronide form after 12 hrs, with no sulfation of T being detected. In contrast to T, 11KT was not glucuronidated as efficiently as T (Fig. 4.4b), with 11KT predominantly present in its free, unconjugated form at 12, 24 and 48 hrs, corroborating our previous findings (Du Toit et al. 2017; Du Toit and Swart 2018). Although 11KT-glucuronide (11KT-G) levels were detected, this steroid was not sulfated. Analysis of 11OHT levels (Fig. 4.4c) showed that this steroid was predominantly present in its free, unconjugated form at 12 and 24 hrs, however, at 48 hrs 11OHT-glucuronide (11OHT-G) formation was higher compared to free, unconjugated 11OHT levels. In addition, while 11OHT-sulfate (11OHT-S) formation was not detected at 12 and 24 hrs, at 48 hrs 11OHT appeared to be sulfated at 48 hrs, however, the difference

110

between 11OHT-G and 11OHT-S levels was not significant. The low 11OHT-G levels, together with negligible free steroid is indicative of substrate conversion to 11KT, 11OHDHT and 11KDHT.
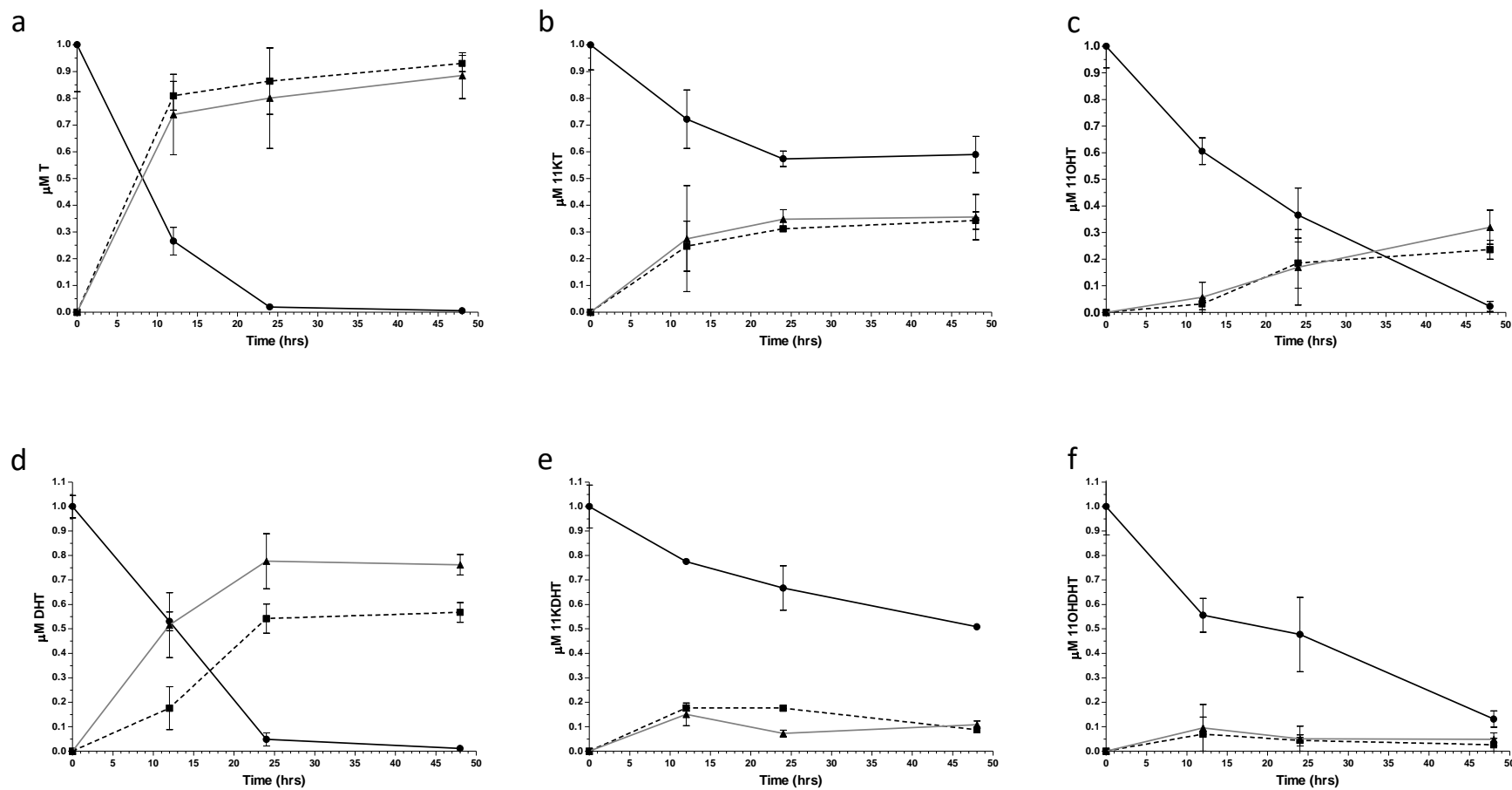
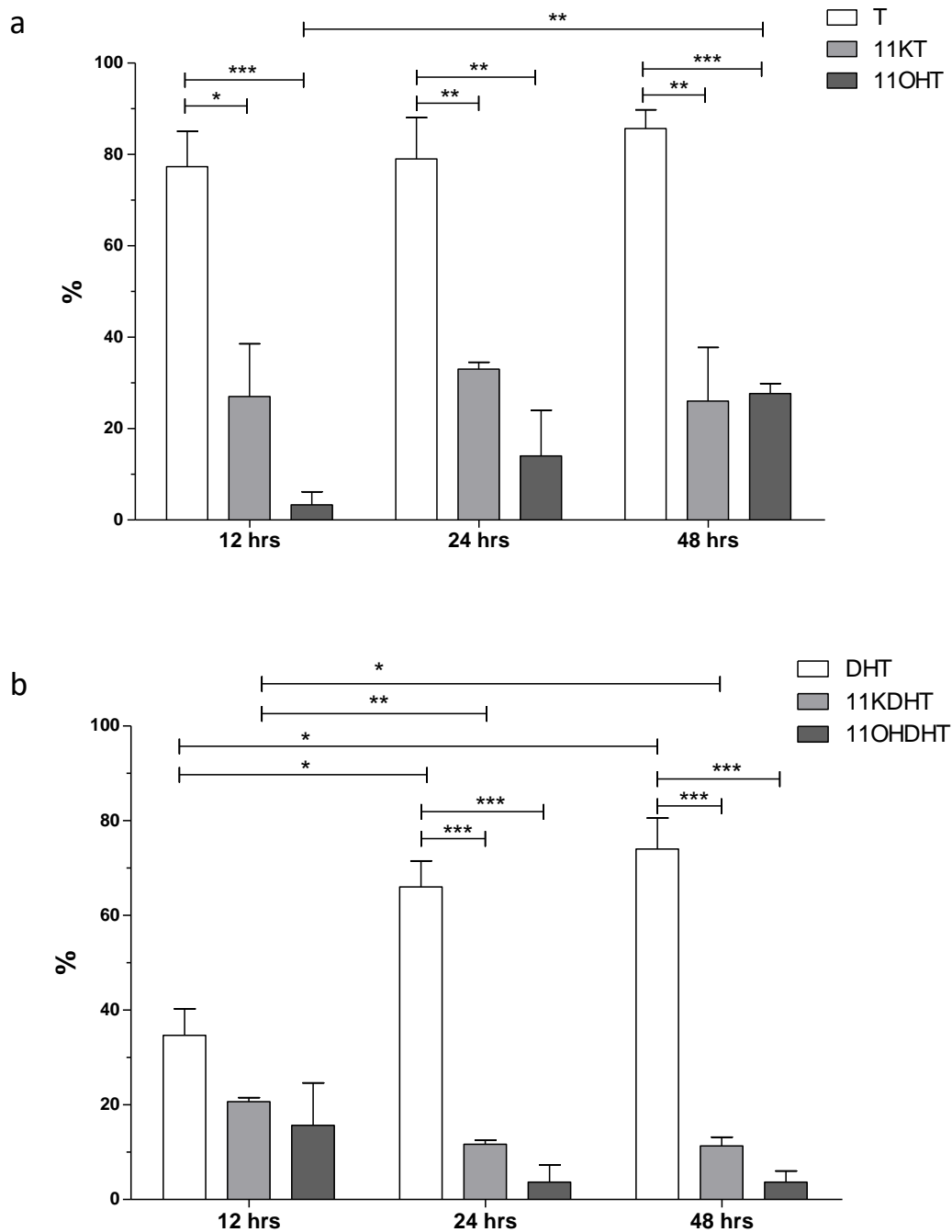**Figure 4.4** Steroid (1 µM) conjugation in LNCaP cells after 12, 24 and 48 hrs. (a) T; (b) 11KT; (c) 11OHT; (d) DHT; (e) 11KDHT; and (f) 11OHDHT. Solid line, unconjugated steroid (A); black dashed line, glucuronidated steroid (B); grey solid line, glucuronidated + sulfated steroid (C). Experiments were performed in triplicate, analysed by UPC^2-MS/MS and the results expressed as the mean ± STD DEV (*n*=3).

Analysis of DHT (Fig. 4.4d) also shows a rapid decrease in unconjugated steroid levels after 24 hrs, similar to T, and DHT was also predominantly glucuronidated after 24 and 48 hrs. Data shows that DHT is sulfated, with the difference between glucuronide and sulfated DHT levels being 2.9-fold (p=0.0998) at 12 hrs, 1.4-fold at 24 hrs and 1.1-fold at 48 hrs. In contrast to DHT, conjugation of 11KDHT (Fig. 4.4e) and 11OHDHT (Fig. 4.4f) was negligible with glucuronidated and sulfated levels below 0.1 μM at 48 hrs. These steroids were predominantly in the free, unconjugated form throughout the assay period with 11KDHT remaining at 0.06 μM and 11ODHT at 0.2 μM, indicating conversion to downstream products.

Percentage conjugated T- and DHT-metabolites

In the analysis of the C_{19} steroids and the C11-oxy C_{19} steroids, conjugated T levels, when compared to those of 11KT and 11OHT, were significant throughout the assay period. 11KT and 11OHT conjugated levels remained <40% (Fig. 4.5a) with T and 11KT in the conjugated form remaining constant, ~80% and ~30%, respectively. In contrast, the % 11OHT in the conjugated form significantly increased, 6-fold, after 12 hrs to ~30% at 48 hrs. Comparing the conjugation of the 5α-reduced metabolites (Fig. 4.5b), at 12 hrs, their levels were not significantly different, however, after 24 hrs, conjugated DHT levels were increased, ~1.9-fold, with the conjugated form of DHT being significantly higher when compared to those of 11KDHT and 11OHDHT. 11KDHT and 11OHDHT conjugation levels, however, remained <30%, with the conjugated derivatives of 11KDHT significantly decreasing after 12 hrs.

Figure 4.5 Steroid conjugation in LNCaP cells. Steroid (1 µM) conversion analysed after 12, 24 and 48 hrs.

(a) % T-metabolites conjugated (glucuronidated + sulfated) and (b) % DHT-metabolites conjugated

(glucuronidated + sulfated). Experiments were performed in triplicate, analysed by UPC^2-MS/MS and the results

expressed as the mean ± STD DEV (*n*=3; ns, not significant; *$P<0.05$, **$P<0.005$, ***$P<0.001$).

Percentage conjugated 3α-reduced metabolites

The 3α-reduced C_{19} metabolites, AST and 3αDIOL, and the C11-oxy C_{19} metabolites, 11OHAST, 11KAST and 11K-3αDIOL, possess a C3α-hydroxy group, which presents these steroids as potentially substrates for glucuronidation and sulfation by enzymes endogenously expressed in LNCaP cells. In addition, only 3αDIOL and 11K-3αDIOL also possess a C17α-hydroxy group. Conjugated levels of 3αDIOL, which has a C3- and C17-hydroxy group, were significantly higher than the conjugated levels of AST (Fig. 4.6), which only has a C3-hydroxy group. Glucuronidated 3αDIOL levels were significantly higher than the levels of free, unconjugated 3αDIOL at 12 hrs (Fig. 4.6 insert). Conjugated 11OHAST and 11KAST levels (~20%) were also higher than those of conjugated AST levels, although not significantly so. While unconjugated 11K-3αDIOL levels were similar to those of 3αDIOL, they were also higher than the conjugated C11-oxy AST metabolites.
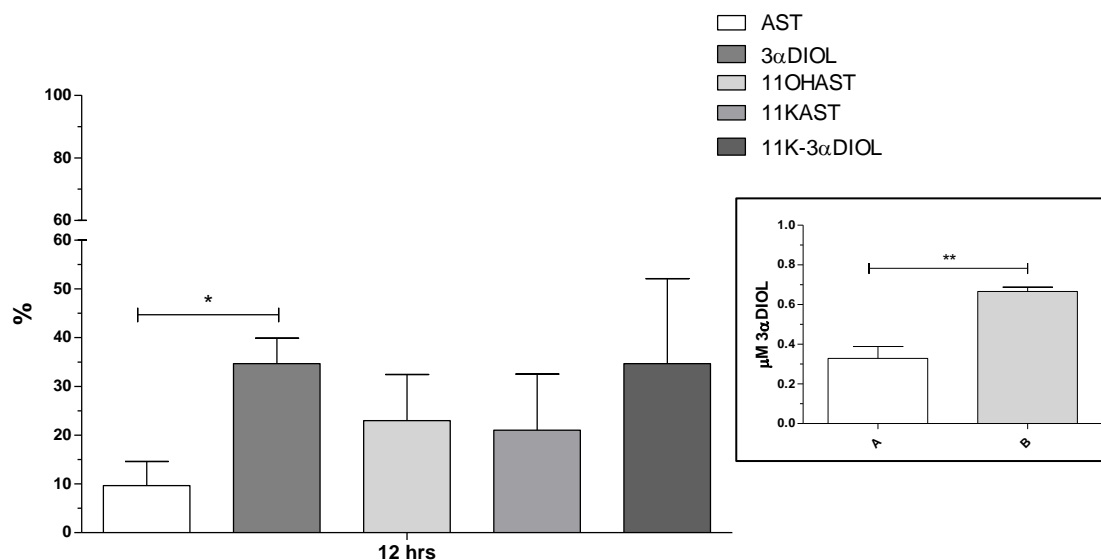
Figure 4.6 Percentage (%) conjugated (glucuronidated and sulfated) steroids. Steroid (1 µM) conversion in LNCaP cells was analysed after 12 hrs. Insert, unconjugated (A) and total, unconjugated + glucuronidated, (B) 3αDIOL

115

levels. Experiments were performed in triplicate, analysed by UPC^2-MS/MS and the results expressed as the mean ± STD DEV (n=3; *P<0.05; **P<0.005).

<u>DHEA and 11OHA4 assays in LNCaP cells</u>

Since the sulfation of ketosteroids have recently been described (Hashiguchi et al. 2017), the sulfation of A4 and 11OHA4 was also investigated. In the analysis of downstream metabolites, only A4 was produced when the metabolism of DHEA was assayed in LNCaP cells (Fig. 4.7a). DHEA was not glucuronidated, nor sulfated (data not shown), and after 24 and 48 hrs, free, unconjugated levels were ~0.65 μM. Since only A4 levels were detected, this suggests DHEA was converted to androstenediol in by 17βHSDs LNCaP cells (Fig. 4.1), this steroid was, however, not quantified. Unconjugated levels of A4 were similar to the total steroid (unconjugated + glucuronidated) levels, ~0.02 μM, indicating that A4 was not glucuronidated. A4 was, however, significantly sulfated after 12 and 24 hrs, 2.81-fold (Fig. 4.7b) although levels remained low (<0.05 μM). We were unable to determine whether SULTs acted on the C3 or C17 keto-groups on the steroid backbone of A4, while A4 was also not directly assayed. Interestingly, when 11OHA4 was assayed, neither glucuronides nor sulfates of 11OHA4 were detected after 12 hrs (Fig. 4.7c). 11OHA4 was, however, metabolized to downstream products with only ~0.4 μM remaining, present in the free, unconjugated form only.
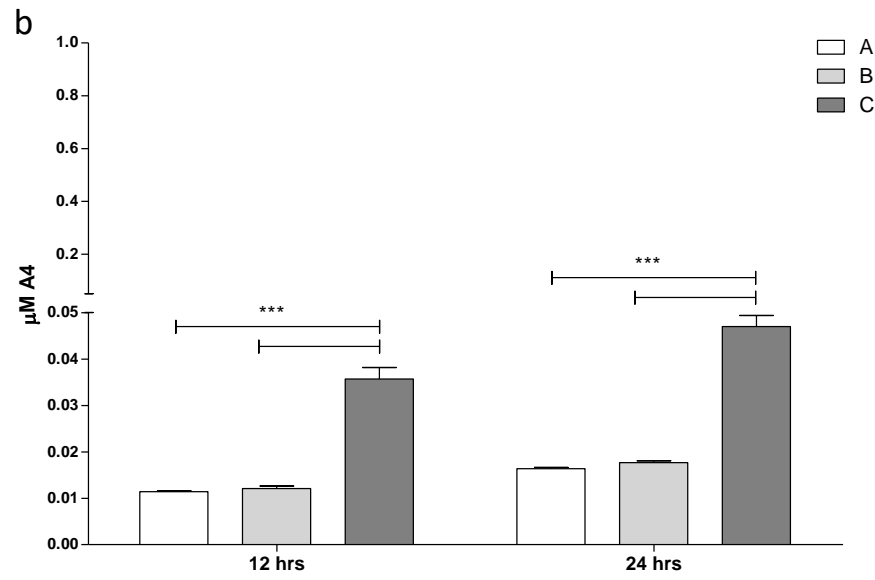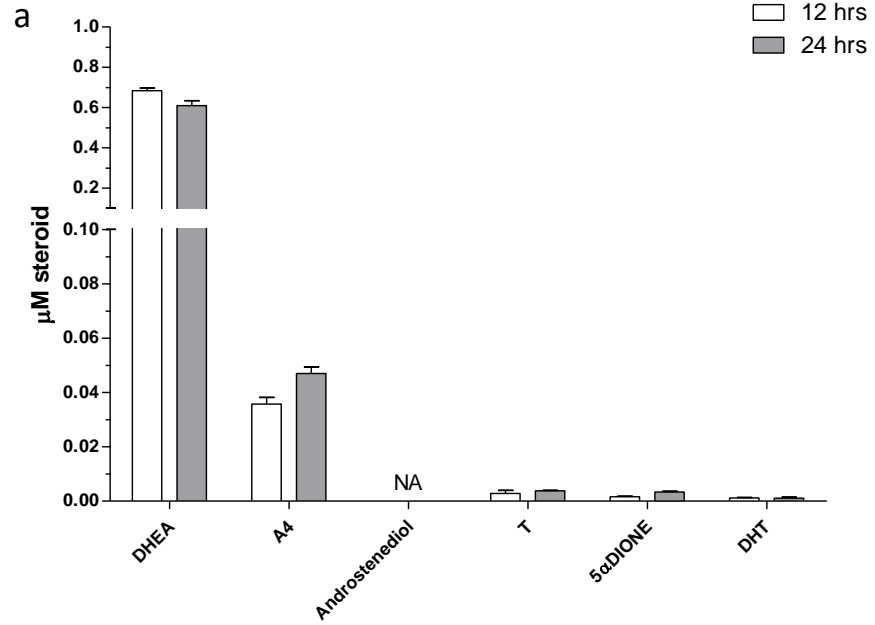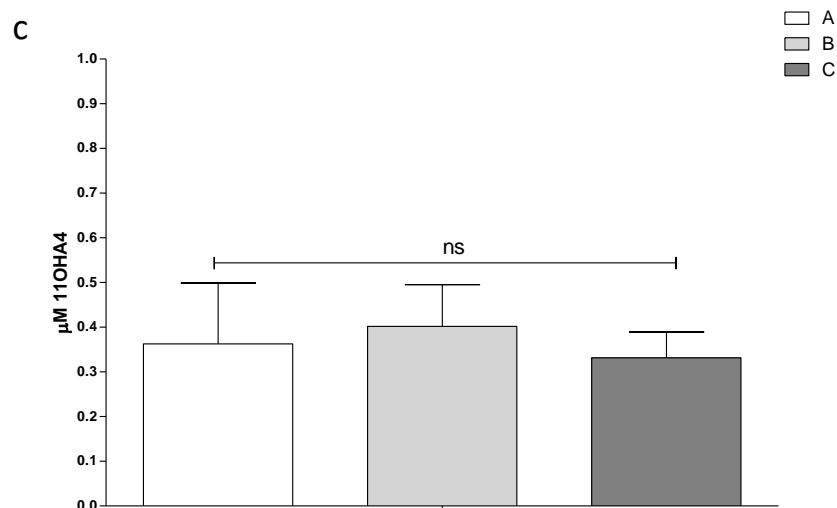
Figure 4.7 - Steroid (1 μM) metabolism in LNCaP cells. (a) Conversion of DHEA and (b) conversion of DHEA to A4 in LNCaP cells after 12 and 24 hrs; and (c) conversion of 11OHA4 in LNCaP cells after 12 hrs. A, unconjugated steroid; B, unconjugated + glucuronidated; C, unconjugated + glucuronidated + sulfated. Experiments were performed in triplicate, analysed by UPC^2-MS/MS and the results expressed as the mean ± STD DEV (n=3; ns, not significant; ***P<0.001; NA, not analysed).

4.3.3 Analyses of steroid sulfates in circulation

4.3.3.1 Male plasma samples

As the sulfation of C11-oxy C_{19} steroids *in vivo* has, to date, not been determined, these steroids together with the C_{19} steroid sulfates were analysed and compared in a healthy male subject and in a patient diagnosed with PCa. In the healthy subject, 11KDHT (59.5 nM) and 11KAST (153.6 nM) sulfates were predominant (Fig. 4.8), while 38.3 nM 3αDIOL-sulfate (3αDIOL-S) was detected, together with low levels of DHT-S (5.8 nM), AST-S (6.5 nM) and 11OHAST-S (3.0 nM). In the PCa plasma, the 3α-reduced metabolites were the most abundant sulfated derivatives, 11OHAST (33.8 nM), 11KAST (222.9 nM) and AST (21.8 nM), while DHT-S (2.9 nM), 3αDIOL-S (11.4 nM) and 11KDHT-S (8.0 nM) levels were low.

Comparing the healthy subject and the PCa patient, DHT-S levels were similar, while AST, 11OHAST and 11KAST sulfate levels were higher and 3αDIOL-S and 11KDHT-S levels were lower, 3.4-fold and 7.4-fold, respectively, in the PCa patient. Results show that steroids possessing either a C3 α-hydroxy group or a C17 β-hydroxy group were sulfated, and present in circulation as sulfate derivatives. Circulatory sulfates of the T-metabolites, 11K-3αDIOL and 11OHDHT were not detected.
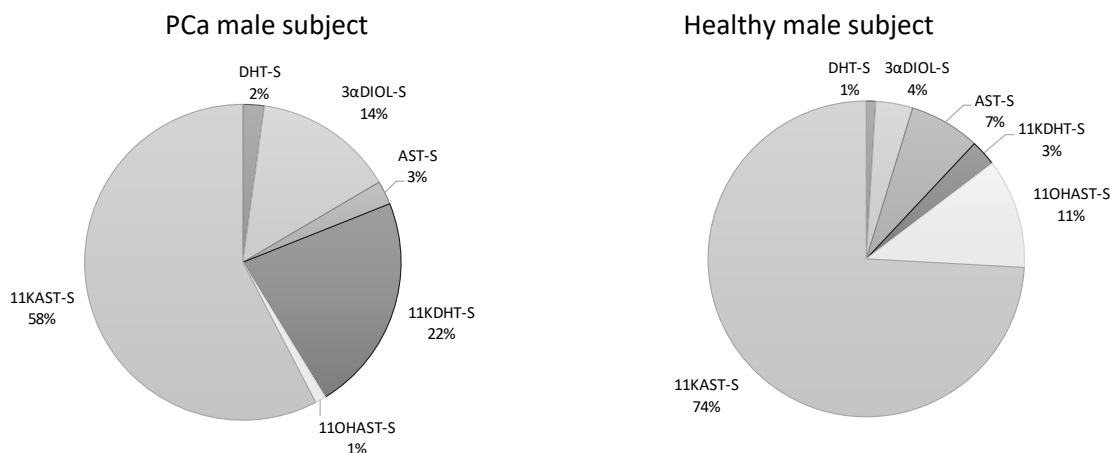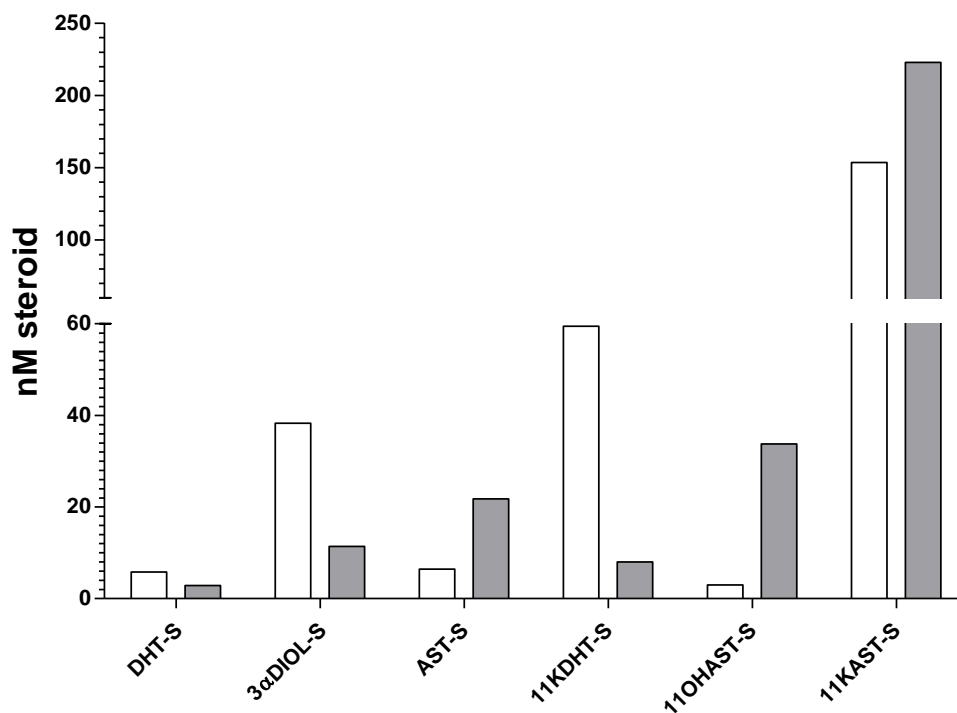
Figure 4.8 UPC^2-MS/MS analyses of circulatory steroid sulfates. Clear bars, healthy male subject; shaded bars, PCa patient. Insert, contribution (%) of sulfated steroids to each profile (11KAST-S, 11KAST-sulfate; 11OHAST-S, 11OHAST-sulfate).

4.3.3.2 Female plasma sample

Profile analyses of conjugated steroid metabolites in circulation showed both glucuronidated and sulfated derivatives to be present (Fig. 4.9). Of the C_{19} steroids, only AST and 3αDIOL were conjugated. Unconjugated AST was not detected, while AST-glucuronide (AST-G) and AST-S were detected at 49 nM and 24.9 nM, respectively. Unconjugated 3αDIOL was negligible detected at ~1.8 nM (below LOQ), with 3αDIOL-glucuronide and 3αDIOL-S detected at 33.8 nM and 19.5 nM, respectively, and analysis was unable to distinguish between conjugation at C3 and C17 or whether at both. DHT levels and T levels (< 1.5 nM) were negligible, as were their conjugated derivatives. Analysis of the C11-oxy C_{19} steroids showed 11OHT and 11KT and their conjugated derivatives also below 1 nM, while free 11KDHT, 11OHAST and 11KAST were not detected. As in the case of the C_{19} steroids, the conjugate levels of the C11-hydroxy 3α-reduced metabolites were high -11OHAST-glucuronide and 11OHAST-S at 51.8 nM and 25.8 nM, respectively, and 11KAST-S was detected at 17.3 nM. 11KAST-G was below the LOQ (~4.6 nM). Interestingly, only 11KDHT-glucuronide was detected, ~2.6 nM (below LOQ), while 11KDHT-S levels were negligible (~0.2 nM). Although these levels were below the LOQ, the data show that 11KDHT conjugate levels are higher than DHT levels. The data also suggests that, in circulation, steroids with C3 α-hydroxy groups are predominantly sulfated, while the C17-hydroxy group of 3αDIOL may also be potentially sulfated. Circulatory sulfates of 11K-3αDIOL and 11OHDHT were not detected.
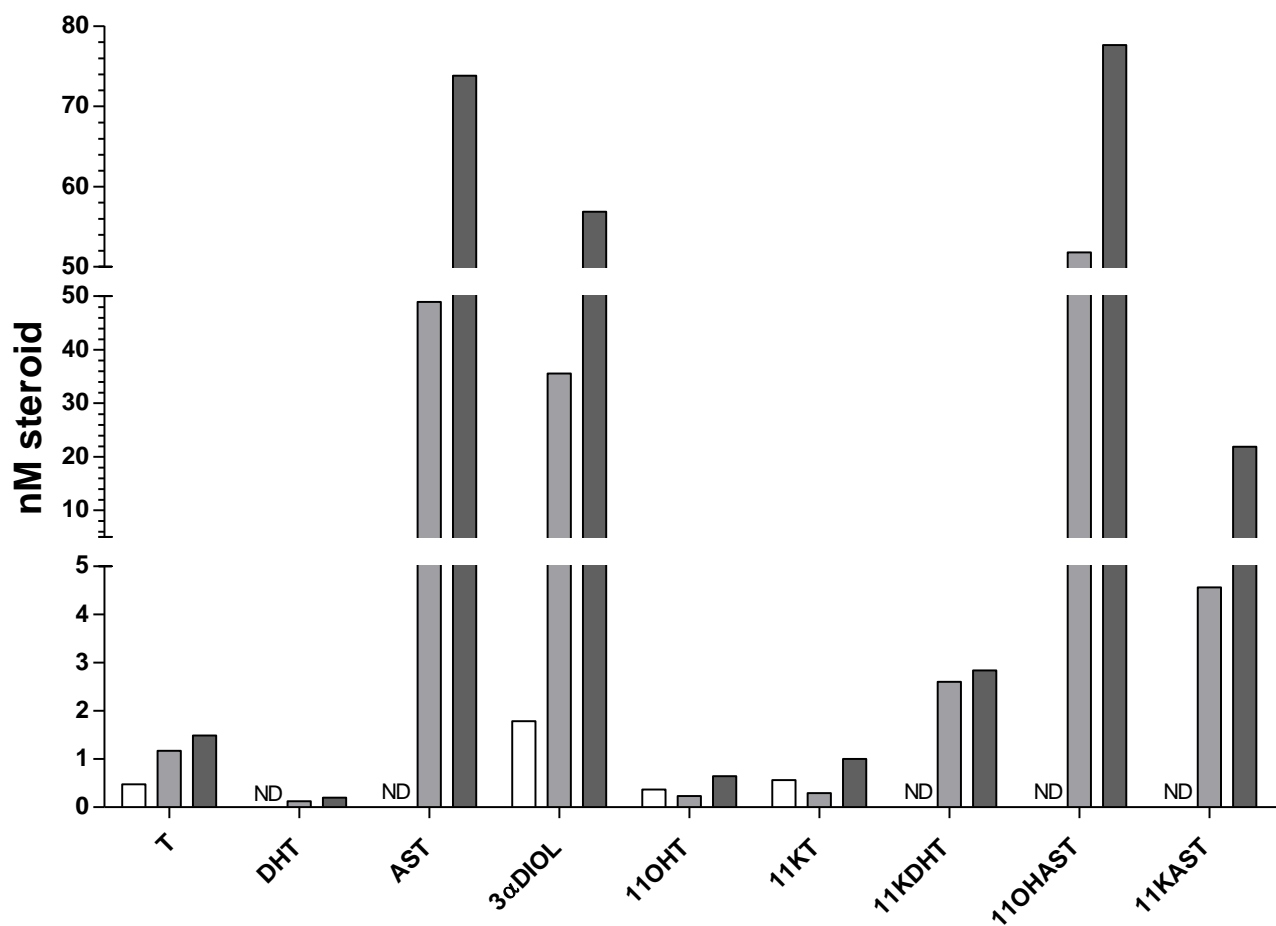
Figure 4.9 UPC^2-MS/MS analysis of circulatory healthy female C_{19} and C11-oxy C_{19} steroid levels. Clear bars, unconjugated steroids (A); light grey bars, unconjugated + glucuronidated steroids (B); dark grey steroids, unconjugated + glucuronidated + sulfated steroids (C). ND, not detected.

4.4 Discussion

While C_{19} steroid conjugates have been detected in circulation, evidence of adrenal and peripheral glucuronidation and sulfation pathways, the conjugation of the C11-oxy C_{19} steroids have not been widely reported. Here, we show that the conjugation of the C11-oxy C_{19} steroids are inefficient compared to the C_{19} steroids *in vitro*, and the analysis shows, for the first time, the presence of C11-oxy C_{19} sulfates in circulation, in both males and females.

121

Of all the C17 α-hydroxy steroid substrates assayed, SULT2B1b appeared to sulfate DHT (Fig. 4.4d), which may be ascribed to the reported increased expression of SULT2B1b in the presence of DHT detected in LNCaP cells. DHT, at 1 and 10 nM, increased the expression of SULT2B1b at the mRNA and protein level, while DHEA and T had no effect on the expression levels of SULT2B1b. This suggests that SULT2B1b is AR mediated —once the AR binds DHT, transcriptional induction of SULT2B1b proceeds (He and Falany 2007), or at least that the AR is involved in the regulation of SULT2B1b, and that the increased expression of this enzyme occurs as a possible feedback mechanism to limit the physiological downstream effect of DHT. LNCaP cells expresses a mutated AR (Veldscholte et al. 1990), which suggests this mutant is involved in this mechanism. However, while 11KDHT has been shown to bind and transactivate the AR and induce AR regulated gene expression in LNCaP cells (Pretorius et al. 2016), neither 11KDHT nor 11OHDHT were sulfated (Fig. 4.4e and f). In addition to the expression of SULT2B1b in LNCaP cells, STS has also been reported to be expressed in LNCaP cells (Day et al. 2009), and while this activity was not assayed in the analyses presented in this chapter, potential STS activity towards 11KDHT may catalyse the steroid's deconjugation and explain the decreased 11KDHT conjugate levels observed during our assay period (Fig. 4.5), and while endogenous β-glucuronidase activity cannot be ruled out, this activity has not been shown in LNCaP cells.

Furthermore, T, 11KT and 11OHT were not significantly sulfated in LNCaP cells (Fig. 4.4), and sulfate derivatives of these steroids were low in circulation (Fig. 4.9). Moreover, the *in vitro* data show that the C11-hydroxy and C11-keto metabolites behave similarly (Fig.4.4) —11KT and 11KDHT were predominantly present in the unconjugated form during the assay period, showing negligible conjugation by sulfation, and while glucuronide derivatives of these steroids were detected, these levels were <40% for 11KT and even lower for 11KDHT (<20%). Although 11OHDHT was not conjugated, this

122

steroid was metabolized to downstream metabolites, as negligible unconjugated steroid levels were detected at the end of the assay period. Similarly, 11OHT was also metabolized to downstream metabolites denoted by the decrease in unconjugated steroid level detected, however, at the end of the assay period conjugated levels of 11OHT was detected. In both cases it is possible that 11βHSD2 converted 11OHDHT and 11OHT to 11KDHT and 11KT, respectively, thus contributing to the pool of active androgens.

The data presented in this chapter show that the active C11-oxy C_{19} steroids are not conjugated as efficiently as the C_{19} steroids (Fig. 4.5), which strongly suggests that the presence of the C11-hydroxy or C11-keto moiety interferes with the binding of the steroid to the conjugating enzymes, thereby allowing the persistence of these steroids in their active forms, especially 11KT and 11KDHT. In this regard, structural modelling of the steroid and the enzyme could potentially contribute to our understanding of the manner in which binding is impeded, thus modulating activity towards specific substrates. Clearly, both 11KT and 11KDHT are less efficiently conjugated than T and DHT, respectively, thus remaining in the free form while 11OHT and 11OHDHT are metabolized efficiently in the 11OHA4-pathway, further contributing to the androgen pool in LNCaP cells. The 3α-reduced C11-oxy steroid conjugate levels were similar to the 3α-reduced C_{19} steroid conjugate levels, however, 3αDIOL was significantly conjugated compared to AST (Fig. 4.6). In addition, while conjugated 11K-3αDIOL was also higher than conjugated C11-oxy AST metabolites, these data suggest that conjugation is favoured at C17. LNCaP cells express high levels of UGT enzymes (Guillemette et al. 1995; Lévesque et al. 2001) which are capable of conjugating at C3 and C17 of 3αDIOL, compared to AST which only possesses a C3-hydroxy group. Although the results discussed above serve to demonstrate conjugation in LNCaP cells, our data is based on a single experiment, and while the results corroborate our previous findings relating to

123

glucuronidation, additional *in vitro* investigations are required to establish the sulfation of the C11-oxy C_{19} steroids.

We have reported that 11KDHT is inefficiently glucuronidated in PCa patients compared to a healthy subject (Du Toit and Swart 2018), and here we report that circulating 11KDHT levels indicate that the steroid was inefficiently sulfated *in vivo*, as shown in the PCa patient compared to a healthy subject (Fig. 4.8). This result suggests that defective SULT activities, leading to increased active steroids in circulation, may contribute to the progression of PCa. As decreased 3αDIOL-S levels were also detected in the plasma of the PCa patient, supporting altered sulfation of the C_{19} steroids in PCa. It is worth mentioning that adrenal and hepatic SULTs contribute to steroid sulfates in circulation, with SULT2A1 being expressed in the adrenals and the liver (Javitt et al. 2001; Riches et al. 2009). SULT2A1 adds a sulfate group to the oxygen moiety at C3 (α- and β-hydroxy groups) of steroids, in addition to the C17-hydroxy group of T (Falany et al. 1989), which suggests that the adrenal and liver are predominantly contributing to the steroid sulfate levels detected in the plasma samples. Sulfate derivatives of AST-metabolites were, however, increased in the plasma of the PCa patient compared to the healthy subject (Fig. 4.8), suggesting the possible upregulation of 3αHSD enzymes in PCa patients, increasing AST, 11OHAST and 11KAST levels, which in turn provided more substrates for prostatic and hepatic SULTs. Furthermore, the DHT-S levels detected in the male plasma samples falls below the range of 50-100 nM reported for circulatory DHT-S (Mueller et al. 2015). In both samples 11KAST was higher than 11OHA4, indicating 11βHSD2 conversions and thus a contribution to 11KAST levels would also feed back to 11KDHT together with 11K-3αDIOL which was not quantitated due to lack of a reference standard.

In contrast, in the female circulatory steroid profile, although 11KDHT was glucuronidated no 11KDHT-S was detected and 11OHAST-S levels were comparable to AST and 3αDIOL, while 11KAST was far lower.

DHT levels were negligible, and comparable to the low levels reported for DHT in premenopausal females (0.08-1.3 nM) (Mueller et al. 2015), with comparable AST-S, 11OHAST-S, 11KAST-S, and 3αDIOL-S, ~22 nM, being efficiently sulfated (Fig. 4.9). In females, the adrenals will contribute 11OHA4 to the circulation, however, its downstream metabolism would be catalysed by steroidogenic enzymes expressed in breast tissue, the ovaries and the uterus (Miller and Auchus 2011). Once 11OHAST and 11KAST is released into circulation, hepatic SULTs would sulfate these metabolites, while the kidneys may also be involved. Interestingly, the C_{19} steroid sulfate levels were similar to the C11-oxy C_{19} steroid sulfate levels, although 11KAST-G and 11KAST-S levels were lower than AST conjugates.

In the current study we also reported on the sulfation of A4 by SULT2B1b expressed in LNCaP cells, and showed that 11OHA4 was not sulfated (Fig. 4.7). Hashiguchi et al. (2017), also reported on the sulfation of these two ketosteroids, however, the authors showed SULT2A1 activity towards A4, while this isoform did not sulfate 11OHA4. Although the data shows that the ketosteroids are very poor substrates as indicated by substrate turnover (Hashiguchi et al. 2017), the data still permits one to suggest that the presence of the C11-hydroxy group may interfere with the binding of the ketosteroid to SULTs and thus the sulfation at C3 and C17 does not occur, with sulfation at C11 unlikely. In the CRPC scenario, both A4 and 11OHA4 are major adrenal steroids which are converted to active androgens in the prostate. The inability of SULTs to sulfate 11OHA4, suggests this steroid is more readily available in its unconjugated form and able to contribute to downstream products in the 11OHA4-pathway, compared to A4. Sulfate derivatives of ketosteroids could not be identified in our *in vivo* analysis and further *in vivo* investigations are therefore needed to establish data regarding the sulfation of ketosteroids. It is worth mentioning that although 11OHA4, 11KA4 and 11OHAST have been detected in neonatal and adult urine samples, the samples had to undergo deconjugation with β-glucuronidase and sulfatase before these metabolites

could be extracted and quantified (Homma et al. 2003; Dhayat et al. 2015) –suggesting that these C11-oxy C_{19} steroids are biotransformed by glucuronidation and sulfation in the human body.

Similarly to sulfation pathways, desulfation is an active pathway in the prostate, but in contrast, desulfation utilizes circulating DHEA-S. DHEA-S is transported into the cell by organic anion transporter proteins (OATPs), desulfated by STS, and then metabolized to downstream androgens such as T and DHT (Mueller et al. 2015). In our LNCaP cell model, however, DHEA-S was not significantly converted to downstream metabolites after 12 and 24 hrs, as negligible DHEA, A4, T and DHT were detected (data not shown). OATPs expression has been reported to be increased in CRPC (Wright et al. 2011) and androgen deprived LNCaP cells showed elevated OATP1A2 expression and increased cell proliferation in the presence of DHEA-S (0.05, 0.5 and 5 µM for 7 days) (Arakawa et al. 2012) -it is interesting that in our hands 1 µM DHEA-S was not metabolised, suggesting either that OATPs did not transport DHEA-S into the cells or the STS catalysed reaction requires more time. When DHEA (1 µM) was assayed in LNCaP cells, negligible downstream metabolites were produced after 12 and 24 hrs (only ~0.02 µM A4 was detected, Fig. 4.7a). Androstenediol was, however, not quantified in the analysis, which may account for the DHEA levels, ~0.65 µM, recovered after 12 and 24 hrs. It has been reported that LNCaP cells should be co-cultured with prostate stromal cells for DHEA to have downstream effects (Arnold et al. 2008; Mizokami et al. 2009), and as such may explain why DHEA was not metabolized more efficiently.

4.5 Summary

This preliminary investigation into the sulfation of C11-oxy C_{19} steroids reports that although C11-oxy C_{19} steroid sulfates were identified in plasma, these steroids were not sulfated in our *in vitro*

assays. In the LNCaP cells, the C11-oxy steroids were not sulfated, which suggests that the adrenal and hepatic SULTs contribute to steroid sulfates in circulation. Only when DHT was assayed were sulfate levels produced in our enzymatic conversion assays, while 11KDHT was not sulfated. In the PCa patient, circulatory 11KDHT-S levels were present at lower levels compared to the healthy subject, while DHT-S levels were negligible. Furthermore, DHT was significantly conjugated compared to 11KDHT in LNCaP cells, thereby underscoring the importance of 11KDHT in PCa. Adrenal 11OHA4 contributes to the androgen pool in peripheral target issue, more so than A4, especially relevant in the ADT treatment by castration in PCa patients. Further investigations into adrenal sulfation may provide *in vivo* evidence of ketosteroid sulfation. Our *in vivo* results show that adrenal, hepatic and prostatic sulfation may be involved in the sulfation at C17 and/or C3 with a α-hydroxyl moiety, and while it has been reported that SULTs prefer substrates with the C3 β-hydroxy orientation, the sulfation of 11OH-epiAST, 11K-epiAST and 11K-3βDIOL, still needs to be determined, in addition to the presence of these 3β-reduced metabolites in circulation.

Our current analysis reports the impeded conjugation of the C11-oxy C_{19} steroids resulting in inefficient inactivation of these C11-oxy steroids, once again highlighting the contribution of these androgens to the androgen pool, with anticipated adverse downstream effects in steroid-dependent diseases.

Chapter 5

An investigation into the metabolism of 11OHA4 and 11OHT and their metabolites in benign prostatic

hyperplasia

5.1 Introduction

In normal prostate growth and development, the biosynthesis of DHT, from its gonadal precursor T,

catalysed by SRD5A is vital. DHT is termed a 'potent' androgen, as it binds the AR, translocates into the

nucleus and subsequently elicits its physiological effects. Consequently, the production of DHT is also

considered the main driving force in the development of prostate diseases, cancers and benign tumours,

such as BPH. BPH is characterized by lower urinary tract symptoms, such as obstruction of the urinary

bladder, due to stromal and epithelial cellular growth, which subsequently enlarges the prostate

(Penning 2010; Kahokehr and Gilling 2014). The hormonal contribution in the development of BPH has

been widely reported (Siiteri and Wilson 1970; Marcelli and Cunningham 1999; Carson and Rittmaster

2003; Andriole et al. 2004), and has resulted in clinical treatments progressing to include SRD5A

inhibitors (Roehrborn et al. 2010; Kahokehr and Gilling 2014). SRD5A inhibitors would block the

production of DHT from T in the classic pathway and, indirectly, from A4 via 5αDIONE in the alternative

pathway (Fig. 5.1). Both T and A4 are produced *de novo* in testicular Leydig cells, however, the adrenal

also produces androgen precursors, including T (low levels), A4 and 11OHA4 (Schloms et al. 2012; Rege

et al. 2013) (Fig. 5.1), with 11OHA4 being implicated in the development of CRPC (Swart et al. 2013; Du

Toit et al. 2017; Du Toit and Swart 2018) and in clinical conditions (Turcu et al. 2016; O'Reilly et al. 2017).

The 11OHA4-pathway yields 11KT and 11KDHT (Fig. 5.1) –androgens capable of binding and activating

the AR, and of induces AR dependent gene expression (Rege et al. 2013; Storbeck et al. 2013;

Pretorius et al. 2016). In the case of these C11-oxy androgens, SRD5A inhibitors would shunt steroids away from 11KDHT, but towards the production of 11KT –an AR agonist, which is inefficiently conjugated *in vivo* and *in vitro* (Du Toit et al. 2017; Du Toit and Swart 2018). In this setting, the 17βHSDs and 11βHSD2 are role players, regulating 11KT levels arising from adrenal 11OHA4 (Fig. 5.1). Of note, the adrenal also produces 11KT, although minimal, together with 11KA4 and 11OHT (Rege et al. 2013), also dependent on the expression of CYP11B1 and CYP11B2, as these enzyme catalyse the production of 11OHA4 from A4 (Fig. 5.1) and 11OHT from T (Swart et al. 2013). 11KT can, therefore, originate in the adrenals and in peripheral tissue given the necessary enzyme machinery is expressed, while no reports, to date, on the production of 11KT or 11KDHT in the testis has been shown.

Figure 5.1 Steroidogenic pathways leading to the production and inactivation of potent androgens DHT, 11KT and 11KDHT (boxed steroids).

In the prostate, the conversion of 11OHA4, 11OHT, 11KA4 and 11KT by SRD5A1 and SRD5A2 are irreversible. 11OHA4, 11OH-5αDIONE and 11OHAST are not substrates for the 17βHSDs, while 11OHT, 11OHDHT, 11KT, 11KDHT and 11K-3αDIOL are substrates for 17βHSD2, and 11KA4, 11K-5αDIONE and 11KAST for 17βHSD3 and AKR1C3. While the conversion of 11OHA4, 11OHT, 11OH-5αDIONE, 11OHDHT and 11OHAST by 11βHSD2 is irreversible, only the presence of 11βHSD1 in the prostate would reverse this reaction (Bloem et al. 2013; Storbeck et al. 2013; Swart et al. 2013). The reversible inactivation of steroids by 3αHSD are dependent on the presence of a keto moiety at C3. Both C_{19} steroids, DHT and 5αDIONE and C11-oxy C_{19} steroids, 11KDHT, 11OH-5αDIONE and 11K-5αDIONE are substrates for 3αHSD, with their respective 3α-reduced products presented as substrates for the reverse reaction catalysed by RL-HSD (Fig. 5.1). These conversions have been reported for the C_{19} steroids, however, for the C11-oxy C_{19} steroids, only the inactivation of 11KDHT and reactivation from 11K-3αDIOL in prostate cell models have been reported (Du Toit and Swart 2018). In addition to inactivation, termination of active androgen signalling proceeds with the glucuronidation of hydroxyl moieties by UGTs either at C3 or C17 on the steroid backbone structure (McNamara et al. 2013).

Although the general clinical approach to BPH is symptomatic relief of the disease affecting the patient's quality of life, medical interventions are currently practised (Kahokehr and Gilling 2014), however, for these interventions to have the best outcome, steroid metabolism in BPH needs to be fully described, with the downstream metabolism of the C11-oxy C_{19} steroids in BPH not yet, to date, clarified. The current study investigated and compared the metabolism of the C11-oxy C_{19} steroids, 11OHA4, 11OHT, 11KA4 and 11KT and the metabolism of A4 and T in BPH-1 cells. The inactivation by 3αHSD enzymes and the reactivation by RL-HSD enzymes which are both endogenously expressed in BPH-1 cells, were also assayed, in so doing generated C_{19} and C11-oxy C_{19} steroid profiles of active and inactive androgens. The

interconversion of C_{19} and C11-oxy C_{19} steroids by 17βHSDs in BPH-1 cells were also investigated and analyses of the unconjugated steroids in prostate tissue of BPH patients produced profiles for comparative analyses of active and inactive androgens.

5.2 Materials and methods

5.2.1 Materials

Steroids (A4, T and DHT), RPMI-1640 medium, β-Glucuronidase (Type VII-A from *E.coli*, 5,292,000 units/g), methyl tert-butyl ether (MTBE) and DCM were purchased from Sigma-Aldrich (St. Louis, MO, USA), and all other steroids from Steraloids (Wilton, USA). All deuterated steroids were purchased from Cambridge isotopes (Andover, MA, USA). BPH-1 cells were a gift from Prof SW Hayward (NorthShore University HealthSystem, Chicago, USA) and HEK293 cells were purchased from ATCC (Johannesburg, South Africa). AKR1C3 pcDNA3, and SRD5A1 pCMV7 and SRD5A2 pCMV7 plasmid constructs were obtained from Prof J. Adamski (Helmholtz Zentrum München, Institute of Experimental Genetics, Neuherberg, Germany) and from Prof DW. Russell (Southwestern Medical Center, University of Texas, Dallas, USA), respectively. Leftover human PCa tissue and samples were anonymously selected following a study investigating PCa clinical markers (reference no. NO9/11/330; Faculty of Medicine and Health Science, Stellenbosch University and Tygerberg Hospital, SA), and stored at -80°C until further use. Analytical grade chemicals and tissue culture requirements were supplied by reliable scientific houses.

5.2.2 Steroid metabolism in BPH-1 cells

BPH-1 cells were cultured in RPMI-1640 medium supplemented with 10% FBS, 1.5 g NaHCO$_3$/L (pH 7), 1% penstrep at 37°C, in an atmosphere of 90% humidity and 5% CO$_2$. After 3-4 passages, confluent cells were replated into 12-well plates at 1 x 10^5 cells/mL and following 48 hrs incubation, the medium was replaced with 1 mL culture medium containing steroid substrates (1 µM): A4, T, 5αDIONE, DHT, AST, 3αDIOL, 11OHA4, 11OHT, 11KA4, 11KT, 11KDHT, 11KAST, 11OHAST, 11OHDHT, 11OH-5αDIONE, 11K-5αDIONE and 11K-3αDIOL. 11OHDHT and 11K-3αDIOL are unavailable commercially, and were prepared as previously described (Du Toit and Swart 2018). Briefly, 11OHT (2 µM) was converted to 11OHDHT in HEK293 cells transfected with SRD5A1/2 and 11KAST (2 µM) was converted to 11K-3αDIOL in cells transfected with AKR1C3 (also reported in Chapter 4, section 4.2.2). After 48 hrs, media was collected and diluted (1:1) with culture media and added at 1 µM to BPH-1 cells. Duplicate 0.5 mL aliquots of T, DHT, AST and 3αDIOL were collected after 48 hrs for analysis of unconjugated (free) steroids and total (unconjugated + glucuronidated) steroids following deconjugation with β-glucuronidase (Du Toit and Swart 2018).

5.2.3 Steroid extraction

Liquid/liquid extractions of steroids (0.5 mL aliquots) were carried out using DCM (10:1) (Storbeck et al. 2013; Swart et al. 2013; Du Toit et al. 2017) with D2T (1.5 ng), D9PROG (15 ng), D7A4 (15 ng) and D711OHA4 (15 ng) added as deuterated internal standards to media aliquots collected from assays carried out in BPH-1 cells. Steroids were extracted from transurethral resection of the prostate (TURP) tissue samples obtained from treatment-naïve BPH patients, using 5 mL MTBE after addition of D2T (1.5 ng), cortisol-D4 (15 ng), D7A4 (15 ng) and D711OHA4 (15 ng) to prostate tissue (100 mg)

homogenate (Du Toit et al. 2017; Du Toit and Swart 2018). Extracted steroids were dried and the residue dissolved in 0.15 mL 50% methanol in water and stored at -20˚C prior to UPC^2-MS/MS analysis.

5.2.4 Separation and quantification of steroid metabolites

Stock solutions of steroids were dissolved in absolute ethanol (2 mg/mL) and stored at -20°C. Standards were prepared as follows: a standard range, 0.00025 – 0.5 ng/μL prepared in deionized water was used in the analysis of tissue samples, a standard range, 0.0001 to 1 ng/μL, prepared in RPMI-1640 cell culture media was used in the analysis of BPH-1 assays. The prepared steroid standards were extracted using the appropriate protocols described above.

The C$_{19}$ and C11-oxy C$_{19}$ steroids were analysed by ACQUITY UPC^2®–MS/MS (Waters Corporation, Milford, USA), separated using an UPC^2® BEH column (3 mm x 100 mm, 1.7 μm particle size) for the A4 and T metabolites and an UPC^2® BEH 2-EP column (3 mm x 100 mm, 1.7 μm particle size) for the C11-oxy C$_{19}$ metabolites, as previously reported (Du Toit et al. 2017; Du Toit and Swart 2018). Modifications to the gradient and the UPC^2 separation of the C$_{19}$ and C11-oxy C$_{19}$ steroids, mass transitions, retention times, LOD, LOQ and other relevant data have been previously published (Du Toit and Swart 2018). Method validation, including recovery and matrix effect (Du Toit et al. 2017) and accuracy and precision (Du Toit and Swart 2018), have been reported. Steroids that were not commercially available were quantified by UPC^2-MS/MS, following peak integrations, using response factors, previously determined by Quanson (2015), and as previously reported (Du Toit and Swart 2018). Data was collected and analysed with the MassLynx 4.1 (Waters Corporation) software program. Experiments were performed in triplicate, representative of at least duplicate experiments and the results are given as means ±STD DEV. Statistics were calculated by an unpaired t-test using GraphPad Prism (version 5) software

133

(GraphPad Software, San Diego, California). Differences were considered statistically significant at $P<0.05$.

5.3. Results

5.3.1 Androgen metabolism in BPH-1 cells

The *in vitro* metabolism of the C11-oxy C_{19} steroids was firstly determined in BPH-1 cells. 11OHA4 was converted by both 11βHSD2 and SRD5A (Fig. 5.2a) yielding low levels of 11KA4 (0.07 μM), and 11OH-5αDIONE (0.017 μM), respectively. The downstream 3α-reduced metabolite, 11OHAST, was detected at 0.02 μM, which was further metabolised to 11KAST (0.05 μM) by 11βHSD2. Although 11KDHT and 11K-3αDIOL levels were negligible, the precursor steroid 11KT (0.03 μM), produced in the conversion of 11KA4 by the 17βHSDs, was also detected. The profile, however, does indicate that 11OHA4 was predominantly present in its unchanged form after 48 hrs with all metabolites below 0.1 μM. Conversely, 11OHT's conversion to downstream metabolites (Fig. 5.2b) was more efficient primarily yielding 11OHA4, 0.48 μM, attributed to the oxidative activity of 17βHSD2 together with 11βHSD2 yielding 11KT, 0.082 μM. 11OHA4 was subsequently converted to 11OH-5αDIONE (0.01 μM), together with 11KA4 (0.013 μM), 11K-5αDIONE (0.015 μM) and 11KAST (0.022 μM), while negligible 5α-reduction of 11OHT to 11OHDHT was observed. In the conversion of 11KA4 (Fig. 5.2c), the formation of 11KT (0.5 μM) indicated reductive 17βHSD activity, together with the SRD5A catalysed reaction converting 11KA4 to 11K-5αDIONE, 0.015 μM. The downstream production of 11OHAST (0.025 μM) suggests possible 11βHSD1 activity –first the conversion of 11K-5αDIONE to 11KAST (3αHSD activity) followed by the production of 11OHAST from 11KAST (11βHSD1 activity). In the conversion of 11KT (Fig. 5.2d) to 11KA4 (0.3 μM), the oxidative 17βHSD activity is most efficient, followed by its subsequent conversion by SRD5A to produce 11K-5αDIONE (0.03 μM). Negligible levels of 11KDHT

(~0.01 µM; below LOQ) were detected, indicative of the conversion of 11K-5αDIONE and/or 11KT by reductive 17βHSDs and/or SRD5As, with only the inactive metabolite detected being 11KAST.
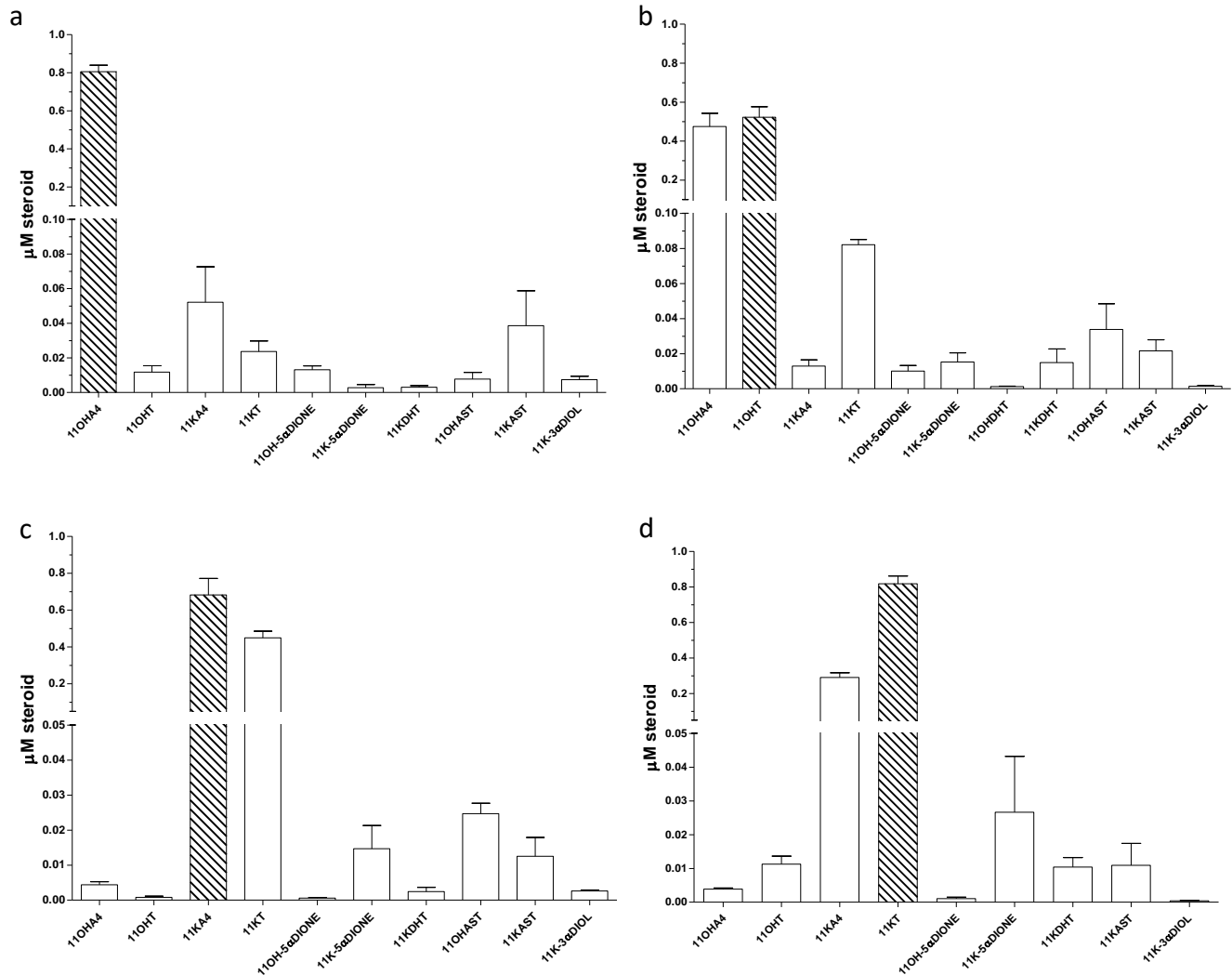
Figure 5.2 C11-oxy C_{19} androgen metabolism in BPH-1 cells. Substrate (1 µM; patterned bars) conversion (a) 11OHA4, (b) 11OHT, (c) 11KA4 and (d) 11KT after 48 hrs. Experiments were performed in triplicate, analysed by UPC^2-MS/MS and the results expressed as the mean ±STD DEV (*n*=6).

The metabolic profile of A4 (Fig. 5.3a) showed that A4 was converted to T (0.3 µM) by reductive 17βHSDs and to 5αDIONE (0.12 µM) by SRD5As. Similarly, in the conversion of T (Fig. 5.3b), the steroid was

predominantly converted to A4 (0.56 µM) by oxidative 17βHSDs, which was subsequently converted to 5αDIONE (0.13 µM). Low levels of DHT (0.02 µM) were detected, formed from both 5αDIONE (17βHSD activity) and T (SRD5A activity). 3αHSD subsequently converted 5αDIONE and DHT to AST and 3αDIOL (Fig. 5.3a and b), respectively.
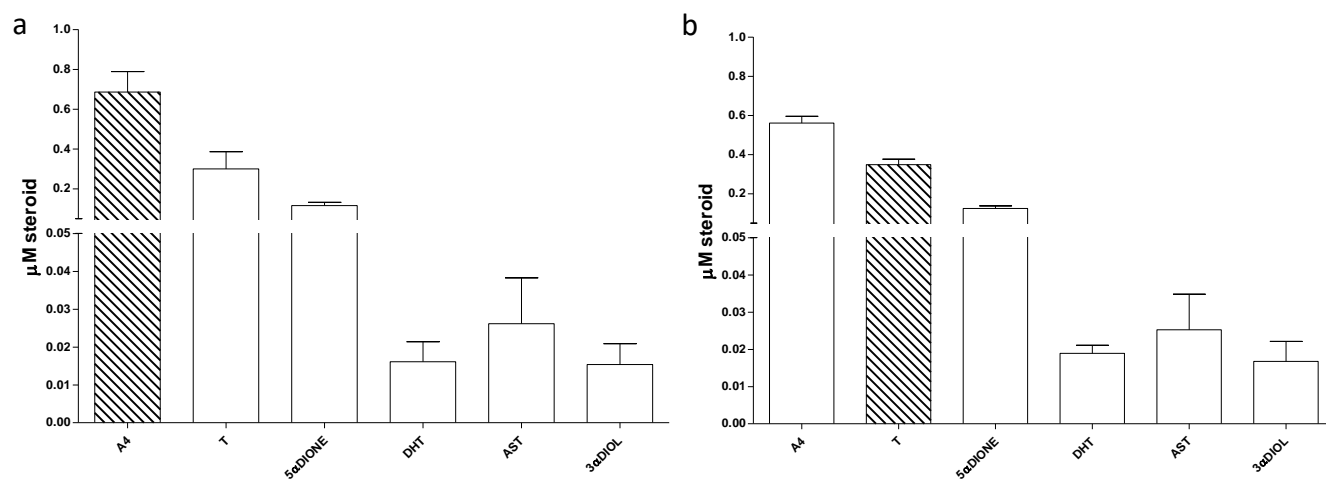
Figure 5.3 C_{19} androgen metabolism in BPH-1 cells. Substrate (1 µM; patterned bars) conversion (a) A4 and (b) T after 48 hrs. Experiments were performed in triplicate, analysed by UPC^2-MS/MS and the results expressed as the mean ±STD DEV (*n*=6).

5.3.2 3αHSD and RL-HSD activity in BPH-1 cells

Prior to the investigation into the 3αHSD and RL-HSD activity in BPH-1 cells, glucuronidation activity was determined in these cells. Following conversion assays of C_{19} steroids, and deconjugation of duplicate aliquots, data indicated that the cell model did not exhibit UGT activity (Fig. 5.4).
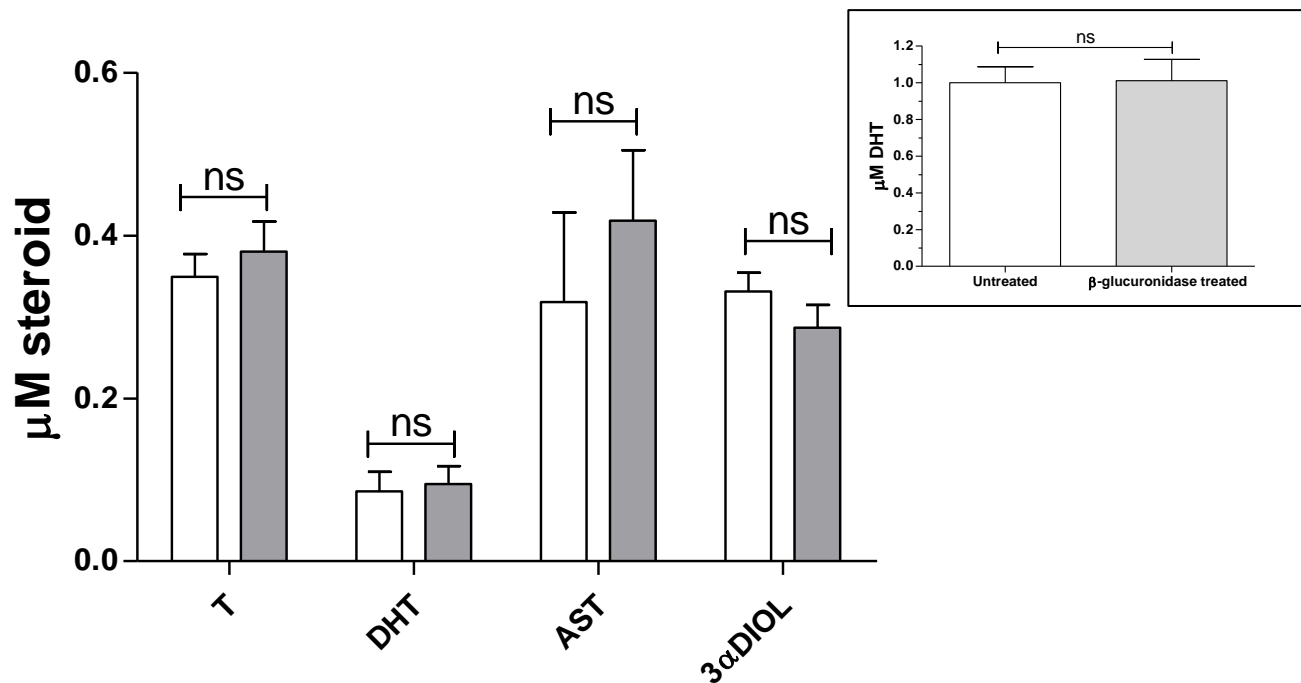
Figure 5.4 Unconjugated and total (unconjugated + glucuronidated) C_{19} steroid levels in BPH-1 cells. T, DHT, AST and 3αDIOL (1 µM) conversion after 48 hrs; clear bars, unconjugated (free) steroids; shaded bars, total steroids. Insert; untreated DHT (1 µM) extracted from media and DHT recovery from DHT-G (1 µM) after 24 hrs incubation with β-glucuronidase served as the control for this experiment. Experiments were performed in triplicate, analysed by UPC^2-MS/MS and the results expressed as the mean ± STD DEV (n=3 for AST; for all other substrates n=6; ns=not significant).

Since no glucuronidation activity was detected the BPH-1 cell model, inactivation and reactivation of active androgens would play an important role in regulating receptor activity. The metabolism of 5αDIONE, AST, DHT, 3αDIOL, 11OHAST, 11OH-5αDIONE, 11KAST, 11K-5αDIONE, 11KDHT and 11K-3αDIOL was subsequently assayed at 1 µM in BPH- cells. Relevant steroids were subsequently analysed to assess the 3αHSD inactivation and RL-HSD reactivation and depicted as ratios (Fig. 5.5). 5αDIONE and DHT were reduced to AST (0.15 µM) and 3αDIOL (0.09 µM) by 3αHSD, respectively, while only AST was efficiently converted back to 5αDIONE (0.07 µM) by RL-HSDs. The inactivation and

137

activation of the C_{19} steroids yielded products in a 2:1 and 7:1 ratio. 3αHSD catalysed the reduction of

11OH-5αDIONE and 11K-5αDIONE producing 11OHAST (0.1 μM) and 11KAST (0.05 μM), respectively.

RL-HSD catalysed the conversion of 11OHAST producing 0.03 μM 11OH-5αDIONE, with the conversion

of 11KAST to 11K-5αDIONE being negligible, resulting in 4:1 and 15:1 ratios, respectively. 11KDHT was

converted to 11K-3αDIOL (0.024 μM), while the reverse reaction proceeded less efficiently to 11KDHT

(0.015 μM), resulting in the 2:1 ratio.
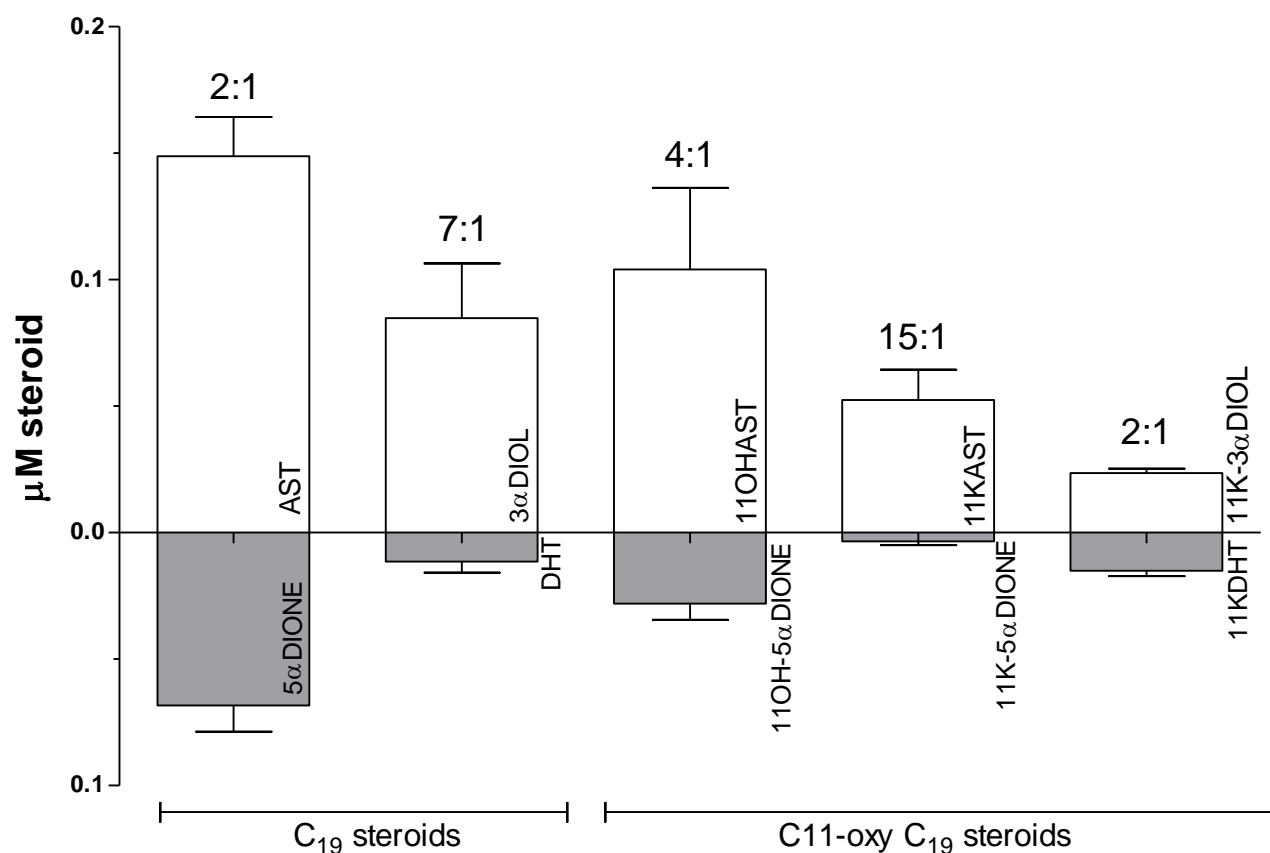
Figure 5.5 Ratios of inactive and active androgens catalysed by 3αHSD and RL-HSD in BPH-1 cells. Cells were

incubated with 5αDIONE, DHT, 11OH-5αDIONE, 11K-5αDIONE and 11KDHT (1 μM) to assess 3αHSD activity and

with AST, 3αDIOL, 11OHAST, 11KAST and 11K-3αDIOL (1 μM) to assess RL-HSD activity. Bars show product

formation catalysed by 3αHSD (white bars) and by RL-HSD (shaded bars) after 48 hrs. Experiments were performed in triplicate, steroids were analysed by UPC^2-MS/MS and the results expressed as the mean ±STD DEV (n=6).

5.3.3 The metabolism of 5α-and 3α-reduced C11-oxy C$_{19}$ steroid metabolites in BPH-1 cells

The complete steroid profiles of the 5α- and 3α-reduced C11-oxy C$_{19}$ and C$_{19}$ steroid metabolites after 48 hrs are shown in figures 5.6 and 5.7, respectively. The C11-oxy C$_{19}$ steroid profiles include the products of the reductive and oxidative 17βHSDs and 11βHSDs. The metabolism of 11OH-5αDIONE (Fig. 5.6a) yielded the 5α-reduced product 11OHAST (0.075 µM), together with the 11βHSD2 product, 11K-5αDIONE (0.02 µM). The subsequent conversion of 11K-5αDIONE by reductive 17βHSDs is evident in the production of 11KDHT (0.04 µM). It should be noted that 11OH-5αDIONE is not a substrate for reductive 17βHSDs and the high levels detected at 0.74 µM after the assay period may be due to 11OHAST being shunted back to the substrate by RL-HSD (Fig. 5.1). The metabolic profile of 11K-5αDIONE (Fig. 5.6b), showed the production of 11KDHT (0.12 µM) catalysed by reductive 17βHSDs, with no conversion to 11OH-5αDIONE by 11βHSD1 being detected. The downstream 3α-reduced metabolites, 11K-3αDIOL and 11KAST detected at ~0.044 µM, may be shunted back to 11K-5αDIONE which was detected at 0.76 µM after the assay period. 11OHDHT was converted (Fig. 5.6c) to 11OH-5αDIONE (0.49 µM) efficiently by oxidative 17βHSD as well as to 11KDHT (0.09 µM) by 11βHSD2. 11OHAST (0.09 µM) was subsequently produced from 11OH-5αDIONE catalysed by 3αHSDs. Negligible levels of 11KAST, 11K-5αDIONE and 11K-3αDIOL were also detected, with 11OHDHT, 0.34 µM, detected after the assay period. The metabolic profile of 11KDHT (Fig. 5.6d) showed no formation of 11OHDHT by 11βHSD1, while oxidative 17βHSD activity efficiently produced 11K-5αDIONE (0.3 µM). 11OH-5αDIONE levels were negligible, however, 11OHAST (0.08 µM) and 11KAST (0.03 µM), were detected, suggesting the conversion of 11K-5αDIONE to 11KAST, followed by the 11βHSD1 catalysed reaction to 11OHAST.

139

11KDHT levels were detected at 0.59 µM after the assay period, suggesting the shunt via 11K-3αDIOL, 11KAST and 11K-5αDIONE possibly contributing to these levels (Fig 5.1). The 11βHSD2 catalysed conversion of 11OHAST to 11KAST (0.04 µM) was confirmed in the metabolic profile of 11OHAST (Fig. 5.6e), and 11OHAST is not a substrate for reductive 17βHSDs. Negligible 11K-5αDIONE (from 11KAST by RL-HSD), 11K-3αDIOL (from 11KAST by reductive 17βHSDs) and 11KDHT (from 11K-3αDIOL by RL-HSD) were also detected, however, 0.92 µM 11OHAST was detected after the assay period. In the conversion of 11KAST (Fig. 5.6f), efficient reductive 17βHSDs produced 11K-3αDIOL (0.3 µM), and the 11βHSD1 catalysed reaction produced 0.02 µM 11OHAST. 11KAST was detected at high levels (0.73 µM) after the assay period, and with 11KDHT (from 11K-3αDIOL by RL-HSD) being detected at 0.01 µM, together with the presence of 11K-5αDIONE indicative of a shunt in these metabolites contributing towards 11KAST levels. The metabolic profile of 11K-3αDIOL (Fig. 5.6g) showed the production of 0.36 µM 11KAST by reductive 17βHSDs, as well as 11KDHT (~0.015 µM) catalysed by RL-HSD. The conversion of 11KAST by 11βHSD1 produced 0.035 µM 11OHAST, while 0.66 µM 11K-3αDIOL was detected after the assay period.
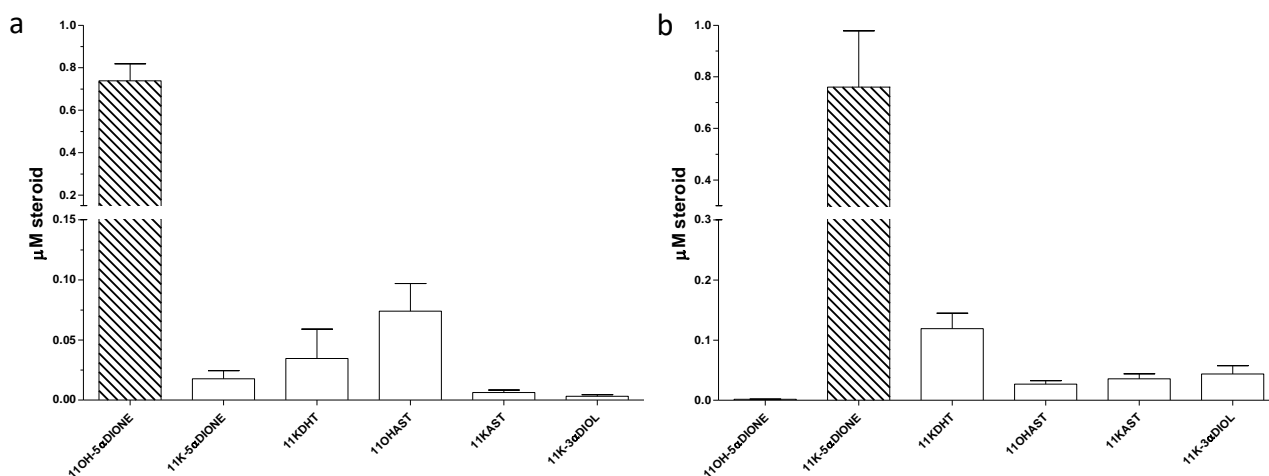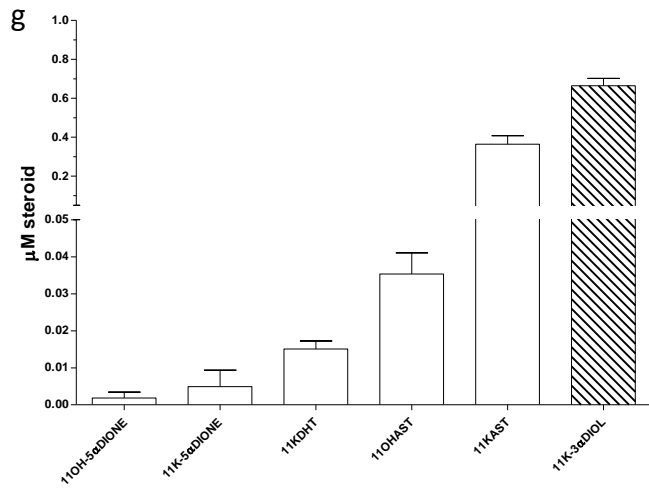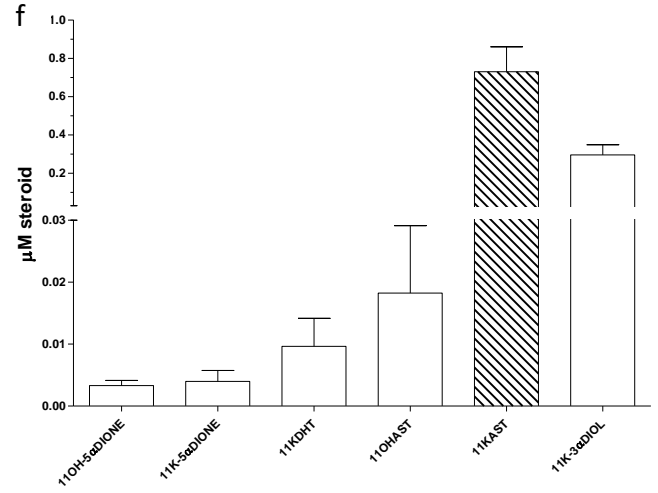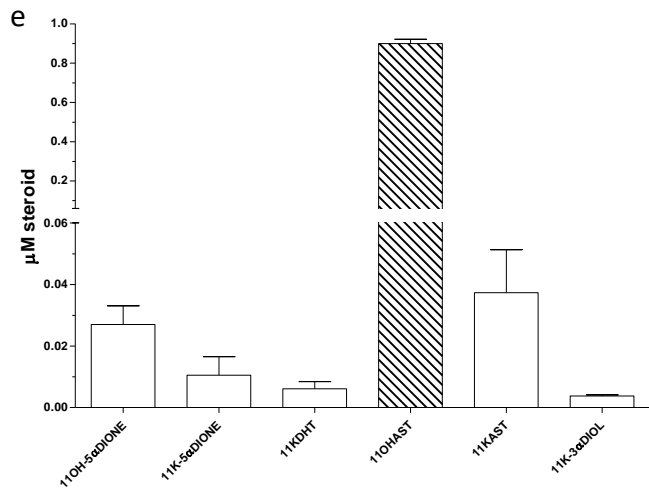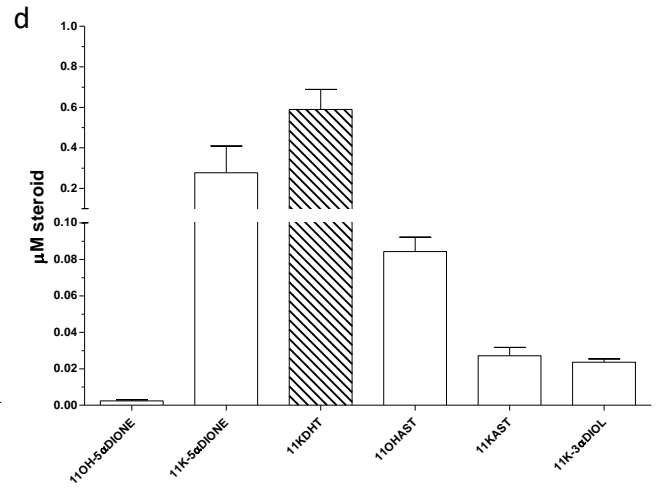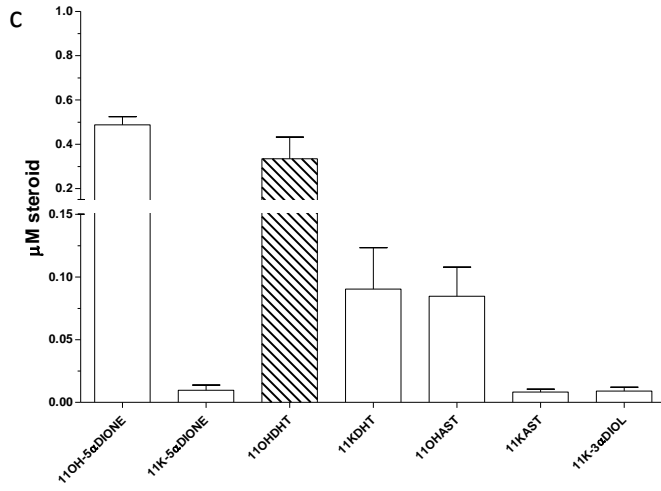
Figure 5.6 C11-oxy C_{19} androgen metabolism in BPH-1 cells. Substrate (1 µM; patterned bars) conversion (a) 11OH-5αDIONE, (b) 11K-5αDIONE, (c) 11OHDHT, (d) 11KDHT, (e) 11OHAST, (f) 11KAST and (g) 11K-3αDIOL after 48 hrs. Experiments were performed in triplicate, analysed by UPC^2-MS/MS and the results expressed as the mean ±STD DEV (*n*=6).

The oxidative and reductive 17βHSD enzymatic activity was subsequently assessed in the conversion of the C_{19} steroid since the 11βHSD enzyme do not compete for these substrates (Fig. 5.1). The metabolic profile of DHT (Fig. 5.7a) showed that DHT was efficiently converted to 5αDIONE (0.42 µM) by oxidative 17βHSDs, as well as to 3αDIOL (0.09 µM) catalysed by 3αHSD. Both products were subsequently converted to AST (0.11 µM). A similar profile was observed in the conversion of 5αDIONE (Fig. 5.7b) produced AST (0.15 µM) and low levels of DHT (0.05 µM) which were subsequently converted to 3αDIOL (0.06 µM), with 0.62 µM 5αDIONE being detected after the assay period. The metabolic profiles of AST (Fig. 5.7c) and 3αDIOL (Fig. 5.7 d) showed their efficient interconversion by the 17βHSDs, yielding a 1:1 ratio, as 0.28 µM 3αDIOL was produced from AST (reductive 17βHSD activity) and 0.3 µM AST was produced from 3αDIOL (oxidative 17βHSD activity). Negligible DHT (0.01 µM) was produced when AST was assayed, while 0.04 µM 5αDIONE was also produced when 3αDIOL was assayed.
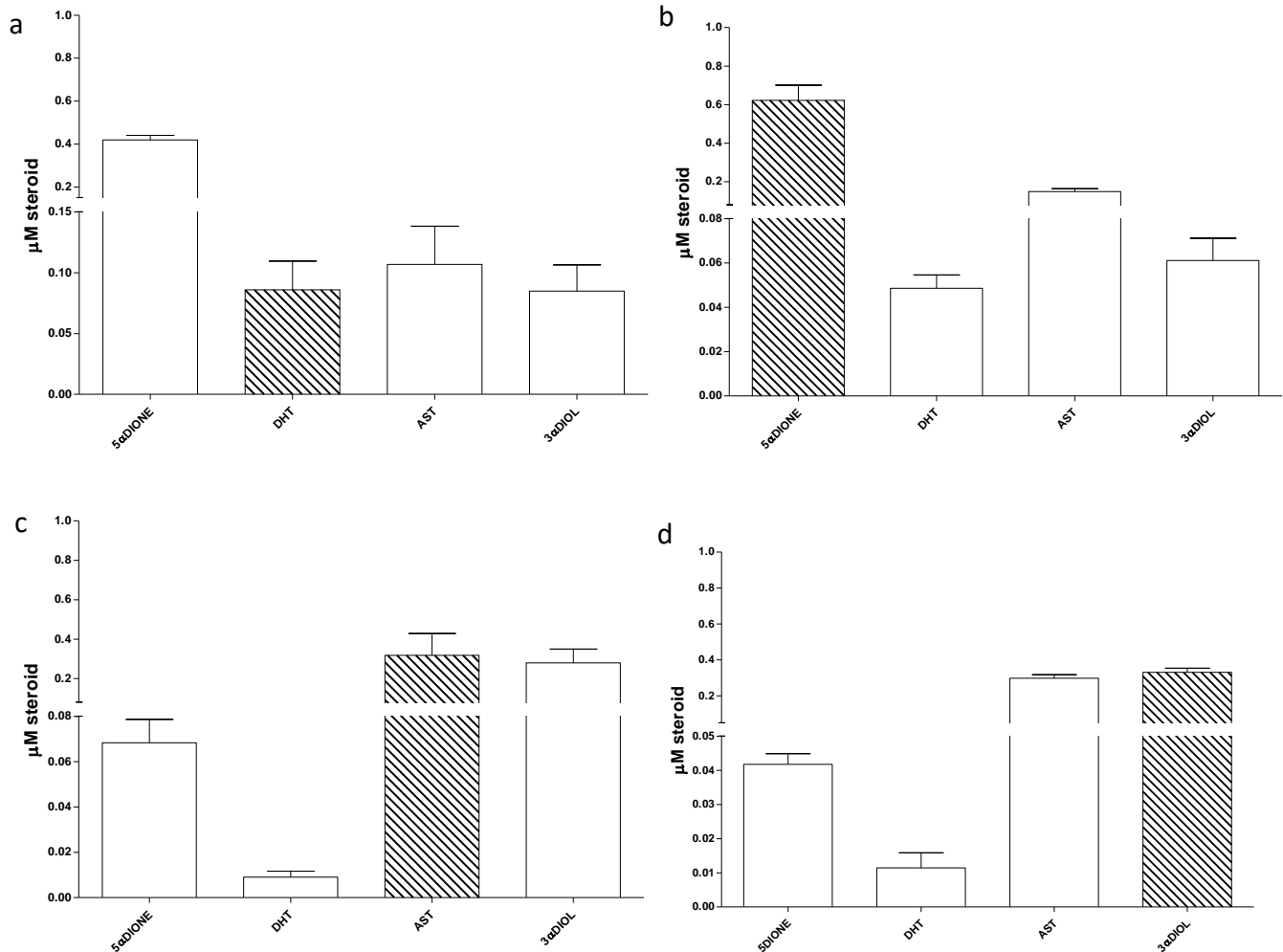
Figure 5.7 C_{19} androgen metabolism in BPH-1 cells. Substrate (1 µM; patterned bars) conversion (a) 5αDIONE, (b) DHT, (c) AST and (d) 3αDIOL after 48 hrs. Experiments were performed in triplicate, analysed by UPC^2-MS/MS and the results expressed as the mean ±STD DEV (*n*=6).

5.3.4 C_{19} and C11-oxy C_{19} steroid profiles in BPH prostate tissue

Analyses of the C_{19} steroid profile in three BPH prostate tissue samples showed only unconjugated A4 present at detectable levels, ~7.5 ng/g (6, 8 and 8 ng/g), of the total androgens analysed (Fig. 5.8). No other C_{19} steroids were detected above the LOQ. In the analyses of the C11-oxy C_{19} steroids, only the 3αHSD inactivated metabolites 11OHAST (18%, 15% and 8% of the total steroids detected) and 11KAST

143

(55%, 35% and 86% of the total steroids detected) were detected at levels above the LOQ, average levels detected at ~8.8 ng/g and ~64.8 ng/g, respectively. Although both 11KDHT and DHT were below the LOQ, 11KDHT levels (1.5-2.5 ng/g) were, in all cases, higher than DHT levels (<1 ng/g).
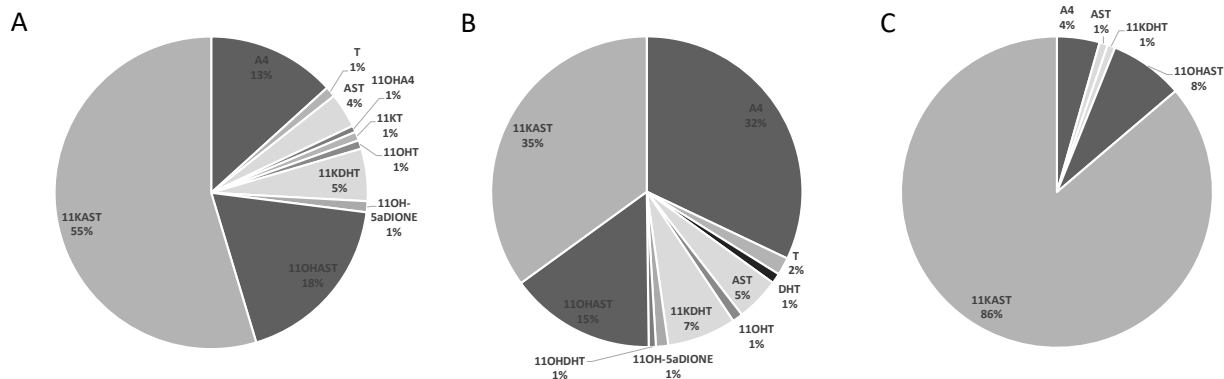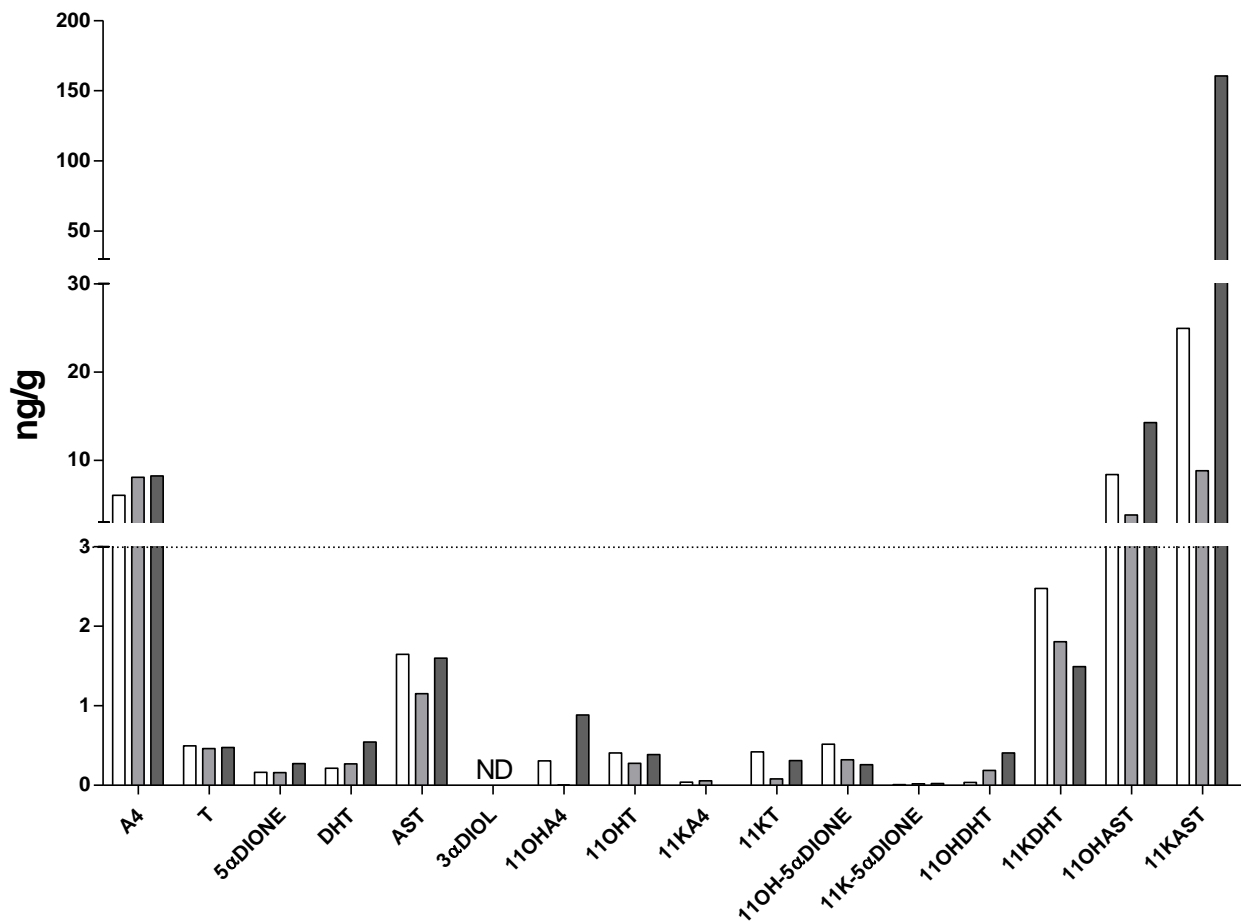
Figure 5.8 UPC^2-MS/MS analysis of unconjugated C$_{19}$ steroid profiles in TURP tissue samples of BPH patients. Clear bars, A, age 69; light grey bars, B, age 55 and dark grey bars, C, age 61. Steroids below the dashed line represent steroids detected below the LOQ. *ND*: not detected. Insert; relative contribution of C$_{19}$ and C11-oxy C$_{19}$ steroids to the steroid profile for each patient.

Although 3αDIOL was not detected in the analysis of the tissue samples, 11K-3αDIOL was. However, the steroid could not be accurately quantified as it is unavailable commercially. Integration of the ionisation signal/peak area of 11K-3αDIOL and that of a deuterated internal standard peak area, enabled the analyses of the response generated by 11K-3αDIOL (Fig. 5.9). The data suggests the *in vivo* inactivation of 11KDHT to 11K-3αDIOL, together with 11KAST also being converted to 11K-3αDIOL by reductive 17βHSDs.
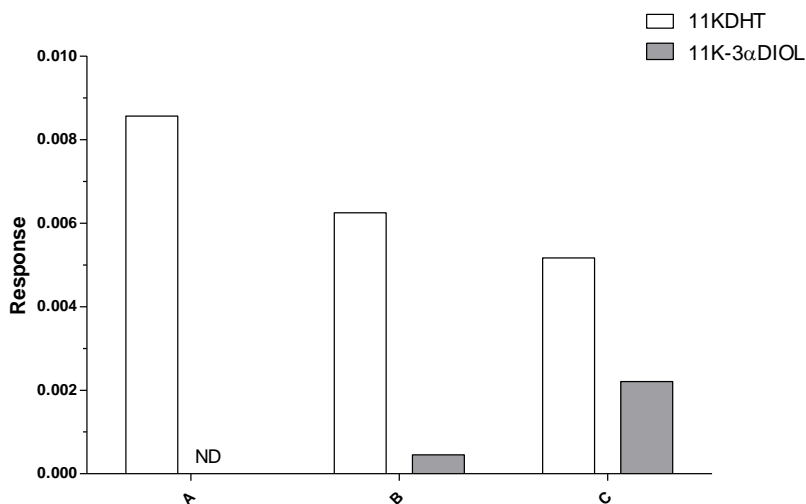
Figure 5.9 UPC^2-MS/MS analysis of unconjugated (free) 11KDHT (shaded bars) and 11K-3αDIOL (clear bars) in TURP tissue samples of BPH patients. A, patient aged 69; B, patient aged 55 and C, patient aged 61. ND: not detected.

145

5.4. Discussion

This study set out to investigate the metabolism of the C_{19} and C11-oxy C_{19} steroids in BPH-1 cells, endogenously expressing enzymes resembling a near normal scenario and potentially that of early stage PCa development. This is the first study reporting on the presence of the C11-oxy C_{19} steroids in BPH tissue and shows the metabolism of the C11-oxy C_{19} steroids in BPH-1 cells yielding active androgens – 11KA4 and 11OHT yielded 11KT, while in tissue downstream inactive steroids, 11OHAST and 11KAST, were identified.

The main contributor to the progression of prostate diseases, including benign tumours, is the intraprostatic production of the potent steroid, DHT, while the production of potent C11-oxy C_{19} steroids may also impact BPH. This study therefore investigated the metabolism of A4, T, 11OHA4 and 11OHT to analyse the production of DHT, 11KT and 11KDHT. Comprehensive profiles enabled the analysis of steroid metabolic pathways and end-products, and established steroid levels after a specific period, as these would be dependent on enzyme expression. SRD5A1 and 2 mRNA are expressed in BPH tissue (Habib et al. 1998; Andriole et al. 2004), together with positive immunostaining for SRD5A1 (Thomas et al. 2003) and a moderate signal for SRD5A3 (Godoy et al. 2011). Quantitative gene expression of oxidative 17βHSD2, 4, 8 and 10, and reductive 17βHSD3, 7 and AKR1C3 have also been shown in BPH tissue (Gianfrilli et al. 2014), while an increase in AKR1C3 mRNA transcript has also been reported in BPH epithelial cells compared to normal prostate epithelial cells (Bauman et al. 2006). However, compared to PCa, BPH expresses substantially more 17βHSD2, 4 and 8, which are primarily oxidative 17βHSDs (Gianfrilli et al. 2014). Interestingly, a 10-fold increase and a 3-fold increase in AKR1C2 and RL-HSD mRNA transcripts, respectively, have been shown in BPH stromal cells compared to normal prostate stromal cells, however, no RL-HSD activity was detected in BPH epithelial cells (Bauman et al. 2006).

146

Steroidogenic enzyme expression is, on the other hand also modulated depending on the stage of PCa progression, as evidenced in the upregulation of SRD5A1 and SRD5A3 and the downregulation of SRD5A2 in CRPC (Titus et al. 2005; Stanbrough et al. 2006; Montgomery et al. 2008; Thomas et al. 2008; Godoy et al. 2011; Azzouni et al. 2012), together with the upregulation of AKR1C3 in PCa (Stanbrough et al. 2006; Luu-The et al. 2008; Mitsiades et al. 2012). In CRPC, 3βHSD1 and 3βHSD2 expression are also increased (Miller and Auchus 2015), while UGT2B15 has also been shown to be upregulated (Stanbrough et al. 2006; Mostaghel 2013).

In the metabolism of A4 and T, conversions catalysed by 17βHSD and 3αHSD, are reversible reactions with the profiles generated (Fig. 5.3a and b) showing equal levels of downstream steroid metabolites detected, suggesting that the equilibrium was reached at this time interval. Considering the downstream metabolites produced, both A4 and T produced the same levels of DHT, 5αDIONE, AST and 3αDIOL, however, our collective data suggest their metabolism is dictated by oxidative and reductive 17βHSD activity. Low 17βHSD activity towards T has been reported, with 7.3% A4 being produced following a 16 hr incubation with [^{3}H]T (Hayward et al. 1995). In addition to our data showing a far more efficient conversion of T to A4, when AST and 3αDIOL were assayed (Fig. 5.7c and d), these steroids were also metabolised efficiently, stabilizing at ~0.33 μM after 48 hrs, with the interconversion by RL-HSD and 3αHSD yielding comparable DHT and 5αDIONE levels, respectively. Clearly, 17βHSDs are major role players in steroid metabolic pathways in BPH-1 cells –regulating potent androgen biosynthesis and inactivation of steroids. Furthermore, DHT production is similar, irrespective of whether A4 or T was assayed, while 3αDIOL and AST levels were also similar. Interestingly, Hayward et al. (1995) also reported the equal downstream production of AST and 3αDIOL from T, yielding 4.6% AST and 4.1% 3αDIOL. Although the data show no glucuronidation of the C$_{19}$ steroids, sulfation of steroid metabolites may

147

contribute to differences in the detected levels, however, in all cases, our analysis of downstream metabolites accounts for the substrate addition at 1 µM.

The steroid profiles determined for the C11-oxy C_{19} steroids are more complex due to 11βHSD activity metabolising these analytes. The adrenals produce, 0.99 nmol/L 11KA4, 0.48 nmol/L 11OHT and 0.39 nmol/L 11KT, however, 11OHA4 levels were detected at 157 nmol/L, which was ~2-fold greater than A4 levels (Rege et al. 2013). Since these steroids also contribute to active androgens, the metabolism of 11OHA4, 11OHT, 11KA4 and 11KT was assayed in BPH-1 cells to ascertain the production of C11-oxy downstream metabolites. Considering the metabolism of 11OHA4 (Fig. 5.2a) –interpreting the profile is facilitated due to 11OHA4 not being a substrate for reductive 17βHSD3 and AKR1C3, with only 11βHSD2 and SRD5A able to convert this adrenal steroid. The conversion of 11OHA4 to 11KA4 by 11βHSD2 led to the subsequent production of 11KT (by reductive 17βHSD activity) and negligible 11KDHT, with the data suggesting that 11βHSD2 levels are higher than SRD5A levels. The metabolism of 11OHT (Fig. 5.2b) yielded high levels of 11OHA4 and 11KT which in turn led to the production of 11KDHT at levels comparable to those reached in the metabolism of 11KT (Fig. 5.2d), however, 11KT levels remained high, with oxidative 17βHSD activity leading to the production of 11KA4. This data suggests that the expression levels of the 17βHSD enzymes are greater than that of 11βHSDs which in turn is greater than the SRD5As.

Interestingly, although SRD5A activity has been reported in this cell model (Hayward et al. 1995), our data showed the enzyme's catalytic activity towards the C11-oxy C_{19} steroids to be very low, as the C11-oxy C_{19} top tier steroid metabolites, 11OHA4, 11OHT, 11KA4 and 11KT were not readily reduced (Fig. 5.2), and the middle and bottom tier metabolites ranged from ~0.04 µM to negligible. Compared to our previously published work, in which 11KDHT was produced, catalysed by SRD5A in VCaP and C4-2B cells (Du Toit and Swart 2018), the pre-cancerous BPH-1 cell model, catalysed the production of 11KDHT

inefficiently, as this steroid was detected <0.018 µM for all substrates assayed. In contrast to the low

SRD5A activity detected towards the top tier steroids, oxidative 17βHSD activity, efficiently converted

11OHT and 11KT to 11OHA4 and 11KA4, respectively (Fig. 5.2), which may be attributed to 17βHSD2, as

the expression of 17βHSD2 has been reported to be higher in BPH tissue than in prostatic tissue

(Gianfrilli et al. 2014). It is worth noting that the conversions by 17βHSDs are reversible, and the data

presented capture steroid levels at the single time interval of 48 hrs. Therefore, although the data show

that 11OHT and 11OHDHT are more readily oxidised by 17βHSDs compared to 11KT and 11KDHT, the

steroid products 11OHA4 and 11OH-5αDIONE (formed from 11OHT and 11OHDHT) are not substrates

for reductive 17βHSDs, and are therefore not converted back to 11OHT and 11OHDHT. The C11 keto

metabolites are, however, converted in the forward and reverse reactions. 17βHSD3, AKR1C3 and

17βHSD2 activities (Bauman et al. 2006; Gianfrilli et al. 2014), were confirmed in the reversible

conversions between 11KA4 and 11KT (Fig. 5.3), with the downstream production of metabolites being

low. Of note, 11βHSD1 catalyses the conversion of C11-keto metabolites to C11-hydroxy metabolites

(Swart et al. 2013), with the oxo-reductase activity of this enzyme observed in this cell line (Fig. 5.6).

Only when 11KAST was directly assayed (Fig. 5.6f), did the 11βHSD1 activity produce 11OHAST. In this

scenario it might be that 11βHSD1 is able to metabolise other C11-hydroxy metabolites, however,

competition with steroidogenic enzymes, such as SRD5A, 17βHSD and 3αHSD, minimise the activity of

11βHSD1.

Although we have reported on the glucuronidation of the C11-oxy C_{19} steroids, their inactivation by

3αHSDs has not been clarified –our group has only reported on the inactivation and reactivation of

11KDHT in LNCaP, C4-2B and VCaP cells (Du Toit and Swart 2018). Since glucuronidation of C_{19} steroids

was not detected in BPH-1 cells, and sulfation questionable, inactivation by 3αHSD and reactivation by

149

RL-HSD would regulate the levels of potent androgens. The analysis of the inactivation and reactivation of C11-oxy C_{19} steroids in BPH-1 cells (Fig. 5.5) showed that 11OH-5αDIONE was more readily reduced by 3αHSD, compared to the 11K-5αDIONE, which in turn was also more efficiently reduced by 3αHSD than 11KDHT. This suggests the presence of a keto group at C11 hampers inactivation. This is also reflected in the 2:1 ratio of 11K-3αDIOL:11KDHT compared to the 7:1 ratio of 3αDIOL:DHT, showing the inefficient inactivation of 11KDHT. We previously reported that the presence of a keto moiety at C11 appears not to affect inactivation by 3αHSD, but rather hampers reactivation in PCa cell models (Du Toit and Swart 2018). In the present study, however, the presence of a C11-oxy moiety appeared to hamper the reduction of the keto group at C3, while the oxidation of the hydroxyl group at C3 was negligible, however, reactivation of 11KDHT was comparable to DHT. Interestingly, 5αDIONE was more readily reduced by 3αHSD than DHT, and the reduced product more readily reactivated by RL-HSD than that of DHT. This may indicate that a keto moiety at C17 may also influence the catalytic activity of 3αHSD and RL-HSD enzymes towards the substrates. Our analyses, furthermore, corroborates reports that RL-HSD activity is minimal in BPH epithelial cells, while 3αHSD (AKR1C2) is upregulated (Bauman et al. 2006).

Our BPH tissue analysis showed only A4 levels above the LOQ, representing the contribution of gonadal, adrenal and *de novo* biosynthesis to the *in vivo* levels of this C_{19} steroid in prostate tissue (Fig. 5.8). The presence of A4 suggests that this steroid can be converted downstream to DHT, however, unconjugated DHT levels were <0.55 ng/g. The present study detected T at ~0.5 ng/g, within range of previously reported levels in untreated BPH tissue, 0.092-2.0 ng/g, with the DHT in the analysis detected at the lower limit compared to previously reported levels of 1.0-8.15 ng/g (Van der Sluis et al. 2011). The C_{19} steroid levels ranged from 0-7.5 ng/g, however, the C11-oxy C_{19} steroid levels ranged from

0.02-64.8 ng/g. The high levels of inactive 11OHAST and 11KAST detected, indicates that the inactivation of the C11-oxy C_{19} steroids appears to be efficient, with the presence of these steroids in their unconjugated forms serving as potential substrates to be reactivated to 11KDHT (as observed in Fig. 5.6e and f). Although, we could not accurately quantify 11K-3αDIOL, the presence of this steroid in tissue, suggest that 11KDHT is inactivated and/or 11KAST is reduced, verifying the contribution of the 11OHA4-pathway to androgens in patients with BPH. Interestingly, these steroid profiles depicted in the current study are similar to the steroid profile of a CRPC patient that we previously published (Du Toit and Swart 2018). This suggest intraprostatic levels of the C11-oxy C_{19} steroids are similar in BPH and CRPC tissue, while the flux through the 11OHA4-pathway is also similar. Only 11OHAST levels were marginally higher in the CRPC tissue compared to the levels in BPH tissue, while 11KDHT levels (also below LOQ) were lower in the CRPC tissue. And while our previous analyses in prostate tissue of PCa patients (Du Toit et al. 2017) did not include the inactivated metabolites, high levels of 11OHA4, 11KA4, 11KT, 11OHT and 11KDHT were detected. These studies were, however, limited by the small sample number. Perhaps, determining circulatory C11-oxy C_{19} steroids in BPH, PCa and CRPC patients, as well as intraprostatic levels, will add to our current understanding of the differences between these diseases and the contribution of the C11-oxy steroids to disease conditions.

In the clinical setting, BPH patients are treated with SRD5A inhibitors as a first line treatment to inhibit the production of DHT. From our *in vitro* analysis, we show that DHT levels are negligible. And while this treatment would also inhibit the production of 11KDHT, the production of 11KT will not be decreased. In this scenario, the question is whether the progression of BPH to PCa is perhaps due to the use of SRD5A inhibitors, which increases the shunt of adrenal C11-oxy C_{19} steroids in the 11OHA4-pathway, subsequently producing the top tier steroids in abundance, and ultimately yielding 11KT. Analysis of

steroid conversions in BPH-1 cells in the presence of SRD5A inhibitors would likely, in the future, shed light on the flux in the pathways altering the levels of potent steroids.

5.5 Summary

Profiling steroids in BPH and at different stages of PCa development is critical to understanding prostate steroidogenesis and enzyme activity, which in turn regulate potent androgen levels. Here we show, for the first time, the 11OHA4-pathway in BPH-1 cells, and highlight the role of the 17βHSD catalysed reactions in this cell model. Furthermore, while the production of DHT and 11KDHT is comparable, 11KT was produced in abundance. Inactivation of DHT was, however, more efficient compared to the inactivation of 11KDHT –suggesting hampered 3αHSD activity due to the presence of the keto group at C11. Our *in vivo* data further establishes the presence of C11-oxy C_{19} steroids in prostate tissue – highlighting the abundantly present downstream metabolites, 11OHAST and 11KAST, as possible role players, able to feed back into the pool of potent androgens. The present study underscores the contribution of adrenal 11OHA4 to the androgen pool in the BPH scenario –suggesting both gonadal and adrenal precursor steroids should be considered in the diagnosis of this disease.

Chapter 6

Profiling steroid metabolic pathways in adrenal-linked endocrine diseases by UPC^2-MS/MS

6. 1 Introduction

Steroid hormones are involved in growth and sexual development, playing pivotal roles in adrenarche, the onset of puberty and pregnancy and while adrenal steroid hormones maintain the electrolyte balance in the body and regulate the metabolism of carbohydrates, proteins and lipids, they also regulate human stress responses. Adrenal steroids therefore play a crucial role in normal physiological homeostasis and human development, with dysregulated androgen production being associated with abnormal development. DSD in neonates and in children, androgen-dependent diseases, including cancers such as breast and PCa, as well as endocrine disorders such as PCOS and CAH, are all driven by abnormal steroid production. Circulatory and urinary steroid reference ranges are therefore necessary, allowing accurate diagnosis of diseases and disorders characterized by androgen deficiency or by androgen excess. Steroid levels have been determined by many analytical methods, including enzyme linked immunoassays (ELISA), radioimmunoassays (RIA) and LC-MS/MS. More recently, supercritical fluid chromatography (SFC), which allows for a more sensitive method for quantifying steroids present in complex matrices, is being applied. Utilizing both liquid and gas chromatographic properties, SFC ensures a faster, more efficient separation per unit time, together with a shorter turn-around time between injections compared to high-performance liquid chromatography (HPLC). Furthermore, coupling SFC with mass spectrometry (MS) greatly enhances steroid detection, with the introduction of the UPC^2-MS/MS system, by the Waters cooperation, propelling steroid separation and quantification into the next era. In addition, this system pumps CO_2 as the predominant mobile phase,

thus labelling this analytical method as environmentally friendly. Utilizing this tool will not only aid in the diagnosis of androgen-dependent diseases, in which only small volumes of samples are often available, but may also assist in the tracking of adrenal disorders and diseases, determining prognosis by enabling the assessment of steroid levels at different phases. In addition, this system allows the separation of multiple, structurally closely related steroids in a single chromatographic step, permitting efficient analyses of complex mixtures of steroids in one sample, in minutes. In addition, steroidogenic pathways can be modelled in patients and steroid biomarkers analysed or identified, allowing clinicians to accurately diagnose and treat patients effectively.

Steroids originate from the adrenals and gonads, with the adrenals able to produce mineralocorticoids, glucocorticoids and androgens, whereas the gonads only produce androgens *de novo* and from adrenal precursors. Adrenal steroids are all dependent on the conversion of cholesterol to PREG by CYP11A1, which is then channelled into the respective pathways of adrenal steroidogenesis (Fig. 6.1). Adrenal precursor steroids, including PROG, 17OHPROG, A4 and T subsequently contribute to the peripheral metabolism of these precursors to potent androgens.
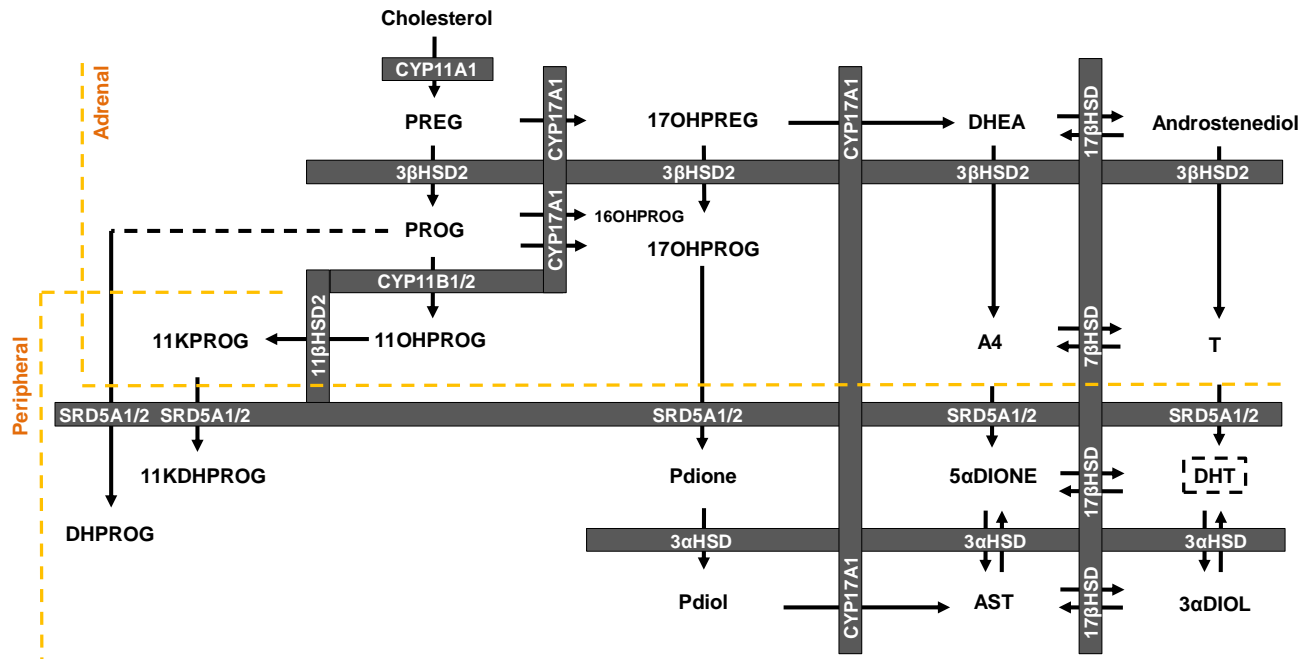
Figure 6.1 Adrenal steroid metabolism leading to the production of steroid precursors for peripheral metabolism (Boxed steroid, potent androgen).

Both A4 and T contribute to the peripheral production of DHT –through the classic and alternative pathways, with both T and DHT able to bind the AR, playing pivotal roles in PCa (Stanbrough et al. 2006; Luu-The et al. 2008; Montgomery et al. 2008; Stein et al. 2012). The adrenal precursor 17OHPROG also leads to the production of DHT in the backdoor pathway, producing intermediates pdione following the conversion by SRD5A, and pdiol following the conversion by 3αHSD (Auchus 2004) (Fig. 6.1). The backdoor pathway has been identified as a dominant pathway in 21OHD patients (Kamrath et al. 2012), where a dysfunction in CYP21A2 activity leads to the accumulation of 17OHPROG (Milewicz et al. 1984; Nahoul et al. 1989), leading to the production of androgens and ultimately DHT.

In addition, the production of 11OHPROG, catalysed by CYP11B1 and CYP11B2 from PROG, subsequently leads to the production of 11KPROG catalysed by 11βHSD2. The peripheral metabolism of PROG and

155

11KPROG by the SRD5As yields DHPROG and 11KDHPROG, respectively. DHPROG has been shown to activate the progesterone receptors (Van Rooyen et al. 2017), and 11KDHPROG, once produced by SRD5A, has been shown to yield another potent androgen, 11KDHT in the backdoor pathway (Van Rooyen et al. 2017).

The role of 11βHSD2 is further highlighted in the peripheral metabolism of 11OHA4, the CYP11B1 and B2 product of A4 (Schloms et al. 2012) (Fig. 6.2). The 11OHA4-pathway leads to the production of 11KDHT, and, due to the conversion of adrenal 11OHA4 and 11OHT by 11βHSD2, produces 11KT, with both 11KDHT and 11KT being AR agonist at 10 nM (Bloem et al. 2015) –playing pivotal roles in CRPC (Swart et al. 2013; Swart and Storbeck 2015). It should be noted that the adrenal also has 11βHSD2 activity and following the biosynthesis of 11OHA4 and 11OHT, produces 11KA4 and 11KT, however, at negligible levels (Rege et al. 2013). These C11-oxy C_{19} steroids impact the progression of CRPC, with our studies having reported high levels of 11OHA4, 11KT and 11KDHT in circulation and in prostate tissue of PCa patients, as well as the inefficient conjugation of 11KT and 11KDHT *in vitro* in cell models, which was also reflected in our analyses of circulatory steroid levels in PCa patients (Du Toit et al. 2017; Du Toit and Swart 2018).
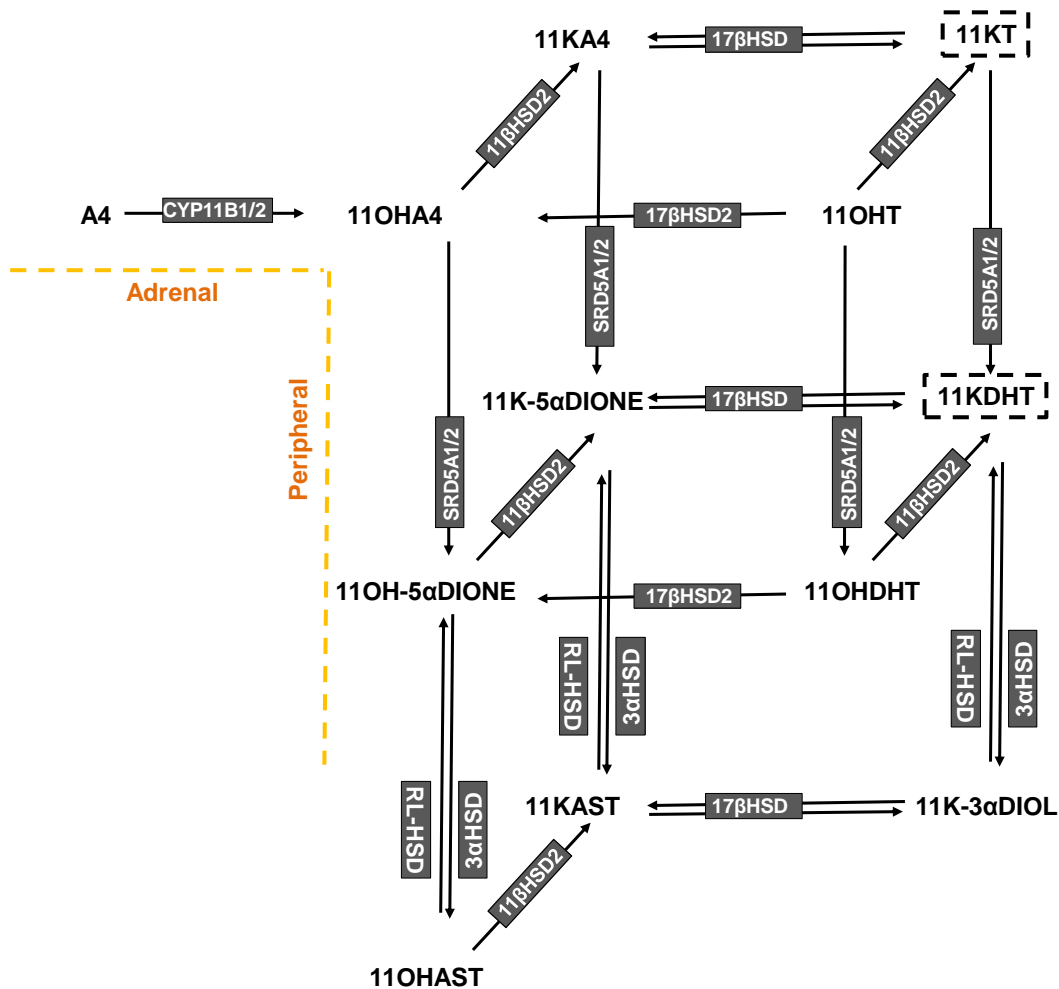
Figure 6.2 Peripheral metabolism of adrenal 11OHA4 in the 11OHA4-pathway (Boxed steroids, potent androgens).

Accurate analytical techniques are required in the diagnosis of androgen-dependent diseases. Traditionally only the quantification of circulatory DHEA, A4 and T are included in the diagnosis of androgen excess in PCOS patients. Other androgens may, however, also be of importance. Recently, C11-oxy C_{19} steroids, including 11OHA4, 11KA4, 11OHT and 11KT, with the increased urinary excretion of 11OHAST, 11OHA4 and 11KA4 were detected in PCOS patients (O'Reilly et al. 2017), using LC-MS/MS and GC-MS. The C11-oxy C_{19} steroids have also been shown to be increased 3-4-fold in 21OH patients, with 11KT levels being the most prominent (Turcu et al. 2016). Furthermore, deficient CYP21A2 activity

in 21OHD patients leads to the excess production of 17OHPROG, 16OHPROG, and 21-dF (Turcu et al. 2015), the latter produced by the hydroxylation of 17OHPROG catalysed by CYP11B1 (Fig. 6.3). These patients have abnormally low cortisol levels, together with increased androgen production. In terms of androgens, our laboratory recently reported the downstream metabolism of 21-dF also leading to the production of novel steroid intermediates, and ultimately to the production of 11KDHT and 11OHDHT in the backdoor pathway (Barnard et al. 2017). Although, the physiological role of these novel steroid intermediates is still unknown, these metabolites should be included in the steroids analysed in 21OHD patients which would only be possible once these steroids can be accurately detected and quantified.
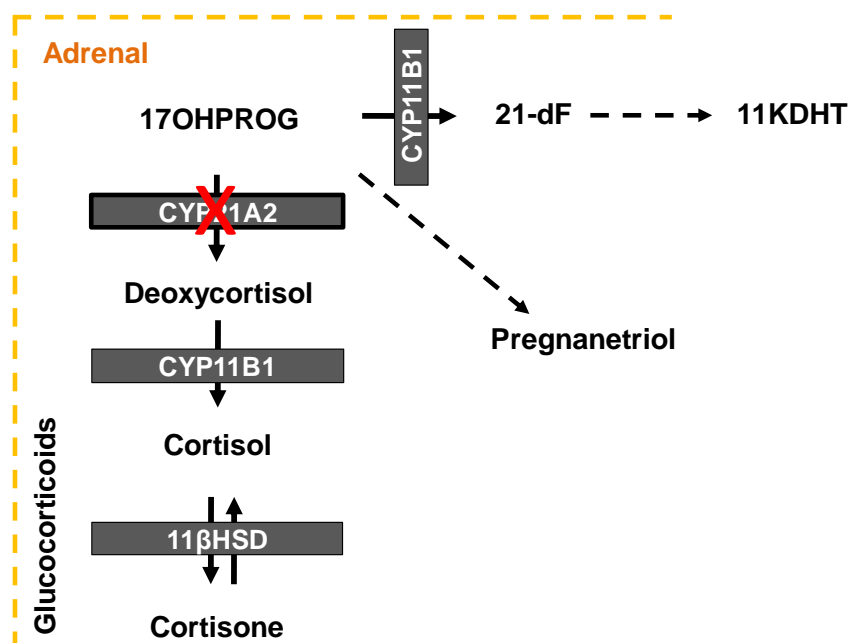
Figure 6.3 Deficient CYP21A2 activity leading to the production of 21-dF, pregnanetriol and 11KDHT.

Another downstream C_{21} steroid of importance is pregnanetriol (5β-pregnan-3α,17α,20α-triol), a urinary steroid metabolite of 17OHPROG monitored in CAH patients (Kamrath et al. 2017), which may be biosynthesized via two routes. It can either be produced from the 5β-reduction of 17OHPROG, followed

by the 3α-reduction of the C3 keto moiety by AKR1C2 and finally the reduction at the C20 keto group.

A second route would follow the reduction at C20 of 17OHPROG, and the subsequent 5β-reduction of the C4-C5 double bond and finally the 3α-reduction by AKR1C2. Another 5β-reduced steroid of importance is etiocholanolone (5β-androstan-3α-ol-17-one), a urinary metabolite detected in 21OHD and PCOS patients (Tsilchorozidou et al. 2003; Kamrath et al. 2012). It is produced from the reduction of A4 by SRD5A, producing 5β-androstanedione (5βDIONE), predominantly in the liver by Δ^4-3-oxosteroid 5β-reductase D1 of the aldo-keto reductase family 1 (AKR1D1). The C3 keto group of 5βDIONE is subsequently reduced by AKR1C2, thereby producing the etiocholanolone metabolite. Furthermore, 11OH-etiocholanolone (5β-androstan-3α,11β-diol-17-one) and 11K-etiocholanolone (5β-androstan-3α-ol-11,17-dione) are also produced as end-metabolites of 11OHA4 and 11KA4, respectively, following the 5β-reduction of the double bond between C4-C5 and the subsequent reduction by AKR1C2. Notably, these C11-oxy metabolites have been detected as urinary metabolites in CAH patients (Jailer et al. 1955) and in healthy neonatal urinary samples (Homma et al. 2003; Dhayat et al. 2015), with increased or decreased levels possibly reflecting hormonal imbalances and abnormal development.

In the following article, the development and validation of a high-throughput UPC[2]-MS/MS method is reported, which can be applied in the separation and quantification of C_{19} and C_{21} steroids, and their respective C11-hydroxy and C11-keto metabolites, particularly relevant in adrenal disorders and steroid-related diseases allowing for the *in vitro* and *in vivo* evaluation of comprehensive steroid panels.[2]

---

[2] Author contribution to the manuscript entitled *A high-throughput UPC[2]-MS/MS method for the separation and quantification of C_{19} and C_{21} steroids and their C11-oxy steroid metabolites in the classical, alternative, backdoor and 11OHA4 steroid pathways*: MAS advised with UPC[2]-MS/MS method development and validation.

A high-throughput UPC^2-MS/MS method for the separation and quantification of C$_{19}$ and C$_{21}$ steroids and their C11-oxy steroid metabolites in the classical, alternative, backdoor and 11OHA4 steroid pathways

Therina du Toit[a], Maria A. Stander[a,b], Amanda C. Swart[a,*]

[a] Department of Biochemistry, Stellenbosch University, Stellenbosch 7600, South Africa
[b] Central Analytical Facility, Stellenbosch University, Stellenbosch 7600, South Africa

ABSTRACT

In the present study an ultra-performance convergence chromatography tandem mass spectrometry (UPC^2-MS/MS) analytical method was developed and validated for the determination of 17 C$_{19}$ and 14 C$_{21}$ steroids, including C11-oxy C$_{19}$ and C11-oxy C$_{21}$ steroids. The limit of detection and limit of quantification ranged from 0.01 to 10 ng/mL and from 0.01 to 20 ng/mL, respectively, and the method shows the recovery, matrix effect and process efficiency of steroids isolated from a serum matrix to be within acceptable limits. Good accuracy, repeatability and reproducibility were also shown and the method provided excellent sensitivity and selectivity as stereoisomers and regioisomers were also resolved and quantified accurately.

Clinical conditions such as congenital adrenal hyperplasia, polycystic ovary syndrome in females and disorders of sex development in neonates and in children, amongst others, are characterized by abnormal steroid levels. Steroid profiling is essential to accurately diagnose steroid levels in the above settings as well as in androgen excess or deficiency in adrenal-linked endocrine diseases. Our method, separating C$_{19}$ and C$_{21}$ steroids in a single chromatographic step, offers a reduced sample turnover rate in the clinical setting, while providing comprehensive steroid profiles of *in vivo* steroids in the nmol/L range. This is, to our knowledge, the first method reported to simultaneously separate C$_{19}$ and C$_{21}$ steroids, together with their C11-hydroxy and C11-keto metabolites –one which may hold promise in the identification of new steroid markers in steroid-linked endocrine diseases, in addition to profiling steroid metabolism and abnormal enzyme activity in patients.

1. Introduction

Steroid hormones are essential to growth and development, playing important roles in the maintenance of normal physiological and endocrinological processes. Diseases and genetic disorders are often characterized by abnormal hormone production, with high circulatory steroid levels associated with clinical conditions. Abnormal androgen production is implicated, amongst others, in breast and prostate cancer (PCa), as well as in polycystic ovary syndrome (PCOS) in females and congenital adrenal hyperplasia (CAH) as well as in disorders of sex development (DSD) in neonates and in children. Diagnosis of these diseases is dependent on reliable reference ranges either identifying specific steroid biomarkers or identifying a number of steroids present at abnormal levels in either plasma, serum or urine samples. Advances in liquid chromatography (LC) and ultra performance LC (UPLC) or ultra high performance LC (UHPLC), together with the coupling of these systems to mass spectrometry (MS) have resulted in improved

chromatographic resolution and increased sensitivity allowing accurate detection and quantification [1–3]. The introduction of the ultra-performance convergence chromatography tandem mass spectrometry (UPC^2-MS/MS) system has furthermore greatly enhanced steroid analysis with the use of supercritical fluid chromatography (SFC) improving detection allowing a more sensitive method for separating steroid compounds even those structurally closely related [4] and present in complex matrices.

In adrenal disorders and disease conditions, adrenal steroid hormones can be either deficient or produced in excess –insufficient cortisol production in Addison's disease, excess cortisol in Cushing's syndrome and increased androgen production in PCOS and in CAH. In adrenal steroidogenesis cholesterol is converted to pregnenolone by P450 side-chain cleavage (CYP11A1), leading to the production of mineralocorticoids, glucocorticoids and androgens. In contrast, the gonads produce androgens only, *de novo* and *via* the metabolism of adrenal steroid metabolites which include progesterone (PROG), 17α-
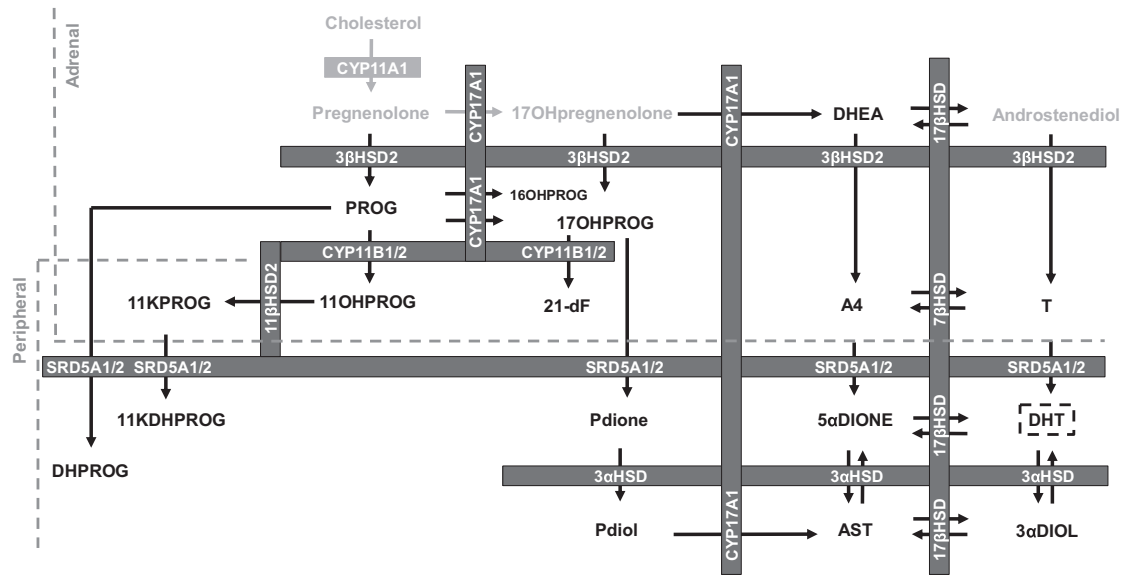
Fig. 1. Adrenal steroid biosynthesis and peripheral metabolism in the classical, alternative and backdoor pathways. Steroids included in the method are indicated by black text. Boxed steroid, potent androgen. CYP11A1, cytochrome P450 side-chain cleavage; CYP17A1, cytochrome P450 17α-hydroxylase; 3βHSD2, 3β-hydroxysteroid dehydrogenase type 2; CYP11B1, cytochrome P450 11β-hydroxylase; CYP11B2, aldosterone synthase; 17βHSD, 17β-hydroxysteroid dehydrogenase; 11βHSD2, 11β-hydroxysteroid dehydrogenase type 2; SRD5A1/2, 5α-reductase type 1/type 2; 3αHSD, 3α-hydroxysteroid dehydrogenase; DHEA, dehydroepiandrosterone/5-androsten-3β-ol-17-one; A4, androstenedione/4-androsten-3,17-dione; T, testosterone/4-androsten-17β-ol-3-one; 5αDIONE, 5α androstanedione/5α-androstan-3,17-dione; DHT, dihydrotestosterone/5α-androstan-17β-ol-3-one; AST, androsterone/5α-androstan-3α-ol-17-one; 3αDIOL, 5α-androstan-3α,17β-diol; PROG, progesterone/4-pregnen-3,20-dione; DHPROG, dihydroprogesterone/5α-pregnan-3,20-dione; 11KPROG, 11keto-progesterone/4-pregnen-3,11,20-trione; 17OHPROG, 17α-hydroxyprogesterone/4-pregnen-17α-ol-3,20-dione; 16OHPROG, 16α-hydroxyprogesterone/4-pregnen-16α-ol-3,20-dione; 11KDHPROG, 11keto-dihydroprogesterone/5α-pregnan-3,11,20-trione; 11OHPROG, 11α-hydroxyprogesterone/4-pregnen-11α-ol-3,20-dione or 11β-hydroxyprogesterone/4-pregnen-11β-ol-3,20-dione; Pdiol, 5α-pregnan-3α,17α-diol-20-one; Pdione, 5α-pregnan-17α-ol-3,20-dione; 21-dF, 21-deoxycortisol/11β,17α-dihydroxypregn-4-ene-3,20-dione.

hydroxyprogesterone (17OHPROG), androstenedione (A4) and testosterone (T) (Fig. 1). Downstream metabolism of both A4 and T yield dihydrotestosterone (DHT), which activates the androgen receptor (AR), playing a pivotal role in PCa [5]. DHT is produced either in the classical pathway in which 5α-reductase (SRD5A) converts T directly to DHT or in the alternative pathway in which A4 is converted to DHT via 5α-androstanedione (5αDIONE) (Fig. 1). The metabolism of the adrenal precursor, 17OHPROG, will also lead to the production of DHT in the backdoor pathway [6]. The backdoor pathway was identified as a dominant pathway in 21-hydroxylase deficient (21OHD) patients [7], where a dysfunction in cytochrome P450 21-hydroxylase (CYP21A2) leads to the accumulation of 17OHPROG [8,9], and thus to the production of DHT (Fig. 1).

Also contributing to the androgen pool are 11keto-testosterone (11KT) and 11keto-dihydrotestosterone (11KDHT), downstream metabolites of adrenal 11β-hydroxyandrostenedione (11OHA4), which we recently showed to be potent androgens and which are associated with clinical conditions. In the 11OHA4-pathway, the C11-oxy C19 steroids lead to the production of 11KDHT [10], impacting on castration-resistant prostate cancer (CRPC) [11–13]. While the adrenal also produces 11β-hydroxytestosterone (11OHT), 11keto-androstenedione (11KA4) and 11KT [14], we recently reported that 11-hydroxyprogesterone (11OHPROG) and 21-deoxycortisol (21-dF), both produced in 21OHD are, together with 11keto-progesterone (11KPROG) and 21-deoxycortisone, reduced by SRD5As channelling these steroids into the backdoor pathway to produce 11KDHT via 11β-hydroxydihydroprogesterone, 11keto-dihydroprogesterone (11KDHPROG), 5α-pregnan-11β,17α-diol-3,20-dione (also known 11OHPdione) and 5α-pregnan-17α-ol-3,11,20-trione (also known as 11KPdione) [15,16].

Standard reference ranges spanning preterm to adult have neither been established for these C11-oxy C19 and C11-oxy C21 steroids nor for their downstream metabolites. Recently, circulating 11OHA4, 11KA4, 11OHT and 11KT, as well as urinary 11β-hydroxyandrosterone (11OHAST) were detected in PCOS patients [17], and while androgen levels were increased in 21OHD patients, C11-oxy C19 steroids were 3 to 4-fold higher than in healthy subjects [18]. In addition, deficient

CYP21A2 activity in 21OHD also results in low cortisol levels, together with a concomitant increase in 16α-hydroxyprogesterone (16OHPROG), 17OHPROG and 21-dF levels [19]. 21-dF and 17OHPROG are routinely analysed in 21OHD, together with the 17OHPROG metabolite, 5β-pregnan-3α,17α,20-triol (pregnanetriol), with analysis often including androsterone (AST) and 5β-androstan-3α-ol-17-one (etiocholanolone), downstream A4 metabolites. The inclusion of the C11-oxy C19 and C11-oxy C21 steroids and their downstream metabolites together with 5β-androstan-3α,11β-diol-17-one (11OH-etiocholanolone), 5β-androstan-3β,11β-diol-17-one (11OH-epietiocholanolone) and 5β-androstan-3α-ol-11,17-dione (11K-etiocholanolone) in diagnostic assessments of adrenal disorders would result in more accurate diagnosis with fewer false positives and negative results.

While some of the aforementioned steroids are currently analysed *in vitro* and *in vivo* by LC-MS/MS, using UPC²-MS/MS for their quantification is not routine practice. The analyses of C19, C11-oxy C19 and C21 steroids have been identified *in vitro* by Schloms et al. [19], using UPLC-MS/MS, followed by Storbeck et al. [10], and Swart et al. [11], reporting on the quantification of these steroids *in vitro* using UPLC-MS/MS. The analysis completed by Schloms et al. [19] separated 21 steroids within 10 min, including T, cortisol, DHEA, A4, cortisone, 11OHA4, 17OHPROG, DHT, 16OHPROG and PROG. Swart et al. [11], separated 17 steroids in 5 min, including cortisol, cortisone, DHEA, A4, T, 11OHA4, 11KA4, 11OHT, 11KT and DHT, while Storbeck et al. [10] separated 11OHA4, 11KA4, 11OHT, 11KT and their 5α-reduced metabolites in 5 min using UPLC-MS/MS. *In vivo* analysis of the C11-oxy C19 steroids by LC-MS/MS in plasma was reported by Rege et al. [14], with their method including 11OHA4, 11KA4, 11OHT and 11KT, and by Turcu et al. [18], which included 11OHA4, 11KA4, 11OHT, 11KT, DHEA, A4 and T. In 2015, Turcu et al. [20] reported on the analysis of 10 C21 steroids, including 21-dF and 11OHPROG, in serum, and in 2017, the same authors reported a method which separated 23 steroids, which included the C11-oxy C19 steroids, using LC-MS/MS [21]. All the above-mentioned methods included some of the C19, C11-oxy C19 and C21 steroids, however, the C11-oxy C21 steroids have not been investigated and UPC²-MS/MS has not been used to quantify the steroids.

More recently, our group quantified C_{19} and C11-oxy C_{19} steroids *in vitro* and *in vivo* using UPC^2-MS/MS [22,23], and the C11-oxy C_{21} steroids which were quantified in a method reported by Barnard et al. [15], while a UPC^2-MS/MS analytical method separating 19 steroids, which included C_{19} and C11-oxy C_{19} steroids, has also been reported [4]. Not any UPC^2-MS/MS method has, to date, been reported which enables the separation and quantification of C_{19}, C_{21} as well as their C11-oxy derivatives in a single chromatographic step without prior derivatization.

The aim of this study was therefore to develop a high-throughput UPC^2-MS/MS method for the separation and quantification of C_{19} and C_{21} steroids, and their C11-hydroxy and C11-keto metabolites, to facilitate the accurate evaluation of steroid panels within the steroid metabolic pathways relevant to adrenal-linked endocrine diseases.

2. Materials and methods

2.1. Materials

Steroids including A4, T, DHT, dihydroprogesterone (DHPROG), dehydroepiandrosterone (DHEA), 17OHPROG, cortisone and cortisol were purchased from Sigma-Aldrich (St. Louis, MO, USA). 11OHA4, 11OHT, 11KA4, 11KT, 11KDHT, 11OHAST, 11keto-androsterone (11KAST), 5α-pregnan-17α-ol-3,20-dione (pdione), 5αDIONE, AST, 5α-androstane-3α,17β-diol (3αDIOL), epietiocholanolone, 5α-pregnan-3α,17α-diol-20-one (pdiol), 11KDHPROG, 11KPROG, 11βOHPROG, 11αOHPROG, 21-dF, 11OH-epietiocholanolone, 11K-etiocholanolone and pregnanetriol were purchased from Steraloids (Wilton, USA). PROG was purchased from BDH Chemicals Ltd. (Poole, England) and 16OHPROG from Toronto Research Chemicals (Toronto, Canada). Deuterated steroid standards were purchased from Cambridge isotopes (Andover, MA, USA): testosterone 1, 2-D2 (D2T); 4-androsten-11β-ol-3,17-dione 2,2,4,6,6,16,16-D7 (D7A4); 4-androstene-3,17-dione 2,2,4,6,6,16,16-D7 (D711OHA4) and progesterone 2,2,4,6,6,17A,21,21,21-D9 (D9PROG). FOODFRESH CO_2 was purchased from Afrox (Cape Town, South Africa), formic acid and methyl tert-butyl ether (MTBE) from Sigma-Aldrich (St. Louis, MO, USA), methanol 215 SpS from ROMIL Ltd. (Cambridge, England) and fetal bovine serum (FBS) from Biochrom GmbH (Berlin, Germany). The ACQUITY UPC^2® ethylene-bridged hybrid (BEH) column (3.0 × 100 mm, 1.7 μm particle size) and VanGuard™ pre-column (2.1 × 5 mm, 3.5 μM) were purchased from Waters (Waters Corporation, Milford, USA).

2.2. Preparation of standards

Steroids were prepared in absolute ethanol (2 mg/mL) and used to prepare three standard master mixes, 20, 200 and 1000 ng/mL in 50% methanol. These were subsequently used to prepare reference standards ranging from 0.01 to 1000 ng/mL by the addition of the appropriate volume to FBS (matrix). Additional samples, used for method validation, were prepared by spiking the matrix and 50% methanol (no matrix) with the appropriate volumes.

2.3. Steroid extraction

Prior to extraction, D2T (1.5 ng), D7A4 (15 ng), D711OHA4 (15 ng) and D9PROG (15 ng) in 100 μL deionized water were added to samples (steroid standards in 500 μL FBS), followed by the addition of 5 mL MTBE. Samples were extracted, as previously described [4,10,11,15,21,22], by vortexing for 26 min, the aqueous phase frozen at −80 °C, after which the organic phase was collected and dried. The dried residue was dissolved in 0.15 mL 50% methanol in water and the samples stored at −20 °C prior to UPC^2-MS/MS analysis. In order to analyse endogenous steroids present in the matrix, FBS (500 μL) was extracted in triplicate according to the protocol described above.

Table 1
Gradient specifications of the UPC^2 separation of steroid metabolites (solvent A, CO_2; solvent B, methanol).

Step	Time (minutes)	Solvent A (%)	Solvent B (%)	Curve
1	0	98	2	Initial
2	2.7	90	10	7
3	3.8	88	12	6
4	4.9	75	25	6
5	5	98	2	1
6	6	98	2	1

2.4. Separation and quantification of steroid metabolites

The C_{19} and C_{21} steroids analysed by UPC$^{2®}$–MS/MS (Waters Corporation, Milford, USA) were separated with an elution gradient described in Table 1. Steroids, injection volume 2 μL, were eluted at a flow rate of 2 mL/min in a total run time of 6 min per sample. The column temperature was set to 60 °C and the automated back pressure regulator (ABPR) to 2000 psi. A Xevo TQ-S triple quadrupole mass spectrometer (Waters, Milford, USA) was used for quantitative mass spectrometric detection and all steroids were analysed in multiple reaction monitoring (MRM) mode, using the positive electrospray ionization (ESI +) mode, with MRM settings shown in Table 2. Table 3 depicts the chemical formulas and structures, molecular mass of each analyte, and the internal reference standard used to quantify each analyte. The internal reference standard chosen for quantification of each steroid metabolite was chosen based on the retention time –the internal standard that eluted the closest to the retention time of the steroid metabolite was chosen as the quantifying reference standard. Preceding the MS line, a make-up pump mixed 1% formic acid in methanol at a constant flow rate of 0.2 mL/min. The following settings were used: capillary voltage of 3.8 kV, source temperature 120 °C, desolvation temperature 500 °C, desolvation gas 1000 L/h and cone gas 150 L/h. Data was collected and analysed with the MassLynx 4.1 (Waters Corporation) software program.

2.5. Method validation

Standard curves were generated for each steroid using standards prepared in FBS with the range spanning 0.01, 0.02, 0.1, 0.2, 1, 2, 10, 20, 100, 200 and 1000 ng/mL, and extracted as described in Section 2.3. The limit of detection (LOD) for each steroid was defined as the lowest concentration at which a signal-to-noise (S/N) ratio > 3 was measured for the quantifier ion. The limit of quantification (LOQ) was defined as the lowest concentration for each steroid at which a S/N ratio > 10 was measured for the quantifier ion and a S/N ratio > 3 for the qualifier ion(s). Linearity of the standard curves was assessed using the Runs test in Graphpad Prism. The presence of endogenous steroids in FBS was analysed in parallel with the validation of our samples and verified not to interfere with our analysis (Supplemental Fig. 1). Accuracy is defined as the percent relative standard deviation (%RSD) from the average response following repeated injections of a single sample and precision is defined as the %RSD from the average response following the injection of independent replicate samples, with the precision repeated over three days to assess inter-day variability [4]. Accuracy and precision were determined for the following reference standard concentrations: 2, 20, 100 and 200 ng/mL, by the addition of the appropriate volumes to FBS (matrix), prior to extraction. Recovery, matrix effects and process efficiency were determined at 2, 20, 100 and 200 ng/mL, according to the protocols reported by Taylor, 2005 [24]. Recovery was calculated by comparing the response of the steroid standards prepared in FBS and extracted as described above, to that of FBS extracts with the post-addition of the same volume (and concentration) of steroids. Matrix effect were determined by comparing FBS extracts with the post-extraction addition of steroids, to
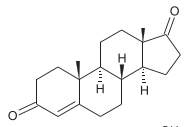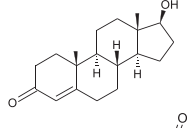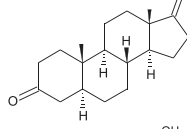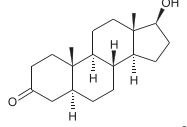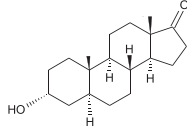
Table 2

UPC²-MS/MS detection and quantification of C_{19} and C_{21} steroid standards. Retention time (RT); molecular ion species and MRM mass transitions; mass spectrometer settings: cone voltages (CV), collision energy (CE); and internal deuterated standards: D2T, D7A4, D9PROG and D711OHA4.

Steroid metabolite	RT (min)	Mass transitions			CV (V)			CE (eV)		
		Quantifier	Qualifier	Qualifier						
A4	1.38	287.2 > 96.9	287.2 > 108.8	–	30	30	–	15	15	–
T	2.47	289.2 > 97.2	289.2 > 109.0	–	30	30	–	22	22	–
5αDIONE	0.87	289.2 > 253.1	289.2 > 97.2	–	22	30	–	16	22	–
DHT	1.80	291.2 > 255.0	291.2 > 273.0	–	25	25	–	15	20	–
AST	1.69	273.2 > 105.3	291.3 > 273.3	–	30	18	–	30	8	–
3αDIOL	2.83	275.2 > 257.0	275.2 > 175.0	–	15	15	–	15	15	–
11OHA4	2.69	303.2 > 267.2	303.2 > 121.0	–	30	30	–	30	15	–
11OHT	3.69	305.3 > 121.0	305.3 > 269.0	–	35	35	–	20	15	–
11KA4	1.99	301.2 > 257.0	301.2 > 265.2	–	35	35	–	25	25	–
11KT	3.14	303.2 > 121.0	303.2 > 267.0	–	30	30	–	20	20	–
11KDHT	2.77	305.2 > 243.0	305.2 > 269.0	–	30	30	–	20	20	–
11OHAST	3.00	289.0 > 271.0	289.0 > 213.0	–	15	15	–	15	15	–
11KAST	2.53	305.0 > 147.0	305.0 > 173.1	–	30	30	–	30	30	–
DHEA	1.88	271.2 > 253.2	271.2 > 243	–	30	–	–	15	–	–
Epietiocholanolone	1.69	273.0 > 105.1	291.2 > 255.0	–	15	15	–	30	15	–
11OH-epietiocholanolone	3.00	289.0 > 271.0	289.0 > 213.0	289.0 > 253.0	15	15	15	15	20	15
11K-etiocholanolone	2.53	305.1 > 147.0	305.1 > 287.0	–	15	15	–	30	20	–
Pregnanetriol	3.57	301.2 > 135.0	301.2 > 81.0	–	25	25	–	15	25	–
PROG	1.32	315.2 > 97.0	315.2 > 109.0	–	28	28	–	20	26	–
DHPROG	0.78	317.0 > 105.2	317.0 > 95.0	317.0 > 175.2	30	30	30	30	30	20
Pdiol	2.90	317.4 > 111.0	317.4 > 299.0	–	20	20	–	15	25	–
Pdione	1.61	333.4 > 159.0	333.4 > 137.0	–	20	20	–	25	25	–
11KPROG	2.00	329.2 > 121.0	329.2 > 84.8	329.2 > 285.0	15	15	15	20	20	20
17OHPROG	2.32	331.1 > 97.0	331.1 > 109.0	–	26	26	–	22	28	–
16OHPROG	3.00	331.2 > 97.0	331.2 > 108.9	–	30	30	–	15	15	–
11KDHPROG	1.45	331.2 > 105.0	331.2 > 147.0	–	25	25	–	30	30	–
11αOHPROG	3.11	331.2 > 295.2	331.2 > 121.0	–	30	30	–	15	30	–
11βOHPROG	2.85	331.2 > 121.0	331.1 > 295.0	–	30	30	–	20	20	–
21-dF	3.37	347.1 > 121.0	347.1 > 269.2	–	20	20	–	25	15	–
Cortisone	3.35	361.2 > 163.0	–	–	30	–	–	30	–	–
Cortisol	3.82	363.0 > 121.0	–	–	30	–	–	20	–	–
D2T	2.47	291.0 > 99.1	291.0 > 111.2	–	30	30	–	20	30	–
D7A4	1.39	294.3 > 100.0	294.3 > 113.0	–	25	25	–	25	25	–
D9PROG	1.32	324.2 > 100.0	324.2 > 113.0	–	30	30	–	20	25	–
D711OHA4	2.68	310.2 > 99.8	310.2 > 147.2	–	25	25	–	30	25	–
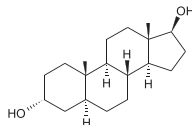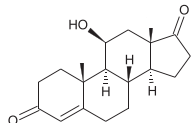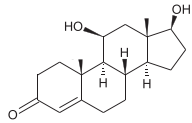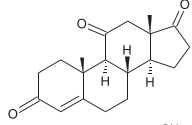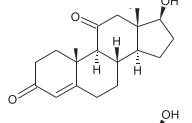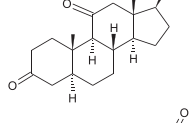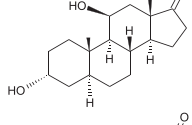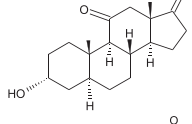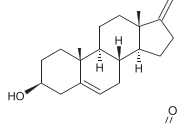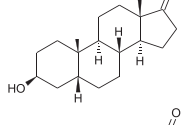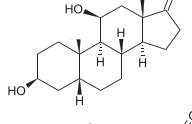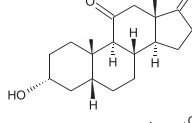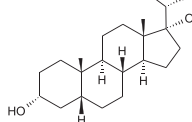
Table 3

Description of steroid analytes including their biochemical names, chemical formulas and structures, molecular mass and the internal reference standard used to quantify each analyte.

Steroid metabolite	Biochemical name	Chemical formula	Chemical structure	Molecular weight	Internal reference standard
A4	4-androsten-3,17-dione	$C_{19}H_{26}O_2$		286.4	D7A4
T	4-androsten-17β-ol-3-one	$C_{19}H_{28}O_2$		288.4	D2T
5αDIONE	5α-androstan-3,17-dione	$C_{19}H_{28}O_2$		288.4	D9PROG
DHT	5α-androstan-17β-ol-3-one	$C_{19}H_{30}O_2$		290.4	D2T
AST	5α-androstan-3α-ol-17-one	$C_{19}H_{30}O_2$		290.4	D2T

Table 3 (*continued*)

Steroid metabolite	Biochemical name	Chemical formula	Chemical structure	Molecular weight	Internal reference standard
3αDIOL	5α-androstan-3α,17β-diol	$C_{19}H_{32}O_2$		292.5	D2T
11OHA4	4-androsten-11β-ol-3,17-dione	$C_{19}H_{26}O_3$		302.4	D711OHA4
11OHT	4-androsten-11β,17β-diol-3-one	$C_{18}H_{28}O_3$		304.4	D2T
11KA4	4-androsten-3,11,17-trione	$C_{19}H_{24}O_3$		300.4	D7A4
11KT	4-androsten-17β-ol-3,11-dione	$C_{19}H_{26}O_3$		302.4	D2T
11KDHT	5α-androstan-17β-ol-3, 11-dione	$C_{19}H_{28}O_3$		304.4	D2T
11OHAST	5α-androstan-3α,11β-diol-17-one	$C_{19}H_{30}O_3$		306.4	D2T
11KAST	5α-androstan-3α-ol-11,17-dione	$C_{19}H_{28}O_3$		304.4	D2T
DHEA	5-androsten-3β-ol-17-one	$C_{19}H_{28}O_2$		288.4	D9PROG
Epietiocholanolone	5β-androstan-3β-ol-17-one	$C_{19}H_{30}O_2$		290.4	D2T
11OH-epietiocholanolone	5β-androstan-3β,11β-diol-17-one	$C_{19}H_{30}O_3$		306.4	D711OHA4
11K-etiocholanolone	5β-androstan-3α-ol-11,17-dione	$C_{19}H_{28}O_3$		304.4	D711OHA4
Pregnanetriol	5β-pregnan-3α,17,20α-triol	$C_{21}H_{36}O_3$		336.5	D2T

Table 3 (*continued*)

Steroid metabolite	Biochemical name	Chemical formula	Chemical structure	Molecular weight	Internal reference standard
PROG	4-pregnen-3,20-dione	$C_{21}H_{30}O_2$		314.5	D9PROG
DHPROG	5α-pregnan-3,20-dione	$C_{21}H_{32}O_2$		316.5	D9PROG
Pdiol	5α-pregnan-3α,17α-diol-20-one	$C_{21}H_{34}O_3$		334.5	D2T
Pdione	5α-pregnan-17α-ol-3,20-dione	$C_{21}H_{32}O_3$		332.5	D7A4
11KPROG	4-pregnen-3,11,20-trione	$C_{21}H_{28}O_3$		328.5	D7A4
17OHPROG	4-pregnen-17α-ol-3,20-dione	$C_{21}H_{30}O_3$		330.5	D2T
16OHPROG	4-pregnen-16α-ol-3,20-dione	$C_{21}H_{30}O_3$		330.5	D2T
11KDHPROG	5α-pregnan-3,11,20-trione	$C_{21}H_{30}O_3$		330.5	D7A4
11αOHPROG	4-pregnen-11α-ol-3,20-dione	$C_{21}H_{30}O_3$		330.5	D2T
11βOHPROG	4-pregnen-11β-ol-3,20-dione	$C_{21}H_{30}O_3$		330.5	D2T
21-dF	4-pregnen-11β,17-diol-3, 20-dione	$C_{21}H_{30}O_4$		346.5	D2T
Cortisone	4-pregnen-17,21-diol-3,11,20-trione	$C_{21}H_{28}O_5$		360.4	D2T
Cortisol	4-pregnen-11β,17,21-triol-3,20-dione	$C_{21}H_{30}O_5$		362.5	D2T

Table 3 (*continued*)
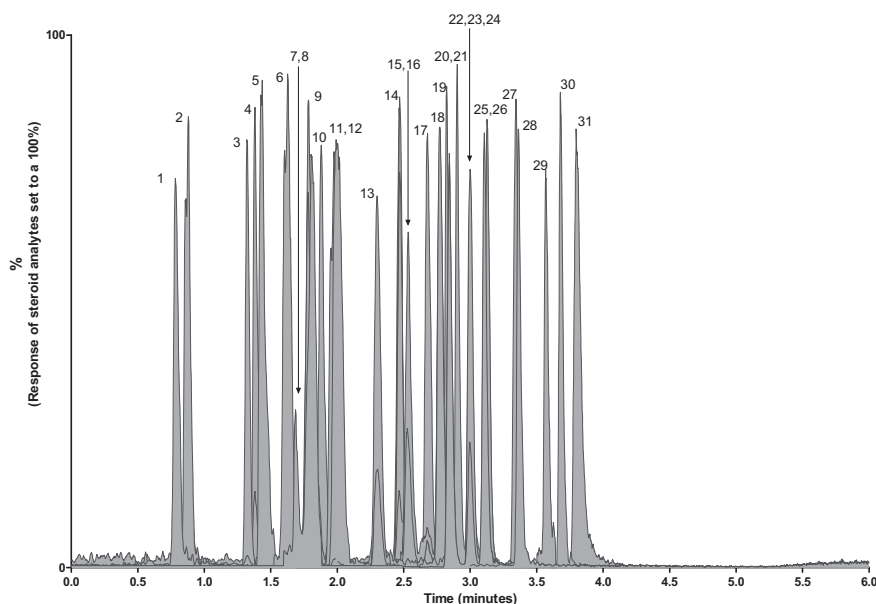
Fig. 2. UPC^2-MS/MS separation of 31 reference standards. C$_{19}$ and C$_{21}$ steroid standards, 100 ng/mL, are depicted in the elution order (1) DHPROG, 0.78 min; (2) 5αDIONE, 0.87 min; (3) PROG, 1.32 min; (4) A4, 1.38 min; (5) 11KDHPROG, 1.45 min; (6) pdione, 1.61 min; (7, 8) epietiocholanolone and AST, 1.69 min; (9) DHT, 1.80 min; (10) DHEA, 1.88 min; (11, 12) 11KA4 and 11KPROG, 2.00 min; (13) 17OHPROG, 2.32 min; (14) T, 2.47 min; (15, 16) 11K-etiocholanolone and 11KAST, 2.53 min; (17) 11OHA4, 2.69 min; (18) 11KDHT, 2.77 min; (19) 3αDIOL, 2.83 min; (20, 21) 11βOHPROG, 2.85 min and pdiol, 2.90 min; (22, 23, 24) 11OH-epietiocholanolone, 11OHAST and 16OHPROG, 3.00 min; (25, 26) 11αOHPROG, 3.11 min and 11KT, 3.14 min; (27) cortisone, 3.35 min; (28) 21-dF, 3.37 min; (29) pregnanetriol, 3.57 min; (30) 11OHT, 3.69 min; and (31) cortisol, 3.82 min.

a pure solution in 50% methanol (no matrix; no extraction) which contained the same volume (and concentration) of steroids. The difference in response between these two samples was divided by the response of the pure solution to calculate the matrix effect. Visually showing the different responses due to the three aforementioned protocols followed, are the generated standard curves shown in Supplemental Fig. 2. Lastly, the process efficiency was calculated by comparing the response of standards prepared in FBS (pre-extraction addition of steroids) to that of the pure solution. In addition, accuracy (bias) is described for all the steroids in Supplemental Table 1, and was calculated by comparing the response of the validation samples (the addition of the appropriate volumes of steroids to FBS and extracted; expected test result) to a reference response (reference value; set as 100%), which was generated using standard curves for each steroid using standards prepared in FBS and extracted, at 20, 100 and 200 ng/mL [25].

3. Results

3.1. UPC^2 separation of steroid standards

The high-throughput UPC^2-MS/MS method allowed the chromatographic separation and quantification of 28 C$_{19}$ and C$_{21}$ steroids, as well as 4 deuterated reference standards in a single 6-min step (Fig. 2). Although some steroids could not be resolved, unique MRMs were determined for accurate quantification. These steroids include 11KA4 and 11KPROG eluting at 2.0 min, and 11OHAST and 16OHPROG eluting at 3.0 min. The stereoisomers (5α, 3α-reduced *vs* 5β, 3α/β-reduced metabolites) AST and epietiocholanolone; 11OHAST and 11OH-epietiocholanolone; and 11KAST and 11K-etiocholanolone could however not be chromatically resolved, and due to their MRMs being similar, the individual stereoisomers could thus not be quantified accurately.

The separation and quantification of steroids which have similar structures, such as the 11αOHPROG and 11βOHPROG stereoisomers, are possible due to the sensitivity and selectivity of the UPC^2-MS/MS system (Fig. 3). Steroids such as 11KPROG and its reduced form, 11KDHPROG, can also be separated and quantified due to the difference in their MRMs. In addition, although the regioisomers, 17OH-PROG and 16OHPROG, have the same MRMs, they ionise differently due to the position of the C17 and C16 hydroxyl group thus enabling separation.

Furthermore, most of the steroid metabolites included in the

method have two qualifiers, however, some steroids have one or three qualifiers (Table 2). The quantifier/qualifier used as MRMs for each steroid metabolite was optimized for the best selectivity, in order to minimize transition cross-talk and to optimize the total ion count (TIC) of each steroid. This allowed an optimal 'points per peak' value for the method, allowing high peak resolution.

3.2. Performance and validation of the method

3.2.1. Calibration range

The calibration range allowed for the accurate determination of LODs and LOQs of each steroid, with LODs and LOQs ranging from 0.01 to 10 ng/mL and from 0.01 to 20 ng/mL, respectively. A linear fit with acceptable r^2-values (> 0.9947) was also obtained for all standard curves (Table 4).

3.2.2. Accuracy and precision

Acceptable %RSDs (< 20%) were obtained for all the steroids for both the accuracy and precision parameters (Table 5). Accuracy was determined to be < 15% for all steroids at 100 and 200 ng/mL, with only epietiocholanolone (17.4%) lying mid concentration, and DHEA (17.9%) and DHPROG (20.0%) in the lower concentration range showing %RSD values > 15%. Accuracy therefore ranged from 1.5% to 20.0% in the lower concentration range, from 1.6% to 17.4% in the middle concentration ranges and from 2.2% to 10.8% in the higher concentration range. Furthermore, intra-day precision and inter-day precision was tested to fully validate the method. Precision ranged from 2.4% to 19.9% for low concentrations, 1.7% to 19.3% for middle concentrations and 1.6% to 14.4% for high concentrations tested during the three-day period.

3.2.3. Recovery, matrix effect and process efficiency

In Table 6, the recovery, matrix effect and process efficiency are described for all the steroids included in the method. Recovery ranged from 63.6% to 100.9% at the lower concentrations, from 45.9% to 110.6% at the middle concentrations, and from 71.5% to 116.3% at the high concentrations. Matrix effect ranged from ionization enhancement of 20.8% for 5αDIONE at the lower concentrations, to ionization suppression of 37.3% and 14.6% for epietiocholanolone at the middle and high concentrations, and ionization enhancement of 23.2% for pregnanetriol at the higher concentrations. Matrix effect therefore ranged from −50.7% to 28.1% over the concentration ranges tested, with
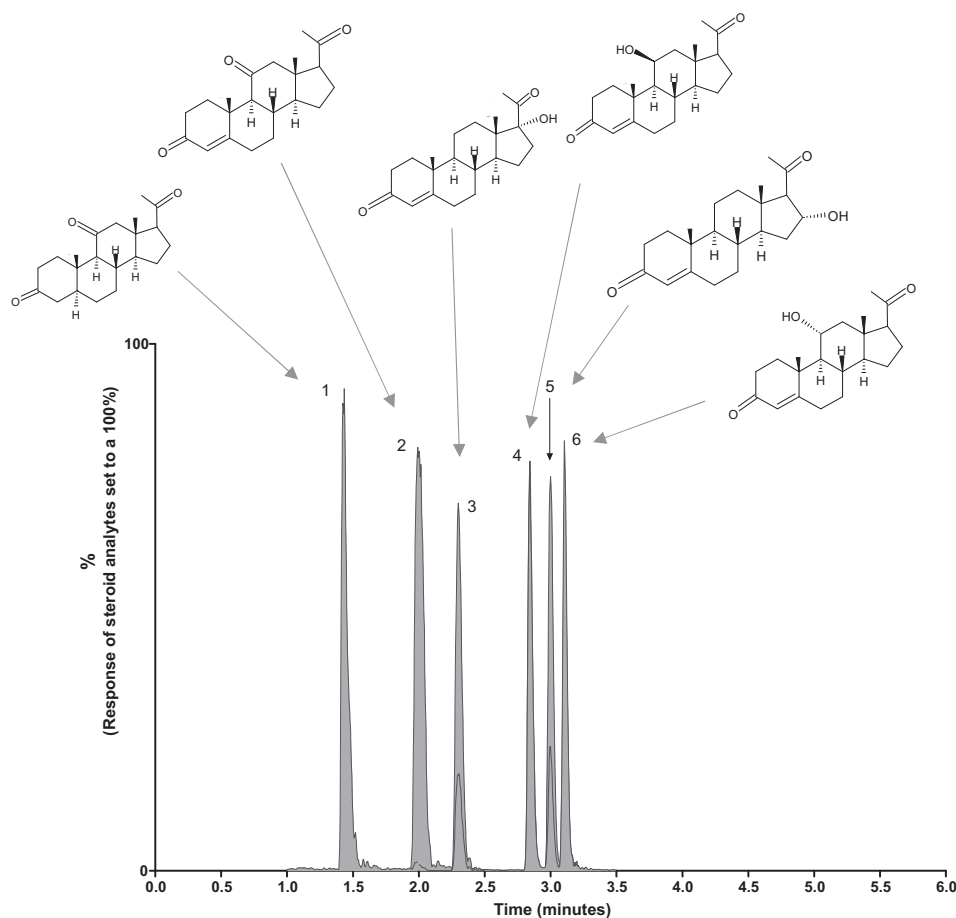
Fig. 3. UPC^2-MS/MS separation of progesterone metabolites. Reference C$_{21}$ steroid standards, 100 ng/mL, are depicted in the elution order (1) 11KDHPROG, 1.45 min; (2) 11KPROG, 2.00 min; (3) 17OHPROG, 2.32 min; (4) 11βOHPROG, 2.85 min; (5) 16OHPROG, 3.00 min and (6) 11αOHPROG, 3.11 min.

ionization suppression of all the steroids determined at 100 ng/mL only. Process efficiency, taking into account the extraction protocol and the matrix, showed values ranging from 39.2% to 109.2% at the lower concentrations, from 36.0% to 100.5% at the middle concentrations and from 87.0% to 118.7% at the higher concentrations. Supplemental Fig. 3 indicates the matrix effect causing ionization suppression, in addition to the recovery and process efficiency percentages obtained for 11OHA4, A4 and DHT at 100 ng/mL.

4. Discussion

This study describes a high-throughput UPC^2-MS/MS method for the separation and quantification of C$_{19}$ and C$_{21}$ steroids, subsequent to organic solvent extraction, without prior derivatization being required, showing good recovery together with the MS system used showing good accuracy, repeatability and reproducibility. Of note, the values obtained for accuracy and precision at 100 ng/mL for the C$_{19}$ and C11-oxy C$_{19}$ steroids were comparable to those reported also using a UPC^2-MS/MS method [4], ranging 2.4–9.5 *vs* 2.6–11.5 and 1.94–17.69 *vs* 2.2–10.2 for accuracy and precision, respectively. The sensitivity of our method, reflected in the low LOD and LOQ values of each steroid, shows that this method can be used to study steroid panels in clinical samples, enabling the detection of steroids in the nmol/L range and at physiological concentrations. Furthermore, the UPC^2-MS/MS showed superior selectivity by separating structurally closely related steroids, including stereoisomers and regioisomers. A limitation of this method, however, is the small number of deuterated reference standards used, as many of the steroids included in our method do not yet have commercially available deuterated forms. In addition, this method was

unable to chromatographically separate the C$_{19}$ 5α, 3α-reduced derivatives (AST, 11OHAST and 11KAST) from the C$_{19}$ 5β, 3α/β-reduced derivatives (epietiocholanolone, 11OH-epietiocholanolone and 11K-etiocholanolone). The quantification of steroids present in a complex matrix may often be confounded by matrix effects causing ion suppression or enhancement. In order to circumvent these effects and possible loss of steroids during the extraction process, standards used to quantify steroids present in a matrix such as plasma, should always include the same amount of deuterated internal standards as in the samples being processed, and steroid extraction should also be from a medium which mimic the matrix effect. Therefore, although matrix effects are observed in the current method, it does not significantly limit the analytical method. In addition, the level of endogenous steroids present in FBS was assessed following extraction and confirmed not to interfere with the quantification of the spiked matrix samples.

As the steroid metabolites included in this method are involved in the classical-, alternative-, backdoor- and 11OHA4-pathway of adrenal and peripheral steroid metabolism, the importance of this method is highlighted in terms of their biosynthesis, activation and inactivation by steroidogenic enzymes (Fig. 1). Cytochrome P450 17α-hydroxylase (CYP17A1) activity, for example, may be assessed by quantifying 17OHPROG and 16OHPROG and their precursor metabolite, PROG, in plasma, serum and tissue with the 3-4:1 ratio (17OHPROG: 16OHPROG) accepted as a normal ratio [20,26], with deviations reflecting CYP17A1 over or under activity characteristic of diseases and adrenal disorders in clinical conditions. CYP11B1 and CYP11B2 activity may also be assessed, together with deficient CYP21A2 activity, occurring in 21OHD and CAH, with increased levels of 17OHPROG and 21-dF determined *in vivo* [8,9], with more comprehensive profiles contributing

Table 4
Method validation data: LOD and LOQ of steroids and the calibration range in ng/mL; linearity (r^2).

Steroid metabolite	LOD (pg on column)	LOQ (pg on column)	Calibration range	r^2
A4	< 0.01 (< 0.07)	0.01 (0.07)	0.01–200	0.9991
T	< 0.01 (< 0.07)	0.01 (0.07)	0.01–200	0.9966
5αDIONE	0.2 (1.33)	1 (6.67)	0.2–1000	0.9999
DHT	1 (6.67)	1 (6.67)	1–200	0.9996
AST	10 (66.67)	20 (133.33)	10–200	0.9977
3αDIOL	0.2 (1.33)	10 (66.67)	0.2–200	0.9974
11OHA4	0.2 (1.33)	1 (6.67)	0.2–1000	0.9999
11OHT	0.1 (0.67)	0.2 (1.33)	0.1–1000	0.9998
11KA4	0.1 (0.67)	0.1 (0.67)	0.1–1000	0.9999
11KT	0.1 (0.67)	0.2 (1.33)	0.1–1000	0.9992
11KDHT	1 (6.67)	10 (66.67)	1–1000	0.9997
11OHAST	2 (13.33)	10 (66.67)	2–1000	0.9949
11KAST	0.2 (1.33)	10 (66.67)	0.2–1000	0.9993
DHEA	1 (6.67)	2 (13.33)	1–1000	0.9969
Epietiocholanolone	10 (66.67)	20 (133.33)	10–200	0.9988
11OH-epietiocholanolone	1 (6.67)	2 (13.33)	1–1000	0.9947
11K-etiocholanolone	0.2 (1.33)	10 (66.67)	0.2–1000	0.9992
Pregnanetriol	0.02 (0.13)	10 (66.67)	0.02–1000	0.9971
PROG	< 0.01 (< 0.07)	0.02 (0.13)	0.01–200	0.9990
DHPROG	1 (6.67)	2 (13.33)	1–1000	0.9987
Pdiol	2 (13.33)	10 (66.67)	2–1000	0.9963
Pdione	10 (66.67)	10 (66.67)	10–1000	0.9977
11KPROG	0.2 (1.33)	0.2 (1.33)	0.2–1000	0.9999
17OHPROG	0.1 (0.67)	0.1 (0.67)	0.1–200	0.9994
16OHPROG	0.1 (0.67)	0.1 (0.67)	0.1–1000	0.9989
11KDHPROG	0.2 (1.33)	1 (6.67)	0.2–1000	0.9995
11αOHPROG	0.2 (1.33)	1 (6.67)	0.2–1000	0.9997
11βOHPROG	0.2 (1.33)	1 (6.67)	0.2–1000	0.9995
21-dF	0.02 (0.13)	1 (6.67)	0.02–1000	0.9979
Cortisone	< 0.01 (< 0.07)	0.01 (0.07)	0.01–1000	0.9997
Cortisol	< 0.01 (< 0.07)	0.01 (0.07)	0.01–1000	0.9984

to the elimination of false positives and negative diagnosis. In addition, CYP11B1 activity is also important in the production of 11OHA4 from A4, as well as 11OHT from T. Subsequent conversion of 11OHA4 and 11OHT by 11β-hydroxysteroid dehydrogenase type 2 (11βHSD2) to 11KA4 and 11KT, respectively, yields 11KT and 11KDHT in the 11OHA4-pathway, potent androgens which, to date, are not routinely assessed in PCa and CRPC patients. 11βHSD2 is also essential in the inactivation of adrenal cortisol to cortisone, with this method able to separate and quantify cortisol and cortisone, together with 11OHPROG and 11KPROG. Both 11OHPROG and 11KPROG have been identified in urinary neonatal samples and levels shown to be age and sex specific [27], further emphasising the application of our method enabling the assessment of comprehensive *in vivo* steroid panels. In addition, while quantifying cortisol levels in disease conditions such as Cushing's syndrome, Addison's disease, PCOS and CAH, the analyses of additional steroid metabolites may further aid diagnosis and the identification of new disease markers. The backdoor pathway could also be analysed in patients, as the current method quantifies 17OHPROG, pdione (SRD5A activity), pdiol (3αHSD activity), AST (CYP17A1 activity), 3αDIOL (17βHSD activity) and DHT (3αHSD activity) (Fig. 1). 21-dF levels together with 11OHAST and 11KDHT, downstream metabolites in the C11-oxy C_{21} backdoor pathway utilizing 21-dF [15], can also be determined in patients. Clearly, this high-throughput UPC^2-MS/MS method facilitates improved diagnosis and prognosis determination in patients suffering from steroid dependent diseases. Although this study reports on the measurement of steroids present in a serum matrix, the extraction protocol and MS method has the potential to be applied in measuring steroids present in complex matrices such as urine, tissue, follicular fluid, saliva and hair.

5. Conclusions

We have developed and validated a method which separates and quantifies key steroids produced in adrenal and peripheral steroid metabolism, and this is, to our knowledge, the first method describing the separation of 17 C_{19} and 14 C_{21} steroids in one chromatographic

Table 5
Method validation data: accuracy ($n = 8$) and precision with inter-day variability ($n = 7$).

Steroid metabolite	Accuracy (%RSD)				Precision (%RSD)											
					Day 1				Day 2				Day 3			
	ng/mL				ng/mL											
	2	20	100	200	2	20	100	200	2	20	100	200	2	20	100	200
A4	3.2	2.6	4.8	3.7	4.7	5.6	1.9	5.7	7.9	2.2	2.2	8.0	13.4	14.7	8.8	4.9
T	3.9	5.2	3.0	3.9	2.4	4.1	2.8	2.6	5.9	6.5	5.5	5.5	10.0	8.7	8.6	3.7
5αDIONE	7.2	6.6	3.5	7.5	7.1	4.5	2.0	9.1	9.5	8.9	9.7	8.0	10.6	10.9	12.7	3.3
DHT	10.0	8.0	9.5	6.3	8.5	6.4	3.0	5.8	4.5	4.5	11.8	8.1	9.1	8.8	4.5	3.6
AST	< LOQ	10.0	7.8	6.6	< LOQ	9.3	11.8	2.8	< LOQ	15.6	14.1	6.8	< LOQ	8.8	4.4	6.3
3αDIOL	< LOQ	9.5	6.5	8.7	< LOQ	6.5	7.3	6.6	< LOQ	8.7	8.8	3.9	< LOQ	10.6	12.9	5.7
11OHA4	5.0	3.9	4.1	3.0	3.3	4.6	2.3	3.1	7.9	6.7	3.0	7.5	4.5	11.1	3.2	4.1
11OHT	8.7	3.1	5.1	9.0	11.8	5.4	3.0	6.0	11.2	9.2	10.7	7.0	9.7	9.5	7.9	6.1
11KA4	10.4	8.2	8.2	3.0	12.3	3.0	7.1	7.8	12.7	9.3	14.7	12.0	14.4	7.3	9.1	6.9
11KT	2.7	4.3	2.4	3.9	4.6	3.9	2.2	2.7	10.0	11.1	8.5	4.9	5.6	6.6	8.1	4.4
11KDHT	< LOQ	3.4	7.0	7.1	< LOQ	5.9	3.4	1.7	< LOQ	10.9	13.5	5.6	< LOQ	10.1	8.9	4.8
11OHAST	< LOQ	10.4	6.0	4.0	< LOQ	8.1	4.0	2.7	< LOQ	5.6	11.1	1.6	< LOQ	13.7	11.9	5.4
11KAST	< LOQ	9.5	6.0	4.5	< LOQ	8.2	4.8	2.8	< LOQ	16.5	17.7	5.7	< LOQ	11.9	9.6	3.8
DHEA	17.9	6.3	10.8	5.3	15.1	10.7	2.3	2.0	15.3	10.5	11.0	8.6	18.1	12.5	11.5	5.3
Epietiocholanolone	< LOQ	17.4	7.2	7.2	< LOQ	13.0	9.9	5.5	< LOQ	7.9	12.6	6.6	< LOQ	19.3	13.3	8.3
11OH-epietiocholanolone	8.7	8.7	8.0	4.0	8.2	5.5	4.1	1.9	12.6	1.7	4.2	3.4	19.9	3.3	2.7	5.3
11K-etiocholanolone	< LOQ	6.9	8.8	4.6	< LOQ	6.2	6.7	5.0	< LOQ	9.1	13.4	5.8	< LOQ	14.5	7.6	6.1
Pregnanetriol	< LOQ	6.4	7.6	10.8	< LOQ	6.0	8.1	14.4	< LOQ	7.3	8.0	10.3	< LOQ	15.1	6.4	7.2
PROG	1.5	3.1	1.6	2.2	4.8	4.3	3.0	4.7	7.4	3.6	3.6	7.5	11.1	17.9	8.7	3.3
DHPROG	20.0	4.8	8.3	5.8	12.4	11.5	6.3	4.1	6.9	10.0	12.4	8.9	19.4	12.8	9.7	8.9
Pdiol	< LOQ	6.6	9.7	4.4	< LOQ	7.7	6.9	4.4	< LOQ	10.4	7.8	5.1	< LOQ	18.4	9.8	4.5
Pdione	< LOQ	7.2	8.0	4.4	< LOQ	4.9	9.3	4.5	< LOQ	13.6	10.7	9.3	< LOQ	13.4	12.1	10.2

(continued on next page)

Table 5 (*continued*)

Steroid metabolite	Accuracy (%RSD)				Precision (%RSD)											
					Day 1				Day 2				Day 3			
	ng/mL				ng/mL											
	2	20	100	200	2	20	100	200	2	20	100	200	2	20	100	200
11KPROG	7.1	9.9	7.6	3.0	9.6	5.1	7.3	3.4	4.2	5.5	12.8	8.9	11.3	10.2	7.0	9.6
17OHPROG	10.2	5.9	8.3	4.4	7.7	8.0	4.4	7.4	12.8	11.4	8.5	7.9	12.5	7.0	11.8	3.7
16OHPROG	8.6	7.1	6.9	5.0	5.8	4.0	5.4	5.3	13.0	12.0	8.5	2.8	14.9	5.2	9.9	6.4
11KDHPROG	10.1	6.7	6.0	5.7	13.6	3.5	4.8	4.2	13.5	5.0	12.4	8.1	18.1	5.9	8.7	10.7
11αOHPROG	5.9	4.7	3.4	3.2	6.3	5.8	2.8	3.5	7.9	6.3	7.7	3.8	9.2	7.4	6.8	5.2
11βOHPROG	13.6	11.6	6.8	6.3	8.9	6.9	4.1	2.4	9.9	9.0	6.1	3.0	8.3	9.6	10.6	2.6
21-dF	9.5	7.1	8.7	10.9	9.7	4.5	6.3	7.9	10.0	5.0	9.1	7.0	6.4	5.4	5.9	6.6
Cortisone	11.9	8.6	7.3	11.6	12.9	6.5	6.4	13.5	6.3	7.6	12.0	10.0	6.6	8.6	7.1	10.6
Cortisol	6.3	6.1	6.9	3.7	16.3	7.7	8.4	7.5	5.6	7.8	8.8	5.9	7.7	6.4	8.1	4.4

step utilizing UPC²-MS/MS. The current method has the analytical power to measure multiple steroids in a run time of under 6 min, thereby effectively condensing sample turnover rate, applicable in both clinical and research fields. Ultimately, this method is able to determine steroid profiles *in vivo* –relating androgen excess or deficiency observed in patients to abnormal enzyme activity. Optimized and validated, our method allows for the accurate quantification of a comprehensive panel of steroids and as such has diverse applications: profiling C11-oxy C_{19} and C11-oxy C_{21} steroids in patients may lead to establishing new biomarkers improving the diagnosis of adrenal disorders with regards to androgen excess or deficiency and while the method may be utilized in prognostic scoring, it can also be applied in determining treatment outcomes in patients. The UPC²-MS/MS analytical method clearly has applications in the field of steroid research as well as in the diagnosis of clinical conditions, dependent on effective and efficient steroid analyses and quantification in which multiple steroid profiling produce informative steroid panels.

Table 6
UPC²-MS/MS method validation for the extraction of steroid from FBS. Recovery (*n* = 3); matrix effect (*n* = 3) and process efficiency (*n* = 3).

Steroid metabolite	Recovery (%)				Matrix effect (%)				Process efficiency (%)			
	ng/mL				ng/mL				ng/mL			
	2	20	100	200	2	20	100	200	2	20	100	200
A4	63.6	47.8	69.0	99.3	−10.7	−17.6	−26.3	2.6	56.8	39.4	50.8	101.8
T	87.1	61.3	66.4	102.2	−38.8	−11.4	−39.8	−1.0	53.3	54.3	40.0	101.1
5αDIONE	90.4	69.1	74.4	101.4	20.8	−4.7	−22.2	10.1	109.2	65.9	57.9	111.6
DHT	81.3	89.8	102.0	105.7	−30.3	−28.8	−46.9	−4.6	56.7	63.9	54.1	100.8
AST	< LOQ	71.3	103.3	98.6	< LOQ	−17.8	−23.4	−0.3	< LOQ	58.6	79.1	98.3
3αDIOL	< LOQ	77.1	99.3	82.8	< LOQ	28.1	−42.3	11.5	< LOQ	98.8	57.3	92.4
11OHA4	91.6	63.9	69.1	108.8	−36.1	−4.0	−42.2	−4.7	58.5	61.4	40.0	103.7
11OHT	74.3	68.8	67.0	80.7	−45.7	−31.0	−38.2	22.2	40.4	47.5	41.4	98.6
11KA4	86.4	54.7	60.7	107.7	−43.0	−24.4	−26.5	6.4	44.6	41.4	44.6	114.5
11KT	73.0	48.7	61.7	99.8	−46.3	−7.9	−41.6	5.5	39.2	44.9	36.0	105.3
11KDHT	< LOQ	87.4	105.2	99.5	< LOQ	15.1	−46.7	3.0	< LOQ	100.5	56.1	102.4
11OHAST	< LOQ	65.2	84.0	103.1	< LOQ	1.9	−46.0	4.8	< LOQ	66.5	45.4	108.0
11KAST	< LOQ	78.4	110.6	107.2	< LOQ	24.8	−33.8	4.1	< LOQ	97.6	73.3	111.6
DHEA	94.1	97.5	84.5	100.4	5.6	1.5	−49.7	−0.3	99.4	99.0	42.5	100.1
Epietiocholanolone	< LOQ	85.1	84.7	116.3	< LOQ	−37.3	−42.3	−14.6	< LOQ	53.4	48.9	99.3
11OH-epietiocholanolone	100.9	83.3	80.7	101.7	−2.6	4.3	−42.7	7.0	98.3	86.9	46.3	108.8
11K-etiocholanolone	< LOQ	83.4	94.4	108.0	< LOQ	−21.8	−45.2	9.9	< LOQ	65.2	51.7	118.7
Pregnanetriol	< LOQ	85.3	98.9	79.0	< LOQ	5.7	−27.7	23.2	< LOQ	90.1	71.5	97.3
PROG	81.5	64.6	62.4	96.8	−27.6	−31.7	−34.9	8.8	59.1	44.1	40.7	105.3
DHPROG	95.8	106.3	81.7	87.1	3.6	−33.4	−47.9	3.4	99.2	70.9	42.5	90.1
Pdiol	< LOQ	76.9	75.7	91.7	< LOQ	−26.2	−33.5	7.9	< LOQ	56.7	50.3	99.0
Pdione	< LOQ	90.4	62.0	101.7	< LOQ	−26.2	−25.1	2.4	< LOQ	56.7	46.5	104.1
11KPROG	87.5	58.3	62.8	104.8	−36.6	−30.4	−21.4	3.5	55.5	40.6	49.3	108.5
17OHPROG	73.8	67.2	68.0	99.0	−25.1	−11.1	−33.6	8.0	55.2	59.7	45.1	107.0
16OHPROG	72.4	55.0	91.1	98.4	−43.5	−24.4	−48.0	7.0	40.9	41.6	47.3	105.3
11KDHPROG	98.2	63.6	78.7	109.0	−45.3	−33.2	−36.7	−6.6	53.7	42.5	49.8	101.9
11αOHPROG	70.2	45.9	66.6	102.7	−41.1	−10.5	−44.9	6.4	41.1	41.1	36.7	109.3
11βOHPROG	98.9	62.5	83.7	99.8	−48.8	1.5	−50.7	4.1	50.6	63.5	41.3	103.9
21-dF	93.3	67.9	82.8	87.7	−49.7	−15.4	−45.9	15.4	47.0	57.4	44.8	101.2
Cortisone	65.0	51.1	71.4	71.5	−27.8	4.0	−48.8	21.7	47.0	53.1	41.5	87.0
Cortisol	76.6	72.5	81.1	92.1	−32.2	−22.8	−34.1	12.0	51.9	56.0	53.5	103.1

Conflict of interest

The authors declare that there is no conflict of interest.

Acknowledgements

Appendix A. Supplementary data

Supplementary data to this article can be found online at https://doi.org/10.1016/j.jchromb.2018.02.023.

References

[1] M.I. Churchwell, N.C. Twaddle, L.R. Meeker, D.R. Doerge, Improving LC–MS sensitivity through increases in chromatographic performance: comparisons of UPLC–ES/MS/MS to HPLC–ES/MS/MS, J. Chromatogr. B 825 (2005) 134–143, http://dx.doi.org/10.1016/j.jchromb.2005.05.037.

[2] F.Z. Stanczyk, N.J. Clarke, Advantages and challenges of mass spectrometry assays for steroid hormones, J. Steroid Biochem. Mol. Biol. 121 (2010) 491–495, http://dx.doi.org/10.1016/j.jsbmb.2010.05.001.

[3] L. Couchman, R.P. Vincent, L. Ghataore, C.F. Moniz, N.F. Taylor, Challenges and benefits of endogenous steroid analysis by LC-MS/MS, Bioanalysis 3 (2011) 2549–2572, http://dx.doi.org/10.4155/bio.11.254.

[4] J.L. Quanson, M.A. Stander, E. Pretorius, C. Jenkinson, A.E. Taylor, K.-H. Storbeck, High-throughput analysis of 19 endogenous androgenic steroids by ultra-performance convergence chromatography tandem mass spectrometry, J. Chromatogr. B 1031 (2016) 131–138, http://dx.doi.org/10.1016/j.jchromb.2016.07.024.

[5] V. Luu-The, A. Bélanger, F. Labrie, Androgen biosynthetic pathways in the human prostate, Best Pract. Res. Clin. Endocrinol. Metab. 22 (2008) 207–221, http://dx.doi.org/10.1016/j.beem.2008.01.008.

[6] R.J. Auchus, The backdoor pathway to dihydrotestosterone, Trends Endocrinol. Metab. 15 (2004) 432–438, http://dx.doi.org/10.1016/j.tem.2004.09.004.

[7] C. Kamrath, Z. Hochberg, M.F. Hartmann, T. Remer, S.A. Wudy, Increased activation of the alternative "backdoor" pathway in patients with 21-hydroxylase deficiency: evidence from urinary steroid hormone analysis, J. Clin. Endocrinol. Metab. 97 (2012) E367–E375, http://dx.doi.org/10.1210/jc.2011-1997.

[8] A. Milewicz, P. Vecsei, S. Korth-Schütz, D. Haack, A. Rösler, K. Lichtwald, S. Lewicka, G.V. Mittelstaedt, Development of plasma 21-deoxycortisol radioimmunoassay and application to the diagnosis of patients with 21-hydroxylase deficiency, J. Steroid Biochem. 21 (1984) 185–191, http://dx.doi.org/10.1016/0022-4731(84)90382-0.

[9] K. Nahoul, J. Adeline, J.P. Bercovici, Radioimmunoassay of plasma 21-deoxycortisol, J. Steroid Biochem. 33 (1989) 1167–1172, http://dx.doi.org/10.1016/0022-4731(89)90426-3.

[10] K.-H. Storbeck, L.M. Bloem, D. Africander, L. Schloms, P. Swart, A.C. Swart, 11β-Hydroxydihydrotestosterone and 11-ketodihydrotestosterone, novel C19 steroids with androgenic activity: a putative role in castration resistant prostate cancer? Mol. Cell. Endocrinol. 377 (2013) 135–146, http://dx.doi.org/10.1016/j.mce.2013.07.006.

[11] A.C. Swart, L. Schloms, K.-H. Storbeck, L.M. Bloem, T. du Toit, J.L. Quanson, et al., 11β-Hydroxyandrostenedione, the product of androstenedione metabolism in the adrenal, is metabolized in LNCaP cells by 5α-reductase yielding 11β-hydroxy-5α-

androstanedione, J. Steroid Biochem. Mol. Biol. 138 (2013) 132–142, http://dx.doi.org/10.1016/j.jsbmb.2013.04.010.

[12] L.M. Bloem, K.-H. Storbeck, L. Schloms, A.C. Swart, 11β-Hydroxyandrostenedione returns to the steroid arena: biosynthesis, metabolism and function, Molecules 18 (2013) 13228–13244, http://dx.doi.org/10.3390/molecules181113228.

[13] A.C. Swart, K.-H. Storbeck, 11β-Hydroxyandrostenedione: downstream metabolism by 11βHSD, 17βHSD and SRD5A produces novel substrates in familiar pathways, Mol. Cell. Endocrinol. 408 (2015) 114–123, http://dx.doi.org/10.1016/j.mce.2014.12.009.

[14] J. Rege, Y. Nakamura, F. Satoh, R. Morimoto, M.R. Kennedy, L.C. Layman, et al., Liquid chromatography – tandem mass spectrometry analysis of human adrenal vein 19-carbon steroids before and after ACTH stimulation, J. Clin. Endocrinol. Metab. 98 (2013) 1182–1188, http://dx.doi.org/10.1210/jc.2012-2912.

[15] L. Barnard, R. Gent, D. Van Rooyen, A.C. Swart, Adrenal C11-oxy C_{21} steroids contribute to the C11-oxy C_{19} steroid pool via the backdoor pathway in the biosynthesis and metabolism of 21-deoxycortisol and 21-deoxycortisone, J. Steroid Biochem. Mol. Biol. (2017), http://dx.doi.org/10.1016/j.jsbmb.2017.07.034.

[16] D. Van Rooyen, R. Gent, L. Barnard, A.C. Swart, The *in vitro* metabolism of 11β-hydroxyprogesterone and 11-ketoprogesterone to 11-ketodihydrotestosterone in the backdoor pathway, J. Steroid Biochem. Mol. Biol. (2017) In press https://doi.org/10.1016/j.jsbmb.2017.12.014.

[17] M.W. O'Reilly, P. Kempegowda, C. Jenkinson, A.E. Taylor, J.L. Quanson, K.-H. Storbeck, et al., 11-Oxygenated C19 steroids are the predominant androgens in polycystic ovary syndrome, J. Clin. Endocrinol. Metab. 102 (2017) 840–848, http://dx.doi.org/10.1210/jc.2016-3285.

[18] A.F. Turcu, A.T. Nanba, R. Chomic, S.K. Upadhyay, T.J. Giordano, J.J. Shield, et al., Adrenal-derived 11-oxygenated 19-carbon steroids are the dominant androgens in classic 21-hydroxylase deficiency, Eur. J. Endocrinol. 174 (2016) 601–609, http://dx.doi.org/10.1530/EJE-15-1181.

[19] L. Schloms, K.-H. Storbeck, P. Swart, W.C.A. Gelderblom, A.C. Swart, The influence of *Aspalathus linearis* (Rooibos) and dihydrochalcones on adrenal steroidogenesis: quantification of steroid intermediated and end products in H295R cells, J. Steroid Biochem. Mol. Biol. 128 (2012) 128–138, http://dx.doi.org/10.1016/j.jsbmb.2011.11.003.

[20] A.F. Turcu, J. Rege, R. Chomic, J. Liu, H.K. Nishimoto, T. Else, et al., Profiles of 21-carbon steroids in 21-hydroxylase deficiency, J. Clin. Endocrinol. Metab. 100 (2015) 2283–2290, http://dx.doi.org/10.1210/jc.2015-1023.

[21] A.F. Turcu, A. Mallappa, M.S. Elman, N.A. Avila, J. Marko, H. Rao, et al., 11-Oxygenated androgens are biomarkers of adrenal volume and testicular adrenal rest tumors in 21-hydroxylase deficiency, J. Clin. Endocrinol. Metab. 102 (2017) 2701–2710, http://dx.doi.org/10.1210/jc.2016-3989.

[22] T. Du Toit, L.M. Bloem, J.L. Quanson, R. Ehlers, A.M. Serafin, A.C. Swart, Profiling adrenal 11β-hydroxyandrostenedione metabolites in prostate cancer cells, tissue and plasma: UPC^2-MS/MS quantification of 11β-hydroxytestosterone, 11keto-testosterone and 11keto-dihydrotestosterone, J. Steroid Biochem. Mol. Biol. 166 (2017) 54–67, http://dx.doi.org/10.1016/j.jsbmb.2016.06.009.

[23] T. Du Toit, A.C. Swart, Inefficient UGT-conjugation of adrenal 11β-hydroxyandrostenedione metabolites highlights C11-oxy C_{19} steroids as the predominant androgens in prostate cancer, Mol. Cell. Endocrinol. 461 (2018) 265–276, http://dx.doi.org/10.1016/j.mce.2017.09.026.

[24] P.J. Taylor, Matrix effects: the Achilles heel of quantitative high-performance liquid chromatography-electrospray-tandem mass spectrometry, Clin. Biochem. 38 (2005) 328–334, http://dx.doi.org/10.1016/j.clinbiochem.2004.11.007.

[25] F.T. Peters, O.H. Drummer, F. Musshoff, Validation of new methods, Forensic Sci. Int. 165 (2007) 216–224, http://dx.doi.org/10.1016/j.forsciint.2006.05.021.

[26] P. Swart, R.W. Estabrook, A.C. Swart, J.I. Mason, M.R. Waterman, Progesterone 16α-hydroxylase activity is catalyzed by human cytochrome P450 17α-hydroxylase, J. Clin. Endocrinol. Metab. 771 (1993) 98–102, http://dx.doi.org/10.1210/jcem.77.1.8325965.

[27] N.A. Dhayat, A.C. Frey, B.M. Frey, C.H. d'Uscio, B. Vogt, V. Rousson, et al., Estimation of reference curves for the urinary steroid metabolome in the first year of life in healthy children: tracing the complexity of human postnatal steroidogenesis, J. Steroid Biochem. Mol. Biol. 154 (2015) 226–236, http://dx.doi.org/10.1016/j.jsbmb.2015.07.024.

6.2 Summary

The novel method described in the manuscript enabled the separation and quantification of 31 steroid metabolites biosynthesised in adrenal and peripheral steroidogenic pathways using a single chromatographic step, permitting separation without prior derivatization. This method has since proved suitable for the quantification of steroid metabolites *in vivo*. Utilizing this method C11-oxy C_{19} and C11-oxy C_{21} steroid levels were determined in healthy neonates in the first 2 days of life, with 11OHA4 and 11KPROG levels detected in plasma of girls and boys (manuscript in preparation), thus emphasizing the value of comprehensive LC-MS/MS analysis in second tier screening in neonates, which may aid in the early diagnosis of steroid-related diseases. This method has also been used to assess androgen excess in a cohort of 35 PCOS patients and 19 healthy controls (manuscript in preparation) –analyses of steroid panels in these patients allowed insight into the activity of adrenal steroidogenic enzymes, together with identifying and quantifying C11-oxy C_{19} and C11-oxy C_{21} steroids which have, to date, not been assessed clinically in PCOS patients. Furthermore, this method was also used to investigate steroid panels in follicular fluid of female patients (unpublished data). Steroid profiles in follicular fluid are currently not widely reported since the research has been limited by analytical methods lacking the sensitivity to measure multiple steroids in small volumes of fluid, hurdles which UPC^2-MS/MS clearly overcomes. Finally, this method was also employed to determine levels of the C11-oxy C_{21} steroids in plasma and tissue of BPH and PCa patients (unpublished data) –further highlighting metabolites not currently considered in the clinical setting.

Taken together, utilizing UPC^2-MS/MS, *in vivo* steroids can be accurately quantified, novel metabolites can be identified and altered steroid metabolic pathways can be linked to defective enzymatic activities.

Furthermore, effective diagnosis of clinical conditions marked by androgen excess can be facilitated by steroid profiling, potentially identifying new steroid markers, using state-of-the-art UPC^2-MS/MS.

Chapter 7

General discussion and conclusion

It is well documented that adrenal C_{19} steroids contribute to the biosynthesis of intratumoral active androgens (Stanbrough et al. 2006; Luu-The et al. 2008; Montgomery et al. 2008), and while 11OHA4 has been shown to be a major contributor to the peripheral biosynthesis of active androgens in the prostate, the monitoring of 11OHA4 and its downstream metabolites has not, to date, been considered in the diagnosis or treatment of BPH, PCa and CRPC, in the clinical setting. The objective of this PhD study was therefore to evaluate the levels of the C11-oxy C_{19} steroids in plasma and in prostate tissue and to study their downstream metabolism, including inactivation and conjugation, in prostate cells, to further ascertain the relevance of these androgens in prostate diseases.

Pre-receptor regulation of C11-oxy C_{19} steroid action is mediated by 11βHSD2, 17βHSDs and SRD5As. Endogenous 11βHSD2 activity was shown in all our cell model assays, while 17βHSD activities were preferred over the SRD5A catalysed reactions. In addition, the 11βHSD2 catalysed biosynthesis of 11KA4 from 11OHA4 was preferred over the SRD5A conversion of 11OHA4 to 11OH-5αDIONE. This highlights the preferred conversion of 11OHA4 to 11KA4, with reductive 17βHSDs subsequently producing 11KT (Fig. 2.4), which was evident in the cell models assayed.

Post-receptor regulation of C11-oxy C_{19} steroid action is mediated by 3αHSD, RL-HSD, UGT2Bs and SULTs. All our cell models displayed endogenous 3αHSD activity and produced inactive 3α-reduced metabolites, and analyses provided steroid profiles including the 3β-reduced C11-oxy metabolites, which were determined in PNT2 cells. 3αHSD activity was most prominent in C4-2B cells when 11KDHT was assayed, followed by VCaP, LNCaP and lastly BPH-1 cells. In contrast, RL-HSD activity was negligible towards

173

11K-3αDIOL in all the cell models assayed, while RL-HSD readily reactivated DHT in C4-2B and VCaP cells, suggesting the C11 keto moiety hampers RL-HSD activity. UGT2B activity towards C_{19} and C11-oxy C_{19} steroids was the highest in LNCaP cells, and while no C11-oxy C_{19} steroid was glucuronidated in C4-2B and VCaP cells, UGT2B activity was also not detected in PNT2 and BPH-1 cells. Interestingly, the C_{19} steroids were readily glucuronidated in LNCaP and VCaP cells, while only DHT was glucuronidated in C4-2B cells. These data highlight that the presence of the C11-oxy moieties interferes with the glucuronidation of the C3 and C17 hydroxyl group of the C11-oxy C_{19} steroids, as well as impeding the inactivation and reactivation of the 5α-reduced C11-oxy C_{19} steroids compared to the C_{19} steroids, as demonstrated in BPH-1 cells. In LNCaP, VCaP and C4-2B cells, however, the inactivation of 11KDHT was more efficient than DHT, while its reactivation was negligible. The C11-oxy C_{19} steroids were shown not to be sulfated in LNCaP cells, and total conjugated levels of 11KT, 11OHT, 11KDHT and 11OHDHT were significantly less compared to T and DHT. Interestingly, A4 was shown to be sulfated in LNCaP cells, and as this steroid is not androgenic, sulfation of A4 may be a mechanism of pre-receptor steroid regulation, thereby hindering the subsequent production of T and DHT. Conversely, 11OHA4 was not sulfated and instead was metabolised to downstream metabolites in these cells. Clearly, *in vitro* steroid action is regulated by the pre-receptor androgen activation and post-receptor inactivation of androgens, which is dependent on the expression of steroidogenic enzymes, which in turn is specific to cell types.

In the present study, it was shown that 11OHA4, 11OHT, 11KA4 and 11KT remained within the top tier of the 11OHA4-pathway in all the cell models when assayed. This shows the necessity for the expression of SRD5As, which would metabolise the top tier C11-oxy steroids, ultimately leading to the production of middle tier metabolites and, in particular, 11KDHT (Fig. 2.4). Since both SRD5A1 and SRD5A2 catalyse the production of 5α-reduced C11 metabolites (Storbeck et al. 2013; Swart et al. 2013), and are

174

expressed in prostate tissue (Russell and Wilson 1994; Uemura et al. 2008; Chang et al. 2011), this suggests that the 11OHA4-pathway would be active *in vivo*. Moreover, even though SRD5A activity is required to produce 11KDHT, which is equipotent to DHT, the top tier steroid that was preferentially produced in all our cell models, 11KT, is equipotent to T at 1 nM, and equipotent to DHT and 11KDHT at 10 nM. 11KT binds and activates the AR and induces the expression of AR-mediated genes (Pretorius et al. 2016), suggesting even with minimal SRD5A activity, the 11OHA4-pathway still contributes an active steroid to the androgen pool. While this study demonstrated that 11KT is readily produced *in vitro*, this study also showed that 11KT is not readily glucuronidated in PCa cells, with unconjugated levels determined in plasma and tissue further contributing to the potency of this steroid.

Our *in vivo* data show low circulatory T levels and negligible DHT levels under castrated conditions (both physical and chemical), while substantial 11OHA4, 11KT and 11KDHT levels were detected in PCa patients, suggesting an increased adrenal output of 11OHA4, together with a greater metabolic shunt in the 11OHA4-pathway in these patients. Furthermore, C11-oxy glucuronide levels were low in plasma of PCa patients, clearly showing impeded glucuronidation contributing to unconjugated steroid levels in circulation. Quantification of C11-oxy sulfates in plasma showed increased 11KDHT-S levels in the healthy subject while in the PCa patient, 11KDHT-S levels were low, and 11KDHT was also not sulfated in the analysis of the female plasma, suggesting impeded sulfation of this C11-keto steroid. However, the limited sample number restricts conclusive analyses. Furthermore, in the analysis of plasma from PCa patients, high circulatory levels of the downstream inactive metabolite, 11OHAST, was detected. This highlights that the steroid shunt in the 11OHA4-pathway is increased in PCa, and while the same shunt in the production of 11OHAST and 11KAST was shown in BPH tissue, as well as in CRPC tissue, high levels of 11OHA4, 11KT, 11OHT and 11KDHT were, however, detected in PCa tissue.

As this study focused on the C11-oxy C_{19} steroids with regards to PCa, it should be noted that the C11-oxy steroids have also been reported to be important in 21OHD and PCOS (Turcu et al. 2016; O'Reilly et al. 2017), while the potential role of the C11-oxy C_{21} steroids in these adrenal-linked endocrine diseases has not been characterized. In this regard the UPC^2-MS/MS analytical method described in this thesis, which quantifies both C11-oxy C_{19} and C11-oxy C_{21} steroids, may have application in shedding light on the levels of these steroids in patients, while also modelling augmented metabolic pathways. It is possible that abnormally high levels of 17OHPROG and 21-dF identified in patients may be identified together with downstream metabolites, linking the backdoor pathway with defective CYP21A2 activity. If, however, high 11OHPROG and 11KPROG levels are detected, adrenal PROG will be identified as a precursor steroid feeding into the backdoor pathway and as such, the activity of CYP11B1, CYP11B2 and 11βHSD2 will be highlighted. In this regard, comprehensive steroid profiles would enable analyses of metabolic pathways and subsequently patient specific clinical aspects, as our analyses clearly shows considerable variations in individual steroid levels detected in tissue and in plasma in PCa patients. Furthermore, our UPC^2-MS/MS method has applications in aiding diagnosis and prognostic scoring in the clinical setting providing critical information on C11-oxy C_{19} and C_{21} steroids in adrenal-linked endocrine diseases. Moreover, the role of C11-oxy C_{19} and C_{21} steroids is as of yet undetermined in diseases and disorders other than 21OHD, PCOS and PCa, with the utilization of the UPC^2-MS/MS potentially providing informative steroid panels in currently undefined physiological events, such as in adrenarche, premature- and delayed adrenarche, menopause, CAH and DSD.

The 'rediscovery' of adrenal 11OHA4 since 2012 and recent reports showing that the adrenals produce high levels of 11OHA4, that it is biosynthesised from A4 by CYP11B1 and B2 catalysed reactions, and that 11OHA4 and its metabolites are metabolised by 11βHSD2, 17βHSDs and SRD5As, producing 11KT and

11KDHT, which are AR agonists, have certainly placed this adrenal steroid under the spotlight and will for many years to come. The present investigation contributes to these findings and describes the metabolism of 11OHA4 and its metabolites in normal, BPH and PCa cell models. This PhD study shows for the first time the presence of 11OHA4 and its downstream metabolites in plasma of PCa patients and in BPH, PCa and CRPC tissue. The glucuronidation of the C11-oxy C_{19} steroid metabolites *in vitro*, and circulatory glucuronide and sulfate C11-oxy C_{19} steroid levels have been identified for the first time. Our analyses provide a comprehensive comparison between the metabolism of the C11-oxy C_{19} steroids and the C_{19} steroids by steroidogenic enzymes –comparing their activation, inactivation, reactivation, glucuronidation and sulfation. Our *in vivo* evidence provides a comparison between the C11-oxy C_{19} and C_{19} steroid levels in plasma and tissue, while also comparing their glucuronide and sulfate levels. In addition, this current study includes the development and validation of three UPC^2-MS/MS methods for the detection and quantification of C_{19} and C_{21} steroid metabolites, which include the C11-oxy C_{19} and C11-oxy C_{21} steroids.

Taken together, this study has shown the presence of the C11-oxy C_{19} steroids in plasma, in the castrated (physical and chemical) PCa scenario, as well as in plasma of healthy subjects, in addition to determining C11-oxy C_{19} steroid conjugates in circulation. Our analyses have also identified C11-oxy C_{19} steroids in tissue, in the castrated CRPC scenario, in PCa undergoing different treatment regimes, as well as in BPH. Furthermore, this study has established the metabolism of the C11-oxy C_{19} steroids in normal and BPH cell models, as well as in PCa cell models, with these representing different stages of PCa progression and CRPC. Clearly, the data in this thesis indicate that the C11-oxy C_{19} steroids are involved in PCa, with adrenal 11OHA4 and its downstream metabolites, 11KT and 11KDHT, now firmly established in the steroid arena.

177

Five key unanswered questions remain:

1. How does the presence of the C11-hydroxy or C11-keto moiety hamper the binding of the steroid substrate to the UGT protein? In this regard, structure modelling and structure/function analyses would allow the examination of substrate binding in the active pocket with the C11 moiety potentially facilitating/hampering substrate/enzyme interaction;

2. Which UGT isoform(s) are able to conjugate the C11-oxy C_{19} steroids? In this regard, intraprostatic and hepatic conjugation could contribute to circulatory glucuronide levels, and organs primarily involved would need to be clarified;

3. What are the quantitative contributions of adrenal 11OHA4 and its metabolites *in vivo*, in circulation in normal, BPH, PCa (castrated and uncastrated) and CRPC patients?;

4. Would profiling C11-oxy C_{19} steroids in PCa patients aid clinicians in the diagnosis and prognostic scoring of the disease, together with determining treatment outcomes?; would C11-oxy C_{21} steroids also need to be considered?;

5. Are there viable targeted treatment options which can be employed to limit the C11-oxy C_{19} steroids in PCa, without adverse effects on normal adrenal steroidogenesis?

Future recommendations

Utilizing UPC^2-MS/MS to profile C11-oxy steroids in adrenal-linked endocrine diseases may identify customized biomarkers, while also modelling steroid metabolic pathways. In this regard, analysis of large cohorts will aid in identifying the role of these C11-oxy steroids in adrenal-related diseases and in PCa. It should be noted that although this study has certainly highlighted the importance of the C11-oxy C_{19}

steroids and the *in vitro* studies conducted were comprehensive, with the *in vivo* data highlighting similar findings, corroborating *in vitro* data, these studies were, however, limited and restricted to small sample numbers. Furthermore, C11-oxy C_{19} steroid glucuronide levels have not yet been established in tissue, while *in vivo* evidence of C11-oxy C_{19} steroid sulfate levels are also lacking. It is worth mentioning that the presence of CYP11B1 and B2 expression in peripheral tissue other than the adrenals, such as the prostate, also require further investigation. As A4 and T are readily produced in peripheral tissue, only the presence of CYP11B1 and B2 will catalyse the biosynthesis of 11OHA4 and 11OHT from A4 and T, respectively. Combined expression of CYP11B1, CYP11B2, 11βHSD2, 17βHSD and SRD5A in peripheral tissue will most certainly contribute to the production of C11-oxy C_{19} steroids, while C11-oxy C_{21} steroids will also be produced from PROG and 17OHPROG precursor steroids, thereby initiating the backdoor pathway. UPC^2-MS/MS can potentially profile all of the previously mentioned metabolic pathways, while intratumoral steroid shunting due to treatment regimens such as enzyme inhibitors, could also be analysed and elucidated. Furthermore, while we show here that the C11-oxy C_{19} steroids are not efficiently glucuronidated, the regiospecific binding of the C11-oxy C_{19} steroids to UGT enzymes or inability to bind, together with compartmentalization and expression levels of the UGT2B isoforms within prostate cells, are still unclear.

This thesis has discussed the C11-oxy C_{19} steroids in the context of disease in PCa –the question arises as to the contribution of these steroids to normal physiological development. Normal circulatory reference ranges throughout the lifespan of males and females are lacking, and while the current study identified circulatory C11-oxy C_{19} steroids in healthy subjects, in males and females, the sample number was limited. Furthermore, our unpublished data has shown the presence of 11OHA4 and 11KPROG in neonates following birth, and while these steroids could also potentially be maternally derived or from

placental origin, the findings suggest these steroids may be involved in embryonic development. Another question arises, as to the contribution of these steroids to puberty. Indeed, this topic has been discussed by Turcu and Auchus (2017), who suggested that these steroids may contribute to adrenarche, a precondition to puberty. Clearly, these C11-oxy C_{19} steroids may be involved in normal development, in which adrenal steroids contribute to steroidogenesis in target tissue as secondary pathways, with 11OHA4 not being an inactive metabolite of A4, as originally speculated (Goldzieher et al. 1978; Bélanger et al. 1993), but rather presenting a new perspective on adrenal precursor steroids and their downstream metabolism.

References

Akinola LA, Poutanen M, Vihko R. Cloning of rat 17β-hydroxysteroid dehydrogenase type 2 and characterization of tissue distribution and catalytic activity of rat type 1 and type 2 enzymes. Endocrinology. (1996) 137(5):1572–1579. doi:10.1210/endo.137.5.8612487.

Albiston AL, Obeyesekere VR, Smith RE, Krozowski ZS. Cloning and tissue distribution of the human 11β-hydroxysteroid dehydrogenase type 2 enzyme. Mol Cell Endocrinol. (1994) 105:R11-17.

Anagnostis P, Athyros VG, Tziomalos K, Karagiannis A, Mikhailidis DP. The pathogenetic role of cortisol in the metabolic syndrome: a hypothesis. J Clin Endocrinol Metab. (2009) 94(8):2692–2701. doi: 10.1210/jc.2009-0370.

Andriole G, Bruchovsky N, Chung LWK, Matsumoto AM, Rittmaster R, Roehrborn C, et al. Dihydrotestosterone and the prostste: the scientific rational for 5α-reductase inhibitors in the treatment of benign prostatic hyperplasia. J Urol. (2004) 172:1399-1403. doi: 10.1097/01.ju.0000139539.94828.29.

Arakawa H, Nakanishi T, Yanagihara C, Nishimoto T, Wakayama T, Mizokami A, et al. Enhanced expression of organic anion transporting polypeptides (OATPs) in androgen receptor-positive prostate cancer cells: Possible role of OATP1A2 in adaptive cell growth under androgen-depleted conditions. Biochem Pharmacol. (2012) 84:1070–1077. doi.org/10.1016/j.bcp.2012.07.026.

Arnold JT, Gray NE, Jacobowitz K, Viswanathan L, Cheung PW, McFann KK, et al. Human prostate stromal cells stimulate increased PSA production in DHEA-treated prostate cancer epithelial cells. J Steroid Biochem Mol Biol. (2008) 111:240–246. doi: 10.1016/j.jsbmb.2008.06.008.

Attard G, Reid AHM, A'Hern R, Parker C, Oommen NB, Folkerd E, et al. Selective inhibition of CYP17 with abiraterone acetate is highly active in the treatment of castration-resistant prostate cancer. J Clin Oncol. (2009) 27:3742–3748. doi: 10.1200/JCO.2008.20.0642.

Auchus RJ, Miller WL. Defects in androgen biosynthesis causing 46,XY disorders of sexual development. Semin Reprod Med. (2012) 30:417–426. doi:10.1055/s-0032-1324726.

Auchus RJ, Rainey WE. Adrenarche - physiology, biochemistry and human disease. Clin Endocrinol. (2004) 60:288–296. doi: 10.1046/j.1365-2265.2003.01858.x.

Auchus RJ. Non-traditional metabolic pathways of adrenal steroids. Rev Endocr Metab Disord. (2009) 10:27-32. doi: 10.1007/s11154-008-9095-z.

Auchus RJ. The backdoor pathway to dihydrotestosterone. Trends Endocrinol Metab. (2004) 15:432e438. doi:10.1016/j.tem.2004.09.004.

Auchus RJ. The classic and nonclassic congenital adrenal hyperplasias. Endocr Pract. (2015) 21:383–389. doi: 10.4158/EP14474.RA.

Azziz R, Black V, Hines GA, Fox LM, Boots LR. Adrenal androgen excess in the polycystic ovary syndrome: Sensitivity and responsivity of the hypothalamic-pituitary-adrenal axis. J Clin Endocrinol Metab. (1998) 83(7):2317–2323.

Azzouni F, Godoy A, Li Y, Mohler J. The 5 alpha-reductase isozyme family: A review of basic biology and their role in human diseases. Advances Urol. (2012), 1–18. doi:10.1155/2012/530121.

Barahona E, Banuelos J, Solis J, Bermudez JA. Preliminary characterization of a new androgen-binding protein in human seminal plasma. Arch Androl. (1980) 4:235 doi: 10.3109/01485018008986969.

Barnard L, Gent R, Van Rooyen D, Swart AC. Adrenal C11-oxy C_{21} steroids contribute to the C11-oxy C_{19} steroid pool via the backdoor pathway in the biosynthesis and metabolism of 21-deoxycortisol and 21-deoxycortisone. J Steroid Biochem Mol Biol. (2017) 174:86-95. https://doi.org/10.1016/j.jsbmb.2017.07.034.

Bauman DR, Steckelbroeck S, Peehl DM, Penning TM. Transcript profiling of the androgen signal in normal prostate, benign prostatic hyperplasia, and prostate cancer. Endocrinology. (2006) 147(12):5806-5816. doi: 10.1210/en.2006-0627.

Beaulieu M, Lévesque E, Hum DW, Bélanger A. Isolation and characterization of a noval cDNA encoding a human UDP-glucuronosyltransferase active on C_{19} steroids. J Biol Chem. (1996) 271(37):22855-22862.

Bélanger A, Couture J, Caron S, Roy R. Determination of nonconjugated and conjugated steroid levels in plasma and prostate after separation on C-18 columns. Ann N Y Acad Sci. (1990) 595:251–259.

Bélanger A, Pelletier G, Labrie F, Barbier O, Chouinard S. Inactivation of androgens by UDP-glucuronosyltransferase enzymes in humans. Trends Endocrinol Metabol. (2003) 14(10):473–479. doi:10.1016/j.tem.2003.10.005.

Bélanger B, Fiet J, Bélanger A. Effects of adrenocorticotropin on adrenal and plasma 11β-hydroxyandrostenedione in the guinea pig and determination of its relative androgen potency. Steroids. (1993) 58:29–34.

Belyaeva OV, Chetyrkin SV, Clark AL, Kostereva NV, SantaCruz KS, Chromwall BM, et al. Role of microsomal retinol/sterol dehydrogenase-like short-chain dehydrogenases/reductases in the oxidation and epimerization of 3α-hydroxysteroids in human tissues. Endocrinology. (2007) 148(5):2148-2156. doi: 10.1210/en.2006-1491.

Berthon P, Cussenot O, Hopwood L, Leduc A, Maitland N. Functional expression of SV40 in normal human prostatic epithelial and fibroblastic cells-differentiaton pattern of nontumorigenic cell-lines. Int J Oncol. (1995) 6(2):333-343.

Bianchini D, Lorente D, Rodriquez-Vida A, Omlin A, Pezaro C, Ferraldeschi P, et al. Antitumour activity of enzalutamide (MDV3100) in patients with metastatic castration-resistant prostate cancer (CRPC) pre-treated with docetaxel and abiraterone. Eur J Cancer. (2014) 50(1):78–84. http://dx.doi.org/10.1016/j.ejca.2013.08.020.

Biancolella M, Valentini A, Minella D, Vecchione L, D'Amico F, Chillemi G, et al. Effects of dutasteride on the expression of genes related to androgen metabolism and related pathway in human prostate cancer cell lines. Invest New Drugs. (2007) 25:491–497. doi: 10.1007/s10637-007-9070-7.

Biswas MG, Russell DW. Expression cloning and characterization of oxidative 17β- and 3α-hydroxysteroid dehydrogenases from rat and human prostate. J Biol Chem. (1997) 272(25):15959-15966. doi: 10.1074/jbc.272.25.15959.

Blanchere M, Berthaut I, Portois MC, Mestayer C, Mowszowicz I. Hormonal regulation of the androgen receptor expression in human prostatic cells in culture. J Steroid Biochem Mol Biol. (1998) 66(5-6):319-326.

Bloch E, Dorfman RI, Pincus G. The conversion of acetate to C_{19} steroids by human adrenal gland slices. J Biol Chem. (1957) 224:737–750.

Bloem LM, Storbeck KH, Schloms L, Swart AC. 11β-Hydroxyandrostenedione returns to the steroid arena: biosynthesis, metabolism and function. Molecules. (2013) 18:13228-13244. doi:10.3390/molecules181113228.

Bloem LM, Storbeck KH, Swart P, Du Toit T, Schloms L, Swart AC. Advances in the analytical methodologies: Profiling steroids in familiar pathways-challenging dogmas. J Steroid Biochem Mol Biol. (2015) 153:80-92. http://dx.doi.org/10.1016/j.jsbmb.2015.04.009.

Bülow HE, Bernhardt R. Analyses of the *CYP11B* gene family in the guinea pig suggest the existence of a primordial *CYP11B* gene with aldosterone synthase activity. Eur J Biochem. (2002) 269: 3838–3846. doi:10.1046/j.1432-1033.2002.03076.x.

Bülow HE, Möbius K, Bähr V, Bernhardt R. Molecular cloning and functional expression of the cytochrome P450 11B-hydroxylase of the guinea pig. Biochem Biophys Res Commun. (1996) 221: 304–312.

Byrns MC, Mindnich R, Duan L, Penning TM. Overexpression of aldo-keto reductase 1C3 (AKR1C3) in LNCaP cells diverts androgen metabolism towards testosterone resulting in resistance to the 5α-reductase inhibitor finasteride. J Steroid Biochem Mol Biol. (2012) 130:7-15. doi:10.1016/j.jsbmb.2011.12.012.

Cai C, Chen S, Ng P, Bubley GJ, Nelson PS, Mostaghel EA, et al. Intratumoral de novo steroid synthesis activates androgen receptor in castration-resistant prostate cancer and is upregulated by treatment with CYP17A1 inhibitors. Cancer Res. (2011) 71(20):6503–6513. doi: 10.1158/0008-5472.CAN-11-0532.

Campana C, Rege J, Turcu AF, Pezzi V, Gomez-sanchez CE, Robins DM, et al. Development of a novel cell based androgen screening model. J Steroid Biochem Mol Biol. (2016) 156:17-22. http://dx.doi.org/10.1016/j.jsbmb.2015.11.005.

Carson III C, Rittmaster R. The role of dihydrotestosterone in benign prostatic hyperplasia. Urol. (2003) 61(suppl 4A):2-7. doi:10.1016/S0090-4295(03)00045-1.

Chang E, Mittelman A, Dao TL. Metabolism of 4-C^{14}-testosterone in normal human adrenal homogenate. J Biol Chem. (1963) 238(3):913–917.

Chang HJ, Shi R, Rehse P, Lin SX. Identifying androsterone (ADT) as a cognate substrate for human dehydroepiandrosterone sulfotransferase (DHEA-ST) important for steroid homeostasis: structure of the enzyme-ADT complex. J Biol Chem. (2004) 279:2689–2696. doi: 10.1074/jbc.M310446200.

Chang HJ, Zhou M, Lin SX. Human dehydroepiandrosterone sulfotransferase: purification and characterization of a recombinant protein. J Steroid Biochem Mol Biol. (2001) 77:159–165. PII: S0960-0760(01)00048-6.

Chang KH, Li R, Papari-Zareei M, Watumull L, Zhao YD, Auchus RJ. Dihydrotestosterone synthesis bypassess testosterone to drive castration-resistant prostate cancer. Proc Natl Acad Sci. (2011) 108(33):13728-13733. www.pnas.org/cgi/doi/10.1073/pnas.1107898108.

Chang KH, Sharifi N. Prostate cancer - from steroid transformations to clinical translation. Nat Rev Urol. (2012) 9:721-724. doi:10.1038.nrurol.2012.175.

Chouinard S, Barbier O, Bélanger A. UDP-glucuronosyltransferase 2B15 (UGT2B15) and UGT2B17 enzymes are major determinants of androgen response in prostate cancer LNCaP cells. J Biol Chem. (2007) 282(46):33466-33474. doi: 10.1074/jbc.M703370200.

Clark BJ, Wells J, King SR and Stocco DM. The purification, cloning and expression of a novel luteinizing hormone-induced mitochondrial protein in MA-10 mouse Leydig tumor cells, characterization of the steroidogenic acute regulatory protein (StAR). J Biol Chem. (1994) 269(45):28314-28322.

Cohn GL, Mulrow PJ. Androgen release and synthesis *in vitro* by human adult adrenal glands. J Clin Invest. (1963) 42(1):64–78.

Cooper MS, Stewart PM. 11β-hydroxysteroid dehydrogenase type 1 and its role in the hypothalamus-pituitary-adrenal axis, metabolic syndrome, and inflammation. J Clin Endocrinol Metab. (2009) 94:4645–4654. doi: 10.1210/jc.2009-1412.

Couchman L, Vincent RP, Ghataore L, Moniz CF, Taylor NF. Challenges and benefits of endogenous steroid analysis by LC–MS/MS. Bioanalysis. (2011) 3(22): 2549–2572. doi: 10.4155/bio.11.254.

Culig Z, Hoffman J, Erdel M, Eder IE, Hobisch A, Hittmair A, et al. Switch from antagonist to agonist of the androgen receptor blocker bicalutamide is associated with prostate tumour progression in a new model system. Br J Cancer. (1999) 81(2):242-251.

Cussenot O, Berger BR, Mowszowicz I, Hojman HP, Teillac A, Le Duc A, et al. Immortalization of human adult normal prostatic epithelial cells by liposomes containing large T-SV40 gene. J Urol. (1991) 146(3):881-886. https://doi.org/10.1016/S0022-5347(17)37953-3.

Dalla Valle L, Toffolo V, Nardi A, Fiore C, Armanini D, Belvedere P, et al. The expression of the human steroid sulfatase-encoding gene is driven by alternative first exons. J Steroid Biochem Mol Biol. (2007) 107:22–29. doi: 10.1016/j.jsbmb.2007.05.004.

Day JM, Purohit A, Tutill HJ, Foster PA, Woo LWL, Potter BVL, et al. The development of steroid sulfatase inhibitors for hormone-dependent cancer therapy. Ann N Y Acad Sci. (2009) 1155:80–87. doi: 10.1111/j.1749-6632.2008.03677.x

Dhayat NA, Frey AC, Frey BM, d'Uscio CH, Vogt B, Rousson V, et al. Estimation of reference curves for the urinary steroid metabolome in the first year of life in healthy children: Tracing the complexity of human postnatal steroidogenesis. J Steroid Biochem Mol Biol. (2015) 154:226-236. http://dx.doi.org/10.1016/j.jsbmb.2015.07.024.

Dillard PR, Lin MF, Khan SA. Androgen-independent prostate cancer cells acquire the complete steroidogenic potential of synthesizing testosterone from cholesterol. Mol Cell Endocrinol. (2008) 295:115-120. doi:10.1016/j.mce.2008.08.013.

Dorfman RI, Rooks WH, Jones JB, Leman JD. Androgenic activity of highly purified 5α-androstane and 5α-androstan-17β-ol. J Med Chem. (1966) 9:930–931.

Dorfman RI. *In vivo* metabolism of neutral steroid hormones. J Clin Endocrinol Metab. (1954) 14:318–325.

Dovio A, Sartori ML, De Francia S, Mussino S, Perotti P, Saba L, et al. Differential expression of determinants of glucocorticoid sensitivity in androgen-dependent and androgen-independent human prostate cancer cell lines. J Steroid Biochem Mol Biol. (2009) 116:29-36. doi:10.1016/j.jsbmb.2009.04.007.

Du Toit T, Bloem LM, Quanson JL, Ehlers R, Serafin AM, Swart AC. Profiling adrenal 11β-hydroxyandrostenedione metabolites in prostate cancer cells, tissue and plasma: UPC^2-MS/MS quantification of 11β-hydroxytestosterone, 11keto-testosterone and 11keto-dihydrotestosterone. J Steroid Biochem Mol Biol. (2017) 166:54-67. http://dx.doi.org/10.1016/j.jsbmb.2016.06.009.

Du Toit T, Swart AC. Inefficient UGT-conjugation of adrenal 11β-hydroxyandrostenedione metabolites highlights C11-oxy C$_{19}$ steroids as the predominant androgens in prostate cancer. Mol Cell Endocrinol. (2018) 461:265-276. https://doi.org/10.1016/j.mce.2017.09.026.

Du Toit T, Swart AC. Perspective on the regulatory role of UGT2B28 as a conjugating enzyme in the progression of prostate cancer. Transl Cancer Res. (2016) 5(suppl 7):S1496-S1502. doi: 10.21037/tcr.2016.12.22.

Dufort I, Rheault P, Huang XF, Soucy P, Luu-The V. Characteristics of a highly labile human type 5 17β-hydroxysteroid dehydrogenase. Endocrinology. (1999) 140(2):568–574.

Dumont M, Luu-The V, De Launoit Y, Labrie F. Expression of human 17β-hydroxysteroid dehydrogenase in mammalian cells. J Steroid Biochem Mol Biol. (1992) 41(3-8):605–608.

Dumont M, Luu-The V, Dupont E, Pelletier G, Labrie F. Characterization, expression, and immunohistochemical localization of 3β-hydroxysteroid dehydrogenase/Δ5-Δ4 isomerase in human skin. J Invest Dermatol. (1992) 99:415–421.

Dyrenfurth I, Lucis OJ, Beck JC, Venning EH. Studies in patients with adrenocortical hyperfunction. III. *In vitro* secretion of steroids by human adrenal glands. J Clin Endocrinol Metab. (1960) 20:765–779.

Ekuase EJ, Liu Y, Lehmler HJ, Robertson LW, Duffel MW. Structure-activity relationships for hydroxylated polychlorinated biphenyls as inhibitors of the sulfation of dehydroepiandrosterone catalyzed by

human hydroxysteroid sulfotransferase SULT2A1. Chem Res Toxicol. (2011) 24:1720–1728. doi: dx.doi.org/10.1021/tx200260h.

Falany CN. Enzymology of human cytosolic sulfotransferases. FASEB (1997a) 11:206–216.

Falany CN, He D, Dumas N, Frost AR, Falany JL. Human cytosolic sulfotransferase 2 B1: Isoform expression, tissue specificity and subcellular localization. J Steroid Biochem Mol Biol. (2006) 102(1–5):214–221. doi: 10.1016/j.jsbmb.2006.09.011.

Falany CN, Vazquez ME, Kalb JM. Purification and characterization of human liver dehydroepiandrosterone sulphotransferase. Biochem J. (1989) 260:641–646.

Falany CN, Wheeler J, Oh TS, Falany JL. Steroid sulfation by expressed human cytosolic sulfotransferases. J Steroid Biochem Mol Biol. (1994) 4(8):369–375.

Farnsworth WE. Human prostatic dehydroepiandrosterone sulfate sulfatase. Steroids. (1973) 21:647–664.

Fernlund P, Gershagen S. 2-Iodoestradiol binds with high affinity to human sex hormone binding globulin (SHBG). J Steroid Biochem. (1990) 36(1-2):75-81. https://doi.org/10.1016/0022-4731(90)90115-9.

Flück CE, Meyer-Boni M, Pandey AV, Kempna P, Miller WL, Schoenle EJ, et al. Why boys will be boys: Two pathways of fetal testicular androgen biosynthesis are needed for male sexual differentiation. Am J Hum Genet. (2011) 89:201-218. doi: 10.1016/j.ajhg.2011.06.009.

Fuda H, Lee YC, Shimizu C, Javitt NB, Strott CA. Mutational analysis of human hydroxysteroid sulfotransferase SULT2B1 isoforms reveals that exon 1B of the SULT2B1 gene produces cholesterol sulfotransferase, whereas exon 1A yields pregnenolone sulfotransferase. J Biol Chem. (2002) 277:36161–36166. doi: 10.1074/jbc.M207165200.

Fung KM, Samara ENS, Wong C, Metwalli A, Krlin R, Bane B, et al. Increased expression of type 2 3α-hydroxysteroid dehydrogenase /type 5 17β-hydroxysteroid dehydrogenase (AKR1C3) and its relationship with androgen receptor in prostate carcinoma. Endocr-Relat Cancer. (2006) 13:169–180. doi:10.1677/erc.1.01048.

Ganguly A, Meikle AW, Tyler FH, West CD. Assessment of 11β-hydroxylase activity with plasma corticosterone, deoxycorticosterone, cortisol, and deoxycortisol: role of ACTH and angiotensin. J Clin Endocrinol Metab. (1977) 44:560–568.

Geese WJ, Raftogianis RB. Biochemical characterization and tissue distribution of human SULT2B1. Biochem Biophys Res Commun. (2011) 288:280–289. doi:10.1006/bbrc.2001.5746.

Ghayee HK, Auchus RJ. Basic concepts and recent developments in human steroid hormone biosynthesis. Rev Endocr Metab Disord. (2007) 8:289-300. doi: 10.1007/s11154-007-9052-2.

Gianfrilli D, Pierotte S, Pofi R, Leonardo C, Ciccariello M, Barbagallo F. Sex steroid metabolism in benign and malignant intact prostate biopsies: individual profiling of prostate intracrinology. BioMed Res Int. (2014) 1-8. http://dx.doi.org/10.1155/2014/464869.

Godoy A, Kawinski E, Li Y, Oka D, Alexiev B, Azzouni F, et al. 5α-reductase type 3 expression in human benign and malignant tissues: A comparative analysis during prostate cancer progression. Prostate. (2011) 71:1033–1046. doi:10.1002/pros.21318.

Goldzieher JW, Beering SC. Metabolism of 11β-hydroxyandrostenedione, adrenosterone and hydrocortisone to urinary 11-oxy 17-ketosteroids. J Clin Endocrinol Metab. (1969) 29:171–178.

Goldzieher JW, de la Pena A, Aivaliotis MM. Radioimmunoassay of plasma androstenedione, testosterone and 11β-hydroxyandrostenedione after chromatography on Lipidex-5000 (hydroxyalkoxypropyl sephadex). J Steroid Biochem. (1978) 9:169–173.

Gomez-Sanchez CE, Qi X, Verlarde-Miranda C, Plonczynski MW, Parker CR, Rainey W, et al. Development of monoclonal antibodies against human CYP11B1 and CYP11B2. Mol Cell Endocrinol. (2014) 383:111-117. http://dx.doi.org/10.1016/j.mce.2013.11.022.

Guillemette C, Hum DW, Bélanger A. Specificity of glucuronosyltransferase activity in the human cancer cell line LNCaP, evidence for the presence of at least two glucuronosyltransferase enzymes. J. Steroid Biochem. Mol. Biol. (1995) 55(3/4):355e362. http://dx.doi.org/10.1016/0960-0760(95)00183-2.

Gulcan HO, Duffel MW. Substrate inhibition in human hydroxysteroid sulfotransferase SULT2A1: studies on the formation of catalytically non-productive enzyme complexes. Arch Biochem Biophys. (2011) 507:232–240. doi: 10.1016/j.abb.2010.12.027.

Gupta MK, Guryev OL, Auchus RJ. 5α-reduced C_{21} steroids are substrates for human cytochrome P450c17. Arch Biochem Biophys. (2003) 418(2):151–60. doi:10.1016/j.abb.2003.07.003.

Habib FK. The prostate: New concepts and developments. Taylor and Francis (2004).

Habib FK, Ross M, Bayne CW, Grigor K, Buck AC, Bollina P, et al. The localisation and expression of 5α-reductase type I and II mRNAs in human hyperplaia prostate and in prostate primary cultures. J Endocrinol. (1998) 156:509-517.

Hammer GD, Parker KL, Schimmer BP. Minireview: Transcriptional regulation of adrenocortical development. Endocrinology. (2005) 146(3):1018-1024. doi: 10.1210/en.2004-1385.

Hanley NA, Arlt W. The human fetal adrenal cortex and the window of sexual differentiation. Trends Endocrinol Metab. (2006) 17(10):391–7. doi:10.1016/j.tem.2006.10.001.

Hashiguchi T, Kurogi K, Shimohira T, Teramoto T, Liu M-C, Suiko M, et al. Δ4-3-ketosteroids as a new class of substrates for the cytosolic sulfotransferases. BBA - General Subjects (2017) 1861:2883–2890. http://dx.doi.org/10.1016/j.bbagen.2017.08.005.

Hayward SW, Dahiya R, Cunha GR, Bartek J, Deshpande N, Narayan P. Establishment and characterization of an immortalized but non-transformed human prostate epithelial cell line: BPH-1. In vitro Cell Dev Biol. (1995) 31(1):14-24.

He D, Falany CN. Characterization of proline-serine rich carboxyl terminus in human sulfotransferase 2B1b: Immunogenicity, subcellular localization, kinetic properties, and phosphorylation. Drug Metab Dispos (2006) 34(10):1749–1755. doi: 10.1124/dmd.106.011114.

He D, Falany CN. Inhibition of SULT2B1b expression alters effects of 3β-hydroxysteroids on cell proliferation and steroid hormone receptor expression in human LNCaP prostate cancer cells. Prostate. (2007) 67:1318–1329. doi: 10.1002/pros.20615.

He D, Meloche CA, Dumas NA, Frost AR, Falany CN. Different subcellular localization of sulphotransferase 2B1b in human placenta and prostate. Biochem J (2004) 379:533–540

Hemmerich S, Verdugo D, Rath VL. Strategies for drug discovery by targeting sulfation pathways. Drug Discov Today. (2004) 9:967–975. PII: S1359-6446(04)03272-6.

Hempel N, Barnett AC, Bolton-Grob RM, Liyou NE, McManus ME. Site-directed mutagenesis of the substrate binding cleft of human estrogen sulfotransferase. Biochem Biophys Res Commun. (2000) 276:224–230. doi: 10.1006/bbrc.2000.3473.

Her C, Wood TC, Eichler EE, Mohrenweiser HW, Ramagli LS, Siciliano MJ, et al. Human hydroxysteroid sulfotransferase SULT2B1: two enzymes encoded by a single chromo- some 19 Gene. Genomics. (1998) 53:284–295.

Heracek J, Richard H, Martin H, Luboslav S, Jana S, Jitka K. Tissue and serum levels of principal androgens in benign prostatic hyperplasia and prostate cancer. Steroids. (2007) 72(4):375-380. https://doi.org/10.1016/j.steroids.2007.01.004.

Heyns CF, Basson J, Van der Merwe A, Zarrabi AD. Clinical (non-histological) diagnosis of advanced prostate cancer: Evaluation of treatment outcome after androgen deprivation therapy. S Afr J Surg. (2014) 52(3):82-85. doi:10.7196/SAJS.1689.

Hofland J, Van Weerden WM, Dits NFJ, Steenbergen J, Van Leenders GJLH, Jenster G, et al. Evidence of limited contributions for intratumoral steroidogenesis in prostate cancer. Cancer Res. (2010) 70(3):1256–1264. doi: 10.1158/0008-5472.CAN-09-2092.

Holownia P, Owen EJ, Conway GS, Round J, Honour JW. Studies to confirm the source of 11β-hydroxyandrostenedione. J Steroid Biochem Mol Biol. (1992) 41(3–8): 875–880.

Holzbeierlein J, Lal P, LaTulippe E, Smith A, Satagopan J, Zhang L, et al. Gene expression analysis of human prostate carcinoma during hormonal therapy identifies androgen-responsive genes and mechanisms of therapy resistance. Am J Pathol. (2004) 164(1):217–27. doi:10.1016/S0002-9440(10)63112-4.

Homma K, Hasegawa T, Masumoto M, Takeshita E, Watanabe K, Chiba H, et al. Reference values for urinary steroids in japanese newborn infants: gas chromatography/mass spectrometry in selected ion monitoring. Endocr J. (2003) 50:783-792. http://doi.org/10.1507/endocrj.50.783.

Horoszewicz JS, Leong SS, Kawinski E, Karr JP, Rosenthal H, Chu TM, Mirand EA, Murphy GP. LNCaP model of human prostatic carcinoma. Cancer Res. (1983) 43:1809–1818.

Huang XF, Luu-The V. Molecular characterization of a first human 3(α/β)-hydroxysteroid epimerase. J Biol Chem. (2000) 275:29452–29457.

Huggins C, Bergenstal DM. Inhibition of human mammary and prostatic cancers by adrenalectomy. Cancer Res. (1952) 12:134–141.

Huggins C. Prostatic cancer treated by orchiectomy: The five year result. JAMA. (1946) 131(7):576–581.

Imamichi Y, Yuhki KI, Orisaka M, Kitano T, Mukai K, Ushikubi F, et al. 11-Ketotestosterone is a major androgen produced in human gonads. J Clin Endocrinol Metab. (2016) 101:3582–3591. doi: 10.1210/jc.2016-2311.

Jailer JW, Gold JJ, Wiele RV, Lieberman S. 17α-hydroxyprogesterone and 21-desoxyhydrocortisone; their metabolism and possible role in congenital adrenal virilism. J Clin Invest. (1955) 34(11):1639–1646.

Javitt NB, Lee YC, Shimizu C, Fuda H, Strott CA. Cholesterol and hydroxycholesterol sulfotransferases: identification, distinction from dehydroepiandrosterone sulfotransferase, and differential tissue expression. Endocrinology. (2001) 142: 2978–2984.

Jeanloz RW, Levy H, Jacobsen RP, Hechter O, Schenker V, Pincus G. Chemical transformations of steroids by adrenal perfusion. III. Δ^4- androstene-3,17-dione. J Biol Chem. (1953) 203:453–461.

Kahokehr A, Gilling PJ. Landmarks in BPH- from aetiology to medical and surgical management. Nat Rev Urol. (2014) 11:118–122. doi: 10.1038/nrurol.2013.318.

Kamrath C, Hochberg Z, Hartmann MF, Remer T, Wudy SA Increased activation of the alternative "backdoor" pathway in patients with 21-hydroxylase deficiency: evidence from urinary steroid hormone analysis. J Clin Endocrinol Metab. (2012) 97:E367–E375. https://doi.org/10.1210/jc.2011-338 1997.

Kamrath C, Wettstaedt L, Boettcher C, Hartmann MF, Wudy SA. The urinary steroidome of treated children with classic 21-hydroxylase deficiency. J Steroid Biochem Mol Biol. (2017) 165:396–406. http://dx.doi.org/10.1016/j.jsbmb.2016.08.006.

Koh E, Noda T, Kanaya J, Namiki M. Differential expression of 17β-hydroxysteroid dehydrogenase isozyme genes in prostate cancer and noncancer tissues. Prostate. (2002) 53(2):154–9. doi:10.1002/pros.10139.

Korenchuk S, Lehr JE, Mclean L, Lee YG, Whitney S, Vessella R, et al. VCaP, a cell-based model system of human prostate cancer. In Vivo. (2001) 15(2):163–168.

Kowal J, Simpson ER, Estabrook RW. Adrenal cells in tissue culture. V. On the specificity of the stimulation of 11β-hydroxylation by adrenocorticotropin. J Biol Chem. (1970) 245: 2438–2443.

Kowal J. Adrenal cells in tissue culture. III. Effect of adrenocorticotropin and 3', 5'-cyclic adenosine monophosphate on 11β-hydroxylase and other steroidogenic enzymes. Biochemistry. (1969) 8:1821–1831.

Kumagai J, Hofland J, Erkens-Schulze S, Dits NFJ, Steenbergen J, Jenster G, et al. Intratumoral conversion of adrenal androgen precursors drives androgen receptor-activated cell growth in prostate cancer more potently than de novo steroidogenesis. Prostate. (2013) 73:1636-1650. doi: 10.1002/pros.22655.

Labrie F, Luu-The V, Labrie C, Simard J. DHEA and its transformation into androgens and estrogens in peripheral target tissue: Intracrinology. Frontiers Neuroendocrinol. (2001) 22:185-212. doi:10.1006/frne.2001.0216.

Lazard D, Zupko K, Poria Y, Nef P, Lazarovits J, Horn S, et al. Odorant signal termination by olfactory UDP glucuronosyl transferase. Nature. (1991) 349:790-793.

Lee KA, Fuda H, Lee YC, Negishi M, Strott CA, Pedersen LC. Crystal structure of human cholesterol sulfotransferase (SULT2B1b) in the presence of pregnenolone and 3'-phosphoadenosine 5'-phosphate. J Biol Chem. (2003) 278:44593–44599 doi: 10.1074/jbc.M308312200.

Lévesque É, Turgeon D, Carrier JS, Montminy V, Beaulieu M, Bélanger A. Isolation and characterization of the UGT2B28 cDNA encoding a novel human steroid conjugating UDP-glucuronosyltransferase. Biochem. (2001) 40: 3869e3881. http://dx.doi.org/10.1021/bi002607y.

Lewbart ML, Schneider JJ. Enzymatic synthesis of steroid sulfates. J Biol Chem. (1956) 222:787–794.

Lin H, Steckelbroeck S, Fung K, Jones AN, Penning TM. Characterization of a monoclonal antibody for human aldo-keto reductase AKR1C3 (type 2 3α-hydroxysteroid dehydrogenase/type 5 17β-hydroxysteroid dehydrogenase); immunohistochemical detection in breast and prostate. Steroids. (2004) 69:795–801. doi:10.1016/j.steroids.2004.09.014.

Lipsett MB, Sarfaty GA, Wilson H, Bardin CW, Fishman LM. Metabolism of testosterone and related steroids in metastatic interstitial cell carcinoma of the testis. J Clin Invest. (1966) 45(11):1700–1709.

Locke JA, Guns ES, Lubik AA, Adomat HH, Hendy SC, Wood CA, et al. Androgen levels increase by intratumoral de novo steroidogenesis during progression of castration-resistant prostate cancer. Cancer Res. (2008) 68(15):6407-6415. doi:10.1158/0008-5472.CAN-07-5997.

Loriot Y, Bianchini D, Ileana E, Sandhu S, Patrikidou A, Pezaro C et al. Antitumour activity of abiraterone acetate against metastatic castration-resistant prostate cancer progressing after docetaxel and enzalutamide (MDV3100). Ann Oncol. (2013) 24(7):1807–1812. doi:10.1093/annonc/mdt136.

Løvås K, Gjesdal CG, Christensen M, Wolff AB, Almas B, Svartberg J, et al. Glucocorticoid replacement therapy and pharmacogenetics in Addison's disease: effects on bone. Eur J Endocrinol. (2009) 160(6):993–1002. doi: 10.1530/EJE-08-0880.

Luo J, Dunn TA, Ewing CM, Walsh PC, Isaacs WB. Decreased gene expression of steroid 5 alpha-reductase 2 in human prostate cancer: Implications for finasteride therapy of prostate carcinoma. Prostate. (2003) 57:134–139. doi: 10.1002/pros.10284.

Luu-The V, Bélanger A, Labrie F. Androgen biosynthetic pathways in the human prostate. Best Pract Res Clin Endocrinol Metab. (2008) 22:207-221. doi:10.1016/j.beem.2008.01.008.

Luu-The V. Analysis and characteristics of multiple types of human 17β-hydroxysteroid dehydrogenase. J Steroid Biochem Mol Biol. (2001) 76:143-151. PII: S0960-0760(00)00155-2.

Marcelli M, Cunningham GR. Hormonal signaling in prostatic hyperplasia and neoplasia. J Clin Endocrinol Metab. (1999) 84:3463–3468.

Mariani AJ, Glover M, Arita S. Medical versus surgical androgen suppression therapy for prostate cancer: A 10-year longitudinal cost study. J Urol. (2001) 165(1):104-107. http://dx.doi.org/10.1097/00005392-200101000-00026.

Martel C, Rhéaume E, Takahashi M, Trudel C, Couët J, Luu-The V, et al. Distribution of 17β-hydroxysteroid dehydrogenase gene expression and activity in rat and human tissues. J Steroid Biochem Mol Biol. (1992) 41(3-8):597–603.

Marti N, Galván JA, Pandey AV, Trippel M, Tapia C, Müller M, et al. Genes and proteins of the alternative steroid backdoor pathway for dihydrotestosterone synthesis are expressed in the human ovary and seem enhanced in the polycystic ovary syndrome. Mol Cell Endocrinol. (2017) 441:116-123. http://dx.doi.org/10.1016/j.mce.2016.07.029.

Masuda M. Urinary ketosteroid excretion patterns in congenital adrenal hyperplasia. J Clin Endocrinol Metab. (1957) 17:1181–1190.

Mathew PA, Mason JI, Trant JM, Sanders D, Waterman MR. Amino acid substitutions Phe[66]→Leu and Ser[126]→Pro abolish cortisol and aldosterone synthesis by bovine cytochrome $P450_{11\beta}$. J Biol Chem. (1990) 265:20228–20233.

Matthews J, Wihlén B, Tujague M, Wan J, Ström A, Gustafsson JÅ. Estrogen receptor (ER) β modulates ERα-mediated transcriptional activation by altering the recruitment of c-Fos and c-Jun to estrogen- responsive promoters. Mol Endocrinol. (2006) 20:534-543. doi: 10.1210/me.2005-0140.

McEwan IJ. Gene regulation through chromatin remodelling by members of the nuclear receptor superfamily. Biochem Soc Trans. (2000) 28:369–373.

McNamara KM, Nakamura Y, Miki Y, Sasano H. Phase two steroid metabolism and its roles in breast and prostate cancer patients. Frontiers in Endocrinol. (2013) 4:1-7. doi: 10.3389/fendo.2013.00116.

Meloche CA, Falany CN. Expression and characterization of the human 3β-hydroxysteroid sulfotransferases (SULT2B1a and SULT2B1b). J Steroid Biochem Mol Biol. (2001) 77:261–269.

Messiano S, Jaffe RB. Development and function of the primate fetal adrenal cortex. Endocr Rev. (1997) 18(3):378-404.

Milewicz A, Vecsei P, Korth-Schütz S, Haack D, Rösler A, Lichtwald K, et al. Development of plasma 21-deoxycortisol radioimmunoassay and application to the diagnosis of patients with 21-hydroxylase deficiency. J Steroid Biochem. (1984) 21:185–191. http://dx.doi.org/10.1016/0022-4731(84)90382-0.9.

Miller W, Auchus R. The molecular biology, biochemistry and physiology of human steroidogenesis and its disorders. Endocr Rev. (2011) 32(1):81–151. doi: 10.1210/er.2010-0013.

Mitsiades N, Sung CC, Schultz N, Danila DC, He B, Eedunuri VK, et al. Distinct patterns of dysregulated expression of enzymes involved in androgen synthesis and metabolism in metastatic prostate cancer tumors. Cancer Res. (2012) 72:6142–6152. doi: 10.1158/0008-5472.CAN-12-1335.

Mizokami A, Koh E, Izumi K, Narimoto K, Takeda M, Honma S, et al. Prostate cancer stromal cells and LNCaP cells coordinately activate the androgen receptor through synthesis of testosterone and dihydrotestosterone from dehydroepiandrosterone. Endocr Relat Cancer. (2009) 16:1139–1155. doi: 10.1677/ERC-09-0070.

Mizrachi D, Auchus RJ. Androgens, estrogens, and hydroxysteroid dehydrogenases. Mol Cell Endocrinol. (2009) 301:37–42. doi:10.1016/j.mce.2008.08.029.

Mohler JL, Gregory CW, Ford III OH, Kim D, Weaver CM, Petrusz P, et al. The androgen axis in recurrent prostate cancer. Clin Cancer Res. (2004) 10(2):440–448. doi:10.1158/1078-0432.CCR-1146-03.

Montgomery RB, Mostaghel EA, Vessella R, Hess DL, Kalhorn TF, Higano CS, et al. Maintenance of intratumoral androgens in metastatic prostate cancer: a mechanism for castration-resistant tumor growth. Cancer Res. (2008) 68(11):4447–54. doi:10.1158/0008-5472.CAN-08-0249.

Mostaghel EA. Beyond T and DHT – Novel steroid derivatives capable of wild type androgen receptor activation. Int J Biol Sci. (2014) 10(6):602-613. doi: 10.7150/ijbs.8844.

Mostaghel EA. Steroid hormone synthetic pathways in prostate cancer. Transl Androl Urol. (2013) 2(3):212-227. doi: 10.3978/j.issn.2223-4683.2013.09.16.

Mueller JW, Gilligan LC, Idkowiak J, Arlt W, Foster PA. The regulation of steroid action by sulfation and desulfation. Endocr Rev. (2015) 36(5):526-563. doi: 10.1210/er.2015-1036.

Muthusamy S, Andersson S, Kim HJ, Butler R, Waage L, Bergenheim U, et al. Estrogen receptor β and 17β-hydroxysteroid dehydrogenase type 6, a growth regulatory pathway that is lost in prostate cancer. Proc Natl Acad Sci. (2011) 108(50):20090-20094. www.pnas.org/cgi/doi/10.1073/pnas.1117772108.

Nahoul K, Adeline J, Bercovici JP. Radioimmunoassay of plasma 21-deoxycortisol. J Steroid Biochem. (1989) 33:1167–1172.

Nakamura Y, Suzuki T, Fukuda T, Ito A, Endo M, Moriya T, et al. Steroid sulfatase and estrogen sulfotransferase in human prostate cancer. Prostate. (2006) 66:1005–1012. doi: 10.1002/pros.20426.

Nardi A, Pomari E, Zambon D, Belvedere P, Colombo L, Dalla Valle L. Transcriptional control of human steroid sulfatase. J Steroid Biochem Mol Biol. (2009) 115:68–74. doi: 10.1016/j.jsbmb.2009.02.017.

Noonan KL, North S, Bitting RL, Armstrong AJ, Ellard SL, Chi KN. Clinical activity of abiraterone acetate in patients with metastatic castration-resistant prostate cancer progressing after enzalutamide. Ann Oncol. (2013) 24(7):1802–1807. doi:10.1093/annonc/mdt138.

Noordam C, Dhir V, McNelis JC, Schlereth F, Hanley NA, Krone N, et al. Inactivating *PAPSS2* mutations in a patient with premature pubarche. N Engl J Med. (2009) 360:2310–2318.

O'Reilly MW, Kempegowda P, Jenkinson C, Taylor AE, Quanson JL, Storbeck KH, et al. 11-Oxygenated C19 steroids are the predominant androgens in polycystic ovary syndrome. J Clin Endocrinol Metab. (2017) 102:840–848. https://doi.org/10.1210/jc.2016-3285.

Page N, Warriar N, Govindan MV. 11β-Hydroxysteroid dehydrogenase and tissue specificity of androgen action in human prostate cancer cell LNCaP. J Steroid Biochem Mol Biol. (1994) 49: 173-81.

Paquet S, Fazli L, Grosse L, Tetu B, Rennie PS, Bélanger A, et al. Differential expression of the androgen-conjugating UGT2B15 and UGT2B17 enzymes in prostate tumor cells during cancer progression. J Clin Endocrinol Metab. (2012) 97:428–432. doi:10.1210/jc.2011-2064.

Pelletier G, Luu-The V, Li S, Ouellet J, Labrie F. Cellular localization of mRNA expression of enzymes involved in the formation and inactivation of hormonal steroids in the mouse prostate. J Histochem Cytochem. (2004) 52(10): 1351-1356. doi: 10.1369/jhc.4A6311.2004.

Pelletier G. Expression of steroidogenic enzymes and sex-steroid receptors in human prostate. Best Prac Res Clin Endocrinol Metab. (2008) 22(2):223-228. doi:10.1016/j.beem.2008.02.004.

Penning TM, Burczynski ME, Jez JM, Hung CF, Lin HK, Ma H, et al. Human 3α-hydroxysteroid dehydrogenase isoforms (AKR1C1-AKR1C4) of the aldo-keto reductase superfamily: functional plasticity and tissue distribution reveals roles in the inactivation and formation of male and female sex hormones. Biochem J. (2000) 351:67-77.

Penning TM, Byrns MC. Steroid hormones transforming aldo-keto reductase and cancer. Steroid enzymes and cancer: Ann N Y Acad Sci. (2009) 1155:33-42. doi: 10.1111/j.1749-6632.2009.03700.x.

Penning TM, Steckelbroeck S, Bauman DR, Miller MW, Jin Y, Peehl DM, et al. Aldo-keto reductase (AKR) 1C3: Role in prostate disease and the development of specific inhibitors. Mol Cell Endocrinol. (2006) 248:182–191. doi:10.1016/j.mce.2005.12.009.

Penning TM. Androgen biosynthesis in castration-resistant prostate cancer. Endocr- Relat Cancer. (2014) 21:T67-T78. doi: 10.1530/ERC-14-0109.

Penning TM. New frontiers in androgen biosynthesis and metabolism. Curr Opin Endocrinol Diabetes Obes. (2010) 17(3):233-239. doi:10.1097/MED.0b013e3283381a31.

Pia A, Vignani F, Attard G, Tucci M, Bironzo P, Scagliotti G, et al. Strategies for managing ACTH dependent mineralocorticoid excess induced by abiraterone. Cancer Treatment Rev. (2013) 39:966-973. http://dx.doi.org/10.1016/j.ctrv.2013.03.003.

Pretorius E, Africander D, Vlok M, Perkins MS, Quanson JL, Storbeck KH. 11-Ketotestosterone and 11-ketodihydrotestosterone in castration resistant prostate cancer: potent androgens which can no longer be ignored. PLoSONE. (2016) 11:e0159867. doi: 10.1371/journal.pone.0159867.

Prins GS. Molecular biology of the androgen receptor. Mayo Clin Proc (2000) 75 Suppl: S32–35.

Quanson JL. The characterisation of the catalytic activity of human steroid 5α-reductase towards novel C19 substrates, MSc thesis (2015) Stellenbosch University, http://scholar.sun.ac.za/handle/10019.1/97057.

Quanson JL, Stander MA, Pretorius E, Jenkinson C, Taylor AE, Storbeck KH. High-throughput analysis of 19 endogenous androgenic steroids by ultra-performance convergence chromatography tandem mass spectrometry. J Chromatogr B. (2016) 1031:131-138. http://dx.doi.org/10.1016/j.jchromb.2016.07.024.

Rainey WE, Nakamura Y. Regulation of the adrenal androgen biosynthesis. J Steroid Biochem Mol Biol. (2008) 108:281–286. doi: 10.1016/j.jsbmb.2007.09.015.

Rang HP, Dale MM, Ritter JM, Moore PK. The pituitary and adrenal cortex. 5th ed. Philadelphia, PA: Elsevier Churchill Livingstone. (2003) 404-420.

Rathkopf DE, Smith MR, De Bono JS, Logothetis CJ, Shore ND, De Souza P, et al. Updated interim efficacy analysis and long-term safety of abiraterone acetate in metastatic castration-resistant prostate cancer patients without prior chemotherapy (COU-AA-302). Urol Eur. (2014) 66:815-825. http://dx.doi.org/10.1016/j.eururo.2014.02.056.

Rauh M. Steroid measurement with LC-MS/MS in pediatric endocrinology. Mol Cell Endocrinol. (2009) 301:272-281. doi:10.1016/j.mce.2008.10.007.

Reed MJ, Purohit A, Woo LW, Newman SP, Potter BV. Steroid sulfatase: molecular biology, regulation, and inhibition. Endocr Rev. (2005) 26:171–202. doi: 10.1210/er.2004-0003.

Rege J, Karashima S, Lerario AM, Smith JM, Auchus RJ, Kasa-Vubu JZ, et al. Age-dependent increases in adrenal cytochrome b5 and serum 5-androstenediol-3-sulfate. J Clin Endocrinol Metab. (2016) 101:4585-4593. doi: 10.1210/jc.2016-2864.

Rege J, Nakamura Y, Satoh F, Morimoto R, Kennedy MR, Layman LC, et al. Liquid chromatography-tandem mass spectrometry analysis of human adrenal vein 19-carbon steroids before and after ACTH stimulation. J Clin Endocrinol Metab. (2013) 98:1182–1188. doi: 10.1210/jc.2012-2912.

Rege J, Nakamura Y, Wang T, Merchen TD, Sasano H, Rainey WE. Transcriptome profiling reveals differentially expressed transcripts between the human adrenal zona fasciculata and zona reticularis. J Clin Endocrinol Metab. (2014) 99:E518–E527. doi: 10.1210/jc.2013-3198.

Rege J, Nanba AT, Auchus RJ, Ren J, Peng HM, Rainey WE, et al. Adrenocorticotropin acutely regulates pregnenolone sulfate production by the human adrenal in vivo and in vitro. J Clin Endocrinol Metab. (2017) (In press). doi: 10.1210/jc.2017-01525.

Rege J, Rainey WE. The steroid metabolome of adrenarche. J Endocrinol. (2012) 214:133-143. doi: 10.1530/JOE-12-0183.

Riches Z, Stanley EL, Bloomer JC, Coughtrie MW. Quantitative evaluation of the expression and activity of five major sulfotransferases (SULTs) in human tissues: the SULT "pie". Drug Metab Dispos. (2009) 37:2255–2261. doi: 10.1124/dmd.109.028399.

Risbridger GP, Davis ID, Birrell SN, Tilley WD. Breast and prostate cancer: more similar than different. Nat Rev Cancer. (2010) 10(3):205–212.

Roehrborn CG, Siami P, Barkin J, Damião R, Major-Walker K, Nandy I, et al. The effects of combination therapy with dutasteride and tamsulosin on clinical outcomes in men with symptomatic benign prostatic hyperplasia: 4-year results from the CombAT study. Eur Urol. (2010) 57:123-131. doi:10.1016/j.eururo.2009.09.035.

Rosemberg E, Dorfman RI. Biological activity of 9 alpha-fluoro-11 beta-hydroxy-delta 4-androstene-3, 17-dione. Proc Soc Exp Biol Med. (1958) 99:336–338.

Ross RW, Xie W, Regan MM, Pomerantz M, Nakabayashi M, Daskivich TJ, et al. Efficacy of androgen deprivation therapy (ADT) in patients with advanced prostate cancer: association between Gleason score, prostate-specific antigen level, and prior ADT exposure with duration of ADT effect. Cancer. (2008) 112:1247-1253. doi: 10.1002/cncr.23304.

Russell DW, Wilson JD. Steroid 5α-reductase: two genes/two enzymes. Annu Rev Biochem. (1994) 63:25–61.

Ryan CJ, Smith MR, De Bono J, Molina A, Logothetis CJ, De Souza P, et al. Abiraterone in metastatic prostate cancer without previous chemotherapy. N Engl J Med. (2013) 368(2):138–148.

Savard K, Dorfman RI, Baggett B, Fielding LL, Engel LL, McPherson HT, et al. Clinical, morphological and biochemical studies of a virilizing tumor in the testis. J Clin Invest. (1960) 39:534–553.

Schloms L, Storbeck KH, Swart P, Gelderblom WCA, Swart AC. The influence of *Aspalathus linearis* (Rooibos) and dihydrochalcones on adrenal steroidogenesis: quantification of steroid intermediates and end products in H295R cells. J Steroid Biochem Mol Biol. (2012) 128(3-5):128–38. doi: 10.1016/j.jsbmb.2011.11.003.

Schrader AJ, Boegemann M, Ohlmann CH, Schnoeller TJ, Krabbe LM, Hajili T, et al. Enzalutamide in castration-resistant prostate cancer patients progressing after docetaxel and abiraterone. Eur Urol. (2014) 65 (1):30–36.

Seo YK, Mirkheshti N, Song CS, Kim S, Dodds S, Ahn SC, et al. SULT2B1b sulfotransferase: induction by vitamin D receptor and reduced expression in prostate cancer. Mol Endocrinol. (2013) 27:925–939. doi: 10.1210/me.2012-1369.

Shah SK, Trump DL, Sartor O, Tan W, Wilding GE, Mohler JL. Phase II study of dutasteride for recurrent prostate cancer during androgen deprivation therapy. J Urol. (2009) 181:621–6. doi:10.1016/j.juro.2008.10.014.

Sharifi N, Auchus RJ. Steroid biosynthesis and prostate cancer. Steroids. (2012) 77(7):719–726. doi:10.1016/j.steroids.2012.03.015.

Sharifi N. The 5α-androstanedione pathway to dihydrotestosterone in castration-resistant prostate cancer. J Investig Med. (2012) 60(2):1-8. doi:10.231/JIM.0b013e31823874a4.

Siiteri PK, Wilson JD. Dihydrotestosterone in prostatic hypertrophy. I. The formation and content of dihydrotestosterone in the hypertrophic prostate of man. J Clin Invest. (1970) 49:1737–1745.

Slominski A, Ermak G, Mihm M. ACTH receptor, CYP11A1, CYP17 and CYP21A2 genes are expressed in skin. J Clin Endocrinol Metab. (1996d) 81(7):2746–2749.

Slominski A, Zbytek B, Nikolakis G, Manna PR, Skobowiat C, Zmijewski M, et al. Steroidogenesis in the skin: Implications for local immune functions. J Steroid Biochem Mol Biol. (2013) 137:107–123. http://dx.doi.org/10.1016/j.jsbmb.2013.02.006.

Slominski A, Zjawiony J, Wortsman J, Semak I, Stewart J, Pisarchik A, et al. A novel pathway for sequential transformation of 7-dehydrocholesterol and expression of the P450scc system in mammalian skin. Eur J Biochem. (2004c) 271:4178–4188. doi:10.1111/j.1432-1033.2004.04356.x.

Smith DF, Toft DO. Minireview: Steroid receptors and their associated proteins. Mol Endocrinol. (1993) 7:4–11.

Soronen P, Laiti M, Torn S, Harkonen P, Patrikainen L, Li Y, et al. Sex steroid hormone metabolism and prostate cancer. J Steroid Biochem Mol Biol. (2004) 92:281-286. doi:10.1016/j.jsbmb.2004.10.004.

Stanbrough M, Bubley GJ, Ross K, Golub TR, Rubin MA, Penning TM. Increased expression of genes converting adrenal androgens to testosterone in androgen-independent prostate cancer. Cancer Res. (2006) 66(5):2815-2825. doi:10.1158/0008-5472.CAN-05-4000.

Starka L, Hampl R, Hill M, Lapcik O, Bilek R, Petrik R. Epitestosterone in human blood and prostatic tissue. Eur J Clin Chem Clin Biochem. (1997) 35:469–73.

Steckelbroeck S, Jin Y, Gopishetty S, Oyesanmi B, Penning TM. Human cytosolic 3α-hydroxysteroid dehydrogenases of the aldo-keto reductase superfamily display significant 3β-hydroxysteroid dehydrogenase activity: Implications for steroid hormone metabolism and action. J Biol Chem. (2003) 279:10784–10795. doi: 10.1074/jbc.M313308200.

Stein MN, Goodin S, Dipaola RS. Abiraterone in prostate cancer: a new angle to an old problem. Clin Cancer Res. (2012) 18:1848–1854. http://dx.doi.org/10.1158/1078-0432.CCR-11-1805.

Storbeck K, Bloem LM, Africander D, Schloms L, Swart P, Swart AC. 11β-hydroxydihydrotestosterone and 11-ketodihydrotestosterone, novel C19 steroids with androgenic activity: A putative role in

castration resistant prostate cancer? Mol Cell Endocrinol. (2013) 377:135-146. http://dx.doi.org/10.1016/j.mce.2013.07.006.

Storbeck KH, Swart AC, Goosen P, Swart P. Cytochrome b_5: Novel roles in steroidogenesis. Mol. Cell. Endocrinol. (2013) 371: 87-99. http://dx.doi.org/10.1016/j.mce.2012.11.020.

Strott CA. Sulfonation and molecular action. Endocr Rev. (2002) 23:703–732. doi: 10.1210/er.2001-0040.

Swart AC, Schloms L, Storbeck KH, Bloem LM, Du Toit T, Quanson JL, et al. 11β-Hydroxyandrostenedione, the product of androstenedione metabolism in the adrenal, is metabolized in LNCaP cells by 5α-reductase yielding 11β-hydroxy-5α-androstanedione. J Steroid Biochem Mol Biol. (2013) 138:132-142. http://dx.doi.org/10.1016/j.jsbmb.2013.04.010.

Swart AC, Storbeck KH. 11β-hydroxyandrostenedione: Downstream metabolism by 11βHSD, 17βHSD and SRD5A produces novel substrates infamiliar pathways. Mol Cell Endocrinol. (2015) 408:114-123. http://dx.doi.org/10.1016/j.mce.2014.12.009.

Swart P, Estabrook RW, Swart AC, Mason JI, Waterman MR. Progesterone 16α-hydroxylase activity is catalyzed by human cytochrome P450 17α-hydroxylase. J Clin Endocrinol Metab. (1993) 771:98-102, https://doi.org/10.1210/jcem.77.1.8325965.

Taplin ME, Bubley GJ, Shuster T, Frantz ME, Spooner AE, Ogata GK, et al. Mutation of the androgen-receptor gene in metastatic androgen-independent prostate cancer. N Engl J Med. (1995) 332(21):1393–1398.

Ten S, New M, Maclaren N. Clinical review 130: Addison's disease 2001. J Clin Endocrinol Metab. (2001) 86(7):2909–2922.

Thalmann GN, Sikes RA, Wu TT, Degeorges A, Chang SM, Ozen M, et al. LNCaP progression model of human prostate cancer: androgen-independence and osseous metastasis. Prostate. (2000) 44:91–103.

Thiboutot D, Jabara S, McAllister JM, Sivarajah A, Gilliland K, Cong Z, et al. Human skin is a steroidogenic tissue: steroidogenic enzymes and cofactors are expressed in epidermis, normal sebocytes, and an immortalized sebocyte cell line (SEB-1). J Invest Dermatol. (2003) 120:905– 914.

Thigpen AE, Cala KM, Russell DW. Characterization of Chinese hamster ovary cell lines expressing human steroid 5α-reductase isozymes. J Biol Chem. (1993) 268(23):17404-17412.

Thomas LN, Douglas RC, Lazier CB, Too CKL, Rittmaster RS, Tindall DJ. Type 1 and type 2 5α-reductase expression in the development and progression of prostate cancer. Eur Urol. (2008) 53:244-252. doi:10.1016/j.eururo.2007.10.052.

Thomas LN, Douglas RC, Vessey JP, Gupta R, Fontaine D, Norman RW, et al. 5α-reductase type 1 immunostaining is enhanced in some prostate cancers compared with benign prostatic hyperplasia epithelium. J Urol. (2003) 170:2019-2025. doi: 10.1097/01.ju.0000091804.20183.81.

Titus MA, Gregory CW, Ford III OH, Schell MJ, Maygarden SJ, Mohler JL. Steroid 5α-reductase isozymes I and II in recurrent prostate cancer. Clin Cancer Res. (2005) 11(12): 4365–71. doi:10.1158/1078-0432.CCR-04-0738.

Titus MA, Mohler JL. 5α-reductase isozymes in castration-recurrent prostate cancer. In Androgen Action in Prostate Cancer (2009) 175–185. doi:10.1007/978-0-387-69179-4.

Tolis G, Ackman D, Stellos A, Mehta A, Labrie F, Fazekas ATA, et al. Tumor growth inhibition in patients with prostatic carcinoma treated with luteinizing hormone-releasing hormone agonists. Proc Natl Acad Sci USA. (1982) 79:1658–1662.

Touchstone JC, Glazer L, Cooper DY, Roberts JM. The isolation of Δ^4-androstene-11β-ol-3,17-dione from human adrenal incubates. J Clin Endocrinol Metab. (1955) 15:382–384.

Tran C, Ouk S, Clegg NJ, Chen Y, Watson PA, Arora V, et al. Development of a second- generation antiandrogen for treatment of advanced prostate cancer. Science. (2009) 324(5928):787–790.

Tsilchorozidou T, Honour JW, Conway GS. Altered cortisol metabolism in polycystic ovary syndrome: insulin enhances 5α-reduction but not the elevated adrenal steroid production rates. J Clin Endocrinol Metab. (2003) 88(12):5907–5913. https://doi.org/10.1210/jc.2003-030240.

Tukey RH, Strassburg CP. Human UDP-glucuronosyltransferases: Metabolism, expression, and disease. Annu Rev Pharmacol Toxicol. (2000) 40:581-616.

Turcu AF, Auchus RJ. Adrenal steroidogenesis and congenital adrenal hyperplasia. Endocrinol Metab Clin North Am. (2015) 44:275–296. doi: 10.1016/j.ecl.2015.02.002.

Turcu AF, Auchus RJ. Clinical significance of 11-oxygenated androgens. Curr Opin Endocrinol Diabetes Obes. (2017) 24:1-8. doi:10.1097/MED.0000000000000334.

Turcu AF, Nanba AT, Chomic R, Upadhyay SK, Giordano TJ, Shields JJ, et al. Adrenal-derived 11-oxygenated 19-carbon steroids are the dominant androgens in classic 21-hydroxylase deficiency. Eur J Endocrinol. (2016) 174:601–609. doi: 10.1530/EJE-15-1181.

Turcu AF, Rege J, Chomic R, Liu J, Nishimoto HK, Else T, et al. Profiles of 21-carbon steroids in 21-hydroxylase deficiency. J Clin Endocrinol Metab. (2015) 100:2283-2290.

Uemura M, Tamura K, Chung S, Honma S, Okuyama A, Nakamura Y, et al. Novel 5α-steroid reductase (SRD5A3, type 3) is overexpressed in hormone-refractory prostate cancer. Cancer Sci. (2008) 99:81-86. doi: 10.1111/j.1349-7006.2007.00656.x.

Van der Sluis TM, Vis AN, Van Moorselaar RJA, Bui HN, Blankenstein MA, Meuleman EJH, et al. Intraprostatic testosterone and dihydrotestosterone. Part I: concentrations and methods of determination in men with benign prostatic hyperplasia and prostate cancer. BJU Int. (2012) 109:176–182. doi:10.1111/j.1464-410X.2011.10651.x.

Van Rooyen D, Du Toit T, Louw-du Toit R, Africander D, Swart P, Swart AC. The metabolic fate and receptor interaction of 16α-hydroxyprogesterone. Mol Cell Endocrinol. (2017) 441:86-98. http://dx.doi.org/10.1016/j.mce.2016.09.025.

Van Rooyen D, Gent R, Barnard L, Swart AC. The *in vitro* metabolism of 11β-hydroxyprogesterone and 11-ketoprogesterone to 11-ketodihydrotestosterone in the backdoor pathway. J Steroid Biochem Mol Biol. (2017) In press. https://doi.org/10.1016/j.jsbmb.2017.12.014.

Veldscholte J, Ris-Stalpers C, Kuiper GGJM, Jenster G, Berrevoets C, Claassen E, et al. A mutation in the ligand binding domain of the androgen receptor of human LNCaP cells affects steroid binding characteristics and response to anti-androgens. Biochem Biophys Res Commun. (1990) 173(2): 534-540.

Vickman RE, Crist SA, Kerian K, Eberlin L, Cooks RG, Burcham GN, et al. Cholesterol sulfonation enzyme, SULT2B1b, modulates AR and cell growth properties in prostate cancer. Mol Cancer Res. (2016) 14(9):776-786. doi: 0.1158/1541-7786.MCR-16-0137.

Wright JL, Kwon EM, Ostrander EA, Montgomery RB, Lin DW, Vessella R, et al. Expression of SLCO transport genes in castration-resistant prostate cancer and impact of genetic variation in SLCO1B3 and SLCO2B1on prostate cancer outcomes. Cancer Epidemiol Biomarkers Prev. (2011) 20:619–627. doi: 10.1158/1055-9965.EPI-10-1023.

Xing Y, Edwards MA, Ahlem C, Kennedy M, Cohen A, Gomez-Sanchez CE, et al. The effects of ACTH on steroid metabolomic profiles in human adrenal cells. J Endocrinol. (2011) 209:327–335. doi: 10.1530/JOE-10-0493.

Yazawa T, Uesaka M, Inaoka Y, Mizutani T, Sekiguchi T, Kajitani T, et al. Cyp11b1 is induced in the murine gonad by luteinizing hormone/human chorionic gonadotropin and involved in the production of 11-ketotestosterone, a major fish androgen: conservation and evolution of the androgen metabolic pathway. Endocrinology. (2008) 149(4):1786-1792. doi: 10.1210/en.2007-1015.

Yepuru M, Wu Z, Kulkarni A, Yin F, Barrett CM, Kim J, et al. Steroidogenic enzyme AKR1C3 is a novel androgen receptor-selective coactivator that promotes prostate cancer growth. Clin Cancer Res. (2013) 19, 5613–5625. doi:10.1158/1078-0432.CCR-13-1151.

You L. Steroid hormone biotransformation and xenobiotic induction of hepatic steroid metabolizing enzymes. Chem Biol Interact. (2004) 147:233–46. doi:10.1016/j.cbi.2004.01.006.

Scadoosh.